IL
NUOVO CIMENTO
ORGANO DELLA SOCIETÀ ITALIANA DI FISICA
SOTTO GLI AUSPICI DEL CONSIGLIO NAZIONALE DELLE RICERCHE

VOL. IX, N. 3 *Serie decima* 1° Agosto 1958

Über den Einfluß der Eigenrotation des Zentralkörpers auf die Bewegung der Satelliten nach der Einsteinschen Gravitationstheorie.

N. ST. KALITZIN

Bulgarische Akademie der Wissenschaften - Sofia

(ricevuto l'11 Marzo 1958)

Zusammenfassung — Die Aufgabe der Periheldrehung eines Satelliten mit verschwindender Masse im Felde eines rotierenden Zentralkörpers wird auf Grund der Bewegungsgleichungen von EINSTEIN, INFELD, FOCK, RIABUSCHKO u.a. in der Näherung v^2/c^2 exakt behandelt. Zu der Einstein'schen Periheldrehung erhält man hier noch ein Zusatzglied welches von der Rotation des Zentralkörpers herrührt. Dieses Glied entspricht der von LENSE u. THIRRING (1) entdeckten Periheldrehung. Die Abhängigkeit vom Winkel i zwischen der Äquatorebene des Zentralkörpers und der Bahnebene des Satelliten fällt bei Lense u. Thirring verschieden als bei uns aus. Der Unterschied kommt durch die Änderung der Bahnebene des Satelliten (Knotenverschiebung) zustande. Die Periheldrehung in unserer Theorie wird aber in der Bahnebene gemessen. Unser Ergebnis ist von der Kleinheit der Effekte unabhängig. Unsere Betrachtungen sind so durchgeführt, daß sie sich leicht auf den allgemeineren Fall eines sich drehenden Satelliten mit endlicher Masse verallgemeinern lassen.

---

1. – Die Frage über den Einfluß der Eigenrotation des Zentralkörpers auf die Bewegung der Satelliten nach der Einstein'schen Gravitationstheorie ist von J. LENSE und H. THIRRING in (1) (1918) behandelt worden. LENSE und

(1) J. LENSE und H. THIRRING: *Phys. Zeits.*, **19**, 156 (1918).

THIRRING haben die von der Drehung des Zentralkörpers verursachte zusätzliche Drehung des Periheliums eines Satelliten durch die Formel

$$\Delta\omega' = -\frac{\pi^2 r_0^2 J(1 - 3\sin^2(i/2))}{9c^2\tau T^2(1-e^2)^{\frac{3}{2}}}, \tag{1}$$

bestimmt. Dabei bedeutet:

$\Delta\omega'$ = Die Drehung in Bogensekunden pro Jahrhundert,
r_0 = Radius des Zentralkörpers in cm,
J = Anzahl der Tage im Jahr,
c = Lichtgeschwindigkeit in cm s^{-1},
τ = Rotationsdauer das Zentralkörpers in Tagen,
T = Umlaufszeit des Satelliten in Tagen,
e = Exzentrizität der Bahnellipse,
i = Winkel zwischen der Äquatorebene des Zentralkörpers und der Bahnebene.

Auf Grund von Formel (1) hat L. GINZBURG die Periheldrehung eines künstlichen Satelliten der Erde berechnet [2] und bei einer Höhe der Satellitenbahn über die Erdoberfläche von 400 km, $T = 1.54$ Stunden die Periheldrehung von $-43''$ im Jahrhundert gefunden. (Hierbei ist $i = 0$ angesetzt).

Die Berechnung von LENSE und THIRRING erweckt aus folgenden zwei Gründen Bedenken:

1.) LENSE und THIRRING finden die erste relativistische Korrektur zu der Newton'schen Kraft und betrachten diese Korrektur als eine Störungskraft, welche dann in die Gleichungen der klassischen Störungstheorie der Planetenbewegung eingesetzt wird. Diese Störungstheorie ist aber von Euler und Lagrange auf Grund der Newton'schen Mechanik entwickelt. Für eine konsequente Berechnung der von LENSE und THIRRING behandelten Aufgabe müßte man aber von einer auf Grund der relativistisch korrigierten Gleichungen der Mechanik aufgebauten Störungstheorie ausgehen.

2.) Die Periheldrehung, die aus der Eigenrotation des Zentralkörpers herrührt, und die aus der ersten (linearen) Näherung der Einstein'schen Theorie hervorgeht, ist im Allgemeinen zahlenmäßig bedeutend kleiner als die Einstein'sche Periheldrehung, welche erst durch die zweite (nichtlineare) Näherung gewonnen wird. Dementsprechend ist die Vernachläßigung der zweiten Periheldrehung gegenüber der ersten nicht erlaubt. Der Behauptung von

---

[2] W. L. GINZBURG: *Žurn. Exp. Theor. Fiz.*, **30**, 213 (1956).

LENSE und THIRRING, daß diese zwei Periheldrehungen gesondert berechnet und dann linear zusammengesetzt werden können, fehlt wegen der nichtlinearen Gleichungen in der zweiten Näherung die wissenschaftliche Grundlage.

So lesen wir in ([1]), S. 159: «Wenn wir die Glieder mit $\omega r_0 v$ in Rechnung ziehen, so müßen wir erst recht auch jene Glieder in den Bewegungsgleichungen berücksichtigen, welche die Quadrate und Produkte der Geschwindigkeitskomponenten des Massenpunktes enthalten. Tun wir das aber, dann dürfen wir überhaupt nicht mehr mit der ersten Näherung allein rechnen, denn jene Glieder, welche in der zweiten Näherung zu den Newton'schen Gliedern hinzutreten, verhalten sich zu ihnen wie $\alpha/r : 1$, $(\alpha = 2fM)$. Das Geschwindigkeitsquadrat eines Planeten ist aber ebenfalls von der Größenordnung α/r; die Berücksichtigung der quadratischen Glieder in den Geschwindigkeiten bedingt also logisch auch die Berücksichtigung der aus der zweiten Näherung hervorgehenden Glieder. Daraus folgt nun, daß wegen der Gültigkeit der Ungleichung $v > \omega r_0$ die hier angestellten Rechnungen an und für sich keinen Sinn hätten. Man wird sie aber doch praktisch verwenden können, wenn man bedenkt, daß alle hier in Betracht kommenden Störungen ja *so klein sind, daß man sie einander linear überlagern darf*».

Wir wollen hier die Ergebnisse von LENSE und THIRRING in der Näherung v^2/c^2 aus der allgemeinen Relativitätstheorie auf Grund der Bewegungsgleichungen von EINSTEIN, FOCK u.a. streng ableiten. Unsere Ergebnisse sind dementsprechend mit der außerordentliche Kleinheit der Störungseffekte nicht verbunden, wie dies bei LENSE und THIRRING der Fall ist.

2. – Die Aufgabe der Auffindung der Bewegungsgleichungen von n Körpern, die sich wie starre Körper um ihren Schwerpunkten drehen, ist in der $1/c^2$ Näherung von Fock und seiner Gruppe gelöst. (Vergl. ([3])).

Die Bewegungsgleichungen bekommen nach ([3]), S. 358, die Lagrange'sche Form

$$\frac{\mathrm{d}}{\mathrm{d}t}\frac{\partial L}{\partial \dot{a}} - \frac{\partial L}{\partial a_i} = 0\,, \qquad i = 1, 2, 3. \tag{2}$$

a_i bedeuten die Koordinaten des Schwerpunktes des a-ten Körpers. Da wir ein Zweikörperproblem haben, so sollen (x_2, y_2, z_2) die Koordinaten des Schwerpunktes des sich drehenden Zentralkörpers bedeuten, (x_1, y_1, z_1) die Koordinaten des Satelliten. Wir benutzen auch die dreidimensionalen Vektorbezeichnungen $\boldsymbol{r}_1$ und $\boldsymbol{r}_2$. In diesen Bezeichnungen lautet die Funktion von Lagrange nach ([3]), S. 358 u.a. folgendermaßen (die Massenverteilung des Zen-

([3]) V. A. FOCK: *Theorie des Raumes, der Zeit und der Schwere* (Moskau, 1955), (russisch).

tralkörpers besitzt sphärische Symmetrie):

$$(3)\qquad L=\frac{1}{2}m_1\dot{\boldsymbol{r}}_1^2+\frac{1}{2}m_2\dot{\boldsymbol{r}}_2^2+\frac{1}{2}\omega_{ik}^{(2)}\omega_{jk}^{(2)}I_{ij}^{(2)}+\frac{m_1}{8c^2}(\dot{\boldsymbol{r}}_1^2)^2+\frac{m_2}{8c^2}(\dot{\boldsymbol{r}}_2^2)^2+$$
$$+\frac{1}{2c^2}\frac{fm_1m_2}{|\boldsymbol{r}_1-\boldsymbol{r}_2|}(3\dot{\boldsymbol{r}}_1^2+3\dot{\boldsymbol{r}}_2^2-7\dot{\boldsymbol{r}}_1\dot{\boldsymbol{r}}_2)-\frac{1}{2c^2}fm_1m_2\frac{(\dot{\boldsymbol{r}}_1(\boldsymbol{r}_1-\boldsymbol{r}_2))(\dot{\boldsymbol{r}}_2(\boldsymbol{r}_1-\boldsymbol{r}_2))}{|\boldsymbol{r}_1-\boldsymbol{r}_2|^3}+$$
$$+\frac{1}{c^2}fm_1\omega_{si}^{(2)}I_{sj}^{(2)}(2\dot{r}_{2i}-4\dot{r}_{1i})\frac{r_{1j}-r_{2j}}{|\boldsymbol{r}_1-\boldsymbol{r}_2|^3}+f\frac{m_1m_2}{|\boldsymbol{r}_1-\boldsymbol{r}_2|}-\frac{f^2}{2c^2}\frac{m_1m_2(m_1+m_2)}{|\boldsymbol{r}_1-\boldsymbol{r}_2|^2}\quad(*).$$

Punkt bedeutet Ableitung nach der Zeit, f die Newton'sche Gravitationskonstante.

Hier bedeutet $\omega_{si}^{(2)}$ den antisymmetrischen Tensor der Winkelgeschwindigkeit des Zentralkörpers, $I_{kl}^{(2)}$ ist der durch die Gleichung

$$I_{kl}^{(2)}=\int\varrho(\xi_k-a_k)(\xi_l-a_l)(\mathrm{d}\xi)^3$$

definierte Tensor des Trägheitsmomentes des gleichen Körpers. (ϱ — Materiedichte des Körpers). Bei der Ableitung von (3) haben wir die Glieder mit $\omega^2r_0^2/c^2$ vernachläßigt, was auch in [1] gemacht wird, und die sphärische Symmetrie des Zentralkörpers benutzt. Die Winkelgeschwindigkeit setzen wir hier als konstant voraus.

Die Bewegungsgrößen der beiden Körper lauten entsprechend

$$(4)\qquad\begin{cases}P_{1i}=\dfrac{\partial L}{\partial\dot{r}_{1i}}=\dot{r}_{1i}\left(m_1+\dfrac{1}{2}\dfrac{m_1}{c^2}\dot{\boldsymbol{r}}_1^2-\dfrac{1}{2c^2}\dfrac{fm_1m_2}{|\boldsymbol{r}_1-\boldsymbol{r}_2|}\right)+\\ \qquad+\dfrac{7}{2c^2}\dfrac{fm_1m_2}{|\boldsymbol{r}_1-\boldsymbol{r}_2|}(\dot{r}_{1i}-\dot{r}_{2i})-\dfrac{1}{2c^2}fm_1m_2\dfrac{(r_{1i}-r_{2i})(\dot{\boldsymbol{r}}_2(\boldsymbol{r}_1-\boldsymbol{r}_2))}{|\boldsymbol{r}_1-\boldsymbol{r}_2|^3}-\\ \qquad-\dfrac{4}{c^2}fm_1\omega_{si}^{(2)}I_{sj}^{(2)}\dfrac{r_{1j}-r_{2j}}{|\boldsymbol{r}_1-\boldsymbol{r}_2|^3};\quad(+)\\ P_{2i}=\dot{r}_{2i}\left(m_2+\dfrac{1}{2c^2}m_2\dot{\boldsymbol{r}}_2^2-\dfrac{1}{2c^2}fm_1m_2\dfrac{1}{|\boldsymbol{r}_1-\boldsymbol{r}_2|}\right)+\\ +7\dfrac{1}{2c^2}fm_1m_2\dfrac{1}{|\boldsymbol{r}_1-\boldsymbol{r}_2|}(\dot{r}_{2i}-\dot{r}_{1i})-\dfrac{1}{2c^2}fm_1m_2\dfrac{(r_{1i}-r_{2i})(\dot{\boldsymbol{r}}_1(\boldsymbol{r}_1-\boldsymbol{r}_2))}{|\boldsymbol{r}_1-\boldsymbol{r}_2|^3}+\\ \qquad+2\dfrac{1}{c^2}fm_1\omega_{si}^{(2)}I_{sj}^{(2)}\dfrac{r_{1j}-r_{2j}}{|\boldsymbol{r}_1-\boldsymbol{r}_2|^3}.\end{cases}$$

(*) In [3] ,S. 359 ist ein Druckfehler eingelaufen, nämlich ist im Gliede mit ω_{si} den Faktor $1/|\boldsymbol{a}-\boldsymbol{b}|^2$ anstatt $1/|\boldsymbol{a}-\boldsymbol{b}|^3$ geschrieben.

(+) Die zusätzlichen Glieder in (3) und (4), welche von der Rotation des Zentralkörpers herrühren stehen, im Einklang mit den Formeln von A. P. Riabuschko [4] (Formeln (5.5) und (5.6)) und mit jenen von Landau und Lifschitz [5] (S. 291, Formel (1) und (100.7)).

[4] A. P. Riabuschko: *Žurn. Èksp. Theor. Fiz.*, **33**, 6 (12), 1387 (1957).

[5] L. Landau und E. Lifschitz: *Theorie des Feldes* (Moskau, 1948) (russisch).

Das Energieintegral lautet

$$(5)\qquad \frac{\partial L}{\partial \dot r_{1i}}\dot r_{1i}+\frac{\partial L}{\partial \dot r_{2i}}\dot r_{2i}-L=\frac{1}{2}m_1\dot{\boldsymbol r}_1^2+\frac{1}{2}m_2\dot{\boldsymbol r}_2^2+$$

$$+\frac{3}{8}\frac{m_1}{c^2}(\dot{\boldsymbol r}_1^2)^2+\frac{3}{8}\frac{m_2}{c^2}(\dot{\boldsymbol r}_2^2)^2+\frac{1}{2c^2}\frac{fm_1m_2}{|\boldsymbol r_1-\boldsymbol r_2|}(3\dot{\boldsymbol r}_1^2+3\dot{\boldsymbol r}_2^2-7\dot{\boldsymbol r}_1\dot{\boldsymbol r}_2)-$$

$$-\frac{1}{2c^2}fm_1m_2\frac{(\dot{\boldsymbol r}_1(\boldsymbol r_1-\boldsymbol r_2))(\dot{\boldsymbol r}_2(\boldsymbol r_1-\boldsymbol r_2))}{|\boldsymbol r_1-\boldsymbol r_2|^3}-f\frac{m_1m_2}{|\boldsymbol r_1-\boldsymbol r_2|}+f^2\frac{1}{2c^2}\frac{m_1m_2(m_1+m_2)}{|\boldsymbol r_1-\boldsymbol r_2|^2}=$$

$$=\frac{1}{2}\omega_{ik}^{(2)}\omega_{jk}^{(2)}I_{ij}^{(2)}+E=h\,,$$

h eine Konstante; E die gesamte Energie.

Der Drallsatz von [3], S. 366, ergibt in der (xy) Ebene

$$(6)\quad x_1P_y^{(1)}-y_1P_x^{(1)}+x_2P_y^{(2)}-y_2P_x^{(2)}=(x_1\dot y_1-y_1\dot x_1)\left(m_1+\frac{1}{2}\frac{m_1}{c^2}\dot{\boldsymbol r}_1^2+\frac{3}{c^2}\frac{fm_1m_2}{|\boldsymbol r_1-\boldsymbol r_2|}\right)+$$

$$+(x_2\dot y_2-y_2\dot x_2)\left(m_2+\frac{1}{2c^2}m_2\dot{\boldsymbol r}_2^2+\frac{3}{c^2}fm_1m_2\frac{1}{|\boldsymbol r_1-\boldsymbol r_2|}\right)-$$

$$-\frac{7}{2c^2}\frac{fm_1m_2}{|\boldsymbol r_1-\boldsymbol r_2|}(x_1\dot y_2-y_1\dot x_2+x_2\dot y_1-y_2\dot x_1)+$$

$$+\frac{1}{2c^2}\frac{fm_1m_2}{|\boldsymbol r_1-\boldsymbol r_2|^3}(x_1y_2-y_1x_2)(\dot{\boldsymbol r}_1+\dot{\boldsymbol r}_2)(\boldsymbol r_1-\boldsymbol r_2)-$$

$$-\frac{4}{c^2}fm_1I_{sj}^{(2)}\frac{r_{1j}-r_{2j}}{|\boldsymbol r_1-\boldsymbol r_2|^3}(x_1\omega_{s2}^{(2)}-y_1\omega_{s1}^{(2)})+\frac{2}{c^2}fm_1I_{sj}^{(2)}\frac{r_{1j}-r_{2j}}{|\boldsymbol r_1-\boldsymbol r_2|^3}(x_2\omega_{s2}^{(2)}-y_2\omega_{s1}^{(2)})=K_{xy}\,,$$

K_{xy} — eine Konstante.

Wenn wir ein mit dem Schwerpunkt des Systems verbundenes Koordinatensystem einführen, dann lassen sich die Integrale des Schwerpunktes in der Form

$$(7)\qquad m_1\boldsymbol r_1\left(1+\frac{\dot{\boldsymbol r}_1^2}{2c^2}-\frac{1}{2c^2}\frac{fm_2}{|\boldsymbol r_1-\boldsymbol r_2|}\right)+m_2\boldsymbol r_2\left(1+\frac{\dot{\boldsymbol r}_2^2}{2c^2}-\frac{1}{2c^2}\frac{fm_1}{|\boldsymbol r_1-\boldsymbol r_2|}\right)=0\,.$$

darstellen.

Wir führen den Schwerpunkt im Newton'schen Sinne (Vergl. [3], S. 375)

$$(8)\qquad \boldsymbol r_0=\frac{m_1\boldsymbol r_1+m_2\boldsymbol r_2}{m_2+m_2}\,,$$

und die relative Koordinaten

$$(9)\qquad \boldsymbol r=\boldsymbol r_1-\boldsymbol r_2\,.$$

Dann haben wir

$$\text{(10)} \qquad \begin{cases} \boldsymbol{r}_1 = \boldsymbol{r}_0 + \dfrac{m_2}{m_0}\,\boldsymbol{r}, \\ \boldsymbol{r}_2 = \boldsymbol{r}_0 - \dfrac{m_1}{m_0}\,\boldsymbol{r}, \end{cases}$$

wobei

$$m_0 = m_1 + m_2$$

die ganze Masse des Systems bedeutet. Wir führen nach FOCK noch die reduzierte Masse

$$\text{(11)} \qquad m^* = \frac{m_1 m_2}{m_1 + m_2}$$

und bemerken, daß

$$\text{(12)} \qquad m_0 m^* = m_1 m_2 .$$

Es gilt auch

$$\text{(13)} \qquad m_1 \dot{\boldsymbol{r}}_1^2 + m_2 \dot{\boldsymbol{r}}_2^2 = m_0 \dot{\boldsymbol{r}}_0^2 + m^* \dot{\boldsymbol{r}}^2 ,$$

$$\text{(14)} \qquad m_1(x_1\dot{y}_1 - y_1\dot{x}_1) + m_2(x_2\dot{y}_2 - y_2\dot{x}_2) = m_0(x_0\dot{y}_0 - y_0\dot{x}_0) + m^*(x\dot{y} - y\dot{x}) ,$$

$$\text{(15)} \qquad x_2 y_1 - x_1 y_2 = x_0 y - x y_0 .$$

Aus Formel (7) folgt, daß der Radiusvektor $\dot{\boldsymbol{r}}_0$ des Newton'schen Schwerpunktes während der Bewegung eine kleine Größe bleibt, wobei seine Ableitung nach der Zeit ebenfalls klein bleibt. Deswegen können wir in sämtlichen Gliedern, welche c^2 im Nenner enthalten anstatt (10) ansetzen

$$\text{(16)} \qquad \begin{cases} \boldsymbol{r}_1 = \dfrac{m_2}{m_0}\,\boldsymbol{r}; \qquad \dot{\boldsymbol{r}}_1 = \dfrac{m_2}{m_0}\,\dot{\boldsymbol{r}}; \\ \boldsymbol{r}_2 = -\dfrac{m_1}{m_0}\,\boldsymbol{r}; \qquad \dot{\boldsymbol{r}}_2 = -\dfrac{m_1}{m_0}\,\dot{\boldsymbol{r}} . \end{cases}$$

Wenn (16) in (7) eingesetzt wird, ergibt sich

$$\text{(17)} \qquad m_0 \ddot{\boldsymbol{r}}_0 = \frac{m_1 - m_2}{2c^2 m_0}\,\boldsymbol{r}\left(m^* \dot{\boldsymbol{r}}^2 - \frac{f m^* m_0}{\boldsymbol{r}}\right) .$$

Wir schreiben jetzt die Integrale der Energie und des Impulsmoments bei der Annahme, daß $\boldsymbol{r}_0$ klein ist. Auch in den Newton'schen Gliedern von (5) und (6) können wir $\boldsymbol{r}_0$ und $\dot{\boldsymbol{r}}_0$ vernachläßigen, da sie dort nach (13) und (14)

quadratisch auftreten. Wir können also überall die Werte (16) benutzen. So ergibt das Energieintegral, indem wir durch m^* das Resultat teilen

$$(18)\qquad h_0 = \frac{h}{m^*} = \frac{1}{2}\dot{\boldsymbol{r}}^2 - f\frac{m_0}{\tau} + \frac{1}{c^2}\left\{\frac{3}{8}\left(1 - 3\frac{m^*}{m_0}\right)(\dot{\boldsymbol{r}}^2)^2 + \right.$$
$$\left. + \frac{f}{2r}\,\dot{\boldsymbol{r}}^2(3m_0 + m^*) + \frac{1}{2}f\frac{m^*}{r^3}(\dot{\boldsymbol{r}}\boldsymbol{r})^2 + \frac{f^2}{2r^2}\,m_0^2\right\}$$

Bevor wir zum Drallintegral übergehen, machen wir die Annahme, daß die Orbitalbewegung des Satelliten in der Drehungsebene des Zentralkörpers erfolgt, d.h. $\omega_{12}^{(2)} \neq 0$, die übrigen Komponenten von ω_{ik} verschwinden. Da der Zentralkörper sphärischsymmetrische Massenverteilung besitzt, so müssen wir ansetzen:

$$(19)\qquad I_{kl}^{(2)} = I^{(2)}\delta_{kl}\,,$$

$$\delta_{kl} = 1 \text{ für } k = l;\quad \delta_{kl} = 0 \text{ für } k \neq l.$$

Führen wir jetzt die Werte (16) in das Drallintegral ein. Infolge von (15) und (17) kann man das vierte Glied von (6) vernachläßigen. Die übrigen Glieder ergeben

$$(20)\qquad \frac{1}{m^*}K_{xy} + \frac{4}{c^2}fI^{(2)}\frac{1}{r}\omega_{12}^{(2)} + \frac{2}{c^2}f\frac{m_1}{m_2}I^{(2)}\frac{1}{r}\omega_{12}^{(2)} =$$
$$= \left\{1 + \frac{1}{2c^2}\left(1 - 3\frac{m^*}{m_0}\right)\dot{\boldsymbol{r}}^2 + \frac{1}{c^2}\frac{f}{r}(3m_0 + m^*)\right\}(x\dot{y} - y\dot{x})\,.$$

In Falle des Satelliten untersuchen wir die Bewegung einer sehr kleinen Masse $m_1 \to 0$ im Felde einer endlichen Masse m_2. Wir können also in diesem Fall $m^* = 0$ ansetzen. Die Energiegleichung (18) und der Drallsatz (20) ergeben dann

$$(21)\qquad \frac{1}{2}\dot{\boldsymbol{r}}^2 - f\frac{m_2}{r} + \frac{3}{8}\frac{1}{c^2}(\dot{\boldsymbol{r}}^2)^2 + \frac{3}{2}f\frac{m_2}{r}\dot{\boldsymbol{r}}^2\frac{1}{c^2} + \frac{f^2}{2r^2}m_2^2\frac{1}{c^2} = h_0\,,$$

$$(22)\qquad \left\{1 + \frac{1}{2c^2}\dot{\boldsymbol{r}}^2 + \frac{3}{c^2}\frac{f}{r}m_2\right\}\boldsymbol{r}^2\frac{\mathrm{d}\varphi}{\mathrm{d}t} = \mu + \sigma\frac{1}{r}\,,$$

wobei

$$\sigma = \frac{4}{c^2}fI^{(2)}\omega_{12}\,,$$

μ — eine Konstante.

Wenn wir ansetzen

$$u = \frac{1}{r}, \tag{23}$$

dann haben wir die Identität

$$\dot{r}^2 = v^2 = \left(r^2 \frac{\mathrm{d}\varphi}{\mathrm{d}t}\right)^2 \left(\left(\frac{\mathrm{d}u}{\mathrm{d}\varphi}\right)^2 + u^2\right), \tag{24}$$

woraus durch erheben ins Quadrat von (22) sich ergibt

$$v^2 + \frac{1}{c^2} v^4 + \frac{6f}{c^2 r} m_2 v^2 = \left(\mu^2 + 2\mu\sigma \frac{1}{r}\right)\left(\left(\frac{\mathrm{d}u}{\mathrm{d}\varphi}\right)^2 + u^2\right). \tag{25}$$

Aus (21) bestimmen wir näherungsweise $v^2 = \dot{r}^2$ und setzen in (25) ein. Es ergibt sich

$$2h_0 + \frac{h_0^2}{c^2} + 2fm_2\left(1 + 4\frac{h_0}{c^2}\right)u + 6f^2 \frac{m_2^2}{c^2} u^2 = \mu^2 \left(1 + 2\frac{\sigma}{\mu} u\right)\left(\left(\frac{\mathrm{d}u}{\mathrm{d}\varphi}\right)^2 + u^2\right). \tag{26}$$

Wenn wir $1/(1+2(\sigma/\mu)u)$ in Potenzreihe entwickeln, so erhalten wir

$$\mu^2\left(\left(\frac{\mathrm{d}u}{\mathrm{d}\varphi}\right)^2 + u^2\right) = \tag{27}$$

$$= 2h_0 + \frac{h_0^2}{c^2} + 2\left(fm_2 + 4fm_2 \frac{h_0}{c^2} - 2h_0 \frac{\sigma}{\mu}\right) u + 2fm_2\left(3fm_2 \frac{1}{c^2} - 2\frac{\sigma}{\mu}\right) u^2 .$$

Wir differenzieren Gl. (27) nach φ und teilen das Resultat durch $2(\mathrm{d}u/\mathrm{d}\varphi)$. Es ergibt sich

$$\frac{\mathrm{d}^2 u}{\mathrm{d}\varphi^2} + \left[1 - \frac{2fm_2}{\mu^2}\left(3f\frac{m_2}{c^2} - 2\frac{\sigma}{\mu}\right)\right] u = \frac{1}{\mu^2}\left[fm_2 + 4fm_2 \frac{h_0}{c^2} - 2h_0 \frac{\sigma}{\mu}\right]. \tag{28}$$

Das allgemeine Integral von (28) lautet

$$u = \frac{1 + e\cos(\lambda\varphi - \varepsilon)}{p}, \tag{29}$$

wobei e und ε beliebige Konstanten sind. Durch Einsetzen von (29) in (28) erhalten wir

$$\lambda = 1 - \frac{3f^2 m_2^2}{\mu^2 c^2} + 2fm_2 \frac{\sigma}{\mu^3}, \tag{30}$$

$$\frac{1}{p} = \frac{\frac{1}{\mu^2}\left(fm_2 + 4fm_2 \frac{h_0}{c^2} - 2h_0 \frac{\sigma}{\mu}\right)}{1 - \frac{2fm_2}{\mu^2}\left(3f\frac{m^2}{c^2} - 2\frac{\sigma}{\mu}\right)}. \tag{31}$$

Aus (30) und (31) bekommen wir

$$\lambda = 1 - \frac{3fm_2}{pc^2} + \frac{2\sigma}{p\sqrt{fm_2 p}} . \tag{32}$$

Die Periheldrehung für einen Umlauf des Satelliten beträgt

$$\Delta\varphi = \frac{2\pi}{\lambda} - 2\pi = 6\pi \frac{fm_2}{c^2 p} - 4\pi \frac{\sigma}{p\sqrt{fm_2 p}} . \tag{33}$$

Da $\Delta\varphi$ den Faktor $1/c^2$ enthält, so können wir die in (33) vorkommenden Elemente aus der Newton'schen Näherung (der Newton'schen Ellipse) bestimmten. Wir haben

$$p = a(1 - e^2) , \tag{34}$$

$(e < 1)$ $\quad e$ — Exzentrizität der Ellipse.

$$fm_2 = 4\pi^2 \frac{a^3}{T^2} . \tag{35}$$

Dabei bedeutet a die große Halbachse der Ellipse, T ist die Umlaufszeit des Satelliten. Dann erhalten wir aus (33)

$$\Delta\varphi = 24 \frac{\pi^3 a^2}{T^2 c^2 (1 - e^2)} - \frac{8 fm_2 r_0^2 \omega_{12} T}{5 c^2 a^3 (1 - e^2)^{\frac{3}{2}}} . \tag{36}$$

r_0 ist der Radius des Zentralkörpers, $I = m_0 r_0^2/5$.

Pro Jahrundert erhalten wir in Bogensekunden

$$\Delta\varphi = \frac{5}{24} \frac{\pi^2 a^2 J}{T^3 c^2 (1 - e^2)} - \frac{\pi^2 r^2 J}{9 T^2 c^2 \tau (1 - e^2)^{\frac{3}{2}}} . \tag{37}$$

Hier bedeuten

J = Anzahl der Tage im Jahr,

τ = Rotationsdauer des Zentralkörpers in Tagen. T wird ebenfalls in Tagen angegeben.

Das erste Glied auf der rechten Seite von (37) ergibt die Einstein'sche Periheldrehung, das zweite Glied stimmt mit der von LENSE und THIRRING angegebenen Periheldrehung (Formel (1)) überein. Hierbei muß man $i = 0$ ansetzen). Formel (37) ist also die exakte Lösung des Problems in der Näherung v^2/c^2.

Wenn $i \neq 0$ (i ist der Winkel zwischen der Äquatordrehebene des Zentralkörpers und der Bahnebene des Satelliten), dann erhalten wir aus Gleichungen

(6), (21) und (22) (die Koordinatenebene xy ist die Bahnebene des Satelliten)

$$\Delta\varphi = \frac{5}{24}\frac{\pi^2 a^2 J}{T^2 c^2 (1-e^2)} - \frac{\pi^2 r_0^2 J \cos i}{9 T^2 c^2 \tau (1-e^2)^{\frac{3}{2}}}. \tag{38}$$

Der Unterschied zur Formel (1) von Lense und Thirring besteht darin, daß bei Lense und Thirring der Faktor $(1 - 3\sin^2(i/2))$ steht und bei uns $\cos i$. Der Faktor $(1 - 3\sin^2(i/2))$ kann aber, unabhängig von der Ableitung, auch aus folgendem Grund nicht der richtige sein: Bei $i = \pi$ hat er den Wert -2 anstatt -1, wie es sein muß und wie bei $\cos i$ der Fall ist.

Dieser Unterschied kommt dadurch Zustande weil $\Delta\omega'$ von [1] die Knotenverschiebung mitenthält, $\Delta\varphi$ aber ist die in der Bahnebene des Satelliten gemessene Periheldrehung.

RIASSUNTO (*)

Il problema della rotazione del perielio di un satellite di massa trascurabile nel campo di un corpo centrale rotante si tratta esattamente in base alle equazioni del moto di Einstein, Infeld, Fock, Riabuschko *et al.* nell'approssimazione v^2/c^2. Oltre alla rotazione del perielio einsteiniana, si ottiene un altro termine dipendente dalla rotazione del corpo centrale. Questo termine corrisponde alla rotazione del perielio scoperta da Lense e Thirring [1]. La dipendenza dell'angolo i tra piano equatoriale del corpo centrale e piano dell'orbita del satellite risulta per Lense e Thirring differente dalla nostra. La differenza è dovuta alla variazione del piano dell'orbita del satellite (precessione dei nodi). Nella nostra teoria la rotazione del perielio si misura invece nel piano dell'orbita. Il nostro risultato è indipendente dalla piccolezza degli effetti. Le nostre considerazioni sono svolte in modo da essere facilmente estese al caso più generale di un satellite rotante con massa finita.

(*) *Traduzione a cura della Redazione.*

IL NUOVO CIMENTO Vol. IX, N. 3 1° Agosto 1958

The Suppression Effect in Ionization by Fast Electron Pairs (*).

G. H. Burkhardt

Department of Mathematical Physics, University of Birmingham

(ricevuto il 5 Aprile 1958)

Summary. — Electron pairs of very high energies (about 10^{11} eV) were found by Perkins to have reduced ionizing power near their origin. The reason is that the angle between the two paths is very small so that over appreciable distances they stay close enough together for their electric fields very nearly to cancel except for atoms very close to the line of travel. The present paper gives a quantum treatment of this effect and the deviations from the semi-classical result are found negligible, in spite of the fact that the general conditions for the validity of classical mechanics are not satisfied. The phenomenon can be used to estimate the energy of the pair. The limitations of this method, both fundamental and practical, are discussed.

1. – Introduction.

The suggestion by King [1] that electron pairs of very high energy ($> 10^{11}$ eV), produced in cosmic ray showers, have a reduced ionizing power near their origin, due to the proximity of the two opposite charges and their resultant partial screening has been investigated by Perkins [2] and Wolter and Mięsowicz [3]. Their results, while not intended to be primarily a test of any theory, are in accord with simple classical calculations. The effect has an additional interest in that it offers a method for obtaining a measure

(*) This work formed the basis of a Ph. D. thesis, submitted to the University of Birmingham, October, 1957.

(1) D. T. King: unpublished (1950).

(2) D. H. Perkins: *Phil. Mag.*, **46**, 1146 (1955).

(3) W. Wolter and M. Mięsowicz: *Nuovo Cimento*, **4**, 648 (1956).

of the energy of the pair which is applicable in a region in which other methods are difficult and laborious (*).

The object of this paper is to examine this effect from the theoretical point of view. In Sect. 3 the rate of ionization of the pair is calculated quantum mechanically, and the relation of this to the primary photon energy is examined in detail. This raises questions about the nature of the measurement process involved which are considered in Sect. 4 and 5. In Sect. 4, an evaluation is made of the classical view of the effect, used by YEKUTIELI and ČUDAKOV, and the regions of its validity, and an explanation of the agreement of the result is found. In Sect. 5 the effect of the interaction on the pair is studied and the connection with the primary photon energy is considered. In Sect. 6 some numerical results are given as corrections to previous work.

2. – The formulation of the problem.

We wish ultimately to calculate the experimentally observed quantity, which is the grain density along the track of the pair in emulsion. The concept of particular physical interest from the measurement point of view is the rate of ionization, while we shall calculate the rate of energy loss of the pair. The proportionality of these three quantities is normally assumed on an empirical basis ([6]) and we shall do that here, mentioning when necessary the special features of the behaviour of each particular quantity.

The forces being purely electrodynamic, Born approximation is valid in this energy region, as the expansion parameter

$$\frac{e^2}{\hbar v} \sim \frac{1}{137} \ll 1 .$$

We shall use lowest order perturbation theory in the calculation of all matrix elements. We shall therefore neglect the interactions between the negaton and positon of the pair and that between the pair and the nuclear screened Coulomb field, as these produce no excitation of the atomic electrons in lowest order. We shall treat the interaction of the atomic electron with the rest of the atom exactly, using exact atomic wave functions. The perturbation is the interaction between the pair and the atomic electron.

(*) The results of the measurement of the π^0-lifetime by OREAR ([4]) suggest that a re-examination should be made of the experiment of ANAND ([5]), in which the suppression effect should be included.

([4]) J. OREAR, G. HARRIS and S. TAYLOR: *Phys. Rev.*, **106**, 327 (1957).

([5]) B. M. ANAND: *Proc. Roy. Soc.*, A **220**, 183 (1953), Bristol Univ. Ph.D. thesis.

([6]) B. ROSSI: *High-Energy Particles* (New York, 1952) p. 127.

We shall calculate the probability P^i_{n0} of excitation of a given atom i to a given level n, in the laboratory co-ordinate system. The energy loss, in a thickness $\mathrm{d}t$ of material is then

$$-\mathrm{d}E = \sum_{n,i} \omega_{n0} P^i_{n0} , \tag{2.1}$$

where ω_{n0} is the excitation energy of the n-th level and the sum extends over all levels and all atoms in $\mathrm{d}t$. The nucleus of the i-th atom will be taken as the origin of co-ordinates. We shall assume it to be infinitely heavy.

In describing the initial state of the pair it is clearly important to allow for the correlation of the position of the two electrons, but we are not concerned with locating their position absolutely in space, since this is not correlated with the position of the atoms of the medium. The form of the relative moment distribution has been derived by BORSELLINO (7) but it is complicated and for our purpose it may be simplified.

This would suggest taking the initial state of the pair to be

$$\frac{u}{(2\pi)^3} \exp\,[i\boldsymbol{P}\cdot\boldsymbol{R}] \int \mathrm{d}^3\boldsymbol{k} \exp\,[i(\boldsymbol{p}+\boldsymbol{k})\boldsymbol{r}] f(\boldsymbol{k}) , \tag{2.2}$$

where $\boldsymbol{P}$ is the total momentum of the pair, $\boldsymbol{R}$ the position of its centre of mass, $\boldsymbol{r}$ the separation, $\boldsymbol{p}+\boldsymbol{k}$ the relative momentum, u is a spinor factor and f the amplitude of the distribution of relative momentum.

However, such a wave packet is not an energy eigenstate, and since the problem is sensitive to small errors in the energy balance, this would be inconvenient. We therefore introduce a correction to the centre of mass momentum together with the spread in relative momentum: this makes our wave packet

$$\frac{u}{(2\pi)^3} \int \mathrm{d}^3\boldsymbol{k} \exp\,[i\overline{\boldsymbol{P}+\boldsymbol{K}(\boldsymbol{k})}\cdot\boldsymbol{R} + i\overline{\boldsymbol{p}+\boldsymbol{k}}\cdot\boldsymbol{r}] f(\boldsymbol{k}) . \tag{2.3}$$

This, strictly speaking, localizes also the centre of mass of the pair, but we shall see that this is negligible, so that P^i_{n0} is the same for all atoms i, and the summation over atoms is trivial. The essential features of the problem are represented by taking f to be a Gaussian wave packet of mean separation α, and spread β:

$$f = \left(\frac{\beta^2}{\pi}\right)^{\frac{3}{4}} \exp\left[-\frac{\beta^2}{2} k^2 - i\boldsymbol{k}\cdot\boldsymbol{\alpha}\right] . \tag{2.4}$$

Thus, including the initial state $\varphi_0(\boldsymbol{r}_0)$ of the atomic electron, co-ordinate $\boldsymbol{r}_0$,

(7) A. BORSELLINO: *Phys. Rev.*, **89**, 1023 (1953).

the initial state of our system is

$$(2.5) \qquad \frac{\beta^{\frac{3}{2}}}{(2\pi)^3\pi^{\frac{3}{4}}}\, u\cdot\varphi_0(\boldsymbol{r}_0)\int \mathrm{d}^3\boldsymbol{k}\, \exp\left[-\frac{\beta^2}{2}\,k^2 - i\boldsymbol{k}\cdot\boldsymbol{\alpha} + i\overline{\boldsymbol{P}+\boldsymbol{K}(\boldsymbol{k})}\cdot\boldsymbol{R} + i\,\overline{\boldsymbol{p}+\boldsymbol{k}}\cdot\boldsymbol{r}\right].$$

In the final states, over which we finally sum, it is sufficient to use plane waves, so that our wave function is

$$(2.6) \qquad \frac{u'}{(2\pi)^3}\,\varphi_n(\boldsymbol{r}_0)\exp\left[i\boldsymbol{P}'\cdot\boldsymbol{R} + i\boldsymbol{p}'\cdot\boldsymbol{r}\right].$$

With this description we shall calculate the rate of energy loss and study its nature as a measurement process.

3. – The calculation of the mean energy loss.

This follows the method of Bethe ([8]) and Møller ([9]) for the energy loss of a single particle. The energy loss in distance $\mathrm{d}t$, with N atoms per unit volume is

$$(3.1) \qquad -\mathrm{d}E = N\,\mathrm{d}t\sum_n \omega_{n0}P_{n0}\,,$$

where P_{n0} is the transition probability of a given atom from its ground state to state n, due to its interaction with the pair. From standard perturbation theory

$$(3.2) \qquad P_{n0} = \frac{(2\pi)^4}{j_0}\int |M_{n0}|^2\,\mathrm{d}^3\boldsymbol{P}'\,\mathrm{d}^3\boldsymbol{p}'\;\delta(E - E' - \omega_{n0})\,,$$

where M_{n0} is the matrix element of the interaction from initial state (2.4) to final state (2.5) and j_0 is the incident particle flux, which (2.4) implies.

Throughout the calculation we shall use units in which $\hbar = c = 1$. The suffixes 1, 2, 0 refer to the moving negaton, positon and atomic electron respectively; their co-ordinates are

$$(3.3a) \qquad \boldsymbol{R}_1 = \boldsymbol{R} + \boldsymbol{r}\,, \qquad \boldsymbol{R}_2 = \boldsymbol{R} - \boldsymbol{r} \qquad \text{and} \qquad \boldsymbol{r}_0$$

and their momenta before the interaction

$$(3.3b) \qquad \boldsymbol{P}_1 = \tfrac{1}{2}(\boldsymbol{P} + \boldsymbol{p})\,, \qquad \boldsymbol{P}_2 = \tfrac{1}{2}(\boldsymbol{P} - \boldsymbol{p})$$

([8]) H. A. Bethe: *Ann. der Phys.*, **5**, 325 (1930).
([9]) C. Møller: *Ann. der Phys.*, **14**, 531 (1932).

and after the collision similarly, but with primes. Their velocities before the collision

$$\boldsymbol{v}_1 = \boldsymbol{v} + \tilde{\boldsymbol{v}}\,, \qquad \boldsymbol{v}_2 = \boldsymbol{v} - \tilde{\boldsymbol{v}}\,, \tag{3.3c}$$

where $\boldsymbol{v}$, $\tilde{\boldsymbol{v}}$ are here the mean and relative velocities.

Let

$$\boldsymbol{Q} = \boldsymbol{P} - \boldsymbol{P}'\,, \qquad \boldsymbol{q} = \boldsymbol{p} - \boldsymbol{p}'\,. \tag{3.3d}$$

We shall call the direction of $\boldsymbol{P}$ the z-direction, and that of $\boldsymbol{\alpha}$ the x-direction. (The separation is very nearly perpendicular to $\hat{\boldsymbol{z}}$ because of the highly relativistic kinematics.)

j_0 is just equal to the velocity of the incoming particle, v, with this normalization. A change in energy δE is given by

$$\delta H = \delta \boldsymbol{p} \cdot \boldsymbol{v} \tag{3.4}$$

in the limit $\delta p \to 0$, where $\delta \boldsymbol{p}$ is the associated momentum transfer.

Using this expression the requirement of energy conservation becomes

$$\boldsymbol{Q} \cdot \boldsymbol{v} + \boldsymbol{q} \cdot \tilde{\boldsymbol{v}} - \omega_{n0} = 0\,. \tag{3.5}$$

We choose $\boldsymbol{K}(\boldsymbol{k})$ so that

$$\boldsymbol{K} \cdot \boldsymbol{v} + \boldsymbol{k} \cdot \tilde{\boldsymbol{v}} = 0\,, \qquad K_x = K_y = 0\,. \tag{3.6}$$

As the velocity difference along the z direction is very small, $\tilde{\boldsymbol{v}}$ is essentially perpendicular to $\boldsymbol{v}$, and parallel to $\boldsymbol{\alpha}$ so that the opening angle $\theta = \tilde{v}/v$ and $K_z = \theta k_x$. The localization of the centre of mass of the pair is small and only in the z-direction.

The interaction potential V is given by

$$V = -e \int A_\mu(\boldsymbol{r}_0)\, \bar{u}_n \varphi_n^*(\boldsymbol{r}_0) \gamma_0^\mu \varphi_0(\boldsymbol{r}_0) u_0 \, \mathrm{d}^3 \boldsymbol{r}_0\,, \tag{3.7}$$

where

$$A_\mu = -e \int u_{12} \psi(\boldsymbol{R}_1, \boldsymbol{R}_2) \cdot \{ \exp\left[-iE\, \overline{t - |\boldsymbol{R}_1 - \boldsymbol{r}_0|}\, \right] \gamma_1^\mu \exp\left[iE'\, \overline{t - |\boldsymbol{R}_1 - \boldsymbol{r}_0|}\, \right] - \tag{3.8}$$

$$- \exp\left[-iE\, \overline{t - |\boldsymbol{R}_2 - \boldsymbol{r}_0|}\, \right] \gamma_2^\mu \exp\left[iE'\, \overline{t - |\boldsymbol{R}_2 - \boldsymbol{r}_0|}\, \right] \} \psi^{*\prime}(\boldsymbol{R}_1, \boldsymbol{R}_2)\, \bar{u}'_{12} \cdot \mathrm{d}^3 \boldsymbol{R}_1 \mathrm{d}^3 \boldsymbol{R}_2\,,$$

where ψ, ψ' are the space part of the wave functions of the pair. We can now

write the matrix M_{n0} for the transition, taking the Fourier transform of (3.8)

$$(3.9)\qquad M_{n0} = \frac{e^2\beta_2^4}{2\pi^2(2\pi)^6\pi^4}\cdot$$

$$\cdot\int \exp\left[i[\boldsymbol{Q}+\boldsymbol{K}\cdot\boldsymbol{R}+\boldsymbol{q}+\boldsymbol{k}\cdot\boldsymbol{r}-\boldsymbol{k}\cdot\boldsymbol{\alpha}]-\frac{\beta^2}{2}k^2\right]\cdot\varphi_n^*(\boldsymbol{r}_0)\varphi_0(\boldsymbol{r}_0)\,\bar{u}_0'\gamma_0^\mu u_0\cdot$$

$$\cdot\frac{\{\bar{u}_1'\gamma_1^\mu u_1\exp[i\boldsymbol{l}\cdot\overline{\boldsymbol{R}+\boldsymbol{r}-\boldsymbol{r}_0}]-\bar{u}_2'\gamma_2^\mu u_2\exp[i\boldsymbol{l}\cdot\overline{\boldsymbol{R}-\boldsymbol{r}-\boldsymbol{r}_0}]\}}{l^2-\omega_{n0}^2}\cdot\mathrm{d}^3\boldsymbol{r}_0\,\mathrm{d}^3\boldsymbol{r}\,\mathrm{d}^3\boldsymbol{k}\,\mathrm{d}^3\boldsymbol{l}\,.$$

In the spinor interaction terms in this highly relativistic limit,

$$(3.10)\qquad \begin{cases} \bar{u}_1'\gamma_1^0u_1=\bar{u}_2\gamma_2^0u_2=\bar{u}_0'\gamma_0^0u_0=1\,, \\ \bar{u}_1'\gamma_1^zu_1=\bar{u}_2'\gamma_2^zu_2=-\dfrac{v}{c}\,, \qquad \bar{u}_0'\gamma_0^zu_0=-\dfrac{i}{m}\dfrac{\partial}{\partial z}\,. \end{cases}$$

Thus the negaton and positon give opposite and very nearly equal contributions. Specifically spinor effects make negligible contributions, as $Q \ll E_0$ so that

$$(3.11)\qquad M_{n0}=\frac{e^2\beta_2^4}{2\pi\cdot(2\pi)^6\pi^4}\int\exp\left[-\frac{\beta^2}{2}k^2+i[\overline{\boldsymbol{Q}+\boldsymbol{K}+\boldsymbol{l}}\cdot\boldsymbol{R}-\boldsymbol{k}\cdot\boldsymbol{\alpha}]\right]\cdot\varepsilon_n(-\boldsymbol{l})\cdot$$

$$\cdot\frac{\{\exp[i\overline{\boldsymbol{q}+\boldsymbol{k}+\boldsymbol{l}}\cdot\boldsymbol{r}]-\exp[i\overline{\boldsymbol{q}+\boldsymbol{k}-\boldsymbol{l}}\cdot\boldsymbol{r}]\}}{l^2-\omega_{n0}}\mathrm{d}^3\boldsymbol{k}\,\mathrm{d}^3\boldsymbol{l}\,\mathrm{d}^3\boldsymbol{R}\,\mathrm{d}^3\boldsymbol{r}\,,$$

where

$$(3.12)\qquad \varepsilon_n(-\boldsymbol{l})=\int\varphi_n^*(\boldsymbol{r}_0)\exp[-i\boldsymbol{l}\cdot\boldsymbol{r}_0]\cdot\left[\varphi_0(\boldsymbol{r}_0)+i\frac{v}{m}\frac{\partial\varphi_0(\boldsymbol{r}_0)}{\partial z}\right]\mathrm{d}^3\boldsymbol{r}_0\,.$$

Integration over $\mathrm{d}^3\boldsymbol{R}$, $\mathrm{d}^3\boldsymbol{l}$ gives

$$(3.13)\qquad M_{n0}=\frac{e^2\beta_2^4}{2\pi^2(2\pi)^3\pi^4}\int\exp\left[-\frac{\beta^2}{2}k^2-i\boldsymbol{k}\cdot\boldsymbol{\alpha}\right]\frac{\varepsilon_n(\boldsymbol{Q}+\boldsymbol{K})}{(\boldsymbol{Q}+\boldsymbol{K})^2-\omega_{n0}^2}\cdot$$

$$\cdot\{\exp[i(\boldsymbol{q}+\boldsymbol{k}-\overline{\boldsymbol{Q}+\boldsymbol{K}})\boldsymbol{r}]-\exp[i(\boldsymbol{q}+\boldsymbol{k}+\overline{\boldsymbol{Q}+\boldsymbol{K}})\cdot\boldsymbol{r}\}\mathrm{d}^3\boldsymbol{k}\,\mathrm{d}^3\boldsymbol{r}\,.$$

Integration over $\mathrm{d}^3\boldsymbol{r}$ now yields factors $\pm(2\pi)^3\,\delta(q+\boldsymbol{k}\mp\boldsymbol{Q}\mp\boldsymbol{K}(k))$ respectively for the negaton and positon terms. In order to perform the integration $\mathrm{d}^3\boldsymbol{k}$, writing $\boldsymbol{K}(\boldsymbol{k})$ explicitly we have

$$(3.14)\qquad \boldsymbol{q}+\boldsymbol{k}\mp\boldsymbol{Q}\pm k_x\theta\hat{\boldsymbol{z}}=0\,.$$

The solution of which are

$$(3.15)\qquad \begin{cases} -k_x = q_x \mp Q_x\,, \\ -k_y = q_y \mp Q_y\,, \\ -k_z = q_z \mp Q_z \mp q_x\theta + Q_x\theta\,. \end{cases} \qquad \boldsymbol{K} = (q_x\theta \mp Q_x\theta)\hat{\boldsymbol{z}}\,.$$

This is, just an expression of the slight difference in the velocities of the negaton and positon, which we have already neglected in evaluating the spinor factors. We retain it here for the moment, because it is the occurrence of $\boldsymbol{K}$ in the denominator of the matrix element that is most important. Now

$$(3.16)\quad M_{n0} = \frac{e^2\beta^2}{2\pi^2\cdot\pi^{\frac{1}{2}}}\left\{\frac{\varepsilon_n(\boldsymbol{Q}+\overline{\boldsymbol{q}-\boldsymbol{Q}}_r\cdot\theta\hat{\boldsymbol{z}})}{(\boldsymbol{Q}+\overline{\boldsymbol{q}-\boldsymbol{Q}}_r\theta\hat{\boldsymbol{z}})^2-\omega_{n0}^2}\cdot\right.$$

$$\cdot\exp\left[-\frac{\beta^2}{2}(\boldsymbol{q}-\boldsymbol{Q}-\overline{\boldsymbol{q}-\boldsymbol{Q}}_r\theta\hat{\boldsymbol{z}})^2+i(\boldsymbol{q}-\boldsymbol{Q}-\overline{\boldsymbol{q}-\boldsymbol{Q}}_r\theta\hat{\boldsymbol{z}})\cdot\boldsymbol{\alpha}\right]-\frac{\varepsilon_n(\boldsymbol{Q}+\boldsymbol{q}+\boldsymbol{Q}_x\theta\hat{\boldsymbol{z}})}{(\boldsymbol{Q}+\boldsymbol{q}+\boldsymbol{Q}_x\theta\hat{\boldsymbol{z}})^2-\omega_{n0}^2}\cdot$$

$$\left.\cdot\exp\left[-\frac{\beta^2}{2}(\boldsymbol{q}+\boldsymbol{Q}+\boldsymbol{q}+\boldsymbol{Q}_r\theta\hat{\boldsymbol{z}})^2+i(\boldsymbol{q}+\boldsymbol{Q}+\overline{\boldsymbol{q}+\boldsymbol{Q}}_r\theta\hat{\boldsymbol{z}})\cdot\boldsymbol{\alpha}\right]\right\}.$$

We shall examine this more exact expression for M_{n0} later (Sect. **4**), when we have seen the behaviour of the simpler form, which results when we neglect the difference in velocities of the electrons.

If we make the approximation $\vartheta = \theta = 0$ then (3.16) for M_{n0} is greatly simplified giving

$$(3.17)\quad M_{n0} = \frac{e^2\beta^2}{2\pi^2\cdot\pi^{\frac{1}{2}}}\cdot\frac{\varepsilon_n(\boldsymbol{Q})}{Q^2-\omega_{n0}^2}\cdot$$

$$\cdot\left\{\exp\left[-\frac{\beta^2}{2}\overline{\boldsymbol{q}-\boldsymbol{Q}}^2+i\overline{\boldsymbol{q}-\boldsymbol{Q}}\cdot\boldsymbol{\alpha}\right]-\exp\left[-\frac{\beta^2}{2}\overline{\boldsymbol{q}+\boldsymbol{Q}}^2-i\overline{\boldsymbol{q}+\boldsymbol{Q}}\cdot\boldsymbol{\alpha}\right]\right\}.$$

Hence,

$$(3.18a)\qquad P_{n0} = \frac{(2\pi)^4}{j_0}\int|M_{n0}|^2\cdot\delta(\boldsymbol{Q}\cdot\boldsymbol{v}-\omega_{n0})\cdot\mathrm{d}^3\boldsymbol{P}'\,\mathrm{d}^3\boldsymbol{p}'$$

$$(3.18b)\qquad = \frac{(2\pi)^4}{v}\int|M_{n0}|^2\cdot\delta(\boldsymbol{Q}\cdot\boldsymbol{v}-\omega_{n0})\,\mathrm{d}^3\boldsymbol{Q}\,\mathrm{d}^3\boldsymbol{q}$$

$$(3.19)\quad P_{n0} = \frac{4e^4\beta^2}{v\pi^{\frac{3}{2}}}\int\frac{|\varepsilon_n(\boldsymbol{Q})|^2}{[Q^2-\omega_{n0}^2]^2}\cdot\delta(\boldsymbol{Q}\cdot\boldsymbol{v}-\omega_{n0})\cdot$$

$$\cdot(\exp[-\beta^2\overline{\boldsymbol{q}-\boldsymbol{Q}}^2]+\exp[-\beta^2\overline{\boldsymbol{q}+\boldsymbol{Q}}^2]-2\exp[-\beta^2\overline{q^2+Q^2}]\cdot\cos 2\boldsymbol{Q}\cdot\boldsymbol{\alpha})\,\mathrm{d}^3\boldsymbol{Q}\,\mathrm{d}^3\boldsymbol{q}\,.$$

Performing the integrations over $\boldsymbol{q}$ and the angular variables of $\boldsymbol{Q}$

$$P_{n0} = \frac{16\pi e^4}{v^2} \int \frac{|\varepsilon_n(Q)|^2}{[Q^2 - \omega_{n0}^2]^2} \left[1 - \exp\left[-\beta^2 Q^2\right] J_0\left(2\alpha \sqrt{Q^2 - \frac{\omega_{n0}}{v^2}}\right)\right] Q \, \mathrm{d}Q \,. \tag{3.20}$$

The integral over $\mathrm{d}Q$ is now restricted thus,

$$P_{n0} = \int_{Q_{\min}}^{Q_{\max}} P_{n0}(Q) \, \mathrm{d}Q \,. \tag{3.21}$$

$Q_{\min}$ is obtained from energy conservation, which requires

$$Q_{\min} = \frac{\omega_{n0}}{v} \,. \tag{3.22}$$

The value of $Q_{\max}$, the maximum momentum transfer allowed, is fixed by other criteria, which we shall discuss later.

Now we have

$$-\mathrm{d}E = N \, \mathrm{d}t \sum_n \omega_{n0} \int_{Q_{\min}}^{Q_{\max}} P_{n0}(Q) \, \mathrm{d}Q \,, \tag{3.23}$$

$$-\frac{\mathrm{d}E}{\mathrm{d}t} = \frac{16\pi N e^4}{v^2} \sum_n \omega_{n0} \int_{Q_{\min}}^{Q_{\max}} Q \, \mathrm{d}Q \, \frac{|\varepsilon_n(Q)|^2}{[Q^2 - \omega_{n0}^2]^2} \cdot \left[1 - \exp\left[-\beta^2 Q^2\right] J_0\left(2\alpha \sqrt{Q^2 - \frac{\omega_{n0}^2}{v^2}}\right)\right] . \tag{3.24}$$

Let us introduce a change of variable from Q to x, where

$$\begin{cases} x^2 = Q^2 - \dfrac{\omega_{n0}^2}{v^2} \,, & x_{\min} = 0 \,, \\ |\varepsilon_n'(x)|^2 = |\varepsilon_n(Q)|^2 \,, & x_{\max} \doteq Q_{\max} \,. \end{cases} \tag{3.25}$$

Then (3.24) becomes

$$-\frac{\mathrm{d}E}{\mathrm{d}t} = \frac{16\pi N e^4}{v^2} \sum_n \omega_{n0} \int_0^{x_{\max}} x \, \mathrm{d}x \, \frac{|\varepsilon_n'(x)|^2}{[x^2 + (\omega_{n0}^2 / v^2 \gamma^2)]^2} \cdot \left[1 - \exp\left[-\beta^2 \left(x^2 + \frac{\omega_{n0}^2}{v^2}\right)\right] J_0(2\alpha x)\right] , \qquad \gamma^{-2} = 1 - v^2 . \tag{3.26}$$

We shall refer to the two additive parts of (3.26) as the normal and suppression terms.

Let us now divide the region of integration over x into three regions, the boundaries being at values x_1 and x_2 defined from the following considerations. Let us call the integrals over the three regions I_1, I_2, I_3, with the normal suppression terms in each denoted by primed or twice-primed quantities. In the first region, up to x_1 we shall take into account the term $\omega_{n0}^2/v^2\gamma^2$ in the denominator of the integrand, but we wish to expand both $|\varepsilon_n'(x)|^2$ and the suppression factor in this region. Thus we require

$$\left\{\begin{array}{l} \omega_{n0} \ll x_1 \ll e^2 m\ ,\ \beta^{-1}\ ,\ \alpha^{-1}\ , \\ \therefore\quad \beta,\ \alpha \ll 1/e^4 m \sim 10^{-5}\ \text{cm}\ . \end{array}\right. \tag{3.27}$$

We can do the calculation with the less stringent condition

$$\frac{\omega_{n0}}{\gamma} \ll x_1 \ll e^2 m,\ \beta^{-1},\ \alpha^{-1}\ , \tag{3.28}$$

but (3.27) admits the range of α, β where suppression is important, so we shall be content with that, and examine the approach to normal ionization with increasing α, β later.

With this restriction on x_1 we can write from (3.12)

$$|\varepsilon_n'(x)|^2 = |r_{0n}|^2 \cdot \left(x^2 + \frac{\omega_{n0}^2}{v^2\gamma^4}\right)\ , \tag{3.29}$$

where $|r_{0n}|^2$ is the square of the modulus of the dipole moment between the two atomic states.

Substituting (3.29) we find

$$I_1' = \frac{8\pi N e^4}{v^2} \sum_n \omega_{n0} |r_{n0}|^2 \cdot \left[\log \frac{x_1^2}{\omega_{n0}^2/v^2\gamma^2} - v^2\right] \tag{3.30}$$

but ([8])

$$\sum_n \omega_{n0}^2 |r_{n0}|^2 = \frac{1}{2m}\ , \tag{3.31a}$$

$$\sum_n \omega_{n0}^2 |r_{n0}|^2 \log \omega_{n0}^2 = \frac{1}{2m} \log b^2 \left(\frac{e^4 m}{2}\right)^2\ , \tag{3.31b}$$

where b is a constant ~ 1, hence

$$I_1' = \frac{4\pi N e^4}{m v^2} \left[\log \frac{x_1^2 v^2 \gamma^2}{b^2 (e^4 m/2)^2} - v^2\right]\ , \tag{3.32}$$

similarly,

$$(3.33)\quad I_1'' = I_1' - \frac{4\pi N e^4}{m v^2} \cdot \left[(\beta^2+\alpha^2)x_1^2 + c^2\frac{(e^4m)^2}{2} - v^2\beta^2 \log \frac{x_1^2 v^2\gamma^2}{d^2(e^4m/2)^2} - \beta^2 v^2 c^2\,(e^4m/2)^2\right],$$

(c, d are numbers of order unity). From the definition of x_1 and the restriction on α, β it is clear that there is negligible contribution from this region because

$$\beta e^4 m \ll 1\,,$$

so that

$$I_1 = I_1' - I_1'' \ll I_1'\,.$$

For $x_1 < x < x_2$, from (3.27)

$$(3.34)\qquad I_2' = \frac{16\pi N e^4}{v^2} \sum_n \omega_{n0} \int_{x_1}^{x_2} \frac{|\varepsilon_n(x)|^2}{x^3}\,\mathrm{d}x \cdot (1 - \exp[-\beta^2 x^2] J_0(2\alpha x)\,.$$

We can now reverse the order of summation and integration and use the closure relation

$$(3.31c)\qquad \sum_n \omega_{n0} |\varepsilon_n(x)|^2 = \frac{\mathscr{H}^2}{2m}\,,$$

from which we see

$$(3.35)\qquad I_2' = \frac{4\pi N e^4}{m v^2} \log \frac{x_2^2}{x_1^2}\,.$$

For our present purpose we shall assume that either

$$(3.36)\qquad \beta x_2 \gg 1 \qquad \text{or} \qquad \alpha x_2 \gg 1\,,$$

when we can replace the upper limit of I_2'' by ∞. (This does not introduce any serious error, because $\beta Q_{\max} \gg 1$ is always satisfied, and only a small error is introduced by using the form (3.37) of the suppression term over the range of Q from $Q_2 \to Q_{\max}$ so that

$$(3.37)\qquad I_2'' + I_3'' = \frac{8\pi N e^4}{m v^2} \int_{x_1}^{\infty} \frac{\exp[-\beta^2 x^2] J_0(2\alpha x)}{x}\,\mathrm{d}x\,,$$

which, on integration, gives

$$(3.38)\qquad I_2'' + I_3'' = \frac{4\pi N e^4}{m v^2}\left[-Ei(-\beta^2 x_1^2) + Ei\left(-\frac{\alpha^2}{\beta^2}\right) - \log\frac{\Gamma\alpha^2}{\beta^2}\right],$$

where Γ is Euler's constant.

Combining (3.33) and (3.38), we find

$$I'' = \frac{4\pi N e^4}{mv^2}\left|\log\frac{4v^2\gamma^2}{\Gamma^2 b^2 (e^4 m)^2 \alpha^2} + Ei\left(-\frac{\alpha^2}{\beta^2}\right) - v^2\right|. \tag{3.39}$$

The evaluation of I_3, in which suppression is unimportant, is straightforward. The region is characterized by the energy transfer and the momentum transfer once again becoming comparable, as the relativistic effects become important. Also

$$|\varepsilon_k(\boldsymbol{Q})|^2 \doteq \delta(\boldsymbol{Q} - \boldsymbol{k}) \tag{3.40}$$

in this region. This yields

$$I_3' = \frac{4\pi N e^4}{mv^2}\int_{T_2}^{T_{\max}}\frac{\mathrm{d}T}{T}$$

as long as $T_{\max} \ll E_0$, therefore

$$I_3' = \frac{4\pi N e^4}{mv^2}\log\frac{2mT_{\max}}{x_2^2} \tag{3.41}$$

so that

$$I' = \frac{4\pi N e^4}{mv^2}\left[\log\frac{8mT_{\max}v^2\gamma^2}{b^2(e^4 m)} - v^2\right], \tag{3.42}$$

which is the well-known result of Moller, and

$$-\frac{\mathrm{d}E}{\mathrm{d}t} = \frac{4\pi N e^4}{mv^2}\left[\log 2mT_{\max}\Gamma^2\alpha^2 - E_i\left(-\frac{\alpha^2}{\beta^2}\right)\right]. \tag{3.43}$$

It is well-known that $T_{\max}$ is not the kinematic maximum energy transfer, $E_0/2$, as we do not want the true mean of an infinite number of collisions but the most probable energy loss in traversing a small thickness of material. So we must exclude these very improbable collisions with large energy transfer by taking a lower value of $T_{\max}$. It is this that allows us to neglect exchange effects. The logarithmic dependence on $T_{\max}$ makes the exact value unimportant and correspondingly undetermined, but it is around 1 MeV in normal cases. This, however, is one of the cases where the ionization and grain density need further consideration, as the more energetic electrons ejected from atoms of the medium dissipate their energy far away from the track, so that different criteria are needed. The upper limit to energy transfer for the calculation of grain density is that energy for which the electron will just stop

in the grain in which it is produced. This is normally given as about 5 keV ([10]).

The result (3.43) agrees with the classical calculation of YEKUTIELI ([11]) in the case ($\beta \to 0$) of point charges. We shall consider the reasons for this in Sect. **4**. We should note, from (3.19), that the suppression depends on the separation perpendicular to the direction of motion only, as long as $\omega_{n0}\alpha_z/v \ll 1$, which is normally the case. This condition is equivalent to requiring that the time between the impulses from negaton and positon reaching the atom be small compared to an atomic period.

We now examine the approach to normal ionization, removing our restriction on α. To ensure simple analytical expressions, we shall assume that $\beta \ll \alpha$, so that the electrons of the pair are restricted to a region small compared to their separation. The localizing effect of the position measurement implicit in ionization, makes this plausible. Now we allow α to increase without limit, and are particularly interested in values of

$$\alpha \gg \frac{1}{e^2 m} .$$

Then we can write the suppression term as

$$I'' = \frac{16\pi N e^4}{v^2} \sum_n \omega_{n0} |r_{n0}|^2 \int_0^\infty x \, \mathrm{d}x \left[\frac{J_0(2\alpha x)}{x^2 + (\omega_{n0}^2/v^2\gamma^2)} - \frac{\omega_{n0}^2}{\gamma^2} \frac{J_0(2\alpha x)}{[x^2 + (\omega_{n0}^2/v^2\gamma^2)^2]} \right] . \tag{3.44}$$

Hence

$$I'' = \frac{16\pi N e^4}{v^2} \sum_n \omega_{n0} |r_{n0}|^2 \left[K_0\left(\frac{2\alpha\omega_{n0}}{v\gamma}\right) - \frac{\omega_{n0}^2}{\gamma^2} \cdot \frac{2\alpha}{\omega_{n0}/v\gamma} K_1\left(\frac{2\alpha\omega_{n0}}{v\gamma}\right) \right] , \tag{3.45}$$

where K_0, K_1 are Hankel functions of imaginary argument, iz which tend to zero, as $(\pi/2z)^{\frac{1}{2}} e^{-z}$, for arguments greater than ~ 1. Their forms for small arguments are

$$K_0(z) \doteqdot -\log \frac{\Gamma z}{2} , \qquad K_1(z) \doteqdot \frac{1}{z} . \tag{3.46}$$

We see that when $\alpha\omega_{n0}/v\gamma \ll 1$, we recover the form (3.39) with $\beta \ll \alpha$ for $1''$. When z increases so that this condition ceases to hold, I'' tends towards zero like

$$I'' = \frac{8\pi N e^4}{m v^2} \cdot K_0\left(\frac{2b' e^4 m \alpha}{v\gamma}\right) , \tag{3.47}$$

([10]) P. BUDINI: *Nuovo Cimento*, **10**, 236 (1955).

([11]) A. E. ČUDAKOV: *Izv. Acad. Nauk USSR*, **19**, 651 (1955); G. YEKUTIELI: *Nuovo Cimento*, **5**, 1381 (1957).

(where b' is a number of order unity.) The density effect (see Sect. **4**) modifies this result in practice, giving a more rapid approach to normal ionization.

4. – The approximations and their correction.

We have already discussed the use of Born approximation in the calculation, the adequacy of the wave packet (2.4) as a representation of the pair (we shall discuss this in Sect. **5**, but should note here the insensitivity of the ionization to the detailed shape of the packet) and the question of the relation between energy loss and grain density.

An approximation arose in (3.17), when we neglected the difference in the initial momenta of negaton and positon. From (3.16) we see that the minimum values of the denominators of the two terms occur for different values of the vector $\boldsymbol{Q}$, corresponding to the initial directions of the two particles respectively, and that these minimum values are $\omega_{n0}^2/v_1^2\gamma_1^2$ and $\omega_{n0}^2/v_2^2\gamma_2^2$. Thus for $|\boldsymbol{Q}-\boldsymbol{Q}_{\min}|\sim\omega_{n0}/v\gamma$ the two terms are no longer equal and there will be only partial cancellation. The rate of energy loss has a logarithmic form and receives equal contribution from each order of magnitude of momentum transfer: the suppression effect removes the contribution from momenta less than $1/\beta$, $\varkappa$ except for the above contribution from the order of the smallest momentum transfers, which we have neglected in (3.17). The density effect provides further justification for this.

We have so far been concerned with the effect of the pair on the atoms of the medium without any consideration of the influence that the presence of other atoms may have upon this. This is important in the high energy region, not because of its influence on the ionization by the pair but because it reduces that of a single particle, with which the former is compared, by reducing the ionizing power of the particle at large distances. As this is a problem, not connected with the suppression effect itself, and one which has been extensively discussed ([12]), it is not necessary to do so further here, except to remark that it is just from those most distant collisions that the contribution due to the difference of the initial momenta of the negaton and positon arise. We may therefore feel justified in neglecting this. We must, of course, include the principal effect of the momentum difference, namely, the increase of α and β with the distance travelled.

Finally, let us look at the limitations of the classical approach to this problem to understand how it gives (3.43) for the ionization; we shall use arguments like those of WILLIAMS ([13]) for the ionization of a single particle. As in that

([12]) E. FERMI: *Phys. Rev.*, **57**, 485 (1940); R. M. STERNHEIMER: *Phys. Rev.*, **88**, 851 (1953); D. A. TIDMAN: *Nuclear Physics*, **2**, 289 (1956).

([13]) E. J. WILLIAMS: *Rev. Mod. Phys.*, **17**, 217 (1945).

case, we have a situation in which classical mechanics is not valid because the interaction is too weak to give a well-defined angle of scattering for a wave packet; but again, because we have basically a Coulomb interaction, which gives the same scattering in both classical and Born approximation limits, the classical answer has the right form.

However, in neither case are there pure Coulomb interaction. The deviations from this are not given correctly classically and we must understand their effect. In the single particle case, they take the form of cut-offs, at impact parameters ϱ_{max} and ϱ_{min}, due respectively to the binding of the atomic electron, which does not then respond to a slowly varying field, and to the maximum energy transfer already discussed. In the pair problem ϱ_{max} can be taken as proportional to the separation α, because, as we have seen in (3.33), the contribution from the dipole region, which is not given correctly classically, is negligible. Because different parts of the field contribute differently in the classical and quantum limits, there is a different relation between impact parameters and momentum transfer, so that

$$[2mT_{max}]^{\frac{1}{2}} = \frac{e^2}{v\varrho_{min}^{c}} = \frac{\hbar}{\varrho_{min}^{q}}, \tag{4.1}$$

which makes the classical expression for the energy loss too large; an *ad hoc* correction is usually made for this, and this is the same in single particle or pair ionization. ϱ_{max} is given directly as a distance in both problems, collision time and impact parameter being uniquely connected, so that no correction which is different in the two cases, is needed. So if the same correction as for the single particle ionization is used, the pair ionization is correctly given classically. The effect of the interaction on the pair will be considered in the next section.

5. – The dependence of ionization on the primary photon energy.

It has already been remarked that the principal practical importance of this effect lies in the possibility of using it to determine the energy of the pair and of the primary photon which produced it. Therefore, in this section we shall see how much information we can get, from the ionization measurements, about the photon energy, E_0. This will also raise some question of fundamental interest as to the nature of the measurements involved, and its effect on the pair.

We must first look at the distribution of the negaton and positon from the pair production process with particular reference to their relative po-

sition ([7]). The most probable angle of divergence of the pair, θ_p, is given by

$$\theta_P = \frac{2m}{E_0} \cdot \varphi_Z(a) \,, \tag{5.1}$$

where $\varphi_Z(a)$ is a function of a, with only very slight dependence on E_0 and Z, the atomic number of the atom in the field of which the pair was produced; a is the energy partition ratio.

It is not, as we have said, possible to fit this distribution exactly, with the wave packet, which we have chosen to represent the pair. In choosing the form of the wave packet, we required, not only that it be susceptible to mathematical handling, but that it could represent a fair range of circumstances, of which those pertaining near the origin of the pair were only one. We obtain a reasonable fit to the distribution ([7]) (5.1) with our wave packet (2.5), if we take parameters α, β with values

$$\alpha = 0 \,, \qquad \beta = \frac{2m}{E_0} t \,, \tag{5.2}$$

where we have here neglected any effects of earlier interactions, and assume that the separation is proportional to the distance t. The main deviation of this from the actual distribution is that the cut-off at higher angles is too sharp.

Substituting (5.2) in (3.43), we obtain an expression for the mean ionization rate, in terms of the energy of the primary photon.

$$-\frac{\mathrm{d}E}{\mathrm{d}t} = \frac{4\pi N e^4}{mv^2} \log \frac{8m^3 T_{\max} \Gamma t^2}{E_0^2} \,. \tag{5.3}$$

We must now consider the limitations on the accuracy of this method of measuring the primary photon energy, both for one track and for the mean of a number of tracks. We cannot increase our knowledge indefinitely by observing a sufficiently long length of track, not only because the electrons are diverging and for practical reasons, but fundamentally, because each ionization alters the wave packet, so that it contains less information about the primary photon.

The classical view treats each pair as having a well-defined angle of divergence, which will differ for different pairs of the same energy, which are represented quantally by the same wave packet. Thus the fluctuations in ionization from track to track of such pairs would seem to be overestimated by a classical treatment. As a measure of this effect, we calculate, both classically and quantally, the difference between the mean probability of two atoms being excited and the square of the ionization probability for a single atom.

The classical expression for the rate of ionization has the form

$$I = -\frac{\mathrm{d}E}{\mathrm{d}t} = \frac{4\pi N e^4}{mv^2} \log 2mT_{\max} I^2 r^2 , \tag{5.4}$$

which corresponds to a pair of point charges separated by distance r (put $\beta = 0$, $\boldsymbol{\alpha} = \boldsymbol{r}$ in (3.43)). The mean fluctuation in two collisions over a distribution in $\boldsymbol{r}$, $F(\boldsymbol{r})$, for the pairs, is

$$\sigma_c^2 = \overline{I^2} - \overline{I}^2 \tag{5.5}$$

where, if $\xi = \int F(\boldsymbol{r}) \log (r^2/\beta^2)\,\mathrm{d}r$, $\eta = \int F(\boldsymbol{r}) \log^2 (r^2/\beta^2)$:

$$\sigma_c^2 = \left[\frac{4\pi N e^4}{mv^2}\right]^2 \cdot \{\eta - \xi^2\}. \tag{5.6}$$

To make a comparison with the quantum result, we must take a distribution of $\boldsymbol{r}$ corresponding to that in our wave packet. It is implicitly assumed in classical derivations, and is clear from the above, that the suppression is normally sensitive only to separation of the pair perpendicular to the line of motion. We must therefore average over a distribution in a plane equivalent to our wave packet. We shall choose $F(\boldsymbol{r})$ of the form (5.2) (with $\boldsymbol{\alpha} = 0$) so that averaging over angles

$$F(r) = 2r \exp\left[-\frac{r^2}{\beta^2}\right], \tag{5.7}$$

$$\sigma_c^2 = \left[\frac{4\pi N e^4}{mv^2}\right]^2 \frac{\pi^2}{6} . \tag{5.8}$$

The validity of this result depends on that of (5.6) for I. We have already discussed the limitations that this places on β. In the limits of both very large and very small β, the ionization ceases to depend on β and the correlation vanishes as we should expect. We note that σ_c is otherwise independent of β.

For the quantum correlation, we calculate the probability of excitation of two atoms to definite levels. We again use lowest order Born approximation and the calculation proceeds in a similar way to Sect. 3. For comparison, we shall stress the analogy with the simple product of single excitation probabilities.

Let us now use $\boldsymbol{P}$, $\boldsymbol{P}''$, $\boldsymbol{P}'$ to represent the initial, intermediate and final momenta of the centre of mass, and similarly for other quantities. Let us call the co-ordinates of the pair, $\boldsymbol{R}'$, $\boldsymbol{r}'$ when referred to the nucleus of the second atom, which is at a position $\boldsymbol{A}$ from the first. The two electrons have co-ordi-

nates $\boldsymbol{r}_0$, $\boldsymbol{r}_0'$ respectively. We let $\boldsymbol{Q}' = \boldsymbol{P} - \boldsymbol{P}''$ etc. We want first the matrix element for the excitation of one atom to state n, the second atom to state m, using the same incident wave packet as before, and plane waves for the intermediate find final states. We shall treat the simple case $\theta = 0$ from the start. The distance A is assumed to be large compared to the size of the zones of interaction, so that we can neglect the effect of one atom on the other, or their simultaneous effect on the pair.

To preserve the similarity to the product of the separate probabilities mentioned above we shall evaluate the sum over intermediate states first, that is, we perform the integrations with respect to $\boldsymbol{P}''$, $\boldsymbol{p}''$ before the other integrations, as only these variables couple the two halves of the matrix elements. The characteristic of the energy denominator is that it will only contain non-trivially one of the particle momenta, that relating, to the particle scattered in the first interaction. It is thus preferable to evaluate these integrations in terms of $\boldsymbol{P}_1''$, $\boldsymbol{P}_2''$, the individual particle variables, and to transform later to the centre of mass and relative system, which is suitable for describing the suppression effect. In these co-ordinates, the matrix element has the form

$$(5.9)\qquad M_{n\,m,00}^{(2)} = \frac{\beta_2^3 e^4}{\pi^4 (2\pi)^{12} (2\pi^2)^2} \cdot$$

$$\cdot \int \exp\left| -\frac{\beta^2}{2} k^2 + i\left[\overline{\boldsymbol{P}_1 + \frac{\boldsymbol{k}}{2} - \boldsymbol{P}_1''}\cdot\boldsymbol{R}_1 + \boldsymbol{P}_2 - \frac{\boldsymbol{k}}{2} - \boldsymbol{P}_2''\cdot\boldsymbol{R}_2 - \boldsymbol{k}\cdot\boldsymbol{\alpha}\right]\right| \cdot$$

$$\cdot \varphi_n^*(\boldsymbol{r}_0)\varphi_0(\boldsymbol{r}_0)\,\bar{u}_n\gamma'^{\mu}_0 u_0 \left\{\frac{\exp\left[i\boldsymbol{l}\cdot\overline{\boldsymbol{R}_1 - \boldsymbol{r}_0}\right]\cdot\bar{u}_1''\gamma_1^{\mu}u_1 - \exp\left[i\boldsymbol{l}\cdot\overline{\boldsymbol{R}_2 - \boldsymbol{r}_0}\right]\cdot\bar{u}_2''\gamma_2^{\mu}u_2}{l^2 - \omega_{n0}^2}\right\} \frac{1}{E - E'' + i\varepsilon} \cdot$$

$$\cdot \left\{\frac{\exp\left[i\boldsymbol{l}'\cdot\overline{\boldsymbol{R}_1' - \boldsymbol{r}_0'}\right]\bar{u}_1'\gamma_1^{\nu}u_1'' - \exp\left[i\boldsymbol{l}'\cdot\overline{\boldsymbol{R}_2' - \boldsymbol{r}_0'}\right]\bar{u}_2'\gamma_2^{\nu}u_2''}{l'^2 - \omega_{n0}}\right\} \varphi_m^*(\boldsymbol{r}_0')\varphi_0(\boldsymbol{r}_0')\,\bar{u}_m'\gamma_0'^{\nu}u_0' \cdot$$

$$\cdot \exp\left[i(\boldsymbol{P}_1'' - \boldsymbol{P}_1'\cdot\boldsymbol{R}_1' + \overline{\boldsymbol{A}} + \overline{\boldsymbol{P}_2'' - \boldsymbol{P}_2'\cdot\boldsymbol{R}_2' + \boldsymbol{A}})\right] \mathrm{d}^3\boldsymbol{R}_1\,\mathrm{d}^3\boldsymbol{R}_2\,\mathrm{d}^3\boldsymbol{R}_1'\,\mathrm{d}^3\boldsymbol{R}_2'\,\mathrm{d}^3\boldsymbol{r}_0\,\mathrm{d}^3\boldsymbol{r}_0' \cdot$$

$$\cdot \mathrm{d}^3\boldsymbol{l}\,\mathrm{d}^3\boldsymbol{l}'\,\mathrm{d}^3\boldsymbol{k}\,\mathrm{d}^3\boldsymbol{P}_1''\,\mathrm{d}_1^3\boldsymbol{P}_2'' ,$$

We treat the two terms in the first half of the matrix element separately. In the first, in which the electron is scattered, we perform the trivial integral over $\boldsymbol{R}_2$ which gives $(2\pi)^3\delta(\boldsymbol{Q}_2' - \boldsymbol{k}/2)$. We then integrate $\mathrm{d}^3\boldsymbol{Q}_2'$, which ensures that only $\boldsymbol{P}_1$, $\boldsymbol{P}_1''$ enter the energy denominator. We can now consider the integral over $\boldsymbol{P}_1''$

$$(5.10)\qquad A = \int \frac{\exp\left[i\boldsymbol{P}_1''\cdot(\boldsymbol{A} + \boldsymbol{R}_1' - \boldsymbol{R}_1)\right]}{E - E'' + ie}\,\mathrm{d}^3\boldsymbol{P}_1'' .$$

The energy E'' does not depend on the direction of $\boldsymbol{P}_1''$, so that the angular

integration gives

$$A = \frac{4\pi}{|\boldsymbol{A}+\boldsymbol{R}_1'-\boldsymbol{R}_1|}\int_0^\infty \frac{\sin\left(P_1''|\boldsymbol{A}+\boldsymbol{R}_1-\boldsymbol{R}_1'|\right)}{E-E''+i\varepsilon}\,P_1''\,\mathrm{d}P_1'' . \tag{5.11}$$

By contour integration, we find

$$A = \frac{4\pi^2}{B}\,\frac{P_1^0}{v}\cdot\exp\left[iBP_1^0\right], \tag{5.12}$$

where $P_1^0 = |\boldsymbol{P}_1+\boldsymbol{k}/2| - (\omega_{n0}/v)$ and $B = |\boldsymbol{A}+\boldsymbol{R}_1'-\boldsymbol{R}_1|$. In the limit of large A, we may write

$$A = \frac{4\pi^2}{A}\,\frac{P_1^0}{v}\exp\left[i\boldsymbol{P}_1^0\cdot(\boldsymbol{A}+\boldsymbol{R}_1'-\boldsymbol{R}_1)\right], \qquad \boldsymbol{P}_1^0 = \frac{P_1^0}{M}\cdot\boldsymbol{A}. \tag{5.13}$$

An exactly similar calculation for the second term yields the same result for $\boldsymbol{P}_2''$ except that the $\boldsymbol{k}$ is replaced by $-\boldsymbol{k}$. We shall neglect the difference in magnitude between P_1^0 and P_2^0 in the multiplying factor (5.13). We shall discuss these approximations at the end of the calculation. Transforming to centre of mass and relative co-ordinates, we shall formally leave in the integration over $\boldsymbol{Q}'$, $\boldsymbol{q}'$, representing the effect of the sum over intermediate states, (5.13), by a δ-function. Integrating over the co-ordinate variables we find

$$\begin{aligned} M^{(2)}_{nm.00} = {} & \frac{8\beta_2^3 e^4}{\pi^2 v\pi^3}\,\frac{P^0}{A}\int\frac{\varepsilon_n(\boldsymbol{Q}')}{Q'^2-\omega_{n0}^2}\cdot\frac{\varepsilon_m(\boldsymbol{Q}-\boldsymbol{Q}')}{(\boldsymbol{Q}-\boldsymbol{Q}')^2-\omega_{m0}^2}\cdot \\ & \cdot\exp\left[i[\boldsymbol{Q}-\boldsymbol{Q}']\cdot\boldsymbol{A}-\boldsymbol{k}\cdot\boldsymbol{\alpha}\right]-\frac{\beta^2}{2}k^2\Big]\cdot \\ & \cdot[\delta(\boldsymbol{Q}'-\boldsymbol{q}'-\boldsymbol{k})\,\delta(\boldsymbol{Q}'+\boldsymbol{q}'+\boldsymbol{k}-\boldsymbol{s})-\delta(\boldsymbol{Q}'+\boldsymbol{q}'+\boldsymbol{k})\,\delta(\boldsymbol{Q}'-\boldsymbol{q}'-\boldsymbol{k}-\boldsymbol{s})]\cdot \\ & \cdot[\delta(\boldsymbol{Q}-\boldsymbol{Q}'-\boldsymbol{q}+\boldsymbol{q}')-\delta(\boldsymbol{Q}-\boldsymbol{Q}'+\boldsymbol{q}-\boldsymbol{q}')]\cdot\mathrm{d}^3\boldsymbol{Q}'\,\mathrm{d}^3\boldsymbol{q}'\,\mathrm{d}^3\boldsymbol{k}\,, \end{aligned} \tag{5.14}$$

where

$$\boldsymbol{s} = 2\left(\frac{\omega_{n0}}{v}\hat{\boldsymbol{z}}-\frac{P^0}{A}\boldsymbol{A}_\perp\right), \qquad \boldsymbol{A}_\perp = \boldsymbol{A}-(\boldsymbol{A}\cdot\hat{\boldsymbol{z}})\hat{\boldsymbol{z}}\,. \tag{5.15}$$

Integrating $\mathrm{d}^3\boldsymbol{q}'$, $\mathrm{d}^3\boldsymbol{k}$, $\mathrm{d}^3\boldsymbol{Q}'$ yields, putting $\boldsymbol{s}=2\boldsymbol{\sigma}$, $\boldsymbol{Q}-\boldsymbol{\sigma}=\boldsymbol{\tau}$,

$$\begin{aligned} M^{(2)}_{nm.00} = {} & \frac{e^4}{\pi^2\cdot v}\cdot\frac{P^0}{A}\cdot\exp\left[i\boldsymbol{\tau}\cdot\boldsymbol{A}\right]\frac{\varepsilon_n(\boldsymbol{\sigma})}{\sigma^2-\omega_{n0}^2}\cdot\frac{\varepsilon_m(\boldsymbol{\tau})}{\tau^2-\omega_{m0}^2}\cdot \\ & \cdot\left[F(\boldsymbol{\tau}+\boldsymbol{\sigma}-\boldsymbol{q})-F(\boldsymbol{\tau}-\boldsymbol{\sigma}-\boldsymbol{q})-F(-\boldsymbol{\tau}+\boldsymbol{\sigma}-\boldsymbol{q})+F(-\boldsymbol{\tau}-\boldsymbol{\sigma}-\boldsymbol{q})\right], \end{aligned} \tag{5.16}$$

where

$$F(\boldsymbol{k}) = \frac{\beta_2^3}{\pi^3}\exp\left[-\frac{\beta^2}{2}k^2-i\boldsymbol{k}\cdot\boldsymbol{\alpha}\right]. \tag{5.17}$$

Now

$$P^{(2)}_{nm.00} = \frac{(2\pi)^4}{r} \int \left| M^{(2)}_{nm.00} \right|^2 \delta(E' - E)\, \mathrm{d}^3\boldsymbol{q}\, \mathrm{d}^3\boldsymbol{Q}\,. \tag{5.18}$$

We sum over all second atoms by multiplying by N and integrating $\mathrm{d}^3\boldsymbol{A}$ over the appropriate volume. The sum over first atoms gives a factor $N\,\mathrm{d}t$ as in (3.1). By (5.15), it is clear that $(P^{02}/A^2)\,\mathrm{d}A_x\,\mathrm{d}A_y = \mathrm{d}\sigma_x\,\mathrm{d}\sigma_y$ while $\int \mathrm{d}A_z = \mathrm{d}t$ since, in our approximation, $M^{(2)}_{n\,n.00}$ is otherwise independent of A_z.

Let us now look at the form of the suppression factor, $G^{(2)}$, say with (5.17) for $F(\boldsymbol{k})$, then

$$\begin{aligned} G^{(2)} = \frac{\beta^3}{\pi^3} \Big\{ & \exp\left[-\frac{\beta^2}{2} (\boldsymbol{\tau} + \boldsymbol{\sigma} - \boldsymbol{q})^2 - i(\boldsymbol{\tau} + \boldsymbol{\sigma} - \boldsymbol{q})\boldsymbol{\alpha} \right] - \\ & - \exp\left[-\frac{\beta^2}{2} (\boldsymbol{\tau} - \boldsymbol{\sigma} - \boldsymbol{q})^2 - i(\boldsymbol{\tau} - \boldsymbol{\sigma} - \boldsymbol{q})\cdot\boldsymbol{\alpha} \right] - \\ & - \exp\left[-\frac{\beta^2}{2} (-\boldsymbol{\tau} + \boldsymbol{\sigma} - \boldsymbol{q})^2 - i(-\boldsymbol{\tau} - \boldsymbol{\sigma} - \boldsymbol{q})\cdot\boldsymbol{\alpha} \right] + \\ & + \exp\left[-\frac{\beta^2}{2} (-\boldsymbol{\tau} - \boldsymbol{\sigma} - \boldsymbol{q})^2 - i(-\boldsymbol{\tau} - \boldsymbol{\sigma} - \boldsymbol{q})\cdot\boldsymbol{\alpha} \right] \Big\}\,. \end{aligned} \tag{5.19}$$

In (5.17), $\boldsymbol{q}$ only enters in the suppression factor $G^{(2)}$, so let us first evaluate

$$\begin{aligned} \overline{G^{2(2)}} &= \int |G^{(2)}|^2\, \mathrm{d}^3\boldsymbol{q} = \\ &= 4\Big\{ 1 - \exp\left[-\beta^2\tau^2\right] \cos 2\boldsymbol{\tau}\cdot\boldsymbol{\alpha} - \exp\left[-\beta^2\sigma^2\right] \cos 2\boldsymbol{\sigma}\cdot\boldsymbol{\alpha} + \\ &+ \frac{\exp\left[-\beta^2\overline{\boldsymbol{\sigma} + \boldsymbol{\tau}}^2\right]}{2} \cos 2\overline{\boldsymbol{\sigma} + \boldsymbol{\tau}}\cdot\boldsymbol{\alpha} + \frac{\exp\left[-\beta^2\overline{\boldsymbol{\sigma} - \boldsymbol{\tau}}^2\right]}{2} \cos 2\overline{\boldsymbol{\sigma} - \boldsymbol{\tau}}\cdot\boldsymbol{\alpha} \Big\}\,. \end{aligned} \tag{5.20a}$$

Whereas, the product of suppression factor for the separate ionization probabilities is, from (3.19)

$$\begin{aligned} \overline{G^{2(11)}} = 4\Big\{ & 1 - \exp\left[-\beta^2\tau^2\right] \cos 2\boldsymbol{\tau}\cdot\boldsymbol{\alpha} - \exp\left[-\beta^2\sigma^2\right] \cos 2\boldsymbol{\sigma}\cdot\boldsymbol{\alpha} + \\ & + \frac{\exp\left[-\beta^2\overline{\sigma^2 + \tau^2}\right]}{2} \left(\cos 2\overline{\boldsymbol{\sigma} + \boldsymbol{\tau}}\cdot\boldsymbol{\alpha} + \cos 2\overline{\boldsymbol{\sigma} - \boldsymbol{\tau}}\cdot\boldsymbol{\alpha} \right) \Big\}, \end{aligned} \tag{5.20b}$$

the expressions being otherwise equivalent. So that the difference in the suppression factors is

$$\begin{aligned} \overline{\Delta G^2} = 2 \exp\left[-\beta^2\overline{\sigma^2 + \tau^2}\right] \cdot \\ \cdot \Big\{ \left(\exp\left[-2\beta^2\boldsymbol{\sigma}\cdot\boldsymbol{\tau}\right] - 1\right) \cos 2\overline{\boldsymbol{\sigma} + \boldsymbol{\tau}}\cdot\boldsymbol{\alpha} + \left(\exp\left[+2\beta^2\boldsymbol{\sigma}\cdot\boldsymbol{\tau}\right] - 1\right) \cos 2\overline{\boldsymbol{\sigma} - \boldsymbol{\tau}}\cdot\boldsymbol{\alpha} \Big\}. \end{aligned} \tag{5.21}$$

The transition probability can then be written

$$(5.22)\quad P^{(2)}_{nm.00} = \left[\frac{2N\,\mathrm{d}t\,e^4}{v_z^3}\right]^2 \cdot \int \overline{G^2}\,\frac{|\varepsilon_n(\sigma)|^2 v}{[\sigma^2-\omega_{n0}^2]^2}\,\delta(\boldsymbol{\sigma}\cdot\boldsymbol{v}-\omega_{n0})\,\frac{|\varepsilon_m(\tau)|^2}{[\tau^2-\omega_{mn}^2]^2}\,\delta(\boldsymbol{\tau}\cdot\boldsymbol{v}-\omega_{m0})\,\mathrm{d}^3\boldsymbol{\sigma}\,\mathrm{d}^3\boldsymbol{\tau}\,,$$

since from (5.15), $\mathrm{d}\sigma_x\,\mathrm{d}\sigma_y = v\,\delta(\boldsymbol{\sigma}\cdot\boldsymbol{v}-\omega_{n0})\,\mathrm{d}^3\boldsymbol{\sigma}$.

The rate of energy loss in the two planes is now given by

$$(5.23)\quad I^{(2)} = \frac{1}{(\mathrm{d}t)^2}\sum_{n,m}\omega_{n0}\omega_{m0}P^{(2)}_{nm.00}\,.$$

In the simple cases, first when $\alpha=\beta=\infty$, $\overline{G^{2(2)}}=4$ and there is no suppression or correlation. If $\beta=0$, $\overline{G^{2(2)}}$ has the form (5.20*b*) of the product of separate probabilities (cf. (3.19)). This corresponds to a wave packet of δ-function form which, therefore, has very large momentum components which will be unaffected by the momentum transfers in the collision. In both these cases

$$\overline{I^{(2)}} = \overline{I}^2 \qquad \text{and} \qquad \sigma_Q^2 = \overline{I^{(2)}} - \overline{I}^2 = 0\,,$$

which corresponds to the exactly similar classical result.

Looking once again at the general case,

$$(5.24)\quad \sigma_Q^2 = \left[\frac{4Ne^4}{v}\right]\int \frac{|\varepsilon_n(\sigma)|^2}{[\sigma^2-\omega_{n0}^2]^2}\cdot\frac{|\varepsilon_m(\tau)|^2}{[\tau^2-\omega_{m0}^2]^2}\cdot\delta(\boldsymbol{\sigma}\cdot\boldsymbol{v}-\omega_{n0})\,\delta(\boldsymbol{\tau}\cdot\boldsymbol{v}-\omega_{m0})\cdot$$

$$\cdot 2\exp[-\beta^2\sigma^2+\tau^2]\big\{(\exp[-2\beta^2\boldsymbol{\sigma}\cdot\boldsymbol{\tau}]-1)\cos 2\boldsymbol{\sigma}+\boldsymbol{\tau}\cdot\boldsymbol{\alpha}+$$

$$+(\exp[+2\beta^2\boldsymbol{\sigma}\cdot\boldsymbol{\tau}]-1)\cos 2\boldsymbol{\sigma}-\boldsymbol{\tau}\cdot\boldsymbol{\alpha}\big\}\mathrm{d}^3\boldsymbol{\sigma}\,\mathrm{d}^3\boldsymbol{\tau}\,.$$

From this, we see that in both limits, of small σ, τ when suppression is complete, and of large σ, τ where it is unimportant, this correlation term is small, but there will be a contribution from the intervening region, which we shall evaluate in the case $\boldsymbol{\alpha}=0$. This will give the largest correlation, and corresponds to the classical case we have taken; and to (5.2). As values of σ, $\tau \lesssim \beta^{-1}$ do not contribute, we can neglect ω_{n0} and ω_{m0} with respect to σ, τ, when the restrictions (3.27) are satisfied. Then summing over n and integrating

$$(5.25)\quad \sigma_Q^2 = \frac{4Ne^4}{mv^2}\int_{\sigma_{\min}\cdot\tau_{\min}}^{\sigma_{\max}\cdot\tau_{\max}}\frac{\mathrm{d}\sigma}{\sigma}\cdot\frac{\mathrm{d}\tau}{\tau}\exp[-\beta^2\overline{\sigma^2+\tau^2}]\cosh 2\beta^2\boldsymbol{\sigma}\cdot\boldsymbol{\tau}\,\mathrm{d}\psi_\tau\,\mathrm{d}\psi_\sigma\,.$$

Both $\boldsymbol{\sigma}$ and $\boldsymbol{\tau}$ are essentially restricted to the xy plane by energy conservation so $\boldsymbol{\sigma}\cdot\boldsymbol{\tau} = \sigma\tau\cdot\cos(\psi_\tau - \psi_\sigma)$. In view of the above, we can replace the lower limit by zero, and as long as $\beta\sigma_{\max} \gg 1$, we can replace the upper limits by ∞. Performing the integrations we find

$$\sigma_Q^2 = \left[\frac{4\pi N e^4}{mv^2}\right]\frac{\pi^2}{6}\,. \tag{5.26}$$

So with the approximations we have made, the correct correlation is equal to the classical value over the first two ionizations. The absolute magnitude of the correlation is given by

$$\delta^2 = \frac{\sigma^2}{I^2} \sim 10^{-2} \tag{5.27}$$

in typical circumstances. It represents the contribution of one order of magnitude ($\sim\beta$) of the range of momentum transfer.

This result means that as the pair travels through the medium, the wave packet is changed, by an amount δ in the first interaction. These changes are random, so that after $\tilde{N} \sim 1/\delta^2$ such interactions, the wave packet will be determined largely by these interactions and will have lost its original form, corresponding to the primary photon energy E_0. These multiple scatterings are statistical and will vary from track to track. Also, after $\tilde{N}$ observations the ionization will be determined to an accuracy

$$I(\tilde{N}) = \sum_i \frac{I_i}{\tilde{N}} \pm \frac{I(\tilde{N})}{\sqrt{\tilde{N}}} \sim I(\tilde{N}) \pm \delta I(\tilde{N})\,. \tag{5.28}$$

With the logarithmic form of the ionization probability this corresponds to a separation $r \sim \beta \pm \beta$ so that just at that point where the accuracy of observation is becoming sufficient to detect the fluctuations that the classical picture predicts, we find such fluctuations arising in the quantum point of view, from the perturbing effects of the measuring interactions. This is the normal statistical limitation to quantal measurements with an error less than the width of the distribution in the wave packet, but arising in an experiment where the accuracy and perturbation of each individual measurement is small so that the limitation only becomes obvious over many interactions. By the usual arguments, the mean of the measurements on many tracks may have greater accuracy.

In all the above we have neglected the effect of the relative motion of the

pair between collisions, except to discuss how we may allow for the effect of a non-zero angle of divergence. In principle, however, the random momentum transfer in an ionization will lead to alterations in this angle, and therefore will affect the separation of the pair over a finite distance. This effect of the multiple scattering of the pair, was excluded from our quantum correlation calculation when we made the approximation ((5.13) and after) that the intermediate momenta were parallel to $\boldsymbol{A}$. This was consistent, in that the motion in the intermediate state has an effect dependent on A, the separation of the atoms, which is present, but was not included in the classical picture. It is clear also, from our consideration of the motion of the wave packet, that the changes caused by the scattering in a single collision are small compared to the natural spreading of the packet. We shall discuss this further in the next section, only remarking here that this is a quantum mechanical process and if included in both correlation calculations would have given a small difference between the two.

6. – The application to experiment.

The considerations of the last section are related to the understanding of an idealized experiment, in which the position of the individual ionized atoms is observed. We must extend the argument of Sect. 5 to the case where, for practical reasons, we do not extract all the information which it contains from the first section of the track, where $t < \tilde{t}$, say, the distance at which multiple scattering becomes important.

We have now very much poorer statistical information about the photon energy E_0 from this section, and must obtain any extra information that we can from the region, beyond $\tilde{t}$, where the form of the pair is largely determined by its previous interactions. The final accuracy of such an experiment cannot equal that of the idealized experiment of Sect. 5, but will be better than we get in practice from looking at $t < \tilde{t}$ only. Because of the random nature of the scattering process, the distribution for $t > \tilde{t}$ is not now a unique function of E_0 for all tracks, but is a classical statistical distribution of incoherent wave packets whose separation is given by theory of multiple scattering ([14]) and is of the form

$$P(\alpha)\,\mathrm{d}\alpha = \frac{1}{\lambda^2}\exp\left[-\frac{\alpha^2}{2\lambda^2}\right]\alpha\,\mathrm{d}\alpha\,, \tag{6.1}$$

where $\lambda^2 = \mu^2 t^3/E_0^2$, where μ is a constant for the medium. We see from this

([14]) W. D. Scott: *Phys. Rev.*, **76**, 212 (1949).

that $\tilde{t}$, which is given by

$$\left(\frac{2m}{E_0}\right)^2 \tilde{t}^2 = \frac{\mu^2}{E_0^2}\tilde{t}^3 , \tag{6.2}$$

is a constant for the medium independent of energy. This region, $t > \tilde{t}$, is therefore characterized by the spread of the incoherent distribution being large compared to that of the individual coherent component wave packet, so that we have really the quasi-classical situation, and can again average the ionization over that distribution. The distribution itself is not correctly given classically in close analogy to the discussion of Sect. **4** ([13]). Applying our result (3.43), with $\beta \ll \alpha$, we obtain the result of YEKUTIELI. Making the usual generalization of (3.42) to complex atoms and including the density effect, with the parameters of Budini ([11]) for a typical nuclear emulsion we find

$$R = \frac{|\mathrm{d}E\ \mathrm{d}t|_{\alpha,\beta,E_0}}{|\mathrm{d}E_{,}\,\mathrm{d}t|_{\infty,E_0}} = \frac{\log 2m\,T_{\max}\,\Gamma^2\alpha^2 - Ei(-\alpha^2/\beta^2)}{\log(2m\,T_{\max}/\omega\sqrt{\Delta}) - v^2} . \tag{6.3}$$

where $\omega = (4\pi Ne^2/m) = 9.05\cdot 10^{-9}\ \mathrm{m}^2$, $\Delta \sim 1$, $T_{\max} = 5\ \mathrm{keV}$. In the region $t < \tilde{t}$, this has the form

$$R = 3.45 + .357\,(\log_{10} t - \log_{10} E_0) , \tag{6.4}$$

while for $t > \tilde{t}$, averaging α over the appropriate distribution

$$\bar{R} = 3.49 + .357\,(\log_{10} t - \log_{10} E_0) - .077\,5\,Ei\left(-\frac{.021}{t}\right) , \tag{6.5}$$

where E_0 is in MeV, t in cm.

In the original experiment of PERKINS ([2]), the mean ionization of six pairs was measured. Their energies were between 80 and 400 GeV, with a mean about 180 GeV (strictly the geometric mean should be taken). In Table I his results are compared with the theoretical prediction for 180 GeV, from (6.4).

TABLE I.

t (microns)	R (experiment)	R (theory)
15	$.52 \pm .09$	.56
50	$.81 \pm .08$	.75
100	$.78 \pm .08$	.85
200	$.92 \pm .06$	.92

In the experiment of WOLTER and MIĘSOWICZ ([3]), the track of a single pair of somewhat higher energy is measured and the mean ionization over the first 200 μm and the next 1240 μm is recorded. Averaging (6.5) over a distance d cm, from the origin, we obtain

$$(6.6) \qquad R = 3.49 + 0.357\,(\log_{10} d - 0.434 - \log_{10} E_0) - 0.077\,5 \cdot \cdot \left[\left(1 + \frac{.021}{d}\right) Ei\left(-\frac{.021}{d}\right) + \exp\left(-\frac{.021}{d}\right)\right].$$

In Table II we give the results of WOLTER and MIĘSOWICZ and the most probably energies, from (6.6), of the pair.

TABLE II.

t (μm)	R (experiment)	E_0 (GeV)
0-260	.66 $\pm$ .69	$\sim$ 900
260-1500	.93 $\pm$ .05	$\sim$ 1000

Experimental measurement of the energy from the subsequent behaviour of the shower is in accord with these values.

It should be observed that these results are, in only the roughest way, a verification of the theory. Most laborious experiments, involving the measurement in other ways of the energies of numerous pairs of very high energy would be needed to provide an accurate test of the theory. The theory seems to involve no arbitrary assumptions, however, and such experimental verification is not essential.

(6.5) and (6.6) offer a simple method of measuring the mean energy of such pairs, or of obtaining a rough value for the energy of a single pair. They are of course, restricted to the region where the logarithmic dependence on separation is valid, which confines us to the region where

$$(6.7) \qquad 10^{-9}\ \text{cm} \sim \frac{1}{Q_{\max}} < \alpha < \frac{1}{Q_{\min}} \sim 10^{-6}\ \text{cm}\,.$$

Outside these regions, the considerations we discussed at the end of Sect. 3 must be included, but the limitations on accuracy are such that no useful information can be derived. In view of these restrictions (6.7), we shall not attempt to give numerical or graphical tables for the general case.

* * *

My thanks are due to Dr. D. H. PERKINS for suggesting this problem and to Dr. R. H. DALITZ for many helpful discussions. I should especially like to thank Professor R. E. PEIERLS for guidance and stimulation throughout this work. I am grateful for the financial support of the D.S.I.R.

RIASSUNTO (*)

PERKINS ha trovato che coppie di elettroni di altissime energie (circa 10^{11} eV) hanno vicino alla loro origine un potere ionizzante ridotto. La ragione di ciò sta nel fatto che l'angolo fra le due traiettorie è molto piccolo cosicchè lungo cammini di lunghezza apprezzabile i membri della coppia si mantengono abbastanza accostati perchè i loro campi elettrici si annullino reciprocamente quasi completamente, eccetto per atomi assai prossimi alla linea di volo. Il presente lavoro presenta un trattamento quantistico di tale effetto e si trova che le deviazioni dal risultato semiclassico sono trascurabili, ad onta del fatto che le condizioni generali per la validità della meccanica classica non sono soddisfatte. Il fenomeno può essere sfruttato per stimare l'energia della coppia. Si discutono le limitazioni, fondamentali e pratiche, del metodo.

(*) *Traduzione a cura della Redazione.*

Hemispherical Distribution of Cosmic Rays at 25° Geomagnetic Latitude.

P. S. Gill and A. N. Mitra

Department of Physics, Muslim University - Aligarh

(ricevuto il 7 Aprile 1958)

Summary. — A complete investigation has been made of the angular distribution (over various zeniths and azimuths) of the hard component of cosmic rays at the Gulmarg High Altitude Research Observatory (Geomagnetic latitude 24.7° N). The azimuth distribution is found to agree closely with an energy law $E^{-1.80}\mathrm{d}E$ for all the zenith angles. The zenithal distribution is found to be a cosine power law in which the index « n » varies regularly with azimuth. A sinusoidal dependence of « n » on azimuth has also been obtained by the method of least squares.

1. – Introduction.

The study of directional distribution of cosmic ray particles has for long been a fascinating subject of research particularly because of its bearing on the nature and composition of primary cosmic ray particles. This subject got its impetus since the development by Lemaire and Vallarta [1] of Störmer's theory of the motion of charged particles in the earth's magnetic field to apply to cosmic ray particles. The theory in its essentials depends on two simple facts, 1) deflection of charged particles in the earth's magnetic field and 2) the role of Liouville's theorem in determining the intensity at any point on the earth. The earth's magnetic field deflects charged particles of the same energy to different extents depending on the latitude under consideration, the deflection being much larger at the equator than near the poles. Further at a given point on the earth, particles of smaller energies are bent away from

[1] G. Lemaitre and M. S. Vallarta: *Phys. Rev.*, **50**, 493 (1936).

their original paths much more than those of higher energies, so much so, that a certain minimum energy is required for each particle coming in a certain direction with respect to the earth, to reach the latter at all. Thus at each point on the earth, there is a definite *range* of directions such that a particle having an energy higher than a certain minimum value and direction falling within that range is able to reach the earth. This range of directions forms the so-called « allowed cone » which represents the dividing line between particles « acceptable » to a particular point on the earth and those which are not. The intensity at any point can now be calculated simply from a straight-forward application of Liouville's theorem according to which the intensity in any « allowed direction » (in the presence of a magnetic field) is the *same* as would exist in its absence, assuming that the distribution at large distances from the earth is homogeneous and isotropic. In other words, the intensity in an allowed direction is the same as that at infinity, and that in a « forbidden » direction is strictly zero. Now the « allowed cone » was further analyzed by LEMAITRE and VALLARTA into two parts, 1) the « main cone » within which all directions are allowed, and 2) the « shadow cone » outside which all directions are forbidden. There is thus implied a region between these cones which roughly plays the role of the so-called « penumbra », in analogy with the phenomenon of solar eclipses. The « penumbral » region varies with latitude, being almost negligible near the equator, and almost the entire allowed region at high latitudes. Intermediate latitudes (10° to 40°) therefore provide a convenient region for studying the specific penumbral effects which are characterized by a series of « humps » in the azimuthal curves. Theoretical investigations of the structure of the penumbra have been made by SHREMP [2] and particularly by HUTNER [3] who solved the differential equations for the motion of cosmic ray particles by means of a differential analyser.

The earliest experimental investigations on the subject were confined to measurements of east-west asymmetries in the intensities of incident cosmic ray particles at different places on the earth by a large number of workers. All these experiments showed that the intensity from the west was greater than from the east. Now it may be noted that the « allowed cone » opens from the western horizon for positively charged particles and from the eastern horizon in the opposite case. Thus the results on east-west asymmetry indicated broadly that the primary cosmic rays were mostly positively charged particles. The possibility of a more quantitative determination of the charge composition of primary cosmic rays soon came into prominence when in 1939 VALLARTA [4] pointed out that a detailed experimental study of the variation

---

[2] E. J. SHREMP: *Phys. Rev.*, **54**, 153 (1938).
[3] R. A. HUTNER: *Phys. Rev.*, **55**, 15, 614 (1939).
[4] M. S. VALLARTA: *Rev. Mod. Phys.*, **11**, 239 (1939).

of cosmic ray intensity with azimuth for fixed zenith angles (in other words, the specific « penumbral » effects) could be used to provide extensive information on the charge of the primaries. This fact was recognized by GILL in 1941 ([5]) who performed the desired experiment at Lahore (22° N. G. Lat.) at a zenith angle of 60°. The experimental azimuthal curve obtained by him showed the characteristic, penumbral effects in the north-west quandrant, in good agreement with Hutner's theoretical curve calculated on the assumption of positively charged primaries (protons). Later in 1947 VALLARTA *et al.* ([6]) carried out a similar experiment in Mexico City (29° N G Lat.) and obtained similar results. They could, in addition, determine the differential energy spectrum of the primaries which they found to be in agreement with Gill's Lahore data and the result was as follows:

$$F(E)\,\mathrm{d}E = K\,\mathrm{d}E/E^{1.45}\,.$$

Experiments of this nature have, during the years, been carried out by a number of other workers at different places on the earth. However, the data are rather scattered and inadequate in so far as no detailed investigation of the variation with *both* zenith and azimuth at a particular place has yet been available. It may be claimed that any determination of the charge composition of primary cosmic rays in the above manner is considerably obscured by the effects of the earth's atmosphere which undergoes many complex interactions with these particles, so that the laboratory instruments are prevented from detecting the more direct radiation. In fact, it is precisely with the object of avoiding such uncertainties that the tendency in recent times has been to send out these detecting instruments high up in the air by mean of balloon flights, so as to minimize the atmospheric effects. Such experiments certainly provide a much more reliable information about the charge composition of the primaries. Even this fact does not completely do away with the usefulness of carrying out such experiments in the laboratory at least for two reasons. Firstly, the atmospheric path is constant for a given zenith angle, so that at least some of the atmospheric effects which depend on its *depth* remain *constant.* Secondly, the accuracy of such measurements depends largely on whether they can be carried out over rather long periods of time, and in this respect the laboratory conditions are much more favourable than those obtaining in balloon flights. Moreover, the definitions of (Z, A) orientations of the detecting instruments in balloon flights are much more uncertain than those of corresponding instruments in the laboratory.

([5]) P. S. GILL: *Proc. Nat. Inst. Sci. India*, **9**, 251 (1943); *Phys. Rev.*, **67**, 347 (1945); and subsequent papers.

([6]) M. S. VALLARTA *et al.*: *Phys. Rev.*, **71**, 393 (1947).

It was therefore thought worthwhile carrying out a complete and accurate set of measurements of the variation of cosmic ray intensity (hard component) with zenith and azimuth, using the facilities of the Gulmarg High Altitude Research Observatory. The purpose of the investigation was essentially to study the results of these measurements in a systematic way with a view to 1) correlating them with the existing information and 2) making a quantitative analysis of the intensity as a function of the zenith and azimuth, as existing at the latitude of Gulmarg.

2. – Apparatus and measurements.

The experimental set up consisted of 11 triple coincidence telescopes, one being kept always vertical and the others being symmetrically arranged in the same plate at zenith angles of 15°, 30°, 45°, 60° and 75° on either side of the vertical. Each counter telescope was calibrated with the vertical one for the purpose of combining the data. The five telescopes on one side constituted set I and the other five formed set II. Each telescope has 10.2 cm of lead so as to filter out the soft component. The solid angle range covered by each telescope was 10° to 50°.

Set I was regularly interchanged with set II by rotation through 180 degrees, to facilitate comparison of the intensities from opposite directions for each zenith. The azimuths were changed by steps of 15° each time. In this manner twenty four different azimuths were covered for each zenith. The systematic working of the telescopes was checked daily over the period from July '55 to October '55.

For the analysis the data of the two sets were combined. The statistical error of the data discussed is not more than 2% for $Z = 15°$, 30°, 45° and 60°, and not more than 10% for $Z = 75°$. Even taking account of the geometry the over-all error is not more than twice the above values.

The details of the apparatus used are given elsewhere (7).

3. – Analysis of the data.

The cosmic ray intensity at a point in a certain direction defined by the azimuth A and zenith Z is given by

$$I(Z, A) = \int_{E(Z,A)}^{\infty} F(E)\,\mathrm{d}E\,, \tag{1}$$

(7) T. H. Naqvi: *Ph. D. Thesis*, Aligarh University (1956), unpublished. Also *Proc. Nat. Acad. Sci., India* (to be published).

where $F(E)\,\mathrm{d}E$ is the energy spectrum of the primary cosmic rays and $E(Z, A)$ is the minimum energy required by the particle to reach the point of observation in the direction (Z, A) and which, in addition, depends on the location and extension of the penumbral bands at the altitude of the point of observation. The numerical values of $E(Z, A)$ may be obtained brom Shremp's curves ([2]) showing the variation of energy with azimuth at different zeniths and latitudes.

For the energy spectrum we have used the function

$$F(E)\,\mathrm{d}E = \frac{k}{E^c}\,\mathrm{d}E\,, \tag{2}$$

which, with $c = 1.45$, agrees with the earlier results of GILL ([5]) and VALLARTA *et al.* ([6]).

Next, the geomagnetic co-ordinates (Λ, Φ) of a point may be calculated in terms of its geographic co-ordinates (λ, φ) and those of the geomagnetic pole (λ_0, φ_0) in accordance with the formulae ([8])

$$\left\{\begin{array}{l} \mathrm{tg}\,\Phi = -\,\mathrm{tg}\,(\varphi - \varphi_0)\,\sin x\,\sec(x + \lambda_0)\,, \\ \mathrm{tg}\,\Lambda = \quad \cos\Phi\,\mathrm{tg}\,(x + \lambda_0)\,, \end{array}\right. \tag{3}$$

where

$$\mathrm{tg}\,x = \cos(\varphi - \varphi_0)\,\cot\lambda\,. \tag{4}$$

Now the accepted values of λ_0 and φ_0 are (*)

$$\lambda_0 = 78.5^\circ\,\mathrm{N}\,, \qquad \varphi_0 = 291^\circ\,\mathrm{E}\,.$$

Also, the geographic co-ordinates of Gulmarg are

$$\lambda = 34.1^\circ\,\mathrm{N}\,, \qquad \varphi = 74.4^\circ\,\mathrm{E}\,.$$

Substitution of these values in (3) and (4) gives for Gulmarg

$$\Lambda = 24.7^\circ\,\mathrm{N}\,, \qquad \Phi = 327^\circ\,\mathrm{E}\,. \tag{5}$$

(*) These values are supposed to be altered when extremely high altitudes attained in balloon flights are involved. See a recent paper by R. E. DANIELSON and P. S. FREIER: *Phys. Rev.*, **109**, 151 (1958).

([8]) MCNISH: *Journ. Terrestrial Mag.*, **6**, 37 (1947).

One finds from (5) that the geomagnetic latitude of Gulmarg is very close to 25°, which is fortunate since one set of Shremp's curves is available at just 25° latitude, so that no interpolation is necessary (see Fig. 1).

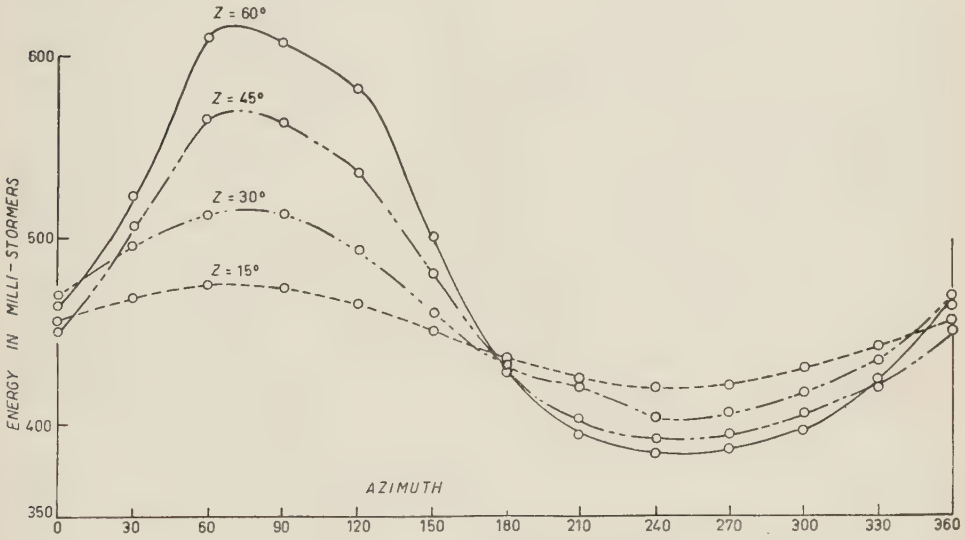

Fig. 1. – Shremp's curves showing the variation of $E(Z, A)$ with azimuth for the zenith angles 15°, 30°, 45° and 75°, at geomagnetic latitude 25° N.

The data are analysed as follows. First, the curves showing the variation of intensity with azimuth for different zenith angles are discussed in relation to the theoretical predictions. Now since at a fixed zenith, the atmospheric length remains constant, and the change in the intensity of cosmic rays arises only through the variation of $E(Z, A)$ with A, it is clear that the azimuthal survey is expected to bring out just the effect of $E(Z, A)$ on the intensity. Next, the observed percentage asymmetries in different azimuthal planes are compared with the calculated values derived from (1) and (2). Finally, the zenithal distribution of intensity for different azimuths is investigated and a simple cosine power law sought for it. The variation of the index with azimuth is also discussed in some detail.

3·1. *Azimuthal distribution.* – Fig. 2 represents the intensity curves as functions of the azimuth for the zenith angles 15°, 30°, 45° and 60°. The one for 75° zenith is not so accurate on account of the statistical errors arising out of a relatively small number of counts, and is accordingly not shown in Fig. 2. The same variation is shown in a different way on a circular graph in Fig. 3 in which the intensity and the azimuth are represented in polar

co-ordinates. For an easy comparison of the variations for the different zenith angles, the intensities for all the zenith angles are normalized to 100 (arbitrary units) in the direction of the polar axis which is taken in the northern direction.

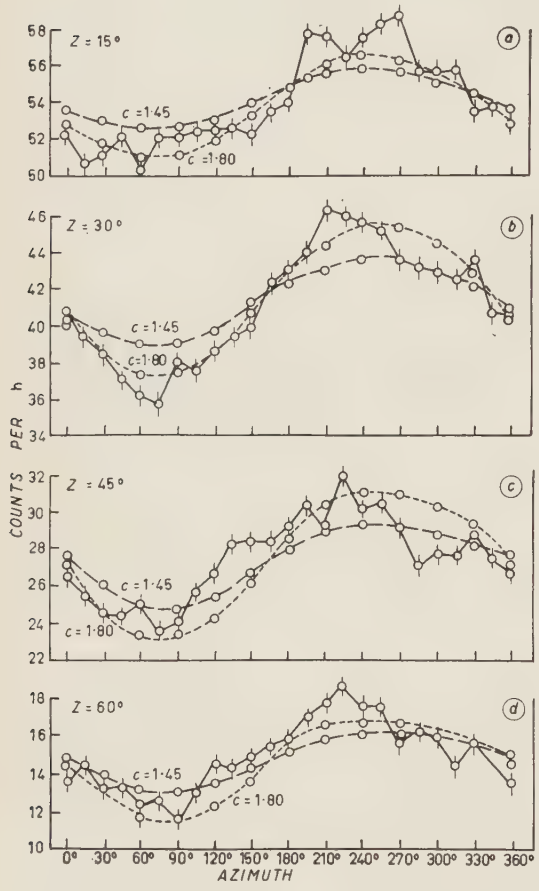

Fig. 2. – Azimuthal variation of intensity for different zenith angles. The solid curves represent the experimental variations. The calculated variations of intensity with azimuth are represented by the dotted and dashed curves corresponding to the exponents $c = 1.80$ and $c = 1.45$ respectively.

From Fig. 2 it is seen that the general trend of the variation of intensity with azimuth is nearly the same for all zenith angles. Also, as expected from the theory of positively charged particles, the intensity shows a minimum near the east and a maximum near the west. More specifically the intensity shows minima in the azimuthal range $60° \div 90°$ (north-east quadrant), the position of the minimum gradually shifting towards the east with increase in zenith angle. The maximum intensity is found to occur in the south-west quadrant, though no simple trend for the gradual shifting of the maximum with increasing zenith angle is discernible, unlike the case of the minimum intensity. This is mostly because of the « penumbral effects » which, according to Hutner's calculations ([3]), manifest themselves in the form of prominent humps in the north-western quadrant in the case of positively charged particles. Moreover, these effects are most marked for smaller zenith angles, say up to 30°, which fact agrees with the results of Figs. 2 and 3, the curves appearing much smoother for $Z = 45°$ and 60° than for $Z = 15°$ and 30°. However, by disentangling the penumbral effects, it is possible to get a clearer picture of the positions of maximum intensity for different zenith angles. For example for $Z = 15°$, one finds three maxima, *viz.* at $A = 210°$,

270° and 315°. The last two may be identified as due to penumbral effects, so that the true maximum occurs at $A \approx 210°$. Similarly, for $Z = 30°$ the true maximum occurs at $A \approx 210°$, the others being due to penumbral effects. Finally, the maxima for $Z = 45°$ and 60° occur at $A \approx 225°$. In this way, one again finds a tendency for the maximum to shift gradually (from south towards west) with increasing zenith angles. Fig. 3 does not of course provide any additional information regarding the various trends, but it at least serves to confirm the above conclusions by facilitating a more direct comparison between the different curves.

Fig. 3. – Variation of intensity with azimuth shown in polar co-ordinates (polar axis taken as the northern direction).

The above results at 60° zenith agree with those of Gill's Lahore data ($\Lambda = 22°$ N), allowing for the difference in Geomagnetic latitude. A theoretical comparison with the experimental curves in Fig. 2, has also been made assuming the primaries to be protons with a spectrum (2). Now the intensity from (1) and (2) is given by

$$I(Z, A) = \frac{k}{c - 1} [E(Z, A)]^{-c+1}, \tag{6}$$

where $E(Z, A)$ can be read off from Fig. 1. The values of $I(Z, A)$ obtained from (6) have been plotted in Fig. 2, for the two cases $c = 1.45$ and 1.80. A comparison shows that except for the fluctuations occurring in the S-W quadrant, agreement is obtained between the two sets, with $c = 1.80$ for all zenith angles except 60° in which case, the experimental curve lies between $c = 1.45$ and 1.80. Thus our investigation suggests an exponent $c = 1.80$ rather than $c = 1.45$ which gives too small fluctuations in the intensity, compared with experiment. This is not really a disagreement with the conclusions of Gill and Vallarta since their investigations had been carried out only

at $Z = 60°$ for which case the exponent 1.45 is not completely ruled out. This is still not the whole story, however. By assuming a certain percentage of heavier primaries (as is quantitatively indicated from balloon flight experiments with emulsion plates), even the lower exponent 1.45 is capable of explaining the experimental curves, since the effect of heavier primaries will be to increase the fluctuations in the curves, which is all that is needed to bring the theoretical curve up to the experimental ones. Our estimate in fact suggests that 85% protons and 15% heavy nuclei (mostly α-particles) can explain the observed curves, though the quantitative validity of these figures cannot be unambiguously established.

3·2. *East-West asymmetry.* – On account of the positive charge of the primaries the intensity in the western direction of a given azimuthal plane is higher than in the eastern direction. The percentage east-west asymmetry for a given azimuth A may thus be defined as

$$(7)\quad P = 200\left|\frac{I(Z, A+180°) - I(Z, A)}{I(Z, A+180°) + I(Z, A)}\right|$$

where P is positive for $0 < A < 180°$. The function P is plotted against A for the cases $Z = 15°$, 30°, 45°, 60° and 75° in Fig. 4, from which it is in fact seen that except for a few stray points the curves are entirely above the line $P = 0$. The maximum asymmetry is seen to occur in the plane $75° \div 255°$ for the zenith angles 30°, 45° and 60°; even for $Z = 15°$ this conclusion is valid if a smooth curve is drawn through the experimental points. Thus the plane of maximum asymmetry is not the east-west plane, but one inclin-

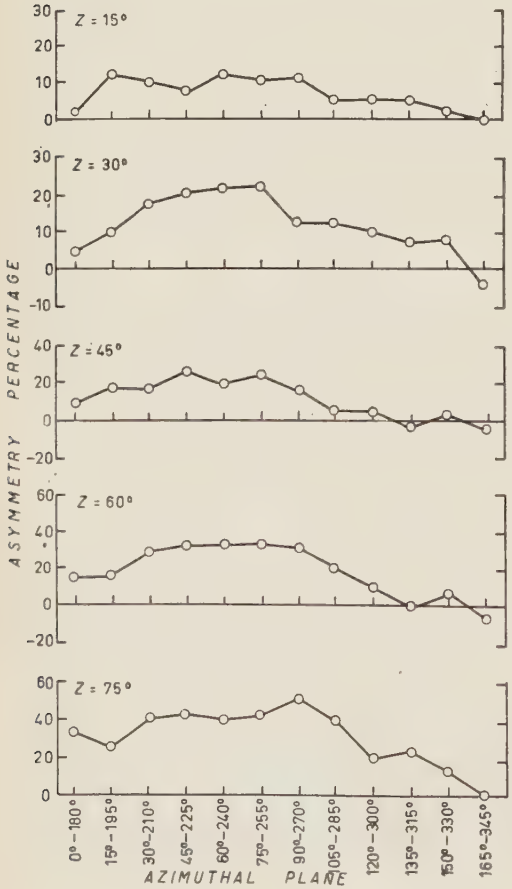

Fig. 4. Percentage east-west asymmetry vs. azimuthal plane for different zenith angles.

ed to it at an angle 15° « north of east » or « south of west ». This deviation seems to be established beyond the limits of experimental errors, though its precise significance needs quantitative investigation. A possible explanation which suggests itself is that the magnetic dipole does not quite pass through the centre of the earth unlike the assumptions of Lemaitre-Vallarta theory and the change so produced may well account for the above deviation from the east-west plane.

Theoretical calculations of the asymmetry have been made only for the east-west and north-south directions using equations (6) and (7) with $c = 1.80$ and $c = 1.45$. The results show that the observed asymmetries in these planes lie between those calculated with the above indices. The fact that the north-south asymmetry (calculated and observed) is also quite significant, provides a good check for the theory.

From Fig. 4 one also gets some idea of the variation of the asymmetry with zenith angle, for given azimuth. The main conclusion is that *at every azimuth* the asymmetry increases with zenith angle even up to 75°, without showing any sign of tapering off. Further the increase is faster in the east-west plane than in the north-south plane. Again the calculated asymmetry *vs.* zenith angle shows very similar trends.

3·3. *Zenithal distribution of intensity.* – In this section we investigate the inverse problem to that of Sect. 3·1, *viz.* the variation of intensity with zenith angle, the azimuth remaining the same. It must be remembered, however, that in this study, the effect of absorption in the atmosphere cannot be ignored as a constant overall factor (unlike the case in azimuthal study) since the length of the atmosphere (and hence its effect) is now dependent on the zenith angle (varying roughly like sec Z). Moreover, even at constant azimuth, the quantity $E(Z, A)$ depends rather sensitively on Z as an inspection of Fig. 1 suggests so that the effects of atmospheric absorption cannot be separated from the directional effects produced by the earth's magnetic field. However, a further inspection of Fig. 1 shows that the minimum energy $E(Z, A)$ *does not vary* with Z for two values of A, *viz.* $A = 0°$ (north) and $A = 180°$ (south), though the constancy of $E(Z, A)$ in the northern direction is not so pronounced on account of the contribution of the shadow cone. Thus, at least in the southern direction, the variation of intensity with zenith would reveal purely the effects of atmospheric absorption.

The zenithal distribution of intensity has been studied by a number of workers and most of them tried to fit a cosine power law to the intensity variations, obtaining indices varying roughly between 2 and 3. The disagreement in the values may be ascribed partly to the fact that the experiments were carried out at particular azimuths (mostly east-west and north-south) and partly to the different experimental arrangements used.

We have here carried out a straightforward analysis of the zenithal distribution for all azimuths without trying to make any comparison with the theory (on account of what has been said already about atmospheric absorption) and the results are shown in Fig. 5. For easy comparison, the curves for A and $A+180°$ have been drawn respectively on the left and right of the vertical from which it is seen that these curves are not quite symmetrical with respect to each other. This asymmetry is quite small for $A = 0°$ (north-south plane) as expected, but it increases gradually with A until it becomes a maximum at $A = 90°$, decreasing again with A in the range $90° < A < 180°$. Since a cosine power law is obviously suggested by the shape of the curves, we have tried to fit functions of the type

$$I_z = I_0 \cos^n Z \,, \tag{8}$$

to each of the 24 curves (12 on either side of the vertical) by the method of least squares. It has been found that for each curve, the best fit is obtained with two values of n, one valid in the range $0° < Z < 30°$ and the other in the range $30° < Z < 75°$. Further the values of n *are different for different azimuths.* Fig. 6 shows the variation of n with A in the form of two curves, valid respectively for $Z < 30°$ and $Z > 30°$. It is seen that n itself varies sinusoidally with A. This has been tested by a least square analysis according to which the variation is rather well represented

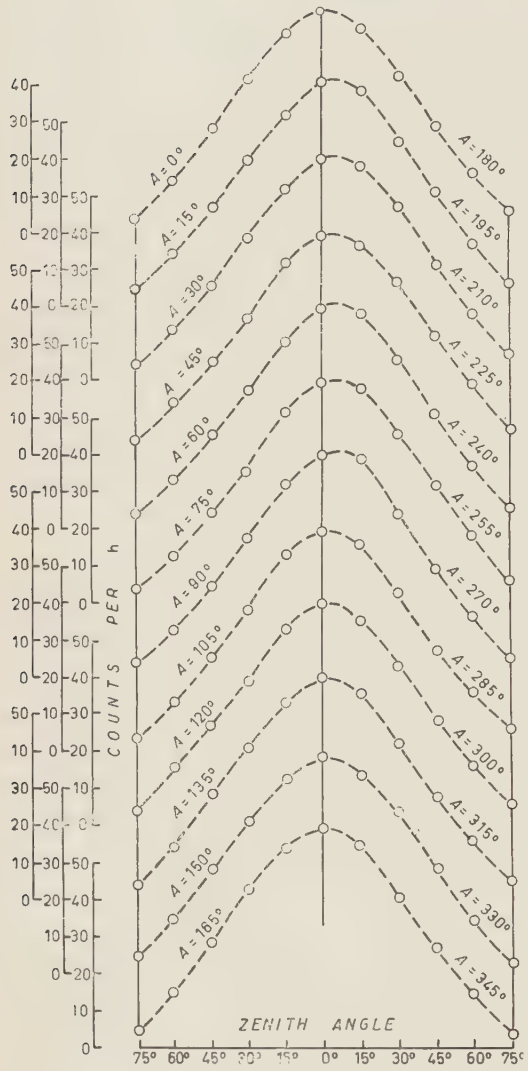

Fig. 5. – Variation of intensity with zenith angle for different azimuths. Curves for A and $A+180°$ are drawn on opposite sides of the line $Z=0$.

by a function of the form

$$n = n_0 + n_1 \cos A \,. \tag{9}$$

To values of the constants n_0 and n_1 for the two regions are (1) for $Z < 30°$ $n_0 = 2.64$, $n_1 = 0.20$ and 2) for $Z > 30°$, $n_0 = 1.80$, $n_1 = 0.06$. These figures show that the variation of n is quite marked for $Z < 30°$, but the exponent

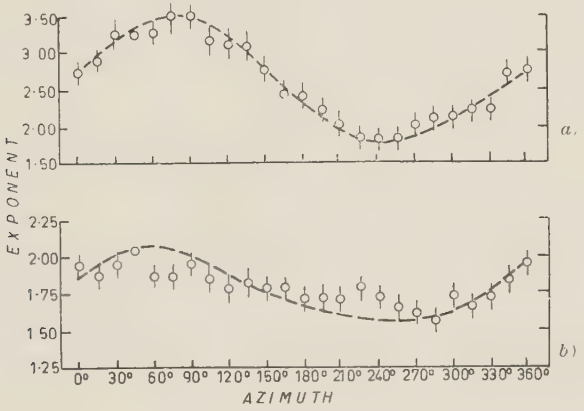

Fig. 6. – Variation with azimuth of the index n of the cosine power law in the zenithal distribution of intensity. Variations for $Z < 30°$ and $Z > 30°$ are shown by curves (a) and (b) respectively (on different scales).

is almost constant for higher zeniths. This is perhaps due to the fact that the atmospheric path length increases rather rapidly with zenith angle, so that the chances of the secondary particles preserving the direction of the primaries become much less for higher zeniths. This effect would tend to smear out the dependence of the exponent on the azimuth as the zenith angle increases.

RIASSUNTO (*)

Si è eseguita un'analisi completa della distribuzione angolare (su vari zenit ed azimut) della componente dura della radiazione cosmica all'Osservatorio di Alta Quota di Gulmarg (latitudine geomagnetica 24.7° N). La distribuzione azimutale si accorda strettamente, per tutti gli angoli zenitali con una legge $E^{-1.80}\,dE$. La distribuzione zenitale segue una legge in potenze del coseno in cui l'indice « n » varia regolarmente con l'azimut. Col metodo dei minimi quadrati si è anche ricavata una dipendenza sinusoidale di « n » dall'azimut.

(*) *Traduzione a cura della Redazione.*

IL NUOVO CIMENTO Vol. IX, N. 3 1° Agosto 1958

The Scattering of μ-Mesons in Lead and Copper.

W. F. Nash and A. J. Pointon

Physical Laboratories, University of Nottingham, England

(ricevuto il 7 Aprile 1958)

Summary. — The scattering distributions of μ-mesons in lead and copper have been investigated using a cloud chamber operated underground at a depth of 40 m w.e. At high momenta the observed scattering distributions are similar to those given by Molière for a « point » nucleus at large angles. It is shown that the results are consistent with a cross-section that varies as A^2 or Z^2 but not as Z or A.

1. – Introduction.

Recently a number of experiments (see Sect. **4**) have been performed to investigate the scattering of μ-mesons in various materials, the experiments being carried out either underground or under large thicknesses of absorbers to ensure that the cosmic ray beam was sensibly free from any high energy nuclear interacting particles. The angular distributions obtained have indicated the existence of a greater number of large-angle scatterings than would be expected on the basis of pure Coulomb effects. This excess of large angles has been termed « anomalous scattering ».

In the experiments reported here the scattering of μ-mesons has been measured in both lead and copper in order that the dependence of the large-angle scattering on the atomic number of the material could be investigated. The experimentally determined scattering distributions have been compared with the expected distributions obtained by averaging the various Coulomb theories (for different forms of the nuclear charge) over the momentum spectrum of the observed particles, suitably corrected for the geometrical bias of the apparatus. The experiment was carried out at a depth of 40 m w.e. and the bulk of the μ-mesons observed lay in the momentum range (0.5 ÷ 20) GeV/c and (0.7 ÷ 20) GeV/c according to the low momentum cut-off imposed by the apparatus.

A comparison has been made between the observed scattering and that expected on extreme models for the nuclear charge distributions, *viz.* OLBERT [1] for a « solid » nucleus of uniform charge density (U.N.M.) and MOLIÈRE [2] for a « point » nucleus. In the case where copper was used as the scattering material, a modified form of Olbert's theory given by LLOYD and WOLFENDALE [3] was also considered. This modified distribution is a more realistic estimate of the scattering and gives a somewhat greater probability of large angles occurring than does the Olbert distribution and it should be noticed that this increase in the case of lead would be only about one-third that in the case of copper.

2. – Experimental arrangement.

The experiment was performed in a cave situated beneath 19.85 m of sandstone rock, equivalent to 39.7 m of water. The surface of the rock was flat over that part covered by the solid angle of the counter telescope used.

The apparatus consisted of a cylindrical cloud chamber of diameter 28 cm and illuminated depth 8 cm, triggered by a threefold coincidence counter telescope as shown in Fig. 1. Between counter trays C_2 and C_3 was placed a thickness of lead, Σ, which gave a low momentum cut-off to the spectrum of the particles observed in the chamber.

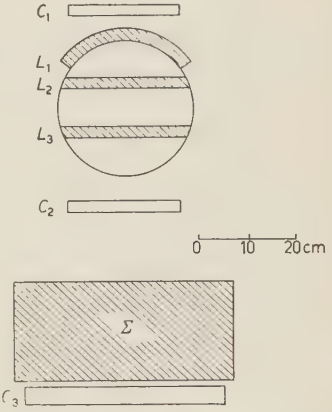

Fig. 1. – Experimental arrangement. C_1 C_2 C_3: counter trays; L_1 L_2 L_3 Σ: lead blocks.

Three separate arrangements were used in which the scattering material contained in the cloud chamber and the thickness of the absorber, Σ, were varied and the results have been grouped accordingly and termed Series I (Pb), Series II (Pb) and Series III (Cu). For Series I and II the scattering material consisted of two 2 cm lead plates placed symmetrically in the cloud chamber and Σ was 32.5 and 47.5 cm thick respectively. In Series III (Cu) the scattering material consisted of a single 5.8 cm thick copper plate placed at the centre of the chamber and Σ was again 47.5 cm.

The tracks were photographed stereoscopically by a camera with lens separation of 7 cm and situated 50 cm from the front plate of the chamber.

(1) S. OLBERT: *Phys. Rev.*, **87**, 319 (1952).
(2) G. MOLIÈRE: *Zeits. f. Naturfor.*, **2***a*, 133 (1948); **3***a*, 78 (1947).
(3) J. L. LLOYD and A. W. WOLFENDALE: *Proc. Phys. Soc.*, A **68**, 1045 (1955).

The projected angles of scatter of the μ-mesons in the scattering material were measured by projecting these photographs onto a circular protractor as described by McDiarmid [4], with such an arrangement that the angles of scatter could be measured with an accuracy of 0.1°.

To check whether any systematic errors existed in the measured angle of scattering the average of the deflections was taken for some 1 000 angles in each series, with the positive and negative directions chosen arbitrarily, and in no case was the error found to be larger than 0.06°. The effect of random errors or « noise level » scattering, which can be much larger than that due to systematic errors, will be discussed for each series separately.

In selecting tracks for measurement only those satisfying the following conditions were accepted:

1) There was little obvious distortion in the track.

2) The track must lie within the solid angle covered by the counter telescope.

3) The particle was not accompanied by any other penetrating particle since otherwise it might have been part of a shower of nuclear interacting particles or of momentum less than that set by Σ.

3. – Experimental results.

An important feature in the calculation of the expected form of the scattering distributions for various theories is a knowledge of the form of the momentum spectrum. An incorrect assumption as to the percentage of the

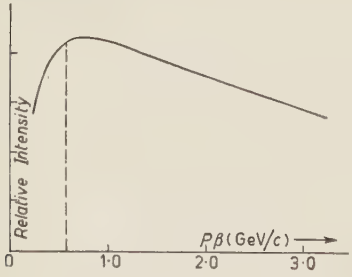

Fig. 2. – Underground spectrum corrected for scattering - Series I (lead).

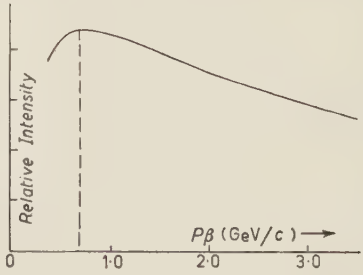

Fig. 3. – Underground spectrum - Series III (copper).

low energy component would either increase or decrease the expected number of large angles. The form of the momentum spectrum at low momenta has

(4) I. B. McDiarmid: *Phil. Mag.*, **45**, 933 (1954); **46**, 177 (1955).

been investigated (NASH and POINTON [5]; GEORGE and SHRIKANTIA [6]) and found to be in good agreement with that derived from the sea level data of HOLMES *et al.* assuming an average energy loss, in the rock, of 2.3 MeV/g/cm². The spectra used in this experiment to calculate the expected distributions for various scattering theories, for lead and copper, are given in Figs. 2 and 3 respectively. The results obtained are given below. All these curves have been corrected for loss of large angles due to geometrical consideration and angular variation of the incident radiation as outlined by COUSINS *et al.* [7].

3·1. *Series* I (Pb). – The total number of angles selected for measurement in this series was 4006 representing 2003 particles each traversing two 2 cm lead plates. The distribution of these angles is shown in integral form in Fig. 4. The curves shown for comparison are the theoretical distributions calculated for Olbert's theory with nuclear radius $= 1.2A^{\frac{1}{3}} \cdot 10^{-13}$ cm; and for Molière's theory for a point nucleus. The spectrum used in calculating these distributions was that given in Fig. 2, with a cut-off of 0.5 GeV/c imposed by the lead, Σ. One event was observed in this series in which the angle of scatter in one plate was 20°. The possibility that this event was a spurious association or a George type interaction could not be completely excluded, and it has not been included in the distribution shown in Fig. 4.

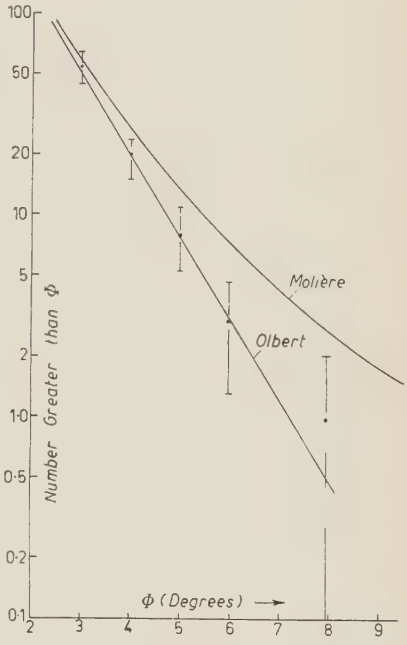

Fig. 4. – Scattering distribution - Series I (lead).

It will be seen that the experimental points are in good agreement with the distribution calculated using Olbert's theory and lie below the distribution calculated using Molière's theory.

3·2. *Series* II (Pb). – In this series a total of 4162 angles were selected for measurement and the distribution of these angles is shown in integral form in Fig. 5. The theoretical distributions were calculated as for Series I (Pb) but with a cut-off to the incident spectrum at 0.7 GeV/c.

(5) W. F. NASH and A. J. POINTON: *Proc. Phys. Soc.*, A **69**, 725 (1956).
(6) E. P. GEORGE and G. S. SHRIKANTIA: *Nuclear Physics*, **1**, 54 (1956).
(7) J. E. COUSINS, W. F. NASH and A. J. POINTON: *Nuovo Cimento*, **6**, 1113 (1957).

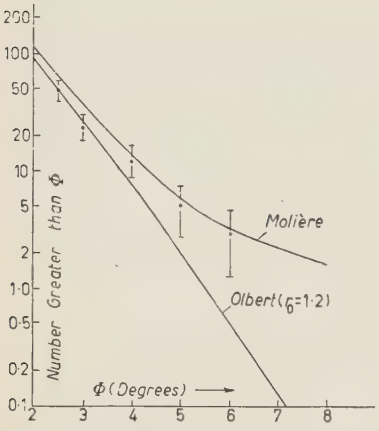

Fig. 5. - Scattering distribution - Series II (lead).

At angles of scatter less than 3° the experimental points are in reasonable agreement with either of the theoretical curves but at angles greater than 3° the experimental results agree well with Molière's distribution and appear to be inconsistent with the U.N.M. theory of Olbert.

In should be noted that in both Series I (Pb) and Series II (Pb) the error due to « noise level » scattering was small; the value calculated from the distribution in r.m.s. angles being less than 0.5° in each case. Hence, at angles greater than about 3° the experimental distributions would not be appreciably affected.

3·3. *Series* III (Cu). – In this case Σ was again fixed to give a momentum cut-off to the spectrum at 0.7 GeV/c. A total of 3892 photographs were selected for measurement and the distribution of these angles is shown in integral form in Fig. 6, where the Olbert and Molière curves are shown together with the theoretical distribution obtained from the modified form of Olbert's theory.

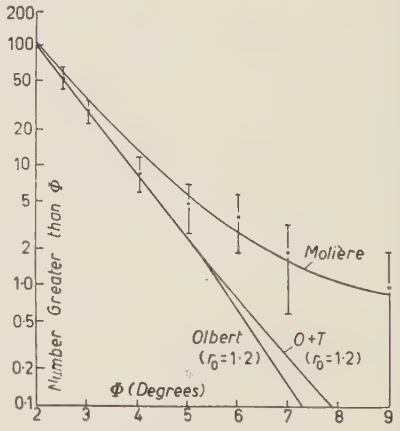

Fig. 6. – Scattering distribution - Series III (copper).

It will be seen that while at angles less than 4° the experimental results are in reasonable agreement with the theoretical curves for both a « solid » and a « point » nucleus, above 4° the results are certainly significantly in excess of the U.N.M. distribution. In fact the probability given by Olbert's theory for an angle of 9° occurring is about 2% and with the modified form of Olbert's theory about 4%. Further, it will be seen from Fig. 6 that the effect of including the single scattering « tail » in the distribution for a « solid » nucleus in no way accounts for the discrepancy between the experimental results and the theoretical curves, although the addition of this « tail » increases the theoretical distribution by far more than any other factor.

In this series the « noise level » scattering was found to be less than 0.3°, which would have a negligible effect on the experimental distributions at angles greater than about 2°.

4. – Comparison with other work.

Experiments which have been carried out on the interaction of slow μ-mesons with nuclei on the basis of the rate of absorption of stopped negative μ-mesons (CONVERSI *et al.* [8]) and others) and the X-ray spectra emitted from μ-mesic atoms (FITCH and RAINWATER [9]) show that the strength of the interaction is of the same order as the β-decay constant. That the μ-meson acts in the same way as an electron, at least for energies up to about 600 MeV, has been confirmed by PANOFSKY *et al.* [10] who found μ-meson pairs produced by high energy γ-quanta. Thus it would be assumed that the scattering of μ-mesons would be purely electromagnetic and follow the theory given by Olbert or a modified form of this theory based on phase shift analysis. Such a form has been shown to hold for 125 MeV electrons by BROWN and ELTON [11], who found the value for the mean nuclear radius as $R = 1.2 \cdot 10^{-13} A^{\frac{1}{3}}$ cm, in agreement with the work of FITCH and RAINWATER.

Therefore it appears that the work reported here is not in agreement with the theoretically expected results. However, it is in agreement with previous work on the scattering of μ-mesons at high energies and a few direct comparisons may be made.

4'1. *The cross-section for large angle scattering.* – The cross-section for angles of scatter greater than 5° has been estimated for Series II (Pb) and Series III (Cu) and from the results given by MCDIARMID [4] for his Group (3) lead and Group (3) iron. In the present experiment the mean momentum was slightly less than that for McDiarmid's Groups (3). This would be expected to increase slightly the values of cross-section found in our experiment.

Present experiment		MCDIARMID	
Series II Lead	$(7.7 \pm 3.4) \cdot 10^{-29}$ cm²/nucleon	Group (3) Lead	$(6.7 \pm 2.0) \cdot 10^{-29}$ cm²/nucleon
Series III Copper	$(4.9 \pm 2.2) \cdot 10^{-29}$ cm²/nucleon	Group (3) Iron	$(3.6 \pm 1.3) \cdot 10^{-29}$ cm²/nucleon

(8) M. E. CONVERSI, E. PANCINI and E. PICCIONI: *Phys. Rev.*, **71**, 209 (1947).

(9) V. L. FITCH and J. RAINWATER: *Phys. Rev.*, **92**, 987 (1953).

(10) W. K. H. PANOFSKY, G. E. MASEK and A. J. LAZARUS: *Phys. Rev.*, **103**, 374 (1956).

(11) G. E. BROWN and L. R. B. ELTON: *Phil. Mag.*, **45**, 164 (1955).

These results are in reasonable agreement in view of the statistical errors inherent in this type of experiment and the differences in the μ-meson spectra and scattering materials.

4·2. *The angular dependence of large angle scattering.* – The agreement between the experimental results and the predictions of Molière's theory indicate that the scattering law at large angles is of the form φ^{-n} where $n = 3$. However, it can be shown that the results given here are consistent with values of the exponent, n, in the range $n = 3$ to $n = 5$. These values compare with those found from the results of WHITTEMORE and SHUTT [12] and MCDIARMID [4] where the range in each case is from $n = 3$ to $n = 5$. The results of LLOYD and WOLFENDALE [3] give a range of n values from $n = 2$ to $n = 5$ but the actual range varies with the part of the momentum spectrum considered.

4·3. *Dependence of large angle scattering on A or Z.* – The agreement with the predictions of Molière indicates that the measurements are consistent with a scattering cross-section varying as Z^2/nucleus. However the results can be shown to be consistent with an A^2 dependence. Since the momentum spectra for Series II (Pb) and Series III (Cu) are very similar, the number of angles greater than 5° expected for Series III (Cu) can be predicted from the number of angles greater than 5° observed for Series II (Pb). If it is assumed that a Z^2 dependence is correct the predicted values can be expressed as a ratio of the values given by the Molière curve for various A or Z dependencies. Their ratios are given here for both the present experiment and for McDiarmid's Group (3) Iron predicted from the Group (3) Lead:

A or Z dependence	Ratio to MOLIÈRE (POINTON and NASH)	Ratio to MOLIÈRE (MCDIARMID)
Z^2	1	1
A^2	0.75	0.73
A	2.45	2.7
Z	2.82	3.2

Thus it is seen that the results are consistent with a Z^2 or A^2 dependence and inconsistent with a Z or A dependence. A similar conclusion was drawn from the results of LLOYD and WOLFENDALE [3].

[12] W. L. WHITTEMORE and R. D. SHUTT: *Phys. Rev.*, **88**, 1312 (1952).

5. – Discussion.

Since the results given here and those of other workers have shown a marked discrepancy between experiment and theory it is perhaps pertinent to consider the theories which have been used. The agreement between the theory given for a « point » nucleus and the results indicates that it is unlikely that any modification of the theory for a « solid nucleus » on the basis suggested by McDiarmid [4] (*i.e.* allowing a form factor in the scattering smaller than $\lambda\!\!\!^{-}/R$) would bring this theory into agreement with the results unless the nuclear radius is reduced to about $R = 0.3 \cdot 10^{-13} A^{\frac{1}{3}}$ cm which is a value very much smaller than that found from other experiments, where the charge distribution has been measured.

One contribution to scattering is that due to incoherent effects which have been estimated by Gatto [13] for large angles as $1/Z$ times the scattering due to a « point » nucleus and is less than this at small angles. Thus it is seen that while the observed dependence on angle and $p\beta$ value are predicted the values given for the magnitude and the Z dependence are totally inconsistent with experimental results. In the present experiment this would only contribute 1.2 % of the Molière curve in the case of lead and 3.4 % in the case of copper. It seems doubtful whether a more accurate estimate of the contribution due to incoherent scattering would account for the observed anomalous scattering of μ-mesons.

Bethe [14] has pointed out that the meson field of the nucleons may be expected to influence the scattering of high energy electrons. A similar consideration would be expected in the scattering of μ-mesons and it is possible that the scattering theories should be modified to allow for this.

Since in the Born approximation, the scattering cross-section depends only on the momentum transfer in the scattering collision, it is interesting to compare the momentum transfers for the experiments with electrons and μ-mesons. If the angle of 8°, observed in Series I (Pb) is considered the minimum possible value for the momentum transfer is 70 MeV/c. If, however, the scattered μ-mesons is assumed to have a $p\beta$ value 2.5 GeV/c (the mean value for particles with $p\beta < 5$ GeV/c) then the mean momentum transfer would be 350 MeV/c. These values compare with the maximum momentum transfer, 230 MeV/c, observed in the experiments of Hofstadter *et al.* [15]. Thus it is seen that on the Born approximation, the scattering theories would not be greatly affected. The possible difference in momentum transfers, although not

---

(13) R. Gatto: *Nuovo Cimento*, **10**, 1559 (1953).

(14) H. A. Bethe: *Experimental Nuclear Physics*, (New York, 1951). Vol. I, p. 281.

(15) R. Hofstadter, H. Fechter and J. A. McIntyre: *Phys. Rev.*, **92**, 978 (1953).

large, and the higher momenta of the μ-mesons might be expected to affect a phase shift calculation. However such an effect would not be expected to account for the differences in the experiments on electron and μ-meson scattering.

Recently FOWLER ([16]) has shown that the elastic scattering cross-section of μ-mesons at large angles is affected by inelastic scattering of the μ-meson when the energy transfer is $\geqslant 150$ MeV. The resulting contribution to the scattering was shown to have an A^2 dependence and be proportional to $1/(p\beta)^2$, this is consistent with the results given here. Furthermore if the cross-section for star production may be taken as $(1 \div 2) \cdot 10^{-29}$ cm^2 then the single scattering cross-section would approach that for a point nucleus. The theory also predicts a momentum dependence in that little or no anomaly is expected below about 600 MeV/c. This is in accord with the present results.

However, it has been pointed out recently by LLOYD (see FOWLER and WOLFENDALE, ([17]), to be published) that this theory is not firmly based, and may require serious revision before final judgement can be made.

6. – Conclusions.

1) The scattering distributions of μ-mesons, in both lead and copper, are inconsistent with the usual theory of Coulomb scattering at large angles. The μ-mesons considered all had $p\beta$ values greater than 0.5 GeV/c but the contribution to the theoretical scattering distributions by particles of momenta greater than 5 GeV/c is virtually negligible.

2) The observed scattering distributions are in better agreement with the predictions of the theory given by Molière for a « point » nucleus at large angles.

3) The properties of the scattering cross-section for the anomalous component of the scattering distributions may be enumerated

a) The cross-section is approximately proportional to $1/(p\beta)^2$.

b) The cross-section varies as φ^{-n} where $n = 3$ to 5.

c) The results are consistent with a cross-section which varies as A^2 or Z^2 but not as Z or A.

4) The results of the present experiment are in agreement with those of other workers in that the anomalous component is small at small values of momenta.

([15]) G. N. FOWLER: *Nuclear Physics*, **3**, 121 (1957).
([17]) G. N. FOWLER and A. W. WOLFENDALE: (to be published).

5) It would appear that Fowler's latest theory on anomalous scattering, in terms of a photo-nuclear interaction, does give a result which is similar to the experimental results. However, there are objections to his work and it would seem that a more rigorous treatment of the problem is required before a final conclusion may be reached.

6) The explanation of the observed anomalous scattering in terms of any known short range nuclear forces does not seem possible but it is doubtful whether some new form of nuclear interaction could be justifiably proposed until the possibility of modifying the scattering theories has been more fully investigated.

* * *

We are glad to record our indebtedness to Professor L. F. BATES for his interest in these experiments and to Dr. A. W. WOLFENDALE for many helpful discussions. We also thank the Nottingham Corporation for permission to work in the cave. One of us (A.J.P.) is indebted to the Department of Scientific and Industrial Research for the provision of a maintenance grant.

The apparatus used in this work was built in part with a grant from the Government Grant Committee of the Royal Society.

RIASSUNTO (*)

Si sono studiate le distribuzioni dello scattering dei mesoni μ in piombo e in rame per mezzo di una camera a nebbia posta sotto terra alla profondità di 40 m a.e. Per momenti elevati le distribuzioni di scattering osservate sono simili a quelle date da MOLIÈRE per un nucleo « puntiforme » sotto grandi angoli. Si dimostra che i risultati sono comparabili con una sezione d'urto variabile come A^2 o Z^2 ma non come Z o A.

(*) *Traduzione a cura della Redazione.*

On the Abundances of the $K_{\mu 3}$ and K_{e3} Decay Modes of Positive K Mesons.

M. Bruin, D. J. Holthuizen and B. Jongejans

Natuurkundig Laboratorium, Universiteit van Amsterdam, Nederland

(ricevuto il 28 Aprile 1958)

Summary. — The abundances of the $K_{\mu 3}$ and K_{e3} decay modes were checked in a large stack of Birge *et al.* (1), using the additional criteria of Alexander *et al.* (2). Our results agree completely with those of Birge *et al.* The weighted average of these and comparable corrected results of others yields a relative abundance of $(3.9 \pm .5)$ % for $K_{\mu 3}$ and of $(5.1 \pm .8)$ % for K_{e3} decay. Available experimental data on the electron spectrum of the K_{e3} decay mode are compiled and compared to theoretical calculations by Furuichi *et al.* (3). No evidence is found for an abnormally short mean free path of the positive secondary pions from $K_{\pi 2}$ decay as previously reported by Alexander *et al.* (2).

1. – Introduction.

The decay modes of K^{+}-mesons have been systematically investigated by a number of groups (1,2,4-8). Of the work hitherto published the statistically most important contributions were those by Birge *et al.* (1) and by Alexander

(1) R. W. Birge, D. H. Perkins, J. R. Peterson, D. H. Stork and M. N. Whitehead: *Nuovo Cimento*, **4**, 834 (1956).

(2) G. Alexander, R. H. W. Johnston and C. O'Ceallaigh: *Nuovo Cimento*, **6**, 478 (1957).

(3) S. Furuichi, T. Kodama, S. Ogawa, Y. Sugahara, A. Wakasa and M. Yonezawa: *Progr. Theor. Phys.*, **17**, 89 (1957).

(4) G. Stack-collaboration: *Nuovo Cimento*, **2**, 1063 (1955).

(5) J. Crussard, V. Fouché, J. Hennessy, G. Kayas, L. Leprince-Ringuet, D. Morellet and F. Renard: *Nuovo Cimento*, **3**, 731 (1956).

(6) D. M. Ritson, A. Pevsner, S. C. Fung, M. Widgoff, G. T. Zorn, G. Goldhaber and S. Goldhaber: *Phys. Rev.*, **101**, 1085 (1956).

(7) T. F. Hoang, M. F. Kaplon and G. Yekutieli: *Phys. Rev.*, **102**, 1185 (1956).

(8) T. F. Hoang, M. F. Kaplon and G. Yekutieli: *Phys. Rev.*, **105**, 278 (1957).

et al. (2), in the following abbreviated as B and A respectively. The least precisely known frequencies of occurrence are those of the relatively rare decay modes $K_{\mu 3}$ and K_{e3}, the accurate determination of which is also the most difficult from the technical point of view. The values given for these abundances by A and B were:

$$\text{A:} \qquad (5.9 \pm 1.3)\,\%\ K_{\mu 3}\,, \qquad (5.1 \pm 1.3)\,\%\ K_{e3}\,,$$

$$\text{B:} \qquad (2.83 \pm 0.95)\,\%\ K_{\mu 3}\,, \qquad (3.23 \pm 1.30)\,\%\ K_{e3}\,.$$

These percentages are based on the total numbers of K-mesons, thus including the τ and τ' decay modes.

The determination of the abundances of the various decay modes by the Berkeley group essentially depended on tracing and blobcounting samples of K-meson secondaries, having a specified potential tracklength, as far as possible. In the case of the Dublin group the discrimination scheme essentially consisted of performing blob counts as well as multiple scattering measurements over the first and the fourth cm of pathlength of the charged decay products.

The difference between the $K_{\mu 3}$ and K_{e3} abundances as obtained by B and A is thought to be significant by the latter authors. It should be stressed however that for the small numbers of events available the used root-mean-square errors may hardly be called an adequate measure of statistical significance. Nevertheless the present investigation was undertaken to check whether a systematic bias was inherent in the methods of measurement used by B as compared to those of A. For this purpose the stacks previously used in Berkeley were kindly lent to us. We compared the two sampling methods, and as no reason for systematic deviations on account of these were found, we investigated samples used by B according to procedures employed by A. This implied the additional determination of the values of $p\beta$ over a certain length of the K-meson secondary tracks.

2. – Measurements.

2·1. *Measuring technique.* – All measured tracks belonged to the samples of « stack 20 » from which B had determined the relative abundances of the K^--meson decay modes.

The scattering measurements were performed with a Koristka MS2 microscope, so that the stage noise contribution to the observed signal could be ignored. A cut-off was applied at four times the mean second difference and the usual noise elimination procedure was followed taking 100 μm and 200 μm cells.

The scattering constant was determined in the following way. The experimentally determined second differences D_{exp} of a track using a cell size s (in units of 100 μm) may be expressed ([9]) as:

$$D^2_{exp} = \frac{(100 \cdot 2\pi)^2 K^2 g^2(s, \beta)}{(360)^2 (p\beta)^2} s^3 + \varepsilon^2 ,$$

in which K is the scattering constant for $s = 1$, p is the momentum in MeV/c, $\beta = v/c$ and ε is the noise. The function g expresses the variation of the scattering constant with the cell size and with the velocity of the particle. For a muon of the $K_{\mu 2}$ decay in the first four cm from the decay point g is practically independent of the velocity β. The value of $p\beta$ may be derived from the known masses of the K-meson and the secondary particles. Using the Berkeley tables of high energy particle data ([10]), one finds for the first cm an average $p\beta = 209$ MeV/c and for the fourth cm an average $p\beta = 191$ MeV/c in the case of the $K_{\mu 2}$ decay mode. From the graphs of Voyvodic ([11]) one may derive that for $s = 1, 2, 4$ and 8 the appropriate scattering constants may respectively be expressed as K, $1.04K$, $1.07K$ and $1.10K$. The function $g^2(s, \beta)$ was therefore taken to be $g^2(1, \beta) = 1.00$, $g^2(2, \beta) = 1.08$, $g^2(4, \beta) = 1.14$, $g^2(8, \beta) = 1.21$.

For 27 cases, presumably $K_{\mu 2}$ decays, the second differences were determined over the first and fourth cm path length of the charged secondary from the decay point. The scattering measurements were performed with a cell size of 100 μm. The values of the second differences for 100, 200, 400 and 800 μm cells were averaged for the 27 cases. It was possible a priori that the sample contained a high energy $K_{\mu 3}$ case. This would however have had no significant influence on these mean values. The data obtained for the first and for the fourth cm path length were used separately to obtain a value of K. The best fit to these experimental data employing least square and graphical methods was found for a numerical value of the scattering constant $K = 24.3 \pm .9$.

2·2. *Resolution of decay modes.* – When looking for ambiguities which might give rise to a faulty determination of the relative abundance of $K_{\mu 3}$ events one has the following possibilities:

a) Below a secondary energy of 60 MeV there may be confusion with τ' decay. These cases were all traced to rest, so that there could be no doubt about the identity.

([9]) M. G. K. Menon, C. O'Ceallaigh and O. Rochat: *Phil. Mag.*, **42**, 932 (1951).
([10]) J. H. Atkinson and B. H. Willis: *UCRL*-2426 II (rev.) (1957).
([11]) L. Voyvodic: *Progr. Cosm. Ray Phys.*, **2**, 273 (1954).

b) If the secondary has an energy of about 100 MeV confusion is possible with the $K_{\pi 2}$ decay mode. In these cases A performed measurements over the whole available track length.

c) In the region where the secondary has an energy near 130 MeV it might be confused with a $K_{\mu 2}$ event. A called those cases suspect where a value of $p\beta$ was found in the first and fourth cm segment that was at least 10% lower than expected for $K_{\mu 2}$ decay, whereas also both values of the blob density b^* were at least one standard deviation higher than calculated for such a muon. If this was the case they performed extended measurements.

As far as the K_{e3} decay mode is concerned unfortunate statistics may cause confusion with the $K_{\pi 2}$ or even more with $K_{\mu 2}$ decays when relying on blob counting results near the decay point. Scattering measurements and especially comparison of the $p\beta$ values of successive segments will have to show the electron identity if the particle cannot be followed far enough to recognize it as such.

The first sample restudied consisted of those tracks which had a potential length in the emulsion of 21 cm. No scattering measurements were performed on tracks which were unambiguously identified. This was the case for a number of secondaries that came to rest in the emulsion, interacted in flight, or showed an obvious electron behaviour. We combined the results of the blob counting which had been carried out in Berkeley with the results of our scattering measurements. There turned out to be *no events* in the above mentioned ambiguous regions for which the original classification by B had to be altered.

In Fig. 1 a plot is shown of b^* versus the distance from the decay point for the charged secondaries of $K_{\pi 2}$, $K_{\mu 2}$ and the upper limit of $K_{\mu 3}$ decay. The blob density is expressed in terms of the plateau blob density. The hatched areas indicate a three percent statistical in-

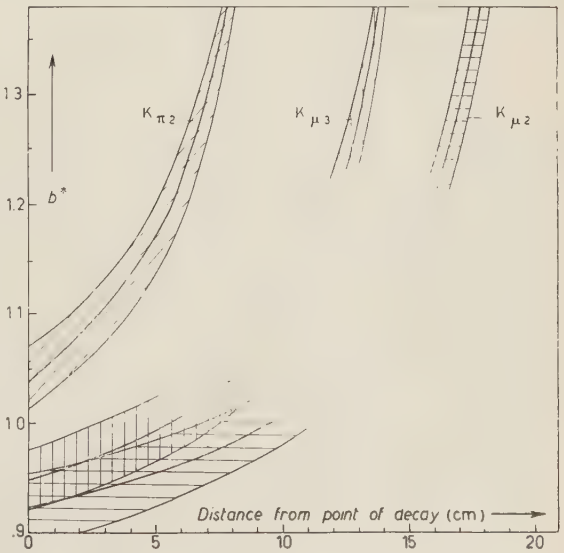

Fig. 1. – Blob density b^* (relative to plateau blob density) versus distance from the point of decay for the charged secondaries of $K_{\pi 2}$, $K_{\mu 2}$, and the upper limit of $K_{\mu 3}$ decay. The hatched areas indicate a 3% error.

accuracy, obtained by counting about 1000 blobs. Fig. 2 shows $p\beta$ as a function of the traversed path for the same decay modes. Here the hatched areas indicate an error of 20%. These curves were calculated from combined data taken from references ([10]) and ([12]). The statistical errors which should be ascribed to scattering measurements can be obtained from DI CORATO *et al.* ([13]). If one carries out measurements over 1 cm using 100 μm cells, so that about 50 cells of 200 μm are available and when one has little stage and reading noise the standard deviation is about 15%. However for long series of measurements it is often not practicable to take each reading a sufficiently large number of times to keep the reading error negligible. It is therefore felt that a total error of about 20% will in general be a better measure of the inaccuracy in such a type of measurement.

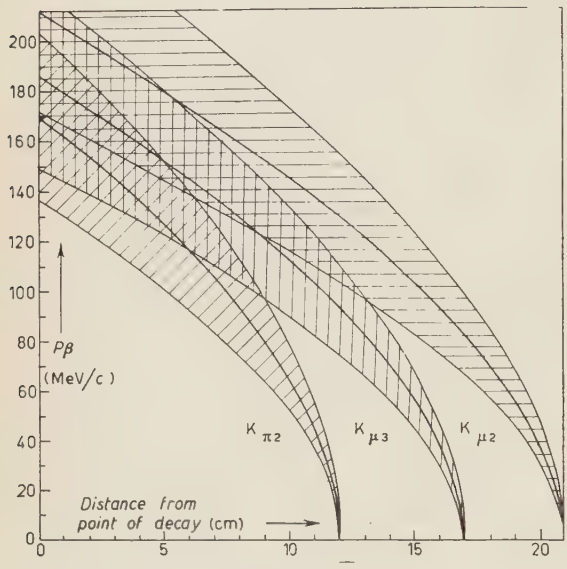

Fig. 2. – Value of $p\beta$ versus distance from the point of decay for the charged secondaries of $K_{\pi 2}$, $K_{\mu 2}$ and the upper limite of $K_{\mu 3}$ decay, The hatched areas indicate a 20% error.

This was found to be consistent with our observations. It should of course be kept in mind that even then about one out of three cases will be outside the probability limits given by the hatched areas in Fig. 2. One may thus see that using the scheme of A the discrimination between a μ from $K_{\mu 2}$ and a high energy μ from $K_{\mu 3}$ is not evident, and that scattering measurements would be reliable only near the end of the range of that particle. For a muon of $K_{\mu 3}$ which has a lower energy the possibility of confusion with $K_{\mu 2}$ becomes less, but then there is more overlap with the $K_{\pi 2}$ decay mode.

We noticed that in the first sample checked the blob counting at the farthest segment of the track gave a far better resolution for $K_{\mu 3}$ than ob tained from the scattering measurements. This is what should be expected

([12]) G. ALEXANDER and R. F. W. JOHNSTON: *Nuovo Cimento*, **5**, 363 (1957).

([13]) M. DI CORATO, B. LOCATELLI and D. HIRSCHBERG: *Suppl. Nuovo Cimento*, **4**, 448 (1956).

also, comparing the Figs. 1 and 2. Therefore for the tracks of our second sample (which were followed over a mean length of 6.5 cm) no additional scattering measurements were carried out in the fourth cm when searching for $K_{\mu 3}$ events.

In order to obtain information in this sample about possible electrons from K_{e3} decay, the value of $p\beta$ was checked over the first cm by scattering measurements. If not readily recognized by their typical behaviour, electrons might have been hidden especially among the cases of $K_{\mu 2}$ decay. If namely the blob counting should have given the main information on the μ or electron identity, these particles would only be well recognizable beyond about 11 cm of path length. From there the blob density of the muon starts to increase above the plateau value. It is of course clear that the electron shows in general large losses at a much lower traversed path length. All tracks which yielded a value of $p\beta$ lower than 180 MeV/c in the first cm were scattered over a longer range in order to check whether the particle was indeed an electron. For eventual electrons above 180 MeV/c we relied on the following through and blob counting procedure.

No additional electrons were found in this way, and the number of particles to which extended scattering measurements had to be applied agreed with statistical expectation.

3. – Results and discussion.

3·1. *Possibility of systematic deviations.* – In our measurements no indication can be found that the methods used by [1] give rise to a systematic underestimate of the rare decay modes $K_{\mu 3}$ and K_{e3}. In the work of A attention was drawn to the fact that secondaries of the $K_{\tau 2}$ decay mode seemed to have an abnormally short mean free path for interaction. With their value of (11.2 ± 2.4) cm, we have to compare the value determined for the stack of B of (39 ± 13) cm, obtained from 11 events out of 427 cm tracklength. As the geometric mean free path is about 28 cm we do not seem to find a significant deviation from this value. The fact that A found a shorter mean free path for these pions, together with a somewhat lower $K_{\tau 2}$ abundance could at first sight suggest that some cases of non-interacting $K_{\pi 2}$ had been called $K_{\mu 3}$, thus raising the $K_{\mu 3}$ abundance. However, if one would change even as many as 10 events called $K_{\mu 3}$, no appreciable decrease of the mean free path for interaction would result. Besides, their $K_{\mu 3}$ spectrum gives no evidence for such a misclassification.

In principle for the K_{e3} decay a source of error that might give rise to too many electrons could be a contamination with electron decays from stopped muons that arise from π-μ decays in flight. It is evident that such a case can

be recognized by following the primary track for a few mm. Besides this effect would yield electrons with an energy below 55 MeV whereas in that region no anomalous number of events is to be seen in the experimental spectrum.

There is no evidence either that the methods used by ([2]) would give rise to a systematic overestimation of the rare decay modes. It is clear that in photographic emulsion unambiguous results can only be obtained from tracing to rest a sufficiently large sample of K-meson secondaries. If one uses statistical considerations to find high energy $K_{\mu 3}$ decays from a sample of particles, which have only a limited path in the emulsion, this method is certainly not reliable.

Apart from the fact that the $K_{\mu 3}$ decay mode is the most difficult one to identify in the high energy region of the muon, it is also most subject to corrections applied for scanning bias. This is due to the fact that a fraction of the $K_{\mu 3}$ muons belongs to the easily visible secondaries.

The abundance of the K_{e3} decay mode will be less easily underestimated and also be less dependent on the fraction of light secondaries missed in scanning.

3·2. *Relative abundances of* $K_{\mu 3}$ *and* K_{e3} *decay modes.* – From various results ([1,2,4-8]) the number of cases of $K_{\mu 3}$ and K_{e3} decay were collected. Only those cases were taken which had been obtained in a way similar to those of B and A. Total sample numbers were calculated by correcting the number of K-mesons actually found. If the authors did not state the magnitude of the scanning loss for one or more types of decays, a correction was applied using *e.g.* the number of τ-mesons they found as a standard. This was taken to be a fraction of all K-mesons equal to the average percentage from B and A. The data thus arrived at are collected in the following table. This material was combined giving each result a weight inversely proportional to the mean square relative error. The abundances obtained in this way are:

$$K_{\mu 3}: \qquad (3.9 \pm .5)\,\% ,$$

$$K_{e3}: \qquad (5.1 \pm .8)\,\% .$$

The mean value for the abundances of $K_{\mu 2}$ and $K_{\pi 2}$ as given by A and B are respectively $(58 \pm 3)\,\%$ and $(26 \pm 3)\,\%$. Therefore one has the branching ratios:

$$(1) \qquad \frac{K^- \to \mu^- + \nu + \pi^0}{K^- \to e^- + \nu + \pi^0} = 0.8 \pm 0.2 ,$$

$$(2) \qquad \frac{K^- \to e^- + \nu + \pi^0}{K^+ \to \mu^+ + \nu} = 0.09 \pm 0.02 ,$$

$$\frac{K^+ \to \mu^+ + \nu + \pi^0}{K^+ \to \pi^+ + \pi^0} = 0.15 \pm 0.04 , \tag{3}$$

$$\frac{K^+ \to e^+ + \nu + \pi^0}{K^+ \to \pi^+ + \pi^0} = 0.20 \pm 0.06 . \tag{4}$$

TABLE I. – *Cases of* $K_{\mu 3}$ *and* K_{e3} *decay with corresponding sample numbers.*

	Number of events	Corrected sample	Percentage		Reference
$K_{\mu 3}$	9	3075	.3	2.9	(1)
	5	340	1.5		
	2	186	1.1		
	21	358		5.9	(2)
	5	108		4.6	(4)
	3.5	487	.7	4.0	(5)
	2	62	3.3		
	6	1156	.5	1.4	(6)
	1	75	.9		
	7.5	502	1.5	3.5	(8)
	1	50	2.0		
K_{e3}	6	186		3.2	(1)
	18	358		5.0	(2)
	5	82		6.1	(4)
	5	62		8.1	(5)
	1	56		1.8	(6)
	5	50		10	(8)

One may theoretically obtain values for these ratios assuming strong interactions followed by a universal Fermi interaction. COSTA and DALLAPORTA [14] obtained for the ratios (3) and (4) 0.37 and 0.95 respectively. Their theoretical value for (1) proved to be 0.39. The ratio (1) was directly computed by ONEDA and WAKASA [15] and yielded 0.44. GOTÔ [16] calculated the relative frequencies on the assumption of a scalar meson with gradient coupling and equal coupling

[14] G. COSTA and N. DALLAPORTA: *Nuovo Cimento*, **2**, 519 (1955).
[15] S. ONEDA and A. WAKASA: *Nuclear Physics*, **1**, 445 (1956).
[16] S. GOTÔ: *Progr. Theor. Phys.*, **17**, 107 (1957).

constants for $K_{\mu 3}$ and K_{e3} decay. For the ratios (1) and (2) he arrives at a value of 0.8 and 0.1 respectively. Considering the coarse experimental material and the speculative nature of the theoretical assumptions, not too much weight should be given yet to an exact agreement.

3·3. *Spectrum of electrons from the* K_{e3} *decay mode.* – For the muons of the $K_{\mu 3}$ decay mode it is at present difficult to compose a decay spectrum as the numbers obtained over various energy intervals have different weights.

The combined electron data are shown in Fig. 3, together with theoretical curves given by FURUICHI *et al.* [3].

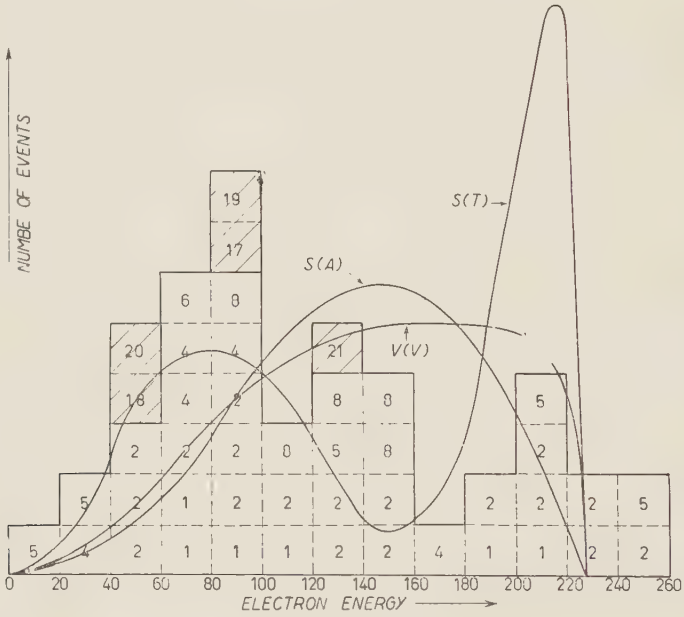

Fig. 3. – Experimental and theoretical energy distribution for the electrons from K_{e3} decay. The hatched areas represent old cases not included in the normalization of the curves. The numbers in the blocks indicate the references.

The indices $S(T)$, $S(A)$ and $V(V)$ imply what the principal assumptions are, namely:

$S(T)$: scalar K-meson with tensor coupling,

$S(A)$: scalar K-meson with pseudoscalar coupling,

$V(V)$: vector K-meson with vector coupling.

Other possible combinations of particle and coupling types can be found in references ([3]) and ([17]). Some of these curves give the same distributions, whereas others are not essentially different from the $S(A)$ and $V(V)$ features.

The curve $S(A)$ was also given by GOTÔ ([16]). In the calculations Lorentz invariance of the transition matrix and a universal Fermi interaction for the decay were assumed to be valid, and only lowest order terms were considered. The theoretical curves have been normalized to 40 events. This is the number of events found by systematical searching procedures. It should be borne in mind that a precise determination of the electron energy is very difficult and that therefore the measurements have large errors. In addition five older cases ([18-22]) are indicated by hatched areas. They were not included in the normalization of the curves, as these events are thought to have a larger bias. The numbers in the histogram refer to the publications the electron data were taken from.

It seems that the tensor type of interaction in the K_{e3} decay mode is not ruled out by the experimental material. Its salient features not attained by other combinations, are the rapid rise at the low energy side and the minimum in the high energy region. As was pointed out by FURUICHI *et al.* ([3]), the second peak of $S(T)$ can be lowered to any level by mixing. If one assumes that the experimental distribution does not show too much distortion one would be inclined to think that a mixture ([15]) of $S(P)$ and $S(T)$ would give a better representation of the data.

It is clear however that the experimental material is still too scanty to allow any definite conclusions.

* * *

This work is part of the research program of the Institution for Fundamental Research of Matter (F.O.M.), financially supported by the Netherlands Organization for Pure Scientific Research (Z.W.O.).

We wish to express our gratitude to Dr. R. W. BIRGE and Dr. M. N. WHITE-

([17]) S. FURUICHI, Y. SUGAHARA, A. WAKASA and M. YONEZAWA: *Nuovo Cimento*, **5**, 285 (1957).

([18]) M. W. FRIEDLANDER, D. KEEFE, M. G. K. MENON and L. VAN ROSSUM: *Phil. Mag.*, **45**, 1043 (1954).

([19]) C. DAHANAYAKE, P. E. FRANCOIS, Y. FUJIMOTO, P. IREDALE, C. J. WADDINGTON and M. YASIN: *Phil. Mag.*, **45**, 1219 (1954).

([20]) R. H. W. JOHNSTON and C. O'CEALLAIGH: *Phil. Mag.*, **46**, 393 (1955).

([21]) W. W. CHUPP, G. GOLDHABER, S. GOLDHABER, S. J. GOLDSACK, J. E. LANNUTTI, F. M. SMITH and F. H. WEBB: *Phys. Rev.*, **99**, 335 (1955).

([22]) H. H. HECKMANN: *UCRL 3003* (1955).

HEAD for putting the stacks at our disposal and for their friendly cooperation in providing us with all relevant data on their measurements. It is a pleasure to thank Prof. Dr. G. W. RATHENAU for his stimulating interest.

RIASSUNTO (*)

Le abbondanze dei modi di decadimento $K_{\mu 3}$ e K_{e3} furono esaminate in un grosso pacco di emulsioni di BIRGE *et al.* (1) usando i criteri addizionali di ALEXANDER *et al.* (2). I nostri risultati si accordano perfettamente con quelli di BIRGE *et al.* La media ponderata di questi ed altri risultati corretti per renderli omogenei dà un'abbondanza relativa del $(3.9 \pm .5)\%$ per i decadimenti $K_{\mu 3}$ e del $(5.1 \pm .8)\%$ per i K_{e3}. Si elaborano i dati sperimentali disponibili per lo spettro elettronico del decadimento K_{e3} e si confrontano col calcolo teorico di FURUICHI *et al.* (3). Non si trovano prove per un cammino libero medio anormalmente corto dei pioni secondari positivi da decadimento $K_{\pi 3}$, come precedentemente riferito da ALEXANDER *et al.* (2).

(*) *Traduzione a cura della Redazione.*

IL NUOVO CIMENTO Vol. IX, N. 3 1° Agosto 1958

On the Universal Fermi Interaction (*)(+).

S. A. Bludman

Radiation Laboratory, University of California - Berkeley, Cal.

(ricevuto il 6 Maggio 1958)

Summary. — The parity-non-conserving, V-A form of Fermi interaction is derived from a principle of invariance under a continuous group of transformations, in analogy with the ordinary gauge-invariance derivation of the minimal electromagnetic interaction of charged particles. This assumption is a stronger restriction on the form of Fermi interactions than that invoked by Sudarshan and Marshak, Gell-Mann and Feynman, and Sakurai, and leads to additional predictions that are subject to experimental check. If these transformations were symmetry transformations of the entire Lagrangian, then the β- and μ-decay coupling constants would be precisely equal. The implications of extending this Fermi gauge invariance to a group depending on space-time functions is discussed. The possibility that Fermi interactions involving change of strangeness are unallowed is considered, and the results of assuming a universal Yukawa V-A parity-non-conserving interaction are tabulated. Such a Yukawa interaction, involving one new coupling constant, leads to reasonable K-meson and hyperon decay rates and allows π-meson decay into μ+ν without any appreciable decay into e+ν.

1. – Introduction.

The recent experimental evidence on the electron asymmetry from polarized nuclei or muons, on the electron polarization, on the nuclear recoil, and on the μ-decay ϱ value tends to indicate that in both β and μ decay the four-fermion interaction is of the same strength g and of the same V-A form.

$$g\bar{\psi}_1\gamma_\mu\tfrac{1}{2}(1+\gamma_5)\tau_+\psi_1\bar{\psi}_2\gamma_\mu\tfrac{1}{2}(1+\gamma_5)\tau_-\psi_2+\text{h. c.} \tag{1}$$

(*) Reported on at the *New York meeting of the American Physical Society*, Jan, 29 1957; *Bull. Am. Phys. Soc.*, Ser. II, **3**, 20 (1958).

(+) This work was done under the auspices of the U.S. Atomic Energy Commission.

Here $\tau_{\pm}$ are charge-raising and -lowering operators and ψ_1 refers to the electron-neutrino, ψ_2 to the neutron-proton or muon-neutrino field operators. It has also been conjectured that the same interaction obtains in electron or μ capture and perhaps in other Fermi interactions, although definitive experiments have not yet been done (1).

A theoretical basis for this V-A form of interaction has recently been suggested by SUDARSHAN and MARSHAK (2), FEYNMAN and GELL-MANN (3), and SAKURAI (4). These authors all assume that the Fermi interaction obtains between pairs of charged and neutral fermions and then, motivated by principles of « chirality invariance » (2), use of two-component fields (3), or « mass-reversal invariance » (4), they assume, that the Fermi interactions are invariant under the discrete transformation

$$\psi \to \psi' = i\gamma_5\psi \,, \tag{2'}$$

applied to all Fermi fields separately. They are then led directly to the parity-non-conserving charge-exchange V-A interaction, Eq. (1).

Now the vectorial nature of the Fermi interaction suggests a stronger assumption analogous to the assumption of gauge invariance in electrodynamics. In this paper we consider the consequences of assuming for the Fermi interactions an invariance under a *continuous* group of transformations applied to various fermions *simultaneously*. One motivation for this farther-reaching assumption is that the charge-exchange character, expressed by the operators $\tau_{\pm}$ in Eq. (1), can be incorporated more naturally. A second motivation is that certain conservation laws, to be discussed in Sect. **3**, would follow if the entire Lagrangian were invariant under these continuous Fermi gauge transformations. Since the mass terms, and probably also the strong interactions, are not invariant under these transformations, we will be led to speculate on the origin of the strong interactions and the blocking of the symmetry of the weak interactions.

In Sect. **3** we also discuss two structure problems connected with the weak interaction: the ϱ value, and the Gamow-Teller Fermi coupling constant ratio. Sect. **4** discusses the possibility of allowing Fermi gauge transformations which depend arbitrarily on space-time. This leads to a vector meson intermediary field in Fermi interactions, with serious implications that are discussed.

(1) G. PUPPI: *Nuovo Cimento*, **5**, 587 (1948); O. KLEIN: *Nature*, **161**, 897 (1948); T. D. LEE, M. ROSENBLUTH and C. N. YANG: *Phys. Rev.*, **75**, 905 (1949); J. TIOMNO and J. WHEELER: *Rev. Mod. Phys.*, **21**, 153 (1949).

(2) E. C. G. SUDARSHAN and R. E. MARSHAK: *Padua-Venice International Conference*, September, 1957; *Phys. Rev.*, **109**, 1860 (1958).

(3) R. P. FEYNMAN and M. GELL-MANN: *Phys. Rev.*, **109**, 193 (1958).

(4) J. J. SAKURAI: *Nuovo Cimento*, **7**, 649 (1958).

(5) M. GELL-MANN: *Suppl. Nuovo Cimento*, **4**, 848 (1956).

We are inclined to believe that the Fermi interactions do not allow changes in strangeness. Since this philosophy—which is in agreement with experimental results on the absence of hyperon β decay—is more restrictive than the usual one ([5]), we are led to introduce in the Appendix a universal weak Yukawa interaction. This additional interaction (with one new coupling constant) is sufficient to explain the observed rates of most meson and hyperon decay processes, and leads to verifiable predictions about the asymmetries and nucleon polarizations to be expected in hyperon decay.

The weak interactions have been generally regarded solely as destructive of the reflection and charge-conjugation symmetry laws. The point of view suggested in this paper, on the other hand, is that the weak interactions actually show some symmetry not shared by the strong interactions.

2. – A symmetry principle for the Fermi interactions.

2·1. *Fermi gauge transformations.* – If mass differences are neglected, the members of a charge multiplet are distinguished only by the electromagnetic interaction. This equivalence can be expressed for the neutron-proton, electron-neutrino, and muon-neutrino systems by arranging these fermions into two component spinors in charge space, $\psi_j = (\mathrm{pn})$, (νe), $(\nu\mu)$, and asserting invariance under arbitrary unitary unimodular transformations.

We assume that the weak interactions are those distinguishing $\psi_+ = \frac{1}{2}(1+\gamma_5)\psi$ from $\psi_- = \frac{1}{2}(1-\gamma_5)\psi$ in the same way as the electromagnetic field distinguishes between the projections $\frac{1}{2}(1+\tau_3)\psi$ and $\frac{1}{2}(1-\tau_3)\psi$. Then we identify the weak interactions as those that are invariant under the transformation

$$\psi \to \psi' = \exp\left[i\tfrac{1}{2}(1+\gamma_5)\,\boldsymbol{\tau}\cdot\boldsymbol{\omega}\right]\psi\,. \tag{2}$$

This transformation is admitted by the interactions $\bar{\psi}\gamma_\mu\psi$ and $\bar{\psi}\gamma_\mu\gamma_5\psi$. Because $\bar{\psi}\sigma_{\mu\nu}\psi$, $\bar{\psi}\gamma_5\psi$, and $\bar{\psi}\psi$ couple ψ_+ and ψ_-, such terms in the Lagrangian, including particularly the ordinary mass term, are not invariant under transformation (2).

The transformation (2) is a canonical transformation generated infinitesimally by the charge-space vector

$$\boldsymbol{F} = \int \mathrm{d}\sigma_\mu \boldsymbol{J}^\mu\,, \tag{3}$$

where

$$\boldsymbol{J}^\mu = \sum_j i\bar{\psi}_j\gamma_\mu\tfrac{1}{2}(1+\gamma_5)\boldsymbol{\tau}\psi_j \tag{4}$$

is an Hermitian current density composed additively of the fermion doublets introduced. By use of the anticommutation relations for ψ_j, Eq. (4) may be written more symmetrically:

$$\boldsymbol{J}^{\mu} = \sum_j \frac{i}{2}\{\overline{\psi}_j\gamma_\mu \tfrac{1}{2}(1+\gamma_5)\boldsymbol{\tau}\psi_j - \overline{\psi}_j^c\gamma_\mu \tfrac{1}{2}(1-\gamma_5)\boldsymbol{\tau}^T\psi_j^c\}\,, \tag{4'}$$

where $\psi^c = C\overline{\psi}$, with $C\gamma_\mu C^{-1} = -\gamma_\mu^T$, is the charge conjugate to ψ.

Thus we have

$$\begin{cases} [\boldsymbol{F}, \psi_i] = \tfrac{1}{2}(1+\gamma_5)\boldsymbol{\tau}\psi_i\,, \\ [\boldsymbol{F}, \psi_i^c] = -\tfrac{1}{2}(1-\gamma_5)\boldsymbol{\tau}^T\psi_i^c\,. \end{cases} \tag{5}$$

Particle and antiparticle contribute with opposite signs to $\boldsymbol{F}$, which we entitle the Fermi charge (with three components!) or Fermi spin.

Since F_1 and F_2 do not commute with the electric charge, states of definite charge cannot be diagonal in $F_{1,2}$ (any more than they can be diagonal in the charge-conjugation operator, say). Indeed it is precisely the electromagnetic field that distinguishes the members of the degenerate ψ_i doublets.

Note that the upper and lower members of ψ are positive and neutral for the nucleons, and neutral and negative for the leptons. This is summarized in the formula for the charge

$$Q = \tau_3 + l/2\,,$$

where the charge displacement l is 1 for nucleons and -1 for leptons.

2·2. *Minimal coupling.* – In addition to assuming Fermi gauge invariance of the weak interactions, we also assume that the weak interactions are specifically the interactions of this current with itself,

$$\mathcal{L}_{\text{int}} = g\boldsymbol{J}_\mu\cdot\boldsymbol{J}_\mu = \sum_{i,j}\{g[\overline{\psi}_i\gamma_\mu(1+\gamma_5)\tau_+\psi_i][\overline{\psi}_j\gamma_\mu(1+\gamma_5)\tau_-\psi_j] + \tag{6}$$

$$+\left(\frac{g}{4}\right)[\overline{\psi}_i\gamma_\mu(1+\gamma_5)\tau_3\psi_i][\overline{\psi}_j\gamma_\mu(1+\gamma_5)\tau_3\psi_j]\}\,.$$

This assumption corresponds exactly to the assumption of minimal interaction in electrodynamics.

The interaction (6) contains three kinds of terms:

a) The part involving $\tau_\pm = \frac{1}{2}(\tau_1 \pm i\tau_2)$ and $i \neq j$,

$$\sum_{i\neq j} g(i\tau_+ i)(j\tau_- j) = g[(pn)(e\nu) + (pn)(\mu\nu) + (\nu e)(\mu\nu) + \text{h. c.}]\,, \tag{7}$$

leads to the familiar parity-non-conserving V-A charge-exchange interactions. (We use an abbreviated notation in which i, j, p, n, e, μ, etc., stand for the corresponding field operators and the spin matrices $\gamma_\mu(1+\gamma_5)$ have been suppressed.)

b) The part involving $\tau_\pm$ and $i=j$

$$\sum_i g(i\tau_+ i)(i\tau_- i) = g[(pn)(np) + (\nu e)(e\nu) + (\nu\mu)(\mu\nu)] \tag{8}$$

leads to weak lepton-lepton and nucleon-nucleon scattering processes which have been already suggested by FEYNMAN and GELL-MANN ([3]).

c) The part involving τ_3 leads to

(i) weak nucleon-nucleon scattering processes,

$$\frac{g}{4}(pp\text{-}nn)(pp\text{-}nn)\,; \tag{9}$$

(ii) weak nucleon-lepton processes,

$$\frac{g}{2}(pp\text{-}nn)(2\nu\nu\text{-}ee\text{-}\mu\mu)\,; \tag{10}$$

and

(iii) weak lepton-lepton scattering processes,

$$g\{(\nu\nu)(\nu\nu) + \tfrac{1}{4}(ee)(ee) + \tfrac{1}{4}(\mu\mu)(\mu\mu) + \tfrac{1}{2}(ee)(\mu\mu) - (\nu\nu)(ee) - (\mu\mu)(\nu\nu)\}\,. \tag{11}$$

Provided the spinor fields anticommute, the V-A interaction is invariant under reordering of the four spinors. Hence some of the terms in Eqs. (9) and (11) are equivalent, except for coefficient, to those included in Eq. (8). Consequently:

a) The Feynman–Gell-Mann processes $(\nu e)(e\nu)$ and $(\nu\mu)(\mu\nu)$ are actually not expected on the present theory because of a cancellation between the terms in Eq. (8) and (11).

b) The weak process $(pn)(np)$, if it could be observed, would actually occur with a coupling constant $g/4$.

c) Other scattering processes not considered by FEYNMAN and GELL-MANN are suggested by Eq. (10).

These results, which may be subject to experimental check, are necessary consequences of our development. If τ^+ and τ^- have been introduced in order to obtain the ordinary charge-exchange interactions (7), then τ_3 must occur if a group is to be defined.

2259

2·3. *How universal is the Fermi interaction?* – Because each ψ_i was assumed to contain a neutral and a charged-particle field, pairs like $(e^- e^-)$ or $(e^- \mu^-)$ do not appear. This excludes as first-order processes the decays

$$(12) \qquad \begin{cases} \mu^- \to e^- + \gamma \qquad \text{or} \qquad e^- + e^+ + e^- \\ K^0 \to \mu^+ + e^- \qquad \text{or} \qquad \nu + \bar{\gamma} \end{cases},$$

which have, in fact, never been observed.

The Fermi gauge transformations can certainly be extended to other pairs consisting of members of a charge multiplet such as $(\Xi^0 \Xi^-)$, $(\Sigma^+ X^0)$, $(Y^0 \Sigma^-)$, where $X^0 = \frac{1}{2}(\Lambda^0 + \Sigma^0)$, $Y^0 = \frac{1}{2}(\Lambda^0 - \Sigma^0)$. The rate of β decay $\Xi^- \to \Xi^0 + e^- + \bar{\nu}$ depends on the yet-to-be-discovered $\Xi^0 - \Xi^-$ mass difference. The β decays, $\Sigma^\pm \to \Sigma^0$ proceed at a rate slower than 6 per second.

It would seem, on the other hand, to be an open question whether or not pairs like $(p\Lambda^0)$, consisting of members of *different* charge multiplets, are subject to Fermi gauge transformations. Inclusion of such a pair in the Fermi interaction was suggested by GELL-MANN (5) in order that the strange-particle decays be, at least in principle, a consequence of some universal Fermi interaction. Until we have an over-all symmetry principle assigning both weak and strong interaction properties to all particles, our philosophy ought to be to allow the presence or absence of decays like

$$(13) \qquad \Sigma, \Lambda \to n + e + \bar{\nu}$$

to tell us what is the structure seen by the Fermi interactions.

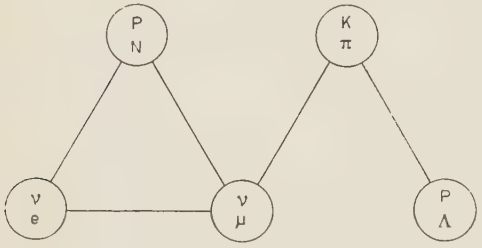

Fig. 1. – The basic weak Yukawa interaction that is assumed, along with the Puppi triangle, in the Appendix to this paper.

The Appendix to this paper presents a treatment of meson and hyperon decays based on a phenomenological universal weak Yukawa V-A interaction. Such a direct Yukawa interaction (which might actually follow from the Fermi interactions) actually gives reasonable values for the meson and hyperon decay rates. If such a weak Yukawa interaction appears as an elementary interaction alongside the conventional Puppi triangle, then the scheme of the weak interactions is that of Fig. 1, instead of the Puppi–Gell-Mann tetrahedron,

3. – Is the Fermi current conserved?

Invariance of the action integral $\int \mathcal{L} \, d^4x$ under an n-parameter group of continuous transformations is equivalent to a set of n integral conservation laws. Electromagnetic charge is, so far as we know, absolutely conserved,

so that ordinary gauge invariance must be an exact symmetry law. If the Fermi gauge transformations were absolute symmetry transformations, $\boldsymbol{F}$ would be absolutely conserved. This would give expression to the conservation of Fermi charge along with electromagnetic charge and would explain [3] the at least approximate equality of the V and A coupling constants in β and μ decay. In this section we wish to consider the limitations, imposed by the strong interactions, to the conception that $\boldsymbol{F}$ is conserved and Eq. (2) is a symmetry operation of the Lagrangian.

3·1. *Comparison of coupling constants in μ and β decay: size effects.* – Feynman and Gell-Mann, in order to explain the apparent equality of the coupling constant g^{β} and g^{μ} in β and μ decay, have considered introducing additional meson-fermion interactions so that the total Fermi current, consisting of the fermion part in Eq. (4) plus a part bilinear in the meson fields, may be conserved. Because for spinless particles the obvious analogue to γ_5 is identically zero, this is difficult to envisage theoretically. In addition, the experimental evidence on the ϱ value in μ decay and on the ratio of Gamow-Teller and Fermi coupling constants in β decay, if taken seriously, requires two different kinds of structure in these weak interactions:

a) Size effects have been invoked [6,7] in μ decay to explain the value $\varrho = (0.68 \pm 0.02) < \frac{3}{4}$ measured [8]. The simplest kind of non-locality [6] in which the (νμ) and (eν) currents are assumed to interact at two different points leads to $\varrho > \frac{3}{4}$ if the weak interaction is supposed to take place through a single intermediary field. With a more complicated three- or four-point interaction involving fermions in intermediate states, a ϱ value less than $\frac{3}{4}$ can be obtained [7]. In any case, *g^{μ} times a form factor* (~ 0.9) is what appears in the μ lifetime and what is remarkably equal to g^{β}. [9].

b) The evidence indicates [10] that the Gamow-Teller and Fermi coupling constants are not precisely equal in β decay,

$$|g_{\mathrm{A}}^{\beta}/g_{\mathrm{V}}^{\beta}| = 1.15 \pm 0.05 \,. \tag{14}$$

If the bare coupling constants are equal this can be attributed only to π or

[6] T. D. Lee and C. N. Yang: *Phys. Rev.*, **108**, 1611 (1957).

[7] S. Bludman and A. Klein: *Phys. Rev.*, **109**, 559 (1958).

[8] C. P. Sargent, M. Rinehart, L. M. Lederman, and K. G. Rogers: *Phys. Rev.*, **99**, 885 (1955); K. Crowe: *Bull. Am. Phys. Soc.*, Ser. II, **2**, 206 (1957); L. Rosenson: *Phys. Rev.*, **109**, 958 (1958).

[9] This observation is originally due to R. Gatto, *UCRL*: (private communication).

[10] See the review by L. Michel: *Rev. Mod. Phys.*, **29**, 223 (1957).

K meson corrections that are different for V and A couplings ([11]). If the Fermi current were absolutely conserved there would be no such corrections.

The present data thus indicate finite but small structure corrections to the idea of a point Fermi interaction with exactly universal coupling constants. This interpretation is subject to additional verification in two ways:

a) g^{μ} and g^{β} can be carefully compared by measuring the ratio of μ capture to K capture in the same nucleus. Because, in the two cases, the same pion structure but far different momentum transfers are involved, this experiment probes the μ-decay structure invoked in connection with the ϱ value.

b) The effect of the pion cloud can be studied by comparing μ capture and μ decay in which the same momentum transfer is involved. If the μ-capture/μ-decay ratio were studied as a function of Z, one might hope to smooth out the uncertainties connected with nuclear structure.

Judging from the magnitude of the deviation of ϱ from $\frac{3}{4}$ and of g_{A} from g_{V} in β decay, $(10 \div 20)\,\%$ structure effects might be expected in experiments of this kind.

3·2. *Role of the strong interactions.* – If all particles were originally massless, so that the Fermi gauge transformations were symmetry operations of the Lagrangian, the physical particles would, in the presence of the Fermi interactions, remain of zero mass and of definite (left) handedness. They would still remain so in the presence of the minimal electromagnetic interactions, which are of the form $\bar{\psi}\gamma_{\mu}\psi A_{\mu}$. Physical particles would then be labeled entirely by the quasigeometrical attributes of handedness and charge. Anomalous magnetic-moment interactions $\bar{\psi}\sigma_{\mu\nu}\psi F^{\mu\nu}$ and scalar or pseudoscalar meson-interaction terms in the Lagrangian, on the other hand, do not admit the Fermi gauge transformations. This tempts one to speculate that the inertial terms $\bar{\psi}m\psi$, like any $\bar{\psi}\sigma_{\mu\nu}F^{\mu\nu}\psi$ terms, are related to those same mysterious effects that introduce the strong meson couplings $\bar{\psi}\gamma_5\boldsymbol{\tau}\cdot\boldsymbol{\varphi}\psi$ or $\bar{\psi}\varphi\psi$ into the Lagrangian. According to this view, all these effects are common consequences of the breakdown of the symmetry, revealed in the weak interactions, by the introduction of some dimension of mass or length ([12]).

This situation corresponds qualitatively to the fact the neutrino, which has neither strong mesonic nor electromagnetic coupling, is massless, whereas baryons that have strong interactions are heavy, and leptons that have electromagnetic but not mesonic interactions, are light. It is important to note that because V and A interactions admit the Fermi gauge group, the lepton mass

([11]) R. Finkelstein and S. A. Moszkoswki: *Phys. Rev.*, **95**, 1695 (1954); S. S. Gerschtein and Ia. B. Zel'dovich: *Soviet Physics* (*JETP*), **2**, 576 (1956); B. Stech: *Zeits. f. Phys.*, **145**, 319 (1956); M. Ross: *Phys. Rev.*, **104**, 1736 (1956).

([12]) See J. Schwinger: *Ann. Phys.*, **2**, 407 (1957).

cannot be attributed entirely to minimal electromagnetic interaction, but must be due, in the first place, to those same mysterious effects which introduce a parameter of mass dimensionality.

One interesting way for a symmetry law to be broken has been suggested by the work of HEISENBERG[13]: perhaps the Lagrangian contains no mass terms and admits the Fermi gauge group, but regularity conditions on the propagators produce the observed masses, destroy the symmetry, and at the same time introduce the effects of strong interaction. (In HEISENBERG's work the Lagrangian contained the isosymmetry of the strong interactions which was somehow destroyed by the weaker electromagnetic effects introduced along with the commutation relations. We find it easier to see the greatest symmetry, closest to the vacuum, in the *weakest* interactions—gravitation, β decay and meson and hyperon decay, electromagnetism because these interactions seem more susceptible to a « geometric » treatment. We see little hope for incorporating the strong interactions into the space-time continuum. The attempt to develop interaction as consequence of a local symmetry principle, the idea of the $\boldsymbol{b}$ field, has not been fruitful where originally proposed in connection with the π-meson interactions[14,15] but, as discussed in the next section, is a possibility for the weak interactions.)

4. – Local Fermi gauge transformations.

In Eq. (2) only restricted Fermi gauge transformations ($\boldsymbol{\omega}$ = arbitrary constant) were considered. If now $\boldsymbol{\omega}$ is promoted to be an arbitrary vector *function* of space-time $\boldsymbol{\omega}(x)$, then a vector-meson field transforming infinitesimally as

$$\boldsymbol{b}_\mu \to \boldsymbol{b}_\mu + 2\boldsymbol{b}_\mu \times \boldsymbol{\omega} + \partial_\mu \boldsymbol{\omega} \tag{15}$$

must be introduced [14] in order that the derivative

$$D_\mu \psi = (\partial_\mu - i\tfrac{1}{2}(1+\gamma_5)\boldsymbol{\tau}\cdot\boldsymbol{b}_\mu)\psi \tag{16}$$

transform covariantly. This approach has the merit of leading directly to a vector interaction

$$\mathcal{L}_{\text{int}} = \boldsymbol{J}_\mu \cdot \boldsymbol{b}_\mu , \tag{18}$$

with the current defined in Eq. (4), without the additional assumption of a specific minimal current interaction.

If this $\boldsymbol{b}$ field is to be interpreted as a real particle, its quanta must be massive in order to explain why $\boldsymbol{b}$ particles have not been detected as products of K- or π-meson decay and in order to explain the effectively local nature of the Fermi interaction. At least two difficulties argue against a

[13] W. HEISENBERG: *Rev. Mod. Phys.*, **29**, 269 (1957).
[14] C. N. YANG and R. L. MILLS: *Phys. Rev.*, **96**, 191 (1954).
[15] S. A. BLUDMAN: *Phys. Rev.*, **100**, 372 (1955).

realistic interpretation of the $\boldsymbol{b}$ field. In the first place, as mentioned above, such an intermediary particle would raise the μ-decay ϱ value above $\frac{3}{4}$, while presently published measurements report a value $\varrho = 0.68 \pm 0.02$ ([16]). In the second place, any charged spin-one particle has a singular non-renormalizable electromagnetic interaction.

Incidentally, beucase of its V coupling, $\boldsymbol{b}$-meson corrections cannot alter the basic V-A lepton interaction to effect the calculated $\pi \to e + \nu / \pi \to \mu + \nu$ ratio. As noted above, a $\boldsymbol{b}$-meson cannot be directly responsible for all the mass of the μ meson.

5. – Concluding discussion.

This development presupposes that we can treat the weak interactions, at least semiquantitatively, without attempting to deal with the strong interactions. A Fermi current has been derived from a continuous group of transformations, which presumably would be symmetry operations in the absence of strong-interaction effects. The weak interactions are supposed to be the interactions of this Fermi current with itself, and possibly with spin-zero mesons.

This assumption goes beyond earlier ones ([3-5]) in three respects:

a) A continuous group of transformations described in Eq. (2), has been introduced here in frank analogy with gauge invariance, general covariance and isotopic spin invariance, in order to give expression to the at-least-approximate conservation of Fermi charge observed in the near equality of Fermi coupling constants. (As stated in Sect. 3 we imagine the Fermi gauge invariance to be blocked, at least partially, by those same phenomena giving rise to strong interactions and mass effects.) Invariance under a discrete group like that in Eq. (2′) does not imply any current conservation law at all.

b) We incorporate the three charge operators τ_+, τ_-, and τ_3 into our symmetry transformation instead of assuming ([3-5]) directly the charge exchange character of the interaction. Because we allow charge-retention Fermi interactions (through τ_3) in addition to the charge-exchange interactions (7) and (8) we expect weak neutrino-nucleon but no neutrino-electron scattering processes.

c) Since we see no reason why the Fermi interaction need extend to *all* fermion pairs, we do not expect hyperon β decays involving strangeness change. If this turns out to be the case, we must assume an additional universal weak Yukawa process to describe meson and hyperon decays.

The consequence of assuming Fermi gauge invariance are in any case far-reaching enough to permit an experimental decision.

([16]) Radiative corrections, which effectively lower the ϱ value, are being investigated for μ-decay through an intermediary $\boldsymbol{b}$ field, in collaboration with H. S. Wong.

Appendix

In this appendix we wish to record the results of assuming a weak interaction between a meson field φ of mass M, and particular pairs of fermions

$$(g/M)2^{-\frac{1}{2}}\partial_\mu\varphi\cdot\bar{\psi}\gamma_\mu(1+\gamma_5)\psi\,. \tag{A.1}$$

As suggested in the right side of Fig. 1, this interaction is assumed to involve only baryons (PΛ), (NΛ), (PΣ), (NΣ), (ΞΛ) belonging to *different* charge multiplets, and only the lepton pair (νμ). From the rate $0.39\cdot10^8\ \mathrm{s}^{-1}$ for π decay we fix

$$g^2/4\pi = 3.67\cdot10^{-15}\,. \tag{A.2}$$

The other decay rates are then calculated from this one coupling constant and compared with experiment in Table I. The rate for $\mathrm{K}\to\mu+\nu$ has been given previously ([17]). For the baryon decays, no attempt has been made to calculate branching raties that would follow, for example, from the $\Delta I=\frac{1}{2}$ rule.

This weak Yukawa interaction discriminates between muon and electron in such a way as to allow the decay $\pi\to\mu+\nu$ while preventing any appreciable $\pi\to\mathrm{e}+\nu$ decay. The strong π coupling to (PN) of course still allows, in addition, π decay through the Fermi interactions that are known to involve ((PN)(νe) as well as (PN)(νμ). The experimental upper limits on the ratio of decay modes of e and μ suggest, however, that these Fermi interactions can be responsible for no more than one tenth of all π decays. (A recent estimate ([18]) of π decay through the channel $\pi\to\mathrm{n}+\bar{\mathrm{n}}\to\mu+\nu$ shows appreciable damping of the pion-nucleon coupling constant. This illustrates how this channel may not contribute significantly in comparison with the direct Yukawa coupling assumed here. It also shows how the amplitude for K decay through $\mathrm{y}+\bar{\mathrm{n}}$ can be comparable with that for π decay through $\mathrm{n}+\bar{\mathrm{n}}$ even though the strong coupling constants are somewhat unequal.)

The interaction (A.1) leads to a ratio of p-wave to s-wave emission

$$\mathrm{tg}\,\nu = [(1-X_-^2)/(1-X_+^2)]^{\frac{1}{2}}\,,$$

which is close to unity in hyperon decay. Here $X_\pm = M/(M_1\pm M_2)$, where M_1 and M_2 are the baryon masses. In the decay of polarized hyperons ([19])

([17]) S. A. Bludman and M. A. Ruderman: *Phys. Rev.*, **101**, 910 (1956). Oneda and collaborators, in *Nuclear Physics*, **1**, 445 (1956) and earlier papers, obtain a different rate for $\mathrm{K}\to\mu+\nu$ because, in the interaction (A1), they omit the factor M^{-1} which is different for π and for K decay.

([18]) M. L. Goldberger and S. B. Treiman: *Phys. Rev.*, **110**, 1178 (1958).

([19]) T. D. Lee and C. N. Yang: *Phys. Rev.*, **108**, 1645 (1957).

large positive asymmetries $\alpha = \sin 2\nu$ and longitudinal polarizations $P_L = -\alpha$ are therefore obtained. The transverse nucleon polarization $P_T = \cos 2\nu$ are, on the other hand, in the plane defined by the decay and the hyperon spin, and relatively small. In this calculation the small effects of final-state interaction have been neglected.

The experimental evidence indicates ([20]) $|\alpha| > 0.77 \pm 0.16$ in Λ decay, which is consistent with the calculated value. The preliminary data probably indicate small asymmetries in Σ decay ([21]), which would be in disagreement with the calculated values listed in Table I. (Such an experimental result would also disagree with the $\Delta I = \frac{1}{2}$ rule, which predicts large asymmetries of opposite signs in at least two of the Σ-decay modes.) In any case the chirality-non-conserving strong interactions can easily wash out the asymmetries and polarizations calculated on the basis of the simple V-A interaction.

TABLE I. – *Decays involving mesons.*

The rates are calculated from the universal weak Yukawa interaction (A1) with coupling constant (A2) derived from the π lifetime. The asymmetry α and transverse polarization P_T of the decay baryon in hyperon decay are given in the convention of LEE and YANG ([19]).

Process	Calculated decay rate (s^{-1})	Observed decay rate (s^{-1}) ([22])	α	P_T
$K \to \mu + \nu$	$55 \cdot 10^6$ ([17])	$48 \cdot 10^6$	—	—
$\Lambda^0 \to p + \pi^-$	$0.10 \cdot 10^{10}$	$0.234 \cdot 10^{10}$	0.89 ([23])	0.45
$\Lambda^0 \to n + \pi^+$		$0.126 \cdot 10^{10}$		
$\Sigma^+ \to p + \pi^0$	$0.62 \cdot 10^{10}$	$0.59 \cdot 10^{10}$	0.98	0.18
$\Sigma^+ \to n + \pi^+$		$0.69 \cdot 10^{10}$		
$\Sigma^- \to n + \pi^-$		$0.64 \cdot 10^{10}$		
$\Xi^- \to \Lambda^0 + \pi^-$	$0.21 \cdot 10^{10}$	$(0.005 - 0.2) \cdot 10^{10}$	0.95	0.30

([20]) L. STEVENSON: *A.P.S. Stanford meeting*, 1957.

([21]) W. H. BARKAS: (*UCRL*) private communication.

([22]) The experimental transition rates into each mode are taken from the survey by M. GELL-MANN and A. H. ROSENFELD, Jr.: *Ann. Rev. Nuclear Sci.*, **7**, (1957).

([23]) J. J. SAKURAI: *Phys. Rev.*, **108**, 491 (1957).

RIASSUNTO (*)

La forma V-A dell'interazione di Fermi non conservante la parità si deriva da un principio d'invarianza rispetto a un gruppo continuo di trasformazioni in analogia colla derivazione ordinaria dell'invarianza di gauge della minima interazione elettromagnetica delle particelle cariche. Questa ipotesi è per la forma delle interazioni di Fermi una restrizione più severa di quella invocata da SUDARSHAN e MARSHAK, GELL-MANN e FEYNMAN, e SAKURAI e conduce ad ulteriori predizioni suscettibili di verifica sperimentale. Se queste trasformazioni fossero trasformazioni della simmetria dell'intera lagrangiana, le costanti di accoppiamento del decadimento β e μ sarebbero esattamente uguali. Si discutono le conseguenze derivanti dall'estensione di questa invarianza di gauge secondo Fermi a un gruppo dipendente da funzioni dello spazio-tempo. Si considera la possibilità che le interazioni di Fermi che comportino un cambiamento di stranezza siano proibite, e si tabulano i risultati derivanti dall'ipotesi di una interazione universale V-A di Yukawa non conservante la parità. Tale interazione di Yukawa, che richiede una nuova costante di accoppiamento conduce a ragionevoli tassi di decadimento dei mesoni K e degli iperoni e permette il decadimento dei mesoni π in $\mu+\nu$ senza apprezzabile decadimento in $e+\nu$.

(*) *Traduzione a cura della Redazione.*

Note on the Decay of ^{82}Sr.

V. Sangiust

Istituto di Fisica Sperimentale del Politecnico - Milano

(ricevuto il 6 Maggio 1958)

Summary. — γ and X radiation accompanying the decay of ^{82}Sr have been investigated. γ rays of 775 and 1400 keV have been found; ^{82}Rb daughter of ^{82}Sr, is shown to decay through β^+ emission, not only to the ground state but also to excited levels of ^{82}Kr.

1. – Introduction.

^{82}Sr can be obtained through a spallation reaction by bombarding rubidium with protons of 40 MeV and over; it decays through electron capture to the ground level of ^{82}Rb with a half-life of 25 days; no transitions to the 6.3 h ^{82m}Rb isomeric state have been observed within a maximum limit of 0.1% ([1,2]).

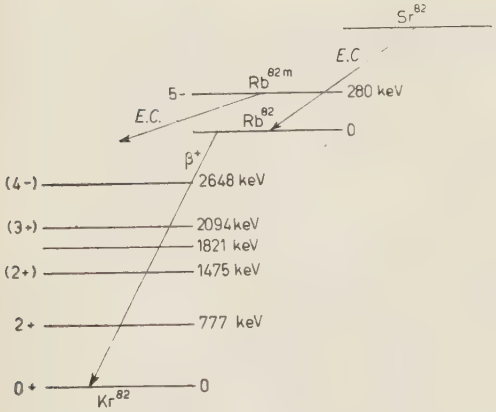

Fig. 1. – Decay scheme of ^{82}Sr.

^{82}Rb (1.25 min) decays through β^+ emission to ^{82}Kr ground state, by an allowed transition; the maximum energy of the β^+ spectrum was found to be at 3.15 MeV ([3]). β^+ transitions to the ^{82}Kr excited levels and γ of disexcitation of these levels have not been observed.

^{82m}Rb decays to ^{82}Kr through electron capture (94%) and β^+ (6%).

([1]) S. V. Castner and D. H. Templeton: *Phys. Rev.*, **88**, 1126 (1952).
([2]) P. Kruger and N. Sugarman: *Phys. Rev.*, **90**, 158 (1953).
([3]) L. M. Litz, S. A. Ring and W. R. Bahlwell: *Phys. Rev.*, **92**, 288 (1953).

On this basis the decay scheme shown in Fig. 1 has been proposed ([4]).

A detailed investigation of the radiation from ^{82}Sr seemed useful to ascertain the possibility of ^{82}Rb decaying to ^{82}Kr excited levels, and to set a precise limit to this type of decay.

2. – Measuring technique.

^{82}Sr was obtained by bombarding rubidium with protons of 40 MeV in the Harwell cyclotron. ^{85}Sr and ^{83}Sr were produced at the same time; ^{85}Sr (half-life 65 days) contributed to the activity by less than 10% and ^{83}Sr (half-life of 33 h) decays to Rb which was separated chemically from the Sr.

The γ radiation from the sample was investigated with a scintillation spectrometer; a cylindrical NaI(Tl) crystal ($1\frac{1}{2}$ in. in diameter and 1 in. high) and a Dumont 6292 photomultiplier were used. The X-radiation accompanying the electron capture was examined with a proportional counter spectrometer (thin window); the counter (3 in. in diameter, 10 in. long) was filled with a mixture of A (90%) and CH_4 (10%) at the pressure of 1.5 atm.

The pulse height was measured by means of a ten-channel fast analyzer ([5]). X-γ and γ-γ coincidence technique was used both between the proportional counter and the γ scintillation spectrometer and between two γ scintillation spectrometers. The coincidence circuit (resolving time $2.5 \cdot 10^{-6}$ s) was triggered only by pulses belonging to a selected photopeak.

3. – Results.

^{82}Sr (half-life 25 days) and ^{82}Rb (half-life 1.25 min) are in equilibrium in the sample, whose activity decays with the half-life of ^{82}Sr.

The half-life of ^{82}Sr was measured with a Geiger counter following the β^+ activity for a period of four half-lives. The value of

$$(25 \pm 0.4)\ \mathrm{d}\,,$$

was obtained, in agreement with data previously reported ([1,3]). An inspection of the γ radiation of the sample in the γ scintillation spectrometer showed the presence of the very intense annihilation peak at 511 keV due to the positrons of ^{82}Rb. At higher energy two weak peaks were observed, of

([4]) D. Stromington, G. M. Hollander and G. T. Seaborg: *Table of Isotopes* (1957), University of California.

([5]) S. Colombo, C. Cottini and E. Gatti: *Nuovo Cimento*, **5**, 748 (1957).

(770±10) keV and (1400±70) keV. The intensities of these lines was found to decay with the same half-life of ^{82}Sr, and so they are not due to impurity present in the sample. No γ-rays of lower energy were found (see Table I).

Table I.

Energies (keV)	Relative intensity
511	100
770 ± 10	2
1400 ± 70	< 0.5

It seems correct to associate these γ radiations at 770 and 1400 keV with the excited levels of ^{82}Kr of the same energy.

Such γ-rays were also found in the decays of ^{82}Br ([6,8]) and ^{82m}Rb ([9,10]).

The γ spectrum in the sample triggered by X-rays at 14 keV coming from the electron capture showed no peak at 770 and 1400 keV (see Table II).

Table II.

Energies (keV)	Relative area of photopeaks
14 (triggering peak)	100
770 ± 10	$< 8 \cdot 10^{-3}$
1400 ± 70	$< 4 \cdot 10^{-3}$

γ-rays of 770 and 1400 keV are practically unconverted ([6]). From this fact and from the data of Table II a maximum limit of 0.2% can be set as the percentage of the decay of ^{82}Sr through the excited state of ^{82m}Rb (6.3 h) which is known to decay through electron capture to ^{82}Kr. This result is in agreement with that of ([3]).

On the contrary the γ spectra of the sample in coincidence with the annihilation peak at 511 keV showed again the lines at 770 and 1400 keV. See Table III.

([6]) R. C. Waddel and E. N. Jensen: *Phys. Rev.*, **102**, 816 (1956).

([7]) S. Hultberg and A. Hedgran: *Arkiv for Fysik*, **11**, 369 (1957).

([8]) V. S. Dubey, C. E. Mandeville and M. A. Rothman: *Phys. Rev.*, **103**, 1430 (1956).

([9]) D. G. Karraker and D. H. Templeton: *Phys. Rev.*, **80**, 646 (1950).

([10]) C. M. Huddleston and A. C. G. Mitchell: *Phys. Rev.*, **88**, 1350 (1952).

TABLE III.

Energies (keV)	Relative areas of photopeak
511 (triggering peak)	100
770 ± 10	$1.4 \cdot 10^{-1}$
1400 ± 70	$< 1.7 \cdot 10^{-2}$

4. – Conclusions.

The results can be summarized and interpreted as follows:

1) ^{82}Sr decays through electron capture to the ground level of ^{82}Rb (1.25 min).

^{82m}Rb (6.3 h) is not the daughter of ^{82}Sr with a maximum limit of 0.2%, in agreement with the data of [1,3].

2) ^{82}Rb decays through β^+ emission not only to ^{82}Kr ground state, but also to 770 and 1400 keV excited levels. From the data of Tables I and III, the branching ratios can be deduced. In Table IV, are reported the maximum energy of the β^+ spectra, the branching, and the values of log *ft* [11] for the three transitions involved, which appear to be alloved transitions. The decay scheme shown in Fig. 2 is consequently proposed.

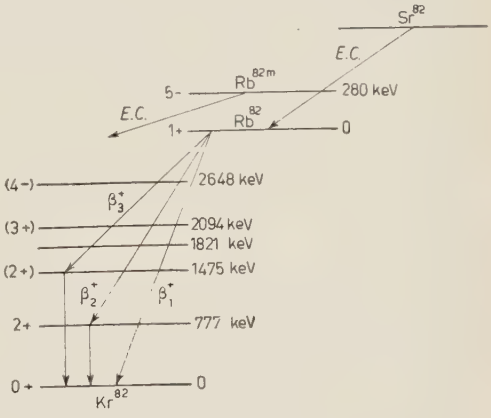

Fig. 2. – Proposed decay scheme of ^{82}Sr.

TABLE IV.

Maximum energies (MeV)	%	log *ft*
3.15 (β_1^+)	95	4.35
2.38 (β_2^+)	4	5.2
1.75 (β_3^+)	< 1	5.3

[11] S. A. MOSKOWSKI: *Phys. Rev.*, **82**, 35 (1951).

The value of $1+$ for spin and parity of ^{82}Rb ground state seems to be probable.

* * *

Thanks are due to Proff. G. Bolla, A. Bisi and L. Zappa for their kind interest in this work.

RIASSUNTO

È stata studiata la radiazione γ e X che accompagna il decadimento dello ^{82}Sr. Sono stati trovati raggi γ di 770 e 1400 keV e si è mostrato che il ^{82}Rb, figlio dello ^{82}Sr, decade per emissione β^+ non solo al livello fondamentale, ma anche ai livelli eccitati di 770 e 1400 keV del ^{82}Kr.

IL NUOVO CIMENTO Vol. IX, N. 3 1° Agosto 1958

Neutral Pion Decay (*).

M. L. Goldberger and S. B. Treiman

Palmer Physical Laboratory, Princeton University - Princeton, N. J.

(ricevuto il 10 Maggio 1958)

Summary. — Neutral pion decay is studied quantitatively with dispersion relation techniques. The process is pictured as proceeding mainly through pion disintegration into baryon pairs, the latter annihilating to produce the photons. In detail we take into account only the nucleon pair, as representative of baryon pair contributions generally. The final expression for the decay rate has a structure very different from what one obtains in perturbation theory. It turns out, however, that the numerical results are not appreciably different.

1. – Introduction.

The dispersion relation techniques which we have recently made use of in a quantitative discussione of $\pi \to \mu + \nu$ decay [1] can be extended without much change to the problem of $\pi^0 \to 2\gamma$ decay; and we shall summarize here some results obtained in connection with the latter process.

As for $\pi \to \mu + \nu$ decay, we pictured this process as occuring through pion disintegration into a nucleon pair, the latter annihilating via axial vector Fermi coupling to produce the leptons. In the approximation adopted no divergent expressions were encountered—in contrast to the perturbation theoretic situation—and the final result for the decay rate turned out to be in remarkably close agreement with experiment. In the case of π^0 decay, we again picture the process as occuring through pion disintegration into a nucleon pair, the latter now annihilating to produce a pair of photons. In this process per-

(*) Supported in part by the Air Force Office of Scientific Research, Air Research and Development Command.

(1) M. L. Goldberger and S. B. Treiman: *Phys. Rev.* (to be published).

turbation theory leads to a finite result. On the experimental side, one has at present only an upper limit on the π^0 lifetime, namely $\tau \lesssim 1 \cdot 10^{-15}$ s ([2]), a value consistent with the result of perturbation theory ([3]). For this reason there is at present no theoretical « problem » in connection with π^0 decay. Our concern is rather methodological: namely, since there is no overwhelming reason to believe in perturbation theory, it is of some interest whenever possible to compare perturbation theory with other schemes of approximation. As a matter of fact, in the approximation adopted here, the final expression for the π^0 decay rate has a structure very different from that of perturbation theory. Nevertheless, the actual numerical predictions are not appreciably different.

A second remark needs to be made. In our discussion of $\pi \to \mu + \nu$ decay we neglected, among other things, possible contributions from intermediate hyperon pairs. We could do so since at the present time there is no evidence for (or against) *direct* Fermi couplings of hyperon pairs (of total strangeness zero) with leptons. But in connection with π^0 decay there is no doubt such hyperon pairs can annihilate into photons, with amplitudes comparable to that for nucleon annihilation.

Indeed, on the global symmetry model ([4]) one finds in perturbation theory ([5]) that cascade pairs and nucleon pairs both contribute, with amplitudes of comparable magnitude but opposite sign. Despite the partial cancellation, however, the final result is still consistent with the experimental upper limit on the π-lifetime. In any case, there is no reason now known to expect that significant cancellations would survive in a more accurate treatment of the problem; and we shall therefore take into account only the nucleon pairs, as representative of baryon pair contributions generally.

2. – Outline of calculation.

The dispersion relation methods employed here have been expounded in connection with the related problem of charged pion decay ([1]). The present analysis is therefore set down only in brief outline, in order to bring out the nature of the approximations and assumptions adopted.

([2]) G. Harris, J. Orear and S. Taylor: *Phys. Rev.*, **106**, 327 (1957).

([3]) R. J. Finkelstein: *Phys. Rev.*, **72**, 415 (1947); J. Steinberger: *Phys. Rev.*, **76**, 1180 (1949); H. Fukuda and Y. Miyamoto: *Prog. Theor. Phys.* (*Japan*), **4**, 347 (1949).

([4]) M. Gell-Mann: *Phys. Rev.*, **106**, 1296 (1957).

([5]) J. Tiomno: *Nuovo Cimento*, **6**, 256 (1957).

In the standard way, the S-matrix element for π^0 decay is written

$$(1) \qquad S = \langle q(\mu), k(\nu) \text{ «out »} | p \rangle = \\ = i(2\pi)^4 \, \delta(p - k - q) \frac{1}{\sqrt{2p_0}} \langle q(\mu), k(\nu) \text{ «out »} | J | 0 \rangle ,$$

where p is the pion four-momentum and μ and ν refer to the polarization states of the photons of momenta q and k respectively; J is the source of the π^0 field: $(m_\pi^2 - \Box)\varphi_\pi = J$. The matrix element is given by

$$(2) \qquad M_{\mu\nu} = \sqrt{2} \sqrt{4k_0 q_0} \langle q(\mu), k(\nu) \text{ out } | J | 0 \rangle = \\ = i\sqrt{2q_0} \int \mathrm{d}^4x \exp [-ik \cdot x] \langle q(\mu) | [j_\nu(x), J] \theta(x) | 0 \rangle ,$$

where j_ν is the source of the electromagnetic field. An equal-time commutator which generally appears makes no contribution here. On general invariance grounds, we know that the matrix element has the structure

$$(3) \qquad M_{\mu\nu} = -i\varepsilon_{\mu\nu\lambda\sigma} k_\lambda q_\sigma F[(k+q)^2] .$$

It is not difficult to show that $F(\xi)$ satisfies a standard dispersion relation and we assume there need be no subtractions:

$$(4) \qquad F(\xi) = \frac{1}{\pi} \int \frac{\operatorname{Im} F(-\xi')}{\xi' + \xi - i\varepsilon} \, \mathrm{d}\xi' .$$

Writing $M_{\mu\nu} = D_{\mu\nu} + iA_{\mu\nu}$, we obtain the absorptive part $A_{\mu\nu}$ in the usual way by inserting in (2) a sum over intermediate states $|s\rangle$; one half the sum of « in » and « out » states is assumed, thought not explicitly written,

$$(5) \qquad A_{\mu\nu} = \pi\sqrt{2q_0} \sum_s \langle q(\mu) | j_\nu | s \rangle \langle s | J | 0 \rangle \, \delta(s - k - q) .$$

Terms with j_ν and J interchanged make no contribution. The states $|s\rangle$ which contribute must have zero nucleon number and must transform like a pseudoscalar. The lowest mass state which can contribute is therefore the three-pion state. This is too difficult to handle: and in line with our picture of π^0 decay proceeding through nucleon pairs, we shall suppose that the most important intermediate state is the nucleon pair state (which, as mentioned earlier, we take to be representative of baryon pair contributions generally). We therefor approximate (5) by writing.

$$(6) \qquad A_{\mu\nu} = \pi\sqrt{2q_0} \sum_{N\bar{N}} \langle q(\mu) | j_\nu | N\bar{N} \rangle \langle N\bar{N} | J | 0 \rangle \, \delta(N + \bar{N} - k - q) .$$

The second factor has the structure

$$\langle N\bar{N} \text{ « out »} | J | 0 \rangle = \sqrt{\frac{m^2}{N_0 \bar{N}_0}}\, G\bar{u}(N) i\gamma_5 \tau_3 v(\bar{N}) K[(N+\bar{N})^2] , \tag{7}$$

where u and v are respectively particle and antiparticle spinors, G is the pion-nucleon coupling constant ($G^2/4\pi \approx 15$) and $K(-m_\pi^2) = 1$. A discussion of the function $K(\xi)$ is given in reference [1].

We turn now to a discussion of the first factor in (6). This is essentially the matrix element for nucleon pair annihilation into photons. Although we require it for physical values of the momenta involved, we cannot appeal to experiment for information concerning this rare process. It can be regarded as an analytical continuation of nucleon Compton scattering but rather than pursue this approach here we discuss the annihilation process by means of dispersion relation techniques. The continuation method will be described elsewhere.

Neglecting an equal-time commutator (whose contribution is absorbed into subtractions to be discussed later), we have

$$N_{\mu\nu} = \left(\frac{2q_0 N_0 N_0}{m^2}\right)^{\frac{1}{2}} \langle q(\mu) | j_\nu | N\bar{N} \text{ « in »} \rangle = \tag{8}$$

$$= -i \left(\frac{2q_0 N_0}{m}\right)^{\frac{1}{2}} \bar{v}(\bar{N}) \int \mathrm{d}^4x \exp\,[i\bar{N}\cdot x] \langle q(\mu) | [j_\nu(0), f(x)] \theta(-x_0) | N \rangle ,$$

where f is the source of the nucleon field and $\bar{v}(\bar{N})$ is a negative energy spinor satisying $\bar{v}(\bar{N})(i\gamma \cdot \bar{N} - m) = 0$. The general structure of $N_{\mu\nu}$ is quite complicated. Imposing the requirements of gauge and charge conjugation invariance, one finds that it can be expressed as a sum of six independent covariants. Only a particular linear combination of these six is relevant for the present purposes, so we shall not describe the general decomposition. The structure of the term, call it $N^{(1)}_{\mu\nu}$, which makes a non-vanishing contribution to (6) is

$$N^{(1)}_{\mu\nu} = \varepsilon_{\mu\nu\lambda\sigma} k_\lambda q_\sigma \bar{v}(\bar{N}) \gamma_5 \tau_3 u(N) Q , \tag{9}$$

where $k = N + \bar{N} - q$ and Q is a scalar function formed from k, q, N, $\bar{N}$. We may limit our attention to $k^2 = q^2 = 0$, in which case $N_{\mu\nu}$ describes precisely the pair annihilation into two photons, as mentioned above.

There is a simple way to obtain Q, given $N_{\mu\nu}$. One needs only multiply $N_{\mu\nu}$ by the covariant $\bar{u}(N)\gamma_5 v(\bar{N})$ and sum over the spin states of N and $\bar{N}$. One finds

$$\frac{(N+\bar{N})^2}{8m^2} \varepsilon_{\mu\nu\varrho\sigma} k_\varrho q_\sigma Q = \sum_{\text{spins}} N_{\mu\nu} \bar{u}(N) \gamma_5 v(\bar{N}) . \tag{9'}$$

The factor $\varepsilon_{\mu\nu\sigma\varrho}k_\varrho q_\sigma$ can also be projected out, but this is unnecessary, since exactly this factor must appear in conjunction with Q.

For dispersion relation purposes it is convenient to regard Q as a function of the two independent scalar products

$$(10)\qquad \begin{cases} \nu = -\dfrac{(\bar{N}+k)\cdot(N+q)}{4m}\,, \\ \Delta^2 = \dfrac{1}{4}(N-q)^2 = \dfrac{1}{4}(\bar{N}-k)^2\,. \end{cases}$$

These are the analogs of the « brick-wall » variables used in discussions of pion-nucleon scattering ([6]). We shall assume that $Q(\nu, \Delta^2)$ satisfies a dispersion relation in ν, for fixed Δ^2. The nature of the assumed dispersion relation, will be discussed later.

Before going on to a discussion of the amplitude Q, we record here the result of inserting (7) and (9) into (6) and carrying out the implied integrations and spin summations to find $A_{\mu\nu}$ and hence, via (3), Im F. One finds

$$(11)\quad \mathrm{Im}\,F[(k+q)^2] = \frac{\pi G}{(2\pi)^3}\int \frac{\mathrm{d}^3 n\,\mathrm{d}^3\bar{n}}{N_0\bar{N}_0}\,(N+\bar{N})^2\,\mathrm{Re}\,(K^*Q)\,\delta(N+\bar{N}-k-q)\,.$$

Let us now write $N^{(1)}_{\mu\nu} = D'_{\mu\nu} + iB_{\mu\nu}$. For the absorptive part $B_{\mu\nu}$ we find, in the familiar way,

$$(12)\quad B_{\mu\nu} = -\pi\sqrt{2q_0}\sqrt{\frac{\bar{N}_0}{m}}\,\bar{v}(\bar{N})\sum_s \big\{\langle q(\mu)|j_\nu|s\rangle\; s|f|N\rangle\,\delta(s-N-\bar{N}) - \\ - \langle q(\mu)|f|s\rangle\langle s|j_\nu|N\rangle\,\delta(s+\bar{N}-q)\big\}\,.$$

The state of lowest mass which contributes to the first term is just the one pion state. From there we would proceed through a series of configurations involving 3, 5, ... pions until we reached a state consisting of a nucleon-antinucleon pair. The evaluation of this contribution involves the product $\langle q(\mu)|j_\nu|N'\bar{N}'\rangle\langle N'\bar{N}'|f|N\rangle$, the first factor of which is the quantity $B_{\mu\nu}$ whereas the second is proportional to the amplitude for nucleon-antinucleon scattering. If this were known we would be led then to a set of integral equations for the various covariants involved in $B_{\mu\nu}$, the solution of which poses a much more formidable problem than we are prepared to undertake.

The second term in Eq. (12) receives its lowest mass contribution from the one nucleon state. Next we encounter that of one nucleon and one pion.

([6]) M. Goldberger: *Proceedings of the Sixth Annual Rochester Conference*, (1956), pp. 1-15.

Both of the factors $\langle q(\mu)|f|N'\pi\rangle\langle N'\pi|j_\nu|N\rangle$ are proportional, essentially, to the amplitude for photopion production and in principle quite a good deal could be said about this contribution. We shall not pursue the matter here but content ourselves in the present note to a consideration of the lowest mass contributions in every case: we take the one pion state for the first term in Eq. (12) and the one nucleon state for the second term. Thus we approximate $B_{\mu\nu}$ by

$$B_{\mu\nu} = -\pi\left(\frac{2q_0N_0}{m}\right)^{\frac{1}{2}}\bar{v}(\bar{N})\Big\{\sum_{p'}\langle q(\mu)|j_\nu|p'\rangle\langle p'|f|N\rangle\,\delta(p'-N-\bar{N}) - \sum_{N'}\langle q(\mu)|f|N'\rangle\langle N'|j_\nu|N\rangle\,\delta(N'+\bar{N}-q)\Big\}, \tag{13}$$

where p' and N' denote respectively the momentum of intermediate pion and nucleon.

Consider first the one pion contribution. The matrix element $\langle p'|f|N\rangle$ is related to the pion-nucleon vertex function. In fact one has

$$\bar{v}(\bar{N})\langle p'|f|N\rangle\,\delta(p'-N-\bar{N}) = \frac{i}{\sqrt{2p_0'}}\sqrt{\frac{\bar{m}}{N_0}}\,G\bar{v}(\bar{N})\gamma_5\tau_3 u(N)\,\delta(p'-N-\bar{N})\,. \tag{14}$$

The factor $\langle q(\mu)|j_\nu|p'\rangle$, on the other hand, is essentially just the matrix element for π^0 decay. Recalling that $p'^2 = -m_\pi^2$, we have from (2) and (3)

$$\langle q(\mu)|j_\nu|p'\rangle = \frac{i}{\sqrt{4q_0p_0'}}\,\varepsilon_{\mu\nu\lambda\sigma}p_\lambda' q_\sigma F(-m_\pi^2)\,. \tag{15}$$

Carrying out the operations implied in (13) we find for the one-pion state contribution to $\mathrm{Im}\,Q$ the result

$$(\mathrm{Im}\,Q)_\pi = \pi G F(-m_\pi^2)\,\delta[(\bar{N}+N)^2 + m_\mu^2]\,, \tag{16}$$

where, in terms of our variables ν and Δ^2,

$$(N+\bar{N})^2 = -m^2 - 2\Delta^2 - 2m\nu\,. \tag{17}$$

Let us now turn to the one-nucleon contribution to $B_{\mu\nu}$. The matrix elements which occur here are simply those which describe the electromagnetic structure of the nucleon. In fact, denoting the electromagnetic form factors by the standard symbols $F_1^{s,v}$, $F_2^{s,v}$ (where the superscripts distinguish the

isotopic scalar (s) and isotopic vector (v) form factors) we have

$$(18)\quad \delta(N'+\bar{N}-q)\langle N'|j_\nu|N\rangle = i\sqrt{\frac{m^2}{N_0\bar{N}'_0}}\,\bar{u}(\bar{N}')\{[F_1^s(0)\gamma_\nu + F_2^s(0)\sigma_{\nu\mu}(N-N')_\mu]+ \\ +[F_1^v(0)\gamma_\nu + F_2^v(0)\sigma_{\nu\mu}(N-N')_\mu]\tau_3\}u(N)\,\delta(N'+\bar{N}-q)\,;$$

and

$$(19)\quad \bar{v}(\bar{N})\langle q(\mu)|f|N'\rangle\,\delta(N'+\bar{N}-q) = i\sqrt{\frac{m}{\bar{N}'_0}}\frac{1}{\sqrt{2q_0}}\bar{v}(\bar{N})\{[F_1^s(0)\gamma_\mu + \\ +F_2^s(0)\sigma_{\mu\nu}(N'+\bar{N})_\nu]+[F_1^v(0)\gamma_\mu + F_2^v(0)\sigma_{\mu\nu}(N'+\bar{N})]\tau_3\}u(N')\,\delta(N'+\bar{N}-q)\,.$$

The important thing to notice is that the form factors here are all evaluated at zero momentum transfer; *i.e.*, we deal only with the static nucleon moments.

Inserting these results into (13), and following our prescription for extracting Q, given in connection with Eq. (9′), we find for the one-nucleon contribution to Im Q

$$(20)\qquad (\mathrm{Im}\,Q)_N = -\pi m\,\frac{\delta[(\bar{N}-q)^2+m^2]}{(\bar{N}+N)^2}\,e^2(1+\mu_p)\,,$$

where μ_p is the anomalous magnetic moment of the proton, measured in units of the nucleon Bohr magneton. We note that

$$(21)\qquad (\bar{N}-q)^2 = -m^2-2\Delta^2+2m\nu\,.$$

We have put off until here discussion of the form of the dispersion relation to be assumed for Q. As can be seen from Eq. (9′) our definition of Q has the possibility of introducing a kind of kinematic singularity at $(N+\bar{N})^2 = \\ = -m^2-2\Delta^2-2m\nu = 0$. In order to avoid introducing artificial poles we write directly a dispersion relation for $(\nu-\nu_0)Q(\nu,\Delta^2)$, where $2m\nu_0 = -m^2-2\Delta^2$, which avoids this difficulty; we allow for a « constant » which in this case may be a function of Δ^2. We have

$$(22)\qquad (\nu-\nu_0)Q(\nu,\Delta^2) = k(\Delta^2)+\frac{1}{\pi}\int_{-\infty}^{\infty}\mathrm{d}\nu'\,\frac{(\nu'+\nu_0)\,\mathrm{Im}\,Q(-\nu',\Delta^2)}{\nu'+\nu+i\varepsilon}\,;$$

or

$$(23)\qquad Q(\nu,\Delta^2) = -\frac{g(\Delta^2)}{2m(\nu-\nu_0)}-\frac{1}{\pi}\int_{\infty}^{\infty}\mathrm{d}\nu'\,\frac{\mathrm{Im}\,Q(-\nu',\Delta^2)}{\nu'+\nu+i\varepsilon}\,,$$

where

$$(23')\qquad -\frac{g(\Delta^2)}{2m} = k(\Delta^2)+\frac{1}{\pi}\int_{\infty}^{\infty}\mathrm{d}\nu'\,\mathrm{Im}\,Q(-\nu',\Delta^2)\,.$$

The function $g(\Delta^2)$ is, of course, unspecified and may be assumed to include the contribution of the equal time commutator dropped in Eq. (8). Before discussing our prescription for specyifing $g(\Delta^2)$, let us record the expression for $\mathrm{Re}\, Q$ obtained by inserting (16) and (20) into (23):

$$\mathrm{Re}\, Q = \frac{g(\Delta^2)}{(N+\bar{N})^2} - \frac{GF(-m_\pi^2)}{(N+\bar{N})^2+m_\pi^2} + \frac{e^2 m(1+\mu_p)}{[(N-q)^2+m^2][(N-k)^2+m^2]}. \tag{24}$$

Suppose now that we calculate the amplitude Q for nucleon pair annihilation into two photons using lowest order perturbation theory, where, however, we include Pauli terms to describe the static anomalous magnetic moments μ_p and μ_n if proton and neutron. A lengthy but straightforward calculation yields the result

$$(\mathrm{Re}\, Q)_{\mathrm{pert}} = -\frac{e^2}{m(N+\bar{N})^2}[2\mu_p - (\mu_p^2-\mu_n)] + \frac{e^2 m(1+\mu_p)}{[(N-q)^2+m^2][(N-k)^2+m^2]}. \tag{25}$$

We observe that this differs from the last term in Eq. (24) (the one nucleon contribution) only by a term which has a singularity at $(N+\bar{N})^2=0$.

We now conjecture that in the neighborhood of this singularity the perturbation theory is, in fact, accurate and we choose $g(\Delta^2)$ so that (24) and (25) agree exactly as $(N+\bar{N})^2 \to 0$. Thus our rule is

$$\mathrm{Re}\, Q = (\mathrm{Re}\, Q)_{\mathrm{pert}} - \frac{GF(-m_\pi^2)}{(N+\bar{N})^2+m_\pi^2}. \tag{26}$$

This is a sort of low energy limit in the sense that as $(N+\bar{N})^2 \to 0$, the photon frequencies must approach zero. We have not as yet attempted to prove the conjecture implied by Eq. (26).

Inserting (25) and (26) into (11) and carrying out the integrations we find, setting $\xi=(k+q)^2$,

$$\mathrm{Im}\, F(\xi) = \frac{\pi G}{(2\pi)^2}\mathrm{Re}\, K(\xi)\left\{\left(1+\frac{4m^2}{\xi}\right)^{\frac{1}{2}}\left[\frac{-\xi GF(-m_\pi^2)}{\xi+m_\pi^2} - \frac{e^2}{m}[2\mu_p-(\mu_p^2-\mu_n^2)]\right] + \frac{4me^2(1+\mu_p)}{\xi}\ln\left(\frac{\sqrt{(-\xi/4)}+\sqrt{(-\xi/4)-m^2}}{m}\right)\right\}\cdot\theta(-\xi-4m^2). \tag{27}$$

Finally, we insert this into the dispersion relation (4) and evaluate $F(-m_\pi^2)$ Matters are simplified if we at this stage set $m_\pi^2=0$, an approximation which

involves very little error. We then find for $F(0)$ the expression

$$F(0) = -\frac{Ge^2}{4\pi^2 m}(1+\mu_p)\left\{\frac{I_0 + \varrho I_1}{1+(G^2/4\pi^2)I_1}\right\}; \tag{28}$$

where

$$\varrho = \frac{2\mu_p - (\mu_p^2 - \mu_n^2)}{1+\mu_p}, \tag{29}$$

$$I_0 = \int_1^\infty \frac{dy}{y^2}\,\mathrm{Re}\,K(-4m^2y)\ln\left(\sqrt{y}+\sqrt{y-1}\right), \tag{30}$$

$$I_1 = \int_1^\infty \frac{dy}{y}\sqrt{\frac{y-1}{y}}\,\mathrm{Re}\,K(-4m^2y). \tag{31}$$

The function $K(\xi)$ which appears above has been discussed by us in connection with the problem of charged pion decay [1]. We found that, in a certain approximation, $K(\xi)$ could be expressed in terms of the (complex) phase shift for physical nucleon-antinucleon scattering in the ${}^1S_0$ isotopic triplet state. An explicit formula for K is given in Eq. (18) of reference [1] [7].

3. – Discussion.

The pion decay rate, expressed in terms of the amplitude F defined in Eqs. (1)–(3), is given by

$$w = \frac{m_\pi^3}{64\pi}F^2(-m_\pi^2). \tag{32}$$

We now observe that in perturbation theory one finds for $F(0)$ the simple expression

$$F_p(0) = -\frac{Ge^2}{4\pi^2 m}. \tag{33}$$

This corresponds in (28) to setting $\mu_p = \mu_n = 0$, neglecting the damping term $(G^2/4\pi^2)I_1$ in the denominator, and setting $I_0 = 1$ (in Eq. (30) this corresponds to setting $\mathrm{Re}\,K = 1$, as expected).

The denominator which appears in Eq. (28) is precisely the same as that in Eq. (24) of reference [1]. It was shown there that $(G^2/4\pi^2)I_1$ is in all probability large compared to unity. In the models considered it was never less

[7] In reference [1], $K(\xi)$ was normalized to $K(-m_\pi^2) = \sqrt{2}\,G$. Here we normalize to $K(-m_\pi^2) = 1$.

than about 3 and probably is much larger (~ 30). Since ϱ is 1.445 the product ϱI_1 ranges from about one to ten. For the same class of models I_0 doesn't vary significantly from unity. In the extreme limit of large I_1, I_0 may be neglected and I_1 itself disappears from (28). We obtain then a result which doesn't depend on the details of the meson nucleon vertex function K, namely

$$\frac{F(0)}{F_p(0)} = (1 + \mu_p)\varrho/(G^2/4\pi^2) = .875 . \tag{34}$$

The decay rate in this limit is then only slightly smaller (by a factor of .77) than that of perturbation theory. The latter yields a lifetime $\tau = 5 \cdot 10^{-17}$ s, which is not in disagreement with the present experimental determination $\tau < 1 \cdot 10^{-15}$ s.

In the approximation where we continue to neglect the unity in the denominator of Eq. (28) but retain I_0 it is clear that the ratio in Eq. (34) can only increase (since we believe K, and hence I_0 to be positive), so the rate may exceed that of perturbation theory. It is perhaps worth remarking that if one attemps to calculate π_0-decay in perturbation theory but with static anomalous moments one encounters divergences. If these are regularized with a Feynman cut-off one also obtains, for all values of the cut-off, a decay rate more rapid than perturbation theory ([8]).

Our calculation, while admittedly rather crude, seems to indicate that there is no evidence for strong pair suppression which would lead to conflict with experiment. It would be very helpful if the lifetime could be determined sufficiently accurately to see if cancellations among various baryon pairs must be expected.

([8]) S. Cohen: *Phys. Rev.*, **98**, 749 (1955).

RIASSUNTO (*)

Si studia quantitativamente il decadimento neutro dei pioni servendosi delle relazioni di dispersione. Si immagina il processo come se si svolgesse principalmente con la disintegrazione di pioni in coppie di barioni e questi si annichilassero producendo i fotoni. Teniamo dettagliatamente conto solo della coppia di nucleoni quali rappresentanti generici dei contributi della coppia di barioni. L'espressione finale per il tasso di decadimento ha una struttura molto differente da quella che si ottiene in teoria delle perturbazioni. Risulta, tuttavia, che i risultati numerici non sono sensibilmente differenti.

(*) *Traduzione a cura della Redazione.*

A Note on an Acausality Test (II).

D. Ito, S. Minami (*) and H. Tanaka (+)

Institute of Physics, Tokyo University of Education - Tokyo
(*) *Department of Physics, Osaka City University - Osaka*
(+) *Istituto di Fisica dell'Università - Bologna*
Istituto Nazionale di Fisica Nucleare - Sezione di Bologna

(ricevuto il 17 Maggio 1958)

Summary. — The forward scattering amplitude $M(\omega)$ (real part $D(\omega)$, imaginary part $A(\omega)$) in pion nucleon scattering is discussed when the acausal spread of the current commutator over the space-like interval is very small. If the acausal smearing is so small as to justify the treating of its effect as a perturbation, the errors of the dispersion relations are proved to be energy independent in the first order approximation. Hence, there would be no guarantee of affecting micro-causality even if the dispersion relations written, as they are, in a form of subtraction $D(\omega) - D(\mu)$ could be in agreement with the experiment.

1. – Introduction.

The dispersion relations derived from the causality condition have been compared recently with the various processes involving protons, mesons or photons. However it should not seem that a satisfactory result in the quantitative arguments have been obtained. The first discrepancy was pointed out by Puppi-Stanghellini [1] in π^--p scattering, and so may be the case also for γ-p scattering [2,3]. Then, the detailed examination of the inaccuracies in the experimental data which might give rise to the discrepancy must appear

[1] G. Puppi and A. Stanghellini: *Nuovo Cimento*, **5**, 1305 (1957).
[2] R. H. Capps: *Phys. Rev.*, **106**, 1031 (1957).
[3] T. Yamagata, L. B. Auerbach, G. Bernardini, I. Filosofo, A. O. Hanson and A. C. Odian: *Bull. Am. Phys. Soc.*, Ser. II, **1**, 350 (1950), and also a private communication from T. Yamagata.

as an important task. But according to the recent work of HAMILTON [4] in such direction the discrepancy in π^--P scattering is, so to say, rather definitive. The discrepancy cannot be removed without contradicting one of the several apparently accurate results. On the other hand, a reconsideration of the basis of the dispersion relations themselves may be also a timely question examining the possible errors due to an eventual violation of causality in a small region of the nucleon. The latter would serve also to make clear the unknown mechanics of the nucleon core found in the high energy electron-proton scattering [5]. From such point of view, in the previous work [6] (cited as (I)) we have given a brief analysis of the error of the dispersion relations. Here, taking this problem again we shall re-examine the acausal error in a different manner.

The spread of the acausal region, if it exists, will be evidently smaller than the ascribed nucleon core radius $\gamma_0 \sim 0.7 \cdot 10^{-13}$ cm. If such acausal region is sufficiently small to treat its effect as a perturbation a possible shift from the normal dispersion relations will be shown, in the following, to be energy independent.

2. – Effect of micro-acausality.

If causality really holds, the forward scattering amplitude $M(z)$ (Fourier transform of $M(\omega)$) in z space is always zero for $z \leqslant 0$.

$$M(z) = 0\,, \qquad \text{for } z \leqslant 0\,, \tag{1}$$

from where the important regularity of $M(\omega)$ on the upper surface of ω space is derived:

$$\lim_{z \to \downarrow^-} M(z) = \lim_{z \to \downarrow^-} \int_{-\infty}^{\infty} M(\omega) \exp\left[-i\omega z\right] \mathrm{d}z = 0\,.$$

However in the acausal case where the current commutator $[J(x), J(0)]$ is spread over the space like region (see Fig. 1), $M(z)$ is no more zero if z approaches to zero passing a certain critical value $-l_0$. In this case, instead

[4] J. HAMILTON: *Phys. Rev.* (in press).
[5] R. HOFSTADTER: *Rev. Mod. Phys.*, **28**, 214 (1956).
[6] D. ITO, S. MINAMI and H. TANAKA: *Nuovo Cimento* **8**, 834 (1958).

of $M(\omega)$ the quantity $M(\omega)\exp[i\omega l_0]$ is now regular on the upper ω surface (*). Then, the Cauchy relation is written for this $M(\omega)\exp[i\omega l_0]$.

$$M(\omega)\exp[i\omega l_0] + \frac{i}{\pi} P \int_{-\infty}^{\infty} \frac{M(\omega')\exp[i\omega' l_0]}{\omega' - \omega} \, \mathrm{d}\omega' = 0 \,. \tag{2}$$

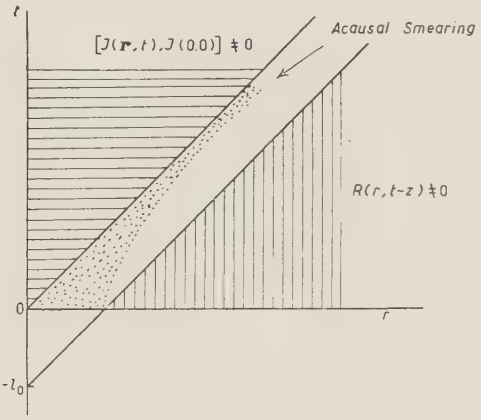

Fig. 1. – $M(z)$, the Fourier transform of the forward scattering amplitude $M(\omega)$ is given by

$$M(z) = \int_{-\infty}^{\infty} \mathrm{d}\omega \, M(\omega)\exp[-i\omega z] = (2\pi)^2 \int_0^{\infty} r \, \mathrm{d}r \int_0^{\infty} \mathrm{d}t \, R(r, t-z) \langle p\lambda | [J(\boldsymbol{r}, t), J(0, 0)] | p\lambda' \rangle \cdot$$

$$R(r, t-z) \quad \frac{1}{\pi} \int_{-\infty}^{\infty} \frac{\sin(\sqrt{\omega^2 - \mu^2}\, r)}{\sqrt{\omega^2 - \mu^2}} \exp[i\omega(t-z)] = \begin{cases} 0 & |t-z| > r, \\ J_0(\mu\sqrt{r^2 - (t-z)^2}) & |t-z| < r. \end{cases}$$

The integral region where $R(r, t-z)$ has non vanishing value is illustrated by vertical hatching. If causality really holds, the commutator $[J(\boldsymbol{r}, t), J(0, 0)]$ is always zero in the space like interval (r, t). If the commutator is spread evenly over the space like region (dotted zone), $M(z)$ is no more zero when z approaches 0 crossing a certain critical value $-l_0$.

Separating the real and imaginary parts of $M(\omega)$

$$M(\omega) = D(\omega) + iA(\omega) \,, \tag{3}$$

(*) This argument of OEHME (7) may be doubtful, but here we shall not enter into such discussion. Another note will be given on this point.

(7) R. OEHME: *Phys. Rev.*, **100**, 1503 (1955).

one gets Oehme's relation:

$$D(\omega)\cos\omega l_0 - A(\omega)\sin\omega l_0 = \frac{1}{\pi} P \int_{-\infty}^{\infty} \frac{A(\omega')\cos\omega' l_0 + D(\omega')\sin\omega' l_0}{\omega' - \omega}\,\mathrm{d}\omega', \tag{4}$$

$$A(\omega)\cos\omega l_0 + D(\omega)\sin\omega l_0 = -\frac{1}{\pi} P \int_{-\infty}^{\infty} \frac{D(\omega')\cos\omega' l_0 - A(\omega')\sin\omega' l_0}{\omega' - \omega}\,\mathrm{d}\omega'. \tag{5}$$

Now it is assumed that l_0 be very small. For example, if l_0 is smaller than 10^{-15} cm, $\varepsilon \equiv \omega l_0$ and $\varepsilon' = \omega' l_0$ will be considered as small quantities when ω' is not so large. For large ω', $\sin\omega' l_0$ and $\cos\omega' l_0$ being strongly oscillating functions, the contributions from such higher energy ω' are expected to be uneffective unless $A(\omega)$ and $D(\omega)$ behave pathologically. So, there must be a limit a which satisfies or nearly satisfies $\int_{-\infty}^{\infty} = \int_{-a}^{a}$. If such a is given by a many values solution we adopt the smallest one in absolute value as the limit a defined above. Thus, the integration interval $-\infty \to \infty$ should be understood in the following as a suitable interval $-a \to a$. Moreover, we now treat ε and ε' as small perturbations of the same order (*).

According to the usual perturbation method $D(\omega)$ and $A(\omega)$ are developped in terms of ε (+):

$$D(\omega) = D_0(\omega) + \varepsilon D_1(\omega) + \varepsilon^2 D_2(\omega) + \dots, \tag{6}$$

$$A(\omega) = A_0(\omega) + \varepsilon A_1(\omega) + \varepsilon^2 A_2(\omega) + \dots. \tag{7}$$

The relations of 0-th and 1-st order with respect to ε (or ε') are obtained in the following form (×):

$$D_0(\omega) = \frac{1}{\pi} P \int_{-\infty}^{\infty} \frac{A_0(\omega')}{\omega' - \omega}\,\mathrm{d}\omega', \tag{8}$$

$$A_0(\omega) = -\frac{1}{\pi} P \int_{-\infty}^{\infty} \frac{D_0(\omega')}{\omega' - \omega}\,\mathrm{d}\omega', \tag{9}$$

(*) In reality, such treatment involves an implicit assumption that the contribution from the $\varepsilon' \gg \varepsilon$ (*i.e.* $\omega' \gg \omega$) region is negligible. For example in the case of $\omega \sim 200$ MeV, it is supposed that ω' higher than 2 GeV should contribute little to the integral in question.

(+) $D_1(\omega)$, $D_2(\omega)$, ... and $A_1(\omega)$, $A_2(\omega)$, ... being functions of ω such development is not an expansion in power series of ω but of l_0.

(×) It is needless to say that $\sin\varepsilon$ (or $\sin\varepsilon'$) and $\cos\varepsilon$ (or $\cos\varepsilon'$) are expanded with respect to ε (or ε').

$$[D_1(\omega) - A_0(\omega)]\,\varepsilon = \frac{1}{\pi} P \int_{-\infty}^{\infty} \frac{[A_1(\omega') + D_0(\omega')]\varepsilon'}{\omega' - \omega}\,\mathrm{d}\omega' . \tag{10}$$

$$[A_1(\omega) + D_0(\omega)]\,\varepsilon = -\frac{1}{\pi} \int_{\infty}^{\infty} \frac{[D_1(\omega') - A_0(\omega')]\varepsilon'}{\omega' - \omega}\,\mathrm{d}\omega' , \tag{11}$$

where, from the crossing symmetry $M(-\omega) = M^*(\omega)$, there must be

$$D_{2n}(-\omega) = \quad D_{2n}(\omega) , \qquad D_{2n+1}(-\omega) = -D_{2n+1}(\omega) ,$$

$$A_{2n}(-\omega) = -A_{2n}(\omega) , \qquad A_{2n+1}(-\omega) = \quad A_{2n+1}(\omega) .$$

The 0-th order relations (8) and (9) are, of course, the well known dispersion relations. Hence, the acausal amplitudes $D_a(\omega)$ and $A_a(\omega)$ defined in the previous paper (I) must be expressed in terms of ε

$$D_a(\omega) = \varepsilon D_1(\omega) + \varepsilon^2 D_2(\omega) + \dots , \tag{12}$$

$$A_a(\omega) = \varepsilon A_1(\omega) + \varepsilon^2 A_2(\omega) + \dots , \tag{13}$$

and if the perturbations are really small so that the higher order terms can be neglected:

$$D_a(\omega) = \varepsilon D_1(\omega) , \tag{12'}$$

$$A_a(\omega) = \varepsilon A_1(\omega) . \tag{13'}$$

While, from the eqs. (9), (10) and (8), (11) one easily has the relations between the amplitudes:

$$\varepsilon D_1(\omega) - \frac{1}{\pi} P \int_{-\infty}^{\infty} \frac{A_1(\omega')\varepsilon'}{\omega' - \omega}\,\mathrm{d}\omega' = \frac{l_0}{\pi} \int_{-\infty}^{\infty} D_0(\omega')\,\mathrm{d}\omega' , \tag{14}$$

$$\varepsilon A_1(\omega) + \frac{1}{\pi} P \int_{\infty}^{\infty} \frac{D_1(\omega')\varepsilon'}{\omega' - \omega}\,\mathrm{d}\omega' = \frac{l_0}{\pi} \int_{\infty}^{\infty} A_0(\omega')\,\mathrm{d}\omega' . \tag{15}$$

Then, taking account of the first order approximation one derives the required relations for the acausal amplitudes $D_a(\omega)$ and $A_a(\omega)$:

$$D_a(\omega) - \frac{1}{\pi} P \int_{-\infty}^{\infty} \frac{A_a(\omega')}{\omega' - \omega}\,\mathrm{d}\omega' = \frac{l_0}{\pi} \int_{-\infty}^{\infty} D_0(\omega')\,\mathrm{d}\omega' , \tag{16}$$

$$A_a(\omega) + \frac{1}{\pi} P \int_{\infty}^{\infty} \frac{D_a(\omega')}{\omega' - \omega}\,\mathrm{d}\omega' = \frac{l_0}{\pi} \int_{-\infty}^{\infty} A_0(\omega')\mathrm{d}\omega' . \tag{17}$$

The left hand sides of these relations are just what we defined as the error of the dispersion relations $\varrho(\omega)$ and $\lambda(\omega)$. (See the eq. (2.17) in (I)). Now what should be emphasized is the energy independence of these errors. That is:

If the spread of the commutator in the space like region $0 \geqslant z \geqslant -l_0$ *is so small as to treat its effect as a small perturbation, the error of the dispersion relations are independent of the incident energy as long as* $\omega \ll 1/l_0$.

As a result, if the errors of the dispersion relations found in the experiment depend strongly on the meson energy the perturbation treatment of ωl_0 should not be reasonable implying that the acausal extension l_0 in the nucleon be rather large.

In this connection, one will take the perturbation to the second order:

$$D_a(\omega) = \varepsilon D_1(\omega) + \varepsilon^2 D_2(\omega)\,, \tag{12''}$$

$$A_a(\omega) = \varepsilon A_1(\omega) + \varepsilon^2 A_2(\omega)\,. \tag{13''}$$

Then, the errors $\varrho(\omega)$ and $\lambda(\omega)$ become

$$\varrho(\omega) \equiv D_a(\omega) - \frac{1}{\pi} P \int_{-\infty}^{\infty} \frac{A_a(\omega')}{\omega' - \omega}\,\mathrm{d}\omega' = \tag{16'}$$

$$= \frac{l_0}{\pi} \int_{-\infty}^{\infty} D_0(\omega')\,\mathrm{d}\omega' + \frac{l_0^2}{\pi} \int_{\infty}^{\infty} D_1(\omega')\omega'\,\mathrm{d}\omega' + \frac{l_0^2}{2\pi} \int_{\infty}^{\infty} (\omega - \omega') A_0(\omega')\,\mathrm{d}\omega'\,,$$

$$\lambda(\omega) \equiv A_a(\omega) + \frac{1}{\pi} P \int_{\infty}^{\infty} \frac{D_a(\omega')}{\omega' - \omega}\,\mathrm{d}\omega' = \tag{17'}$$

$$= \frac{l_0}{\pi} \int_{-\infty}^{\infty} A_0(\omega')\,\mathrm{d}\omega' + \frac{l_0^2}{\pi} \int_{\infty}^{\infty} A_1(\omega')\omega'\,\mathrm{d}\omega' + \frac{l_0^2}{2\pi} \int_{-\infty}^{\infty} (\omega' - \omega) D_0(\omega')\,\mathrm{d}\omega'\,,$$

where the first and second terms are energy independent, while the third terms depend, as expected, on the energy ω.

3. – A remark on the dispersion relations.

As regards the application of the dispersion relations, the following remark will be important. Here the validity of the perturbation treatment in question, *i.e.* the eqs. (16) and (17), is supposed.

From the amplitude $D(\omega)$ one subtracts an amplitude $D(\omega_0)$ at a certain

value ω_0, say, $\omega_0 = \mu$.

$$(18) \quad [D(\omega) - D(\mu)[- \frac{1}{\pi} P \int_{-\infty}^{\infty} \left(\frac{1}{\omega' - \omega} - \frac{1}{\omega' - \mu} \right) A(\omega') \, \mathrm{d}\omega' =$$

$$= \left[D_a(\omega) - \frac{1}{\pi} P \int_{-\infty}^{\infty} \frac{A_a(\omega')}{\omega' - \omega} \, \mathrm{d}\omega' \right] - \left[D_a(\mu) - \frac{1}{\pi} P \int_{-\infty}^{\infty} \frac{A_a(\omega')}{\omega' - \mu} \, \mathrm{d}\omega' = 0 \right].$$

That is, to the first order perturbation the effects of an eventual acausality disappear entirely in such subtraction. In the practical use of the dispersion relations, in order to obtain a strong convergence of the integral one often takes a procedure of subtraction such as $D(\omega) - D(\mu)$,

$$(19) \qquad D(\omega) - D(\mu) = \frac{1}{\pi} P \int_{-\infty}^{\infty} \left(\frac{1}{\omega' - \omega} - \frac{1}{\omega' - \mu} \right) A(\omega') \, \mathrm{d}\omega' .$$

Therefore, even if the $D(\omega)$ in such subtraction representation were in good agreement with the experiment it would not be a guarantee of the effecting micro causality. It must be noted, as seen in (18), that there still remains a possible violation of the micro causality in a very small region.

4. – Discussion.

As the experimental data in the present stage contain a large error it would be premature to estimate the order, if it exists, of an acausal extension. Although nothing can be derived definitly it may be of some meaning to compare the above arguments with the current data.

According to Puppi-Stanghellini the real part $D(\omega)$ of the forward scattering amplitude in π^--p scattering shows a large discrepancy from the dispersion relations with the coupling constant $f^2 = 0.08$ which can reproduce other pion phenomena including the π^+-p scattering also (see Fig. 2). This error $\varrho(\omega)$ seems to be rather energy dependent (see Fig. 5 in (I) also). Hence, according to our above argument such energy dependence indicates that it should not be the case for the perturbation treatment. On the other hand, the acausal spread $l_0 \lesssim 1/4\mu$ (*) conjectured in the previous work (I) basing

(*) Such presumption is, of course, only a preliminary one and may be changed appreciably by an eventual modification of the experimental data (+).

on Puppi-Stanghellini's result is smaller than the proton core radius $\lambda_p \sim 1/2\mu$, but not so small as to treat αl_0 as an expanding parameter in the perturbation series. Consequently, our conclusions in (I) and (II) are consistent requiring a rather large extension of the acausal region (+).

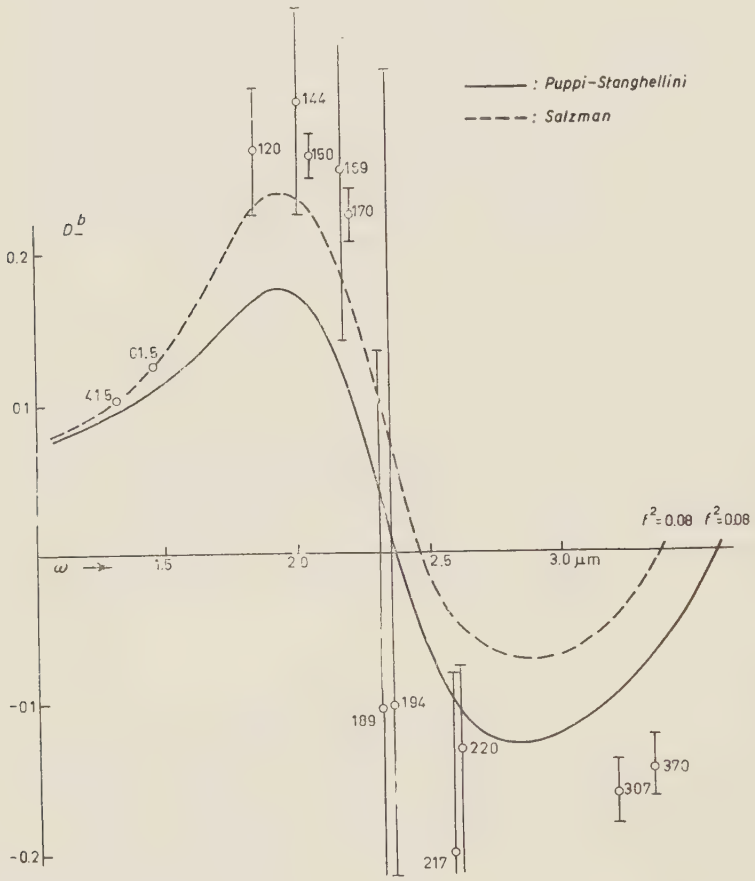

Fig. 2. – Comparison of the dispersion relation with the π^--p scattering data. The continuous curve is given by Puppi-Stanghellini (1) and the dotted curve by Salzman (8).

(+) According to the latest data at 41.5 MeV (Rochester) and at 98 MeV (Liverpool) the discrepancy in the low energy may be remarkable reduced. We thank Dr. GIACOMELLI for his kind information about the subject before the publication of their result (10). (See Fig. 3). As for the situation at high energy one does say nothing because of the large inaccuracies in the experiment. It must be noted that in the Fig. 2 only the statistical errors are given for the 307 MeV and 300 MeV data

(8) G. SALZMAN: to be published. See ref. (4).

The curves of Puppi-Stanghellini are based on rather earlier data and have been recently recalculated by SALZMAN (8) with the data of ANDERSON-PICCIONI (9) (see Fig. 2). As is seen the essential feature remains the same, though much

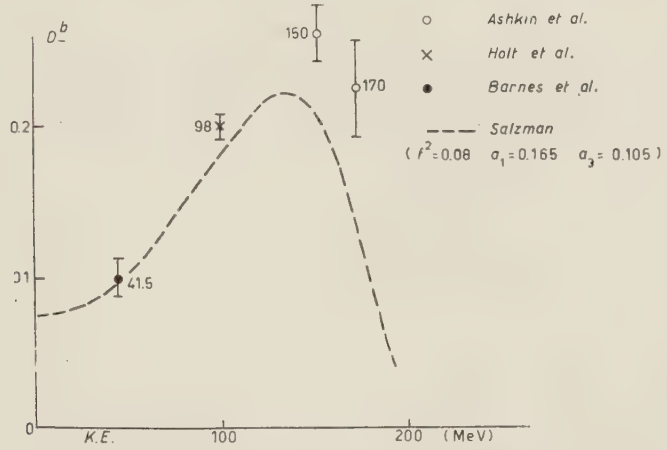

Fig. 3. – Salzman's curve is compared with the latest data (10) at 41.5 MeV (Rochester) and 98 MeV (Liverpool). The discrepancy is considerably reduced in the low energy region.

improved. Or, it seems to show a stronger energy dependence changing the sign of the error $\varrho(\omega)$ before and after the resonance. Anyway, if the discrepancy of the dispersion relations in the present experiment were really ascribed only to a violation of the micro-causality inside the nucleon core, a rather large acausal extension should be expected.

(9) H. L. ANDERSON: *Proceedings of the 6-th Rochester Conference*, P. I, 43 and O. PICCIONI: *Proceedings of the 6-th Rochester Conference*, P. IV, 7.

(10) S. W. BARNES, B. ROSE, G. GIACOMELLI, J. RING and K. MIYAKE: to be published.

RIASSUNTO (*)

Si discute l'ampiezza di scattering in avanti $M(\omega)$ (parte reale $D(\omega)$, parte immaginaria $A(\omega)$) dello scattering pione nucleone, quando la diffusione acausale del commutatore di corrente nell'intervallo spaziale è piccolissima. Se la diffusione acausale è tanto piccola da poter trattare il suo effetto come una perturbazione, gli errori delle relazioni di dispersione risultano indipendenti dall'energia nell'approssimazione del primo ordine. Non si avrebbe quindi alcuna garanzia dell'influenza della microcausalità anche se le relazioni di dispersione, scritte come sono in forma di differenza, $D(\omega) - D(\mu)$, potessero accordarsi coi risultati sperimentali.

(*) *Traduzione a cura della Redazione.*

1965

IL NUOVO CIMENTO Vol. IX, N. 3 1° Agosto 1958

A Dielectric Formulation of the Many Body Problem: Application to the Free Electron Gas.

P. Nozières and D. Pines (*)

Laboratoire de Physique, Ecole Normale Supérieure - Paris

(ricevuto il 19 Maggio 1958)

Summary. — Under suitable conditions it is shown that a generalized dielectric constant $\varepsilon(k, \Omega)$ for an arbitrary many-body problem may be defined by analogy with the macroscopic laws of electrostatics. The ground state energy may then be simply expressed in terms of $\varepsilon(k, \Omega)$ without resort to perturbation theoretic expansions. Within the random phase approximation (RPA), $\varepsilon(k, \Omega) = 1 + 4\pi\alpha(k, \Omega)$, where $\alpha(k, \Omega)$ is the complex polarizability obtained by a generalized Kramers-Heisenberg formula in the plane wave representation. For the free electron gas, this value of $\varepsilon(k, \Omega)$ leads directly to the expression for the ground state energy obtained by Gell-Mann and Brueckner and by Hubbard in the high density limit. It is shown that the treatment of electron interaction within the RPA is equivalent to taking into account only the field of surface charges at the external boundary of the system; it thus corresponds to neglecting all potential and local field corrections. $\varepsilon(k, \Omega)$ may be inferred from the inelastic scattering of fast electrons or from the Compton scattering of X-rays; the circumstances are discussed under which such experiments yield information about the ground state energy of the electron gas.

1. – The aim of this paper is the derivation of an expression for the ground state energy and stopping power of a uniform gas of interacting particles without resort to a perturbation series expansion. This program is realized by the introduction of a generalized dielectric constant at arbitrary frequency Ω and wave vector k, $\varepsilon(k, \Omega)$, in terms of which the above quantities may be simply

(*) National Science Foundation Senior Post Doctoral Fellow on leave of absence from Princeton University, 1957-58.

expressed. The quantity $\varepsilon(k, \Omega)$ is closely related to the Fourier transform of the time dependent pair correlation function introduced by VAN HOVE [1]. (In fact, our derivation of the electron and X-ray scattering cross-sections is essentially equivalent with that given in VAN HOVE's paper). For simplicity, we consider throughout this paper the case of the free electron gas; the methods employed are more general, and apply to any uniform system, of bosons or fermions which displays a linear response to a generalized test charge.

It is particularly simple to evaluate $\varepsilon(k, \Omega)$ within the random phase approximation (RPA). In the RPA, the coupling between different Fourier components of the Coulomb interaction is completely neglected. This approximation, first used for long wave lengths by BOHM and PINES [2], has recently been shown to be valid for all momentum transfers in the case of a very high density electron gas. The calculation of the ground state energy within the RPA has been performed by GELL-MANN and BRUECKNER [3], SAWADA [4], and HUBBARD [5]. The present method enables us to calculate that result in very simple fashion without resort to field-theory techniques or perturbation-theory diagrams [6]. We also calculate the stopping-power in the Born approximation, and establish the connection with the macroscopic approach of HUBBARD [7] and FRÖHLICH [8].

In Sect. 2, we establish a rigorous expression for the ground state energy and stopping power in terms of the *true* dielectric constant of the system defined by analogy with the macroscopic laws of electrostatics. In Sect. 3, we proceed to use the RPA to calculate this dielectric constant, which turns out to be simply given by the usual Kramers-Heisenberg formula (using a plane wave representation). We show how this result may arise from a perturbation series expansion. The corresponding ground state energy is identical with that given by HUBBARD. We then discuss the general behaviour of the results, and show how they may be interpreted as arising from a charge renormalization. In Sect. 4, we discuss the physical meaning of the RPA, along the lines given by us previously. We conclude that the use of RPA is equi-

[1] L. VAN HOVE: *Phys. Rev.*, **95**, 249 (1954). Our approach is closely related to the treatment of the scattering and self energy of charged particles in a free electron gas given by LINDHARD: *Kgl. Danske Mat.-fys. Medd.*, **28**, 8 (1954).

[2] D. BOHM and D. PINES: *Phys. Rev.*, **92**, 609 (1953).

[3] K. A. BRUECKNER and M. GELL-MANN: *Phys. Rev.*, **106**, 364 (1957).

[4] K. SAWADA: *Phys. Rev.*, **106**, 372 (1957); K. A. BRUECKNER, N. FUKUDA, K. SAWADA and R. BROUT: *Phys. Rev.*, **108**, 507 (1957).

[5] J. HUBBARD: *Proc. Roy. Soc.*, A **240**, 539 (1957); A **243**, 336 (1958).

[6] A preliminary report on these results has been given by the authors: *Phys. Rev.*, **109**, 1009 (1958).

[7] J. HUBBARD: *Proc. Phys. Soc.*, A **68**, 441 (1955).

[8] H. FRÖLICH and H. PELZER: *Proc. Phys. Soc.*, A **68**, 525 (1955).

valent to treating only the field of surface charges at the boundary of the system. We then outline various possible corrections to the RPA to take into account potential effects and local field corrections. In Sect. **5**, we discuss the extent to which the quantities involved in our treatment may be obtained experimentally.

2. – Let us consider a gas of free electrons, N per unit volume, from a macroscopic point of view. Their density fluctuation, ϱ_k, is defined as

$$\varrho_k = \sum_i \exp\left[-ik\cdot x_i\right].$$

We now introduce an oscillating test charge of wave vector k and frequency Ω; its charge density is assumed to be

$$e\{r_k \exp\left[-i(\Omega t + \mathrm{k}\cdot\mathrm{r})\right] + \mathrm{c.\,c.}\}.$$

In the absence of the test charge, the average value of $\varrho_{k'}$, $\langle\varrho_{k'}\rangle$, is zero. When we switch on the test charge, $\langle\varrho_{k'}\rangle$ will stay zero for $k' \neq \pm k$, for reasons of translational invariance (this is no longer true if the electrons are imbedded in a periodic potential). On the contrary, $\langle\varrho_{\pm k}\rangle$ will be $\neq 0$. The ratio $\varrho_k/r_k \exp\left[-i\Omega t\right]$ may be related to the dielectric constant $\varepsilon(k, \Omega)$, with the aid of the Fourier expansion of the macroscopic Poisson equations

$$\text{(1)} \qquad \begin{cases} \mathrm{k.}\ \varepsilon E_k = 4\pi e r_k \exp\left[-i\Omega t\right], \\ \mathrm{k.}\ E_k = 4\pi e(r_k \exp\left[-i\Omega t\right] + \langle\varrho_k\rangle). \end{cases}$$

We have

$$\text{(2)} \qquad \frac{\langle\varrho_k\rangle}{r_k \exp\left[-i\Omega t\right]} = \frac{1}{\varepsilon(k, \Omega)} - 1.$$

Obviously, macroscopic arguments will not have much physical meaning for very large k: we then may consider (2) as *a definition* of the *true* dielectric constant $\varepsilon(k, \Omega)$, which, for long wave lengths, agrees with the usual macroscopic definition.

We may write the Hamiltonian of the electrons as

$$\text{(3)} \qquad H_0 = \sum_i \frac{p_i^2}{2m} + \sum_k \frac{2\pi e^2}{k^2}(\varrho_k \varrho_{-k} - N).$$

The test charges then act as a perturbation H_1 on H_0. Since there is an energy transfer, we must switch on the test charges adiabatically in order to avoid

heating up the electrons. We therefore write H_1 as

$$H_1 = \frac{4\pi e^2}{k^2} \cdot (\varrho_{-k} r_k \exp[-i\Omega t] + \text{c. c.}) \exp[\eta t] , \tag{4}$$

where η is small, and will be set equal to zero at the end of our calculations. We calculate $\varepsilon(k\Omega)$ with the aid of the following basic assumption: *the response of the system to the test charge is linear.* In other words, the test charge is sufficiently weak that we may treat H_1 by second-order perturbation theory. For a Coulomb interaction, this is true for small enough r_k (one can then always construct a *weak* test charge). For highly singular interactions (such as a hard sphere repulsion) the response may not be linear, and the following development fails.

We calculate the response of the electron system to the test charge under the assumption that the system is initially in its ground state. Thus if Ψ_n and E_n are the eigenstates and eigenvalues of H_0 (the Ψ_n are many-body wave functions which we do not know how to calculate exactly), we may write the wave function $\Psi(t)$ of the electron gas as

$$\Psi(t) = \sum_n \Psi_n \exp\left[-i \frac{E_n}{\hbar} t\right] a_n(t) ,$$

with the boundary conditions: $a_0(-\infty) = 1$, $a_n(-\infty) = 0$, for $n \neq 0$. If we limit ourselves to the first order in r_k, the time dependent Schrödinger equation for $H_0 + H_1$ is trivially solved and yields:

$$a_n(t) = -\frac{4\pi e^2}{\hbar k^2} \left[\frac{r_k (\varrho_{-k})_{n0} \exp[i(-\Omega + \omega_{n0})t + \eta t]}{-\Omega + \omega_{n0} - i\eta} + \right. \\ \left. + \frac{r_{-k} (\varrho_k)_{n0} \exp[i(\omega_{n0} + \Omega)t + \eta t]}{\omega_{n0} + \Omega - i\eta} \right] . \tag{5}$$

From (5), we calculate the perturbed expectation value of ϱ_k, $\langle \varrho_k \rangle$. The result is considerably simplified if we notice that the translational invariance implies that $(\varrho_{-k})_{n0} = 0$ if $(\varrho_k)_{n0} \neq 0$. We find that, to lowest order in r_k, $\langle \varrho_k \rangle$ is given by [10]

$$\langle \varrho_k \rangle = -\frac{4\pi e^2}{\hbar k^2} r_k \exp[-i\Omega t + \eta t] \cdot \\ \cdot \left[\sum_n |(\varrho_k)_{n0}|^2 \left\{ \frac{1}{-\Omega + \omega_{n0} - i\eta} + \frac{1}{\omega_{n0} + \Omega + i\eta} \right\} \right] . \tag{6}$$

[9] P. Nozières and D. Pines: *Phys. Rev.*, **109**, 762 (1958).

[10] To obtain (6), we have assumed that the system was invariant by reflexion. A detailed discussion of this point is given by the authors in *Phys. Rev.*, **109**, 741 (1958).

Comparing equations (2) and (6), we obtain ε:

$$(7) \qquad \frac{1}{\varepsilon(k,\Omega)} - 1 = -\frac{4\pi e^2}{\hbar k^2} \sum_n |(\varrho_k)_{n0}|^2 \left\{ \frac{1}{-\Omega + \omega_{n0} - i\eta} + \frac{1}{\omega_{n0} + \Omega + i\eta} \right\}.$$

Remark that (7) looks very much like a Kramers-Heisenberg formula. However, the matrix elements and energy differences refer to the true eigenstates of H_0, and not these quantities calculated in a plane wave representation.

We now consider the imaginary part of (7) (letting η go to zero). We find:

$$(8) \qquad \operatorname{Im}\left(\frac{1}{\varepsilon}\right) = \frac{4\pi^2 e^2}{\hbar k^2} \sum_n |(\varrho_k)_{n0}|^2 \{\delta(\omega_{n0} + \Omega) - \delta(\omega_{n0} - \Omega)\}.$$

As has been noticed by FANO [11], the quantity $\operatorname{Im}(1/\varepsilon)$ is closely related to the time dependent pair correlation function $G(r, t)$ introduced by VAN HOVE [1]. In fact, if we denote by $S_0(k, \Omega)$ the Fourier transform of $G(r, t)$ at zero temperature (defined by Equation (4) of VAN HOVE's paper), one has simply

$$(9) \qquad \operatorname{Im}\frac{1}{\varepsilon} = \frac{4\pi^2 e^2}{\hbar k^2} [S_0(k, -\Omega) - S_0(k, +\Omega)].$$

Equation (9) shows clearly that, in general, the correlation function $S(k, \Omega)$ contains more information that $\operatorname{Im} 1/\varepsilon$. However, if we limit ourselves to the ground state, all the ω_{n0} are positive, and $S_0(k, -\Omega) = 0$. We can drop the first δ-function in (8), and it is possible to infer $S(k, \Omega)$ from $\operatorname{Im} 1/\varepsilon$. Such a procedure fails for an excited state.

We now integrate (8) over all frequencies, Ω, and obtain the following basic formula (valid only for the ground state)

$$(10a) \qquad -\int_0^\infty \operatorname{Im}\frac{1}{\varepsilon(k,\Omega)}\,\mathrm{d}\Omega = \frac{4\pi e^2}{k^2} \langle 0 | \varrho_k \varrho_{-k} | 0 \rangle .$$

The relation (10a) enables us to obtain the interaction energy in the ground state, E_{int}, and the static pair correlation function $S(k)$, from a knowledge of the dielectric constant at all wave vectors and frequencies. We have:

$$(10b) \qquad E_{\text{int}} = \langle 0 | H_{\text{coul}} | 0 \rangle = -\sum_k \frac{\hbar}{2\pi} \int_0^\infty \operatorname{Im}\frac{1}{\varepsilon(k,\Omega)}\,\mathrm{d}\Omega - \frac{2\pi N e^2}{k^2}$$

and

$$S(k) = \int_{-\infty}^{\infty} S_0(k, \Omega)\,\mathrm{d}\Omega = \left\langle 0 \left| \frac{\varrho_k^* \varrho_k}{N} \right| 0 \right\rangle = -\frac{\hbar k^2}{4\pi e^2} \int_0^\infty \operatorname{Im}\frac{1}{\varepsilon}\,\mathrm{d}\Omega .$$

[11] U. FANO: *Phys. Rev.*, **103**, 1202 (1956).

The form factor $S(k)$ yields directly the cross-section within the Born approximation for the inelastic scattering of photons or electrons.

In order to obtain the ground state energy E_0 from E_{int}, we use a relation frequently cited in the literature, which is apparently due to PAULI ([12])

$$E_0(g) = E_0(0) + \int_0^g \frac{\mathrm{d}g'}{g'} E_{\text{int}}(g') \,, \tag{11}$$

where g is the coupling constant, in our case e^2. This relation can be demonstrated simply by switching on the Coulomb interaction adiabatically and requiring that the system « follow » the ground state. From (10) and (11), we see that, in the general case, E_0 can be inferred from a knowledge of ε at all k, Ω *and* e^2. The latter requirement is of course difficult to meet experimentally. We shall see however in the next section that, within the RPA, the integration over e^2 can be performed trivially. In any event, we see that the calculation of E_0 may be rigorously reduced to that of $\varepsilon(k, \Omega, e^2)$.

Within this framework, we can evaluate easily the energy transfer of the test charges to the electron gas. Using elementary lowest order time dependent perturbation theory for a harmonic perturbation, we find ([13])

$$\frac{\mathrm{d}W}{\mathrm{d}t} = \frac{2\pi}{\hbar}\left(\frac{4\pi e^2}{k^2}\right)^2 |r_k|^2 |(\varrho_k)_{n0}|^2 \hbar\Omega[\delta(\omega_{n0} - \Omega) - \delta(\omega_{n0} + \Omega)] \,. \tag{12}$$

Comparing (12) with (8), we see at once that

$$\frac{\mathrm{d}W}{\mathrm{d}t} = -\frac{8\pi e^2}{k^2}\,\Omega |r_k|^2 \,\mathrm{Im}\,\frac{1}{\varepsilon(k, \Omega)} \,. \tag{13}$$

This result is identical with that obtained by a direct macroscopic calculation using Ohm's law, in agreement with the correspondence principle. We may also obtain the rate of energy loss of a fast particle, say an electron, with velocity V_0. If V_0 is large, the Born approximation is satisfactory. Each Fourier component of the incoming particle density then behaves like a test charge of density fluctuation $r_k = 1$, with a frequency $\Omega = k \cdot V_0$. The energy loss suffered by the fast electron is therefore

$$\frac{\mathrm{d}E}{\mathrm{d}t} = -\frac{1}{2}\sum_k \frac{8\pi e^2}{k^2}\,(k \cdot V_0)\,\mathrm{Im}\,\frac{1}{\varepsilon(k, k \cdot V_0)} \,.$$

([12]) Private communication from V. WEISSKOPF. This relation is demonstrated in the paper of K. SAWADA (ref. ([4])).

([13]) See footnote ([10]).

If we perform the angular integration over k, assuming V_0 to be very large, we find the well known result ([7,8])

$$\frac{\mathrm{d}E}{\mathrm{d}t} = -\frac{2e^2}{\pi V_0}\int \frac{\mathrm{d}k}{k}\int_0^\infty \Omega \,\mathrm{d}\Omega \,\mathrm{Im}\left(\frac{1}{\varepsilon}\right). \tag{14}$$

Here again, all the information needed for $\mathrm{d}E/\mathrm{d}t$ is contained in the dielectric constant $\varepsilon(k, \Omega)$. Remark that (14) offers a way to measure $\varepsilon(k, \Omega)$ experimentally: in the energy loss experiment first performed by WATANABE ([14]) one measures the absorption of an electron beam as a function of both the energy transfer $\hbar\Omega$ and the momentum transfer k: this yields directly $\varepsilon(k, \Omega)$. (In fact, one even obtains directly the correlation function $S(k, \Omega)$, since, in the scattering of a running wave, there is no mixing of the energy transfers $+\hbar\Omega$ and $-\hbar\Omega$).

As was first emphasized by HUBBARD ([5]), the above formulation may be used to establish in simple fashion the existence of the collective modes of the electron gas, the plasmons. Let us write the complex as $\varepsilon_1 + i\varepsilon_2$. Then $-\mathrm{Im}\,(1/\varepsilon) = \varepsilon_2/\varepsilon_1^2 + \varepsilon_2^2$. For small enough k, $\varepsilon_2(k, \Omega)$ displays the following approximate behaviour: for $\Omega \lesssim kv_0$ (v_0 is the Fermi velocity), ε_2 is non-zero, while for $\Omega \gg kv_0$, ε_2 is very small and in first approximation may be chosen to be zero. Hence if ε_1 happens to go through zero at a certain frequency $\Omega = \omega_{pl}$, ($\Omega \gg kv_0$), $\mathrm{Im}(1/\varepsilon)$ peaks sharply at this frequency. (In the limit $\varepsilon_2(\omega_{pl}, k) = 0$, $\mathrm{Im}\,(1/\varepsilon)$ is simply equal to $\pi\delta(\varepsilon_1)$). The contribution of this peak to the ground state energy and to the stopping power corresponds simply to the ground state energy of the plasmons and to the excitation of plasma modes by the incoming electron. If $\varepsilon_2(\omega_{pl}, k) = 0$, the plasma line is discrete, and there is no damping of the plasmons. In general, $\varepsilon_2(\omega_{pl}, k)$ is small, but $\neq 0$, and the plasmons are damped, giving rise to a finite line width. We remark that it is not necessary to introduce plasmon variables explicitly in order to describe such resonances in the properties of the system; however their explicit introduction often makes possible a simple description of the system properties.

We here note several important properties of $\varepsilon(k, \Omega)$. First of all, for very large Ω, we can expand (7) in powers of $1/\Omega$. We thus find the asymptotic form of ε

$$\varepsilon(k, \Omega) \underset{\Omega\to\infty}{\rightarrow} 1 - \frac{8\pi e^2}{\hbar k^2 \Omega^2}\sum_n \omega_{n0}\,|(\varrho_k)_{n0}|^2 . \tag{15}$$

The summation occurring in (15) is just that involved in the f-sum rule, which has been shown to be rigorous for the representation in terms of the eigen-

([14]) H. WATANABE: *Journ. Phys. Soc. Japan*, **11**, 112 (1956). A discussion of this problem is given by D. PINES: *Rev. Mod. Phys.*, **28**, 184 (1956).

states of H_0 [15]. Therefore (15) reduces to

$$\varepsilon(k, \Omega) \underset{\Omega\to\infty}{\longrightarrow} 1 - \frac{4\pi N e^2}{m\Omega^2} = 1 - \frac{\omega_P^2}{\Omega^2}, \tag{16}$$

where ω_P is the usual free electron plasma frequency.

It is well known that causality requires that ε be analytic with respect to Ω in the upper half complex Ω plane. Furthermore, the system is passive and must always dissipate energy. Therefore ε_2 must have a constant sign in the upper half plane and can only be zero on the real axis. Therefore $1/\varepsilon$ is also analytic in the upper half plane, although it may have poles on the real axis. A simple contour integration then leads to the following relations

$$\begin{cases} \displaystyle\int_0^\infty \varepsilon_2 \Omega \, \mathrm{d}\Omega = \frac{\pi}{2}\omega_P^2, \\ \displaystyle\int_0^\infty \frac{\varepsilon_2}{\varepsilon_1^2 + \varepsilon_2^2} \Omega \, \mathrm{d}\Omega = \frac{\pi}{2}\omega_P^2, \end{cases} \tag{17}$$

(in the second integral, the contour must pass *above* any pole of the integrand on the real axis). Remark that (17*b*) may be deduced directly from (8) and the *f*-sum rule; if we compare it with (14), we find the well known result, due to Bethe, that the total energy loss of a fast particle depends only on the total number of scatterers.

We have defined unambiguously a dielectric constant in terms of the true eigenstates of the system; we have shown that both the ground state energy and stopping power may be rigorously deduced from a knowledge of $\varepsilon(k, \Omega)$ at various coupling constants. In fact, this result is of a purely academic interest as long as we do not have a way to calculate ε. The rigorous results cannot even be used to infer E_0 from the energy loss experiments, since the calculation of E_0 in principle requires a knowledge of $\varepsilon(k, \Omega)$ for different values of the electron charge e. Therefore, approximations are undoubtedly needed, and will, in fact, form the basis for the next section.

Before taking up the calculation of $\varepsilon(k, \Omega)$, we should like to emphasize again the limitations of these results. First, one must be able to define a weak test charge in order to treat H_1 as a perturbation: this requirement imposes certain conditions on the law of interaction between the particles. Second, the foregoing results are only valid for the ground state of the system. For

[15] See for instance a paper by the authors: *Phys. Rev.*, **109**, 741 (1958). The *f* sum rule can be easily established by calculating the quantity $[[H_0, \varrho_k], \varrho_{-k}]_{00}$, first directly, and then in the representation in terms of the Ψ_n.

excited states, HUBBARD ([5]) has shown that essentially the same approach could be used, provided one replaces ε by a slightly modified expression, in which Im $(1/\varepsilon)$ involves the sum of two δ-functions rather than the difference (see Equation (8)). In such a case, in fact, it is easier to work directly with the time dependent pair correlation function $S(k, \Omega)$ of VAN HOVE, which contains all the information needed to get both the dielectric constant and Hubbard's $\varepsilon(k, \Omega)$.

3. – The simplest approximation for ε involves the complete neglect of the Coulomb interaction between the electrons. The eigenstates of H_0 are then Slater determinants of plane waves: we denote such eigenstates as Φ_μ to distinguish them from the true eigenstates Ψ_n. Equation (7) gives ε directly:

$$\frac{1}{\varepsilon} = 1 - 4\pi\alpha \,, \tag{18}$$

where α is the complex polarizability given by the Kramers-Heisenberg formula in this plane wave representation

$$4\pi\alpha(k, \Omega) = \frac{4\pi e^2}{\hbar k^2} \sum_\mu |(\varrho_k)_{0\mu}|^2 \left\{ \frac{1}{\omega_{\mu 0} - \Omega - i\eta} + \frac{1}{\omega_{\mu 0} + \Omega + i\eta} \right\} . \tag{19}$$

For free electrons, α is easily computed, and the result is given by HUBBARD ([4]) With this value of ε, the calculation of the interaction energy E_{int}, (10) is straightforward. We find

$$E_{\text{int}} = \sum_k \frac{2\pi e^2}{k^2} \left\{ \sum_\mu |(\varrho_k)_{0\mu}|^2 - N \right\}. \tag{20}$$

This is just the usual Hartree-Fock exchange energy. Furthermore the integration over de^2 does not introduce any correction to E_0 since E_{int} is linear in e^2. Therefore, this crude approximation is simply the Hartree-Fock approximation, and corresponds to treating the Coulomb interaction by first order perturbation theory.

We may improve our calculation of the energy by taking the Coulomb interaction into account within the RPA (*i.e.* neglecting all coupling between different Fourier components of the interaction). If k is the wave vector of the test charge we would thus only take into account the k-th Fourier component of the electron interaction in computing the system response. The ground state Ψ_0 of the reduced electron system will then consist of an admixture of the plane wave ground state Φ_0 with various excited configurations involving an even number of electron hole pairs each with a total momentum $+k$ or $-k$. The average number of excited electrons will be only of order 1, because

we keep only *one* component of the interaction. If we consider an operator which is diagonal in the plane wave representation, the Coulomb interaction will modify its matrix elements to order $1/N$; such a modification is not negligible if we consider the kinetic energy, since a contribution of order $1/N$ arising from each of the N Fourier components leads to a finite correction. On the contrary, for a diagonal operator A specifically related to the wave vector k, we may replace the expectation value $\langle \Psi_0 | A | \Psi_0 \rangle$ by its plane wave value $\langle \Phi_0 | A | \Phi_0 \rangle$. The matrix elements $(\varrho_k)_{0n}$ will be very different from the imperturbed $(\varrho_k)_{0\mu}$, since ϱ_k leads to creation or destruction of an electron hole pair with momentum k, and therefore connects a large number of configurations involved in Ψ_0 and Ψ_n. We can therefore predict that the expectation value of an operator like $\varrho_k \varrho_{-k}$ will be strongly modified by the Coulomb interaction.

A simple way to calculate the dielectric constant ε is to perform a time dependent canonical transformation to eliminate H_1. Let $\Psi_0(r_k)$ and $\Psi_0(0)$ be the ground state wave function of the system with and without test charge. We may write

$$\Psi_0(r_k) = \exp [iS/\hbar]\Psi_0(0) , \tag{21}$$

where $S(t)$ is a Hermitian operator, proportional to r_k. If $\Psi_0(r_k)$ satisfies the Schrödinger equation

$$-i\hbar \frac{\partial \Psi_0(r_k)}{\partial t} = H\Psi_0(r_k) ,$$

then $\Psi_0(0)$ must obey the following equation

$$-ih \frac{\partial \Psi_0(0)}{\partial t} = \left\{ \exp [-iS/\hbar] H \exp [iS/\hbar] + i\hbar \exp [-iS/\hbar] \frac{\partial}{\partial t} (\exp [iS/\hbar]) \right\} \Psi_0(0) .$$

The solution of the Schrödinger equation is therefore equivalent to finding an operator such that

$$\exp [-iS/\hbar] H \exp [iS/\hbar] + i\hbar \exp [-iS/\hbar] \frac{\partial}{\partial t} (\exp [iS/\hbar]) , \tag{22}$$

does not contain any linear term in r_k. Elementary algebra shows that (22) may be expressed as a series

$$H + \left\{ \frac{i}{\hbar} [H, S] - \frac{\partial S}{\partial t} \right\} + \frac{1}{2} \frac{i}{\hbar} \left[\left\{ \frac{i}{\hbar} [H, S] - \frac{\partial S}{\partial t} \right\}, S \right] + \tag{23}$$

$$+ \ldots + \frac{1}{n!} \left(\frac{i}{\hbar} \right)^n \left[\left[\ldots \left[\left\{ \frac{i}{\hbar} [H, S] - \frac{\partial S}{\partial t} \right\}, S \right] \ldots, S \right], S \right] .$$

To lowest order, S therefore satisfies the following equation

$$\frac{i}{\hbar}[H_0, S] - \frac{\partial S}{\partial t} = -H_1 . \tag{24}$$

The operator S will turn out to be a « one electron » operator (*i.e.*, able only to excite *one* electron hole pair of momentum $\pm k$). Let us write its matrix elements in the plane wave representation in the following way

$$S_{\mu\nu} = g(\omega_{\mu\nu}, \Omega)(\varrho_{-k})_{\mu\nu} r_k \exp[-i\Omega t + \eta t] + \\ + g(\omega_{\mu\nu}, -\Omega)(\varrho_k)_{\mu\nu} r_{-k} \exp[i\Omega t + \eta t] . \tag{25}$$

We must find $g(\omega_{\mu\nu}, \Omega)$. The commutator of S with the kinetic energy is trivially calculated (its matrix elements are simply $\hbar\omega_{\mu\nu} S_{\mu\nu}$). The commutator with the Coulomb interaction may be written

$$\frac{4\pi e^2}{k^2}\{[\varrho_k, S]\varrho_{-k} + \varrho_k[\varrho_{-k}, S]\}.$$

An operator like $[\varrho_k, S]$, being a commutator, is necessarily a one electron operator. The first part of S yields a diagonal contribution: according to the discussion given earlier in this section, this term may be replaced by its expectation value in the state Φ_0. The second term of S gives rise to an operator creating or destroying an electron hole pair with momentum $2k$: this must be neglected within RPA. Therefore, the commutator of the Coulomb interaction with S reduces to:

$$\frac{i}{\hbar}[H_{\text{coul}}, S] = \frac{i}{\hbar}\frac{4\pi e^2}{k^2}\sum_{\mu} |(\varrho_k)_{0\mu}|^2 [g(\omega_{\mu 0}, \Omega) - g(\omega_{0\mu}, \Omega)] \cdot \\ \cdot \varrho_{-k} r_k \exp[-i\Omega t + \eta t] + \text{c. c.} \tag{26}$$

With the help of (26), the correct value of $g(\omega_{\mu\nu}, \Omega)$ may be shown to be given by

$$g(\omega_{\mu\nu}, \Omega) = -\frac{1}{1 + 4\pi\alpha}\frac{4\pi e^2}{ik^2}\frac{1}{\omega_{\mu\nu} + \Omega + i\eta}, \tag{27}$$

where $\alpha(k, \Omega)$ is the polarizability defined in equation (19). We next use (27) to calculate the perturbed expectation value of ϱ_k

$$\langle \varrho_k \rangle = \langle \Psi_0(r_k) | \varrho_k | \Psi_0(r_k) \rangle .$$

From (21), we see at once that, to first order in r_k, $\langle \varrho_k \rangle$ is given by

$$\langle \varrho_k \rangle = \frac{i}{\hbar}[\varrho_k, S]_{00} = -\frac{4\pi\alpha}{1 + 4\pi\alpha} r_k \exp[-i\Omega t + \eta t] . \tag{28}$$

On comparing (28) with the equation (2) defining ε, we conclude that, within the RPA, the complex dielectric constant is given by

$$\varepsilon(k, \Omega) = 1 + 4\pi\alpha(k, \Omega) . \tag{29}$$

The result (29) is in agreement with an earlier treatment [9] in which the effect of real transitions, *i.e.* the imaginary part of ε, was neglected. In the next section, we shall discuss its physical significance.

Although it is not needed for the present reasoning, it is interesting to calculate the second order terms, which are given by

$$\frac{1}{2}\frac{i}{\hbar}[H_1, S] .$$

Using (28), we find

$$\frac{i}{2\hbar}[H_1, S] = \frac{2\pi e^2}{k^2} r_k r_{-k}\left[\frac{1}{\varepsilon(k, \Omega)} + \frac{1}{\varepsilon(-k, -\Omega)}\right] \exp[2\eta t] . \tag{30}$$

If we write $\varepsilon = \varepsilon_1 + i\varepsilon_2$, we see that the Coulomb interaction between the test charges is screened by a factor $\varepsilon_1/(\varepsilon_1^2 + \varepsilon_2^2)$. When $\varepsilon_2 = 0$ this reduces to the usual macroscopic result of electrostatics; furthermore, in such a case, there is no energy transfer of the test charges to the system, and the concept of independent test charges interacting through a screened interaction is physically sensible. On the contrary, if $\varepsilon_2 \neq 0$, the test charges give up energy to the system. (This feature did not appear in the previous calculation because we switched on the test charges adiabatically in such a way that no appreciable. energy transfer could take place.) The test charges then have a finite « life time » τ. If $\Omega\tau \gg 1$. it makes sense to consider the effective interaction (30). On the other hand, if $\Omega\tau \lesssim 1$, the concept of a test charge at frequency Ω loses its meaning. Finally, (30) shows that, although the interaction has a pole at the plasma frequency ($\varepsilon_1 = \varepsilon_2 = 0$), it is regular at frequencies such that $\varepsilon_1 = 0$, $\varepsilon_2 \neq 0$, a definite improvement over the time independent result $(2\pi e^2/k^2\varepsilon_1) r_k r_{-k}$.

Remark that result (29) could have been obtained by a perturbation treatment of the Coulomb interaction, limited to those diagrams appearing within RPA. The first order contribution to $1/\varepsilon$ is that given in (18), and the following orders form a geometrical series which may be trivially summed:

$$\frac{1}{\varepsilon} = 1 - 4\pi\alpha + (4\pi\alpha)^2 + \ldots = \frac{1}{1 + 4\pi\alpha} .$$

Such an expansion only converges when $4\pi\alpha < 1$, while the present calculation does not suffer from that limitation.

If we substitute the value (29) for ε in the expressions for the ground state energy and stopping power given in the preceeding section, we obtain exactly the result of HUBBARD ([5]). The latter is easily seen to be the same as that of SAWADA and hence of GELL-MANN and BRUECKNER. The expression for the ground state energy E_0 may be simplified if we remark that $4\pi\alpha$ is proportional to e^2: the integration over de^2 then yields the following result (cf. HUBBARD)

$$E_0 = E_0(0) + \sum_k \left\{ \frac{\hbar}{2\pi} \int_0^\infty \operatorname{arctg} \frac{\varepsilon_2}{\varepsilon_1} \, d\Omega - \frac{2\pi N e^2}{k^2} \right\}, \tag{31}$$

where $E_0(0) = \frac{3}{5} N E_F$ is the ground state energy of a gas of non-interacting electrons. We wish to emphasize the fact that the result is approximate; its validity depends on the validity of the RPA. In cases in which the RPA is valid, we see that E_0 can be obtained from the experimental data on energy loss of fast electrons, through the following procedure:

$$\begin{cases} 1) \quad \text{Absorption spectrum} \to \operatorname{Im}\left(\frac{1}{\varepsilon}\right), \\ 2) \quad \text{Kramers-Kronig relation} + \operatorname{Im}\left(\frac{1}{\varepsilon}\right) \to \operatorname{Re}\left(\frac{1}{\varepsilon}\right), \\ 3) \quad \operatorname{Im}\left(\frac{1}{\varepsilon}\right) + \operatorname{Re}\left(\frac{1}{\varepsilon}\right) \to \varepsilon \to E_0 . \end{cases}$$

Such a calculation has not been attempted. Remark that, if performed carefully, it might constitute a check of the validity of the RPA. In fact, it is probable that the crystalline periodic field gives rise to important corrections which will tend to mask those arising from RPA, so that this discussion is somewhat academic.

The ground state energy may be written as

$$\begin{cases} E_0 = E_0(0) + \sum_k \Delta E_0(k), \\ \Delta E_0(k) = \frac{\hbar}{2\pi} \int_0^\infty \operatorname{arctg} \frac{\varepsilon_2}{\varepsilon_1} \, d\Omega - \frac{2\pi N e^2}{k^2} . \end{cases} \tag{32}$$

It is interesting to see how $\Delta E_0(k)$ behaves for k much smaller than the Fermi momentum k_0. The arctg has the behaviour shown on Fig. 1: it goes from 0 to π between $\Omega = 0$ and $\Omega = k v_0$ (where v_0 is the Fermi velocity). It then stays equal to π until Ω reaches the plasma frequency ω_{pl} at which ε_1 is zero. For $\Omega > \omega_{pl}$, it is zero. Remark that for small k, ω_{pl} is very close to

$\omega_p = \sqrt{4\pi N e^2/m}$. The integral appearing in (32) may be written as

$$\pi\omega_{\rm pl} - A\,,$$

where A is the shaded area of Fig. 1. The first term corresponds to the zero-point energy of the plasmons, while the second corresponds to the screened long range electron interaction energy (that arising from $H_{\rm rp}$ in the Bohm-Pines formalism). One sees at once that the plasmon energy is k independent, while the individual particle energy is of order k. It is easy to expand E_0 in powers of k along these lines, and one finds exactly the results quoted by the authors in a previous paper ([16]), to which the interested reader is referred. For very large k, on the contrary, arctg $\varepsilon_2/\varepsilon_1$ is only different from 0 in the region $\Omega \sim \hbar k^2/2m$: the first term of $\Delta E_0(k)$ then tends towards $2\pi N e^2/k^2$, so that the result is convergent.

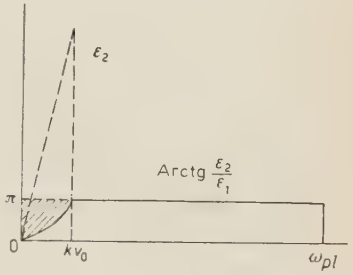

Fig. 1. – arctg $\varepsilon_2/\varepsilon_1$ as a function of Ω. Note the discontinuity at $\omega_{\rm pl}$. In the Hartree-Fock approximation (first order perturbation theory, arctg $\varepsilon_2/\varepsilon_1$ would be replaced by ε_2 (dotted curve).

It should be emphasized that the inclusion of all higher order terms, within the RPA, corresponds to a radical change in the description of the electron system. In the Hartree-Fock approximation, arctg $\varepsilon_2/\varepsilon_1$ shoud be replaced by ε_2 in Equation (32): the energy of the system then arises only from individual particles. Within the RPA, one sees from Fig. 1 that this individual particle contribution is heavily screened (by a factor of order k^2, with even its sign changed). Furthermore, collective effects appear, which extend considerably the frequency range contributing to E_0 (from kv_0 to $\omega_{\rm pl}$). Such a basic change is a consequence of the summation of an infinite perturbation series. The same effect appears in a still clearer fashion in the energy loss of fast electrons. There, the RPA result $\varepsilon_2/(\varepsilon_1^2+\varepsilon_2^2)$ is to be compared with the Hartree-Fock result ε_2. The effect of the electron correlations is to screen the low frequency part, and to concentrate most of the long wave length oscillator strengths at the collective plasma frequency $\omega_{\rm pl}$.

We shall not discuss in detail the numerical details of the calculation for free electrons, since they may be found in HUBBARD's paper. We shall, however, make a few remarks concerning the interpretation of these results. First, we note that the expectation value $E_{\rm int}$ of the Coulomb interaction in the ground state Ψ_0 is equal to the expectation value in the plane wave state Φ_0 of a

([16]) P. NOZIÈRES and D. PINES: submitted to the *Phys. Rev.*

renormalized interaction

$$H^s_{\text{coul}} = \sum_k \frac{2\pi e^2}{k^2}\, \varrho^s_k \varrho^{s*}_k$$

in which ϱ^s_k is a screened density fluctuation, defined by its matrix elements

$$(\varrho^s_k)_{\mu\nu} = \frac{(\varrho_k)_{\mu\nu}}{\varepsilon(k, \omega_{\mu\nu})}\,. \tag{33}$$

This may be interpreted as the replacement of the electric charge $e\varrho_k$ by a renormalized charge $e\varrho^s_k$. (Remark that the screening is frequency dependent, a definite improvement over the Fermi-Thomas method.) Physically, this substitution means that each electron carries a polarization cloud which modifies its effective electric charge.

To conclude this section, we compare the present results with the minority carrier technique described in a previous paper ([9]). There, it was shown that if one neglected resonant transitions (taking principal parts at any pole), it was possible to isolate a group of independent minority carriers, (with density fluctuation $\tilde{\varrho}_k$) which then interact amongst each other through a screened interaction

$$\sum_k \frac{2\pi e^2}{k^2}\, \tilde{\varrho}_{-k} \tilde{\varrho}^{s\prime}_{+k}\,.$$

in which $\tilde{\varrho}^{s'}_k$ was a screened density fluctuation (different from the above ϱ^s_k), defined by

$$(\tilde{\varrho}^{s'}_k)_{\mu\nu} = \frac{(\tilde{\varrho}_k)_{\mu\nu}}{\varepsilon_1(k, \omega_{\mu\nu})}\,.$$

Such minority carriers do not undergo any further correlations, and their contribution to the total energy of the system involves only their kinetic and exchange energy. The latter may be written as

$$\sum_k \left\{ \sum_\nu \frac{2\pi e^2}{k^2} \frac{|(\tilde{\varrho}_k)_{0\nu}|^2}{\varepsilon_1(k, \omega_{\nu 0})} - \frac{2\pi \tilde{N} e^2}{k^2} \right\}, \tag{34}$$

(where $\tilde{N}$ is the number of minority carriers). If we assume that this approach can be extended to all carriers, we find as the ground state energy of the system the following quantity

$$E_0 = E_0(0) + \sum_k \left\{ \frac{\hbar}{2\pi} \int_0^\infty \frac{\varepsilon_2}{\varepsilon_1}\, \mathrm{d}\Omega - \frac{2\pi N e^2}{k^2} \right\}. \tag{35}$$

(35) is the same as (31) but for the replacement of $\operatorname{arctg} \varepsilon_2/\varepsilon_1$ by $\varepsilon_2/\varepsilon_1$. This is not surprising, since ε_2 arises only from the real resonant transitions; taking

principal parts amounts to the neglect of higher powers of ε_2, therefore to the replacement of $\operatorname{arctg} \varepsilon_2/\varepsilon_1$ by $\varepsilon_2/\varepsilon_1$. This discussion shows that the minority carrier treatment presented in ref. ([9]) is only valid when one deals with frequencies such that $\varepsilon_2 \ll \varepsilon_1$ (*i.e.* for Ω much smaller *or* much larger than kv_0). This is the case for many physical problems, particularly for all problems dealing with transitions in an energy shell of width kT around the Fermi surface. On the other hand, the minority carrier approach, although it is suggested by the correspondence principle, does not lead to an accurate calculation of the cohesive energy.

4. – In discussing the meaning of the RPA, it is easier to consider the calculation of the meaning and validity of the RPA in the calculation of the dielectric constant than the ground state energy. A detailed discussion of the meaning and validity of the RPA in the calculation of the dielectric constant may be found in ref. ([9]); we summarize the arguments briefly here. Consider a slab of the electron gas between two condenser plates. Let E be the electric field in the gas arising from the charge on the condenser plates (oscillating at frequency Ω). Consider now a given electron at point M (Fig. 2), and let E_M be the effective electric field at point M, and P the polarization. In order to calculate E_M, we use the method of Lorentz, and draw a sphere around point M: E_M is then the sum of four terms

— the applied field E,

— the field of the polarized matter outside the sphere, which is equivalent

to
$$\begin{cases} \text{the field } E_1 = -4\pi P & \text{of surface charges at the boundary of the specimen} \\ \text{the field } E_2 = \dfrac{4\pi P}{3} & \text{of surface charges at the boundary of the sphere} \end{cases}$$

— the field E_3 of the polarized matter inside the sphere (which we do not know how to calculate).

Let α be the microscopic polarizability: we then have $P = \alpha E_M$. The problem is to calculate ε, which is defined by

$$\varepsilon = \frac{E}{E - 4\pi P}.$$

We therefore need to know both E_3 and α.

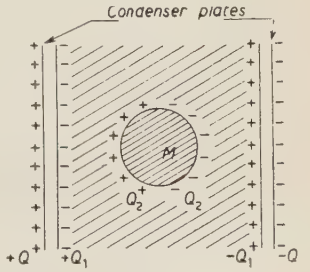

Fig. 2. – The local fields corrections to the dielectric constant. The fields E, E_1, E_2 arise respectively from the charges $\pm Q$, $\pm Q_1$, $\pm Q_2$.

Let us now consider from a qualitative point of view the effects of the Coulomb interaction on these quantities. Let $\varrho(0)$ be the electron charge distribution in the absence of applied electric field ($E = 0$), and $\delta\varrho(E)$ the distortion of this distribution due to E. The effect of $\varrho(0)$ is to modify the restoring forces acting on the electron M, therefore to change the polarizability α. This is typically a « potential » effect, which may be described by an appropriate modification of the electron mass. On the other hand, the effect of $\delta\varrho(E)$ is to modify the electric field at point M, giving rise to the corrections E_1, E_2 and E_3. Of these, E_1 arises from surface charges at the outer boundary of the specimen, and in fact is a direct consequence of the boundary condition of electrostatics, while E_2 and E_3 correspond to the field of polarized electrons *inside* the specimen; the latter fields give rise to the so-called « local field » corrections.

Suppose we neglect the potential correction and thereby assume the polarizability α to be that of free electrons given in the preceeding section: there remains the determination of E_M. If we further neglect completely the electron interaction, thus dropping E_1, E_2 and E_3: we find

$$\frac{1}{\varepsilon} = 1 - 4\pi\alpha\,,$$

which is just equation (8), as might be expected. We might attempt to improve this calculation by keeping E_1, that is, by taking into account the Coulomb interaction, but neglecting the local field corrections: we then find

$$\varepsilon = 1 + 4\pi\alpha\,,$$

which is just (29): the RPA is therefore equivalent to *neglecting potential and local field corrections* taking only into account surface charges at the outer boundary. In fact, this could have been predicted easily: since the RPA does not mix different Fourier components, it is impossible to build wave packets corresponding to the field of localized charges. Therefore the static Coulomb potential and the local field are automatically neglected within RPA. The field E_1 is included because it arises from charges at the boundary of the specimen (we always can take an infinite sample: E_1 then arises from charges at infinity and does not require building a wave packet). Note that we could have made this remark at the beginning, and that, therefore, the Brueckner-Gell-Mann result can be obtained with no calculation at all.

Having thus emphasized the physical meaning of the RPA, we are in a

position to discuss its validity. Except in the case of high density, we know that the corrections are quite appreciable (for low density, they change the entire character of the results). It is convenient to discuss the corrections in the language of diagrams, introduced by GOLDSTONE ([17]), HUGENHOLTZ ([18]) and others. The so-called «polarization» diagrams belong to the general class shown on Fig. 3*a*. As shown by HUGENHOLTZ, the potential effects arise from the replacement of particle propagation lines by any « diagonal » subdiagram, of the general type shown on Fig. 3*b*. Of these diagonal diagrams, the simplest is certainly that shown on Fig. 3*c* which corresponds to the Hartree-Fock potential. Such a potential may be refined: in a further publication, we shall for instance discuss a screened Hartree-Fock potential including all subdiagrams of the type shown on Fig. 3*d*. Of course, this does not exhaust all possible potential corrections, and should be considered as an approximation whose validity must be discussed.

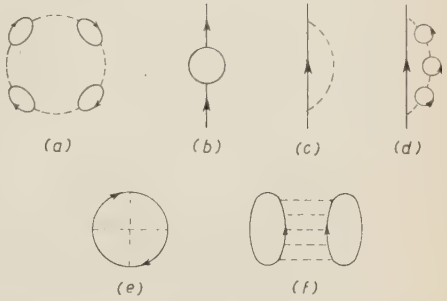

Fig. 3. – The diagrammatic representation of a perturbation expansion. Full lines are particle propagators, dotted lines are interaction lines. 3*a*, polarization diagram; 3*b*, general « diagonal » subdiagram; 3*c*, Hartree-Fock subdiagram; 3*d*, screened Hartree-Fock subdiagram; 3*e*, the second order exchange « cross diagram »; 3*f*, a « ladder » diagram, included in a Brueckner treatment.

In principle, all the other diagrams give rise to local field corrections. From the study of BRUECKNER and GELL-MANN, it appears that among the most important are the « cross diagrams » involving exchange of electrons. In Fig. 3*e* we draw such a diagram in lowest order; it is this diagram which in fact gives rise to the second order exchange energy (the E_b^2 of BRUECKNER and GELL-MANN). As emphasized by HUBBARD, this class of diagrams is important, since for high momentum transfer k, they cancel one half of the RPA diagrams. Unfortunately, it is not possible at present to compute their contribution to all orders, and one must rely on interpolation procedures between the low k and high k limits. Such procedures have been extensively discussed by HUBBARD ([5]) and the authors ([16]).

In the case of the electron gas, these seem to be the leading corrections. Of course, it is possible to consider yet other approaches; for instance one might try to use a Brueckner type calculation to correct the effective interaction and

([17]) J. GOLDSTONE: *Proc. Roy. Soc.*, A **239**, 267 (1957).
([18]) N. HUGENHOLTZ: *Physica*, **23**, 481, 533 (1957).

the one electron potential (including « ladder » diagrams of the type shown on Fig. 3*f*). Such a correction does not seem important in the electron case and nothing has yet been attempted in this direction.

5. – The discussion given in the preceeding section demonstrates the necessity of taking electron correlations into account in a description of any longitudinal phenomenon in the electron gas. The concentration of oscillator strengths at the collective plasma pole, and its counter part, the screening of the low frequency components, are basic features of the system, which are not obtainable from second-order perturbation theory. The RPA represents a considerable improvement over the Hartree-Fock method for the electron gas; it yields a qualitatively sensible physical picture of the system properties, even though it is not quantitatively correct at actual metallic densities. (Thus, as the authors have shown elsewhere ([16]), the RPA is only valid in the long wave length limit ($k \lesssim 0.47 k_0 r_s^{\frac{1}{2}}$); for the short wave length interactions, a perturbation theoretical treatment in which only interactions between electrons of anti-parallel spin are included represents a tolerable approximation).

We should like to emphasize that the results presented in Sect. **3** are not new. The resolution of the many-body problem for free electrons within the RPA is now well understood, and the present approach is but one way to obtain the by now well known result. In our minds, however, the present approach has several advantages.

— It involves quite simple calculations, especially if one realizes at the outset that the RPA is equivalent to neglecting all potential and local field corrections; the calculation of ε is then trivial.

— It does not involve a perturbation series expansion, so that, as in Sawada's approach, there are no accompanying convergence difficulties.

— It affords a direct link between the dielectric properties of the system (*i.e.* the scattering cross-sections for fast electrons), and the ground state energy. (This relation bears some resemblance to the dispersion relations which relate the imaginary and reals parts of the scattering matrix.)

— It yields a very simple discussion of the physical meaning of the approximations.

We have already mentioned that $\varepsilon(k, \Omega)$ is a quantity which may be inferred directly from the energy loss experiments. As has been pointed out by Van Hove, the correlation function, *i.e.* Im $1/\varepsilon$ may also be obtained from the Compton scattering of X-rays by the gas of free electrons ([19]). In the

([19]) The authors wish to thank Prof. H. Curien, for drawing their attention to the interpretation of Compton scattering data.

latter case, in fact, the sensitivity of the experimental apparatus does not allow a spectral analysis of the scattered light, and one only measures with Geiger counters the numbers of photons scattered as a function of angle, which is proportional to the form factor $S(k)$ given in (10*b*) (the calculations are the same as those for the scattering of neutrons by liquid helium). The dielectric constant is therefore an easily measurable quantity. As we already pointed out, where the RPA is valid, one may then compute the ground state energy E_0 from the observed $\varepsilon(k, \Omega)$. (This does not appear to be feasible outside the RPA.)

We remark that, although we have only applied our approach to electrons in the present paper, the method is quite general, and may be extended to other types of systems for which it provides a simple recipe for the calculation of the system properties within RPA. For instance, the method may be applied to the dilute hard sphere boson gas, for which it yields the results of BOGOLJUBOV ([20]) and HUANG, LEE and YANG ([21]) on the ground state energy and excitation spectrum. Details of the calculation will be published elsewhere

To conclude, we see that the RPA yields results which, for actual metallic densities, are qualitatively correct, but that a detailed quantitative analysis requires more insight into both potential and local field corrections. The latter have been already treated by qualitative interpolation procedures, while the former are still an open problem.

* * *

The authors wish to thank Prof. P. AIGRAIN and Prof. J. LUTTINGER for many enlightening discussions on these and related subjects.

([20]) N. N. BOGOLJUBOV: *Journ. Phys. USSR*, **11**, 23 (1947).
([21]) K. HUANG, T. D. LEE and C. N. YANG: *Phys. Rev.*, **106**, 1135 (1957).

RIASSUNTO (*)

Si dimostra che in condizioni opportune si può definire per analogia con le leggi macroscopiche dell'elettrostatica una costante dielettrica generalizzata $\varepsilon(k, \Omega)$ per un problema arbitrario di molti corpi. L'energia dello stato fondamentale si può allora

---

(*) *Traduzione a cura della Redazione.*

esprimere semplicemente in termini di $\varepsilon(k, \Omega)$ senza far ricorso agli sviluppi della teoria delle perturbazioni. Nell'approssimazione della fase casuale (RPA), $\varepsilon(k, \Omega) = 1 + 4\pi\alpha(k\Omega)$, dove $\alpha(k\Omega)$ è la polarizzabilità complessa ottenuta per mezzo di una formula di Kramers-Heisenberg generalizzata nella rappresentazione delle onde piane. Per il gas di elettroni liberi questo valore di $\varepsilon(k, \Omega)$ porta direttamente all'espressione dell'energia dello stato fondamentale ottenuta da GELL-MANN e BRUECKNER e da HUBBARD al limite delle densità elevate. Si dimostra che il trattamento dell'interazione elettronica nei limiti dell'RPA è equivalente a tener conto del solo campo delle cariche superficiali al limite esterno del sistema; corrisponde pertanto a trascurare tutte le correzioni di potenziale e di campo locale. Si può dedurre $\varepsilon(k,\Omega)$ dallo scattering anelastico degli elettroni veloci o dallo scattering Compton dei raggi X; si discutono le condizioni in cui tali esperimenti forniscono dati sull'energia dello stato fondamentale del gas di elettroni.

IL NUOVO CIMENTO Vol. IX, N. 3 1° Agosto 1958

Construction of Potentials from Resonance Parameters.

T. Regge

Istituto di Fisica dell'Università - Torino
Istituto Nazionale di Fisica Nucleare - Sezione di Torino

(ricevuto il 23 Maggio 1958)

Summary. — Gel'fand and Levitan's procedure for the construction of a potential from the spectral measure function is here simplified and made practical. Several theorems of purely mathematical character are also proved and their bearing on concrete problems exhibited.

---

1. – We shall refer here several times to a paper of the author (1) for a review of the properties of Jost's function. These properties are in particular remarkable when the potential is vanishing faster than any exponential for large distances. Indeed in this case Jost's function turns out to be an entire function of the wave number k. The present status of the theory of entire functions is so happily advanced that with its help many results can be derived very simply and elegantly.

The main point of the discussion of (1) was that we established a clear and simple relation between asymptotic behaviour of the large zeros of $f(k)$ and asymptotic beaviour of the potential for large distances. Already the existence of this relation shows how little important these zeros are from the physical point of view.

The extreme tail of the potential has usually no real bearing on physically measurable quantities. If we truncate a Gaussian potential, by letting it vanish identically, farther than several times its range, we shall cause a little change in the phase shifts but drastic changes in the position of the large zeros of Jost's function. The small zeros will remain almost unaffected.

Generally the behaviour of $f(k)$ in the upper plane of k is of negligible

(1) T. Regge: *Nuovo Cimento*, **8**, 671 (19 8).

physical importance. On the other hand we know that when $f(k)$ is entire (and this we suppose to be the case in the following) the knowledge of the zeros alone completely determines ([1]) $f(k)$ and therefore all physically interesting quantities. Since we have just seen that the large zeros do not really have any physical meaning a natural deduction is that all the physics lies in the small ones. Our opinion is also supported by another fact: since we have only a finite number of bound states (*) and of virtual states the large zeros must correspond to radiative states (resonances). Now while there is no clear cut distinction between sharp and broad resonances, we know however that resonance is the more physically interesting and easy to measure the sharper it looks. Broad resonances are bound to mix together and to lose their distinctive features. Now large zeros of $f(k)$ tend to be quite far from the real axis (+) and the corresponding width very large so that the resonance will be difficult to detect.

We have good reasons now to believe that a finite number of zeros provides a fairly good picture of the physical process. We may express this by saying that a table of the zeros is just as good as the whole machinery of phase shifts, binding energies etc. for the description of the scattering process. It has the advantage to be more compact and the disadvantage that in order to know it we need to elaborate a large number of experimental results. On the other hand this knowledge simplifies drastically the construction of an equivalent potential as we shall see in the following.

2. – We have supposed in the above discussion that the potential was such as to make $f(k)$ entire. Most field theoretical potentials, among them Yukawa's potential, do not satisfy this requirement ([2]). Actually the arising singularities of Jost's function fall well beyond the physical region of the small zeros and a reliable approximate description of $f(k)$ in this region can still be accomplished using a polinomial (×). Secondly there is no reason why a Yukawa potential should be better fitted for our purpose that any « entire $f(k)$ » potential. Both are mathematical abstractions both are bound to be equally wrong at some high energy where our non-relativistic approximation does not hold and velocity dependent potentials may change the picture.

Actually only a real attempt to work with experimental data can give an answer to these questions. Until then our improved construction method

(*) The conditions assumed in ([1]) are such that this is true.

(+) One of the results in ([1]) was that large zeros tend to diverge asymptotically from the real axis when their moduli increase.

([2]) T. REGGE: *Nuovo Cimento*, **3**, 295 (1958).

(×) We can approximate $f(k)$, under very large conditions, as much as wanted on the real axis by an entire function.

will be confined to the low energy region where a statical, local and non-relativistic potential has well founded hopes to be succesful. With such an incomplete set of experimental results the potential may be partly undefined. Of course this is no fault of the method by itself, it is just that the postulates on which we based our simplified physical picture do not hold probably in the case of high energy scattering.

3. – From our discussion it appears that there is no real restriction in letting the potential vanish further than a certain distance « a » which shall be taken in any practical case sensibly larger than the extimated range of the forces.

The mathematics implied in the construction of the potential will be considerably simplified without loss of the physical meaning of the theory. With this position we are ready to develop some mathematical machinery which is going to be useful later. To this aim we consider the solutions of the radial Schrödinger equation belonging to some angular momentum L and to the wave number k_n, where k_n is a zero of $f(k)$. For the sake of simplicity we take $L = 0$. We know from [1] that one such solution is given by:

$$\varphi(k_n, x)\,, \qquad \text{where} \qquad \varphi(k_n, 0) = 0\,, \quad \varphi'(k_n, 0) = 1\,. \tag{1}$$

These boundary conditions imply when k_n is a zero, and only then, that:

$$\varphi(k_n, x) = -\frac{f(-k_n)\exp[-ik_n x]}{2ik_n}\,. \qquad x \geqslant a\,. \tag{2}$$

For a given angular momentum there are infinite zeros of $f(k)$. We shall have correspondingly an infinite set of functions $\varphi(k_n, x)$. In spite of the fact that only a finite number of them (the bound states, with k_n below the real axis) are square integrable we can still think of using them as a basis for the expansion of any generical function $\chi(x)$:

$$\chi(x) = \sum_0^\infty \lambda_n \varphi(k_n, x)\,. \tag{3}$$

Completeness on some interval $0 \ldots H$ of the set (3) is equivalent to the completeness of the set:

$$\varphi_0(k_n, x) = \frac{\sin k_n x}{k_n}\,, \tag{4}$$

on the same interval $0 \dots H$. This follows from Gel'fand and Levitan's equation:

$$\varphi(k_n, x) = \varphi_0(k_n, x) + \int_0^x K(x, y)\varphi_0(k_n, y)\,\mathrm{d}y\,, \tag{5}$$

and from general theorems (to this purpose see [3]).

The proof of the completeness of (4) implies the use of some sophysticated mathematical method. We shall sketch it here only in the essential points making use of a number of results from the theory of entire functions which are usually unfamiliar to the physicist. (The reader who wishes to give a closer look to how these results can be established can read [4]).

From [3] we know that completeness on $0 \dots H$ is equivalent to closure of set (4) on the same interval. Closure of (4) means here that for any function $\xi(x)$ which is square integrable on $0 \dots H$ the condition:

$$\int_0^H \varphi_0(k_n, x)\xi(x)\,\mathrm{d}x = 0\,, \qquad \text{for all } n, \tag{6}$$

implies $\xi(x) = 0$ almost everywhere.

The closure of (4) can be proved as follows. We consider the integral:

$$\int_0^H \varphi_0(k, x)\xi(x)\,\mathrm{d}x = I(k)\,. \tag{7}$$

This integral by the inverse of Paley-Wiener's theorem is an entire function of type H (and order 1), in the variable k. If now we suppose (6) to hold this amounts to say that $I(k)$ has all the zeros of $f(k)f(-k)$. We can then write:

$$I(k) = f(k)f(-k)\zeta(k^2) = G(E)\zeta(E)\,, \qquad E = k^2\,. \tag{8}$$

We know however that the type of $I(k)$ is H, while the type of $f(k)f(-k)\zeta(k^2)$ is certainly larger than $2a$. This last statement is true because $I(k)$ is square integrable on the real axis. Now $\zeta(k^2)$ considered as a function of $E = k^2$ is an entire function of order $\frac{1}{2}$ and general theorems make us sure that it can be bounded on a single direction in the E-plane at most. Since $f(k)f(-k) \to 1$ when $k \to \pm\infty$ on the real axis, to obtain square integrability we must have

---

[3] *Fourier Transforms in the complex domain.* By R. E. A. C. Paley and N. Wiener. (*American Mathematical Society Colloquium Publications*, Vol. XIX).

[4] R. P. Boas: *Entire Functions* (New York, 1954).

$\zeta(E)$ to decrease on the real axis of k and therefore, for positive E, $\zeta(k^2)$ is certainly bounded. It follows that it cannot be bounded on any other direction and that the type of $\zeta(k^2)f(k)f(-k)$ is certainly equal or larger than the type of $f(k)f(-k)$ which is $2a$.

Therefore, unless we have $I(k)=0$, we meet a contraddiction if $H<2a$. Now from $I(k)=0$ for any k it follows that $\xi(x)=0$. This result amounts to the proof of the closure and therefore of the completeness of our sets (4) and (3) over the interval $0 \ldots H$, where $H<2a$. If $H=2a$ the proof is slightly more complicated but it can be still carried out.

We have been able therefore to prove the theorem:

a) The sets of functions $\varphi(k_n, x)$ and $\varphi_0(k_n, x)$ are complete in the interval $0 \ldots 2a$.

Additional information is provided by:

b) The sets of functions $\varphi(k_n, x)$ and $\varphi_0(k_n, x)$ are independent in the interval $0 \ldots 2a$.

Proof: By definition the set of functions $\varphi(k_n, x)$ is said to be independent in the interval $2a$ if the relation:

$$\sum_0^\infty \lambda_n \varphi_0(k_n, x) = 0\,, \tag{9}$$

implies $\lambda_n = 0$. Of course independence of $\varphi_0(k_n, x)$ and $\varphi(k_n, x)$ are equivalent. Now the function:

$$G_n(k) - \frac{kG(k^2)}{k^2 - k_n^2}\,. \tag{10}$$

For Paley-Wiener's theorem admits the integral representation:

$$G_n(k) = \int_0^{2a} \vartheta_n(x) \sin kx \,\mathrm{d}x\,, \tag{11}$$

where $\vartheta_n(x)$ is square integrable on $0 \ldots 2a$. This possibility follows from the obvious fact that $G_n(k)$ is an entire function of type $2a$ which is square integrable on the real axis of k. Clearly (11) implies:

$$\int_0^{2a} \varphi_0(k_m, x)\vartheta_n(x)\,\mathrm{d}x = G'(E_m)\delta_{mn}\,, \tag{12}$$

ϑ_n is therefore orthogonal to all $\varphi_0(k_m, x)$ but $\varphi_0(k_n, x)$.

If now we suppose (9) to hold within $0 \dots 2a$ we have:

$$0 = \int_0^{2a} \vartheta_m(x)\left[\sum_n \lambda_n \varphi_0(k_n, x)\right] \mathrm{d}x = \sum_{n=0}^{\infty} \lambda_n \delta_{nm} G'(E_m) = \lambda_m G'(E_m) . \tag{13}$$

This result is completely equivalent to theorem *b*). Theorem *b*) implies that our sets of functions cannot be complete on a wider interval than $0 \dots 2a$. Manifestly if it would be so we could expand with not all vanishing coefficents within $0 \dots H$, with $H > 2a$, a function which vanishes within $0 \dots 2a$ and does not vanish outside. Eq. (9) would hold now within $0 \dots 2a$, thus implying $\lambda_n = 0$ in contraddiction with what assumed in the beginning.

4. – From theorems *a*) and *b*) it follows that any function $\chi(x)$ admits an expansion of the kind:

$$\chi(x) = \sum_0^{\infty} \lambda_n \varphi_0(k_n, x) , \qquad x \leqslant 2a , \tag{14}$$

holding almost everywhere. The coefficents λ_n are given by:

$$\lambda_n = \frac{1}{G'(E_n)} \int_0^{2a} \vartheta_n(x) \chi(x) \, \mathrm{d}x . \tag{15}$$

Similar expansions hold for the perturbed wave functions, $\varphi(k_n, x)$. Clearly:

$$\vartheta_n(x) = \frac{i}{\pi} \int_{\infty}^{\infty} \exp\left[-ikx\right] G_n(k) \, \mathrm{d}k = \frac{2}{\pi} \int_0^{\infty} \sin kx \cdot G_n(k) \, \mathrm{d}k . \tag{16}$$

We have also:

$$\vartheta_n(x) + \exp\left[ik_n x\right] = \frac{i}{\pi} * \int_{\infty}^{\infty} k \exp\left[-ikx\right] \frac{G(k^2) - 1}{k^2 - k_n^2} \, \mathrm{d}k . \tag{17}$$

Here $*\int$ means that the path of integration is taken to be above the zeros of $f(-k)$ and below the zeros of $f(k)$. Applying to both sides the operator $(\mathrm{d}^2/\mathrm{d}x^2) + k_n^2$ we get:

$$\vartheta_n'' + k_n' \vartheta_n = \vartheta , \tag{18}$$

$\vartheta(x)$ is given here by:

$$\vartheta(x) = \frac{i}{\pi} * \int_{-\infty}^{\infty} k \exp[-ikx][1 - G(k^2)]\,\mathrm{d}k\,. \tag{19}$$

Eq. (18) can be solved and yields:

$$\begin{cases} \vartheta_n(x) = -\exp[ik_n x] + \int_0^{2a} G_n(x, y)\vartheta(y)\,\mathrm{d}y; \\ G_n(x, y) = \begin{array}{ll} \varphi_0(k_n, y)\exp[ik_n x], & y \leqslant x, \\ \varphi_0(k_n, x)\exp[ik_n y], & y \geqslant x. \end{array} \end{cases} \tag{20}$$

In this last formula care has been taken of the fact that $\vartheta(x)$ and $\vartheta_n(x)$ as given by (16) and (19) vanish outside $0 \ldots 2a$.

Moreover:

$$\vartheta_n(x) + \exp[ik_n x) \to 0\,. \qquad x \to 0\,. \tag{21}$$

This last property follows from (17).

For the set (3) we can define the functions $\tau_n(x)$ as follows:

$$\frac{G_n(k)}{k} = \int_0^{2a} \varphi(k, x)\tau_n(x)\,\mathrm{d}x\,. \tag{22}$$

The inversion of this formula, like what we have carried out in (16), is somehow complicated by the fact that the free state functions $\varphi(k, x)$ (k real) do not form a complete system, the bound states being also needed. This inversion is most naturally carried out using the complex definition of Dirac's delta function:

$$\delta(x - y) = \frac{1}{\pi} * \int_{\infty} \frac{k^2\,\mathrm{d}k}{G(k^2)}\,\varphi(k, x)\varphi(k, y)\,. \tag{23}$$

We have used here the same path as in (17). (See the appendix for a detailed proof). The result of the inversion is:

$$\tau_n(x) = \frac{1}{\pi} * \int_{\infty}^{\infty} \frac{k^2\varphi(k, x)}{k^2 - k_n^2}\,\mathrm{d}k\,. \tag{24}$$

Putting

$$\varphi(k, x) = \varphi_0(k, x) + \int_0^x K(x, y)\varphi_0(k, y)\,\mathrm{d}y\,,$$

we obtain:

$$\tau_n(x) = \exp[ik_n x] + \int_0^x K(x, y)\exp[ik_n y]\,\mathrm{d}y\,. \tag{25}$$

Account has been taken of the formula:

$$\frac{1}{\pi} * \int_{-\infty}^{\infty} \frac{k \sin kx}{k^2 - k_n^2}\,\mathrm{d}k = \exp[ik_n x]\,. \tag{26}$$

Also interesting is the following differential equation which can be deduced from (25):

$$\tau_n''(x) + k_n^2\tau_n(x) - V(x)\tau_n(x) = \frac{\partial K(x, y)}{\partial y}_{|y\,0}\,. \tag{27}$$

5. – We are now ready to attack the main problem of the inversion. The most important point in the whole procedure is the linear Gel'fand and Levitan's integral equation for the kernel $K(x, y)$:

$$K(x, y) = f(x, y) + \int_0^x K(x, z)f(z, y)\,\mathrm{d}z\,. \tag{28}$$

Here $f(x, y)$ is defined as:

$$f(x, y) = \frac{1}{\pi} * \int_{-\infty}^{\infty} \left[1 - \frac{1}{G(E)}\right] \varphi_0(k, x)\varphi_0(k, y)\,\mathrm{d}k \cdot k^2\,. \tag{29}$$

In the current literature one rather employs an equivalent definition which does not use complex variable integration but Stieltjes integrals over the energy. For what follows our definition is better. $f(x, y)$ can be calculated in principle from the experimental data because $\varphi_0(k, x)$ are known elementary functions and $G(E)$ is simply related to the phase shifts. One solves then eq. (28) and calculates the potential using:

$$-2\,\frac{\mathrm{d}}{\mathrm{d}x} K(x, x) = V(x)\,. \tag{30}$$

Eq. (28) is a Fredholm integral equation in $K(x, y)$. Eqs. (28), (29), (30) contain all what is needed for the reconstruction of the potential. Their practical use is however limited by the intrinsic complicated fashion in which the experimental data appear. A considerable simplification arises using the mathematical machinery which we developed in Sects. **3**, **4**. The first task in trying to solve (28) is of course the calculation of $f(x, y)$ from (29).

To achieve it we espand $f(x, y)$ using set (4). This expansion will be valid only within $0 \ldots 2a$ but this interval is amply sufficient for our problem. The expansion can be written as follows:

$$f(x, y) = \sum_0^\infty \omega_n(x)\varphi_0(k_n, y)\,, \tag{31}$$

where of course from (15) we deduce that:

$$\omega_n(x) = \frac{1}{G'(E_n)} \int_0^{2a} \vartheta_n(y) f(x, y)\,\mathrm{d}y = \frac{1}{\pi G'(E_n)} * \int_{-\infty}^{\infty} \left[1 - \frac{1}{G(E)}\right] \varphi_0(k, x)\, \frac{G(E)}{E - E_n}\, k^2\,\mathrm{d}k. \tag{32}$$

The final result can be written as (see (17)):

$$f(x, y) = \sum_0^\infty \frac{1}{G'(E_n)} \left(\vartheta_n(x) + \exp\left[ik_n x\right]\right) \varphi_0(k_n, y)\,. \tag{33}$$

If $x > y$:

$$\sum_0^\infty \frac{\vartheta_n(x)\varphi_0(k_n, y)}{G'(E_n)} = \delta(x - y) = 0\,,$$

and the expansion takes the simple form:

$$f(x, y) = \sum_0^\infty \frac{1}{G'(E_n)} \exp\left[ik_n x\right]\varphi_0(k_n, y)\,. \tag{34}$$

If $x < y$ we just exchange them in the above formula in virtue of $f(x, y) = f(y, x)$. Expansion (34) does not converge if $x < y$. We could have derived it by writing (29) as:

$$f(x, y) = \frac{i}{\pi} * \int_{-\infty}^{\infty} \left[1 - \frac{1}{G(E)}\right] \exp\left[-ikx\right]\varphi_0(k, y)\,\mathrm{d}k\,, \tag{35}$$

and closing the integration path with an arbitrarily large semicircle in order to enclose all singularities of $f(-k)^{-1}$. This method yields the same result

but it is very difficult to prove that the contribution of the semicircle is negligible. Formulas (33), (34) can be easily extended to the general case of an arbitrary angular momentum. For S waves however we can still simplify it by noticing that:

$$\varphi_0(k, y) = \frac{\exp[iky] - \exp[-iky]}{2ik} .$$

Introducing the function:

$$F(z) = \sum_0^\infty \frac{\exp[ik_n|z|]}{2ik_n G'(E_n)} ,$$

(34) can be written as:

$$f(x, y) = F(x + y) - F(x - y) . \tag{36}$$

For $x = y$ the formulas (34), (36) do not hold any more. Yet we can find the value of $f(x, x)$ by a limiting process because $f(x, y)$ is continuous at $x = y$.

(36) provides a very fast method for the computation of $f(x, y)$ if the position of the zeros is known. It is interesting to notice that zeros with large positive imaginary parts yield small contribution to $F(z)$ as expected and as desirable.

6. – We are facing now the task of solving eq. (28). One obvious way to do it is given by the iteration method. If $f(x, y)$ is small, few terms will be sufficient to provide a good answer. If this is not the case a second approach tries to find the functions $J_n(x)$ in the expansion:

$$K(x, y) = \sum_0^\infty J_n(x)\varphi_0(k_n, y) . \tag{37}$$

Introducing this expansion into (28) and equating the coefficents of $\varphi_0(k_n, x)$ on both sides we find the system:

$$\begin{cases} J_n(x) = \omega_n(x) + \sum_n \left[\int_0^x \varphi_0(k_m, y)\omega_n(y)\,\mathrm{d}y \right] J_m(x) , \\ \sum_0^\infty M_{nm}(x)J_m(x) = \omega_n(x); \qquad M_{nm} = \delta_{nm} - \int_0^x \varphi_0(k_m, y)\omega_n(y)\,\mathrm{d}y . \end{cases} \tag{38}$$

This system can be formally solved by introducing the inverse matrix of

the $M_{mn}(x)$:

$$J_n(x) = \sum_l M_{nl}^{-1}\omega_l(x)\,. \tag{39}$$

The final answer for the potential is therefore:

$$\frac{\mathrm{d}}{\mathrm{d}x}K(x,x) = \frac{\mathrm{d}}{\mathrm{d}x}\sum_{n,l}\varphi_0(k_n,x)M_{nl}^{-1}\omega_l(x) = \tag{40}$$

$$= -\frac{\mathrm{d}}{\mathrm{d}x}\sum_{n,l}\left[\frac{\mathrm{d}}{\mathrm{d}x}M_{ln}(x)\right]M_{nl}^{-1}(x) = -\frac{\mathrm{d}^2}{\mathrm{d}x^2}\log\cdot\det\cdot|M_n|\,.$$

This very compact result strongly resembles a similar one obtained by Jost and Kohn in a related problem ([5]). This determinant can be practically evaluated only if one knows the functions $\omega_n(x)$. These functions can be readily computed from the unique function $\vartheta(x)$ through (20). Eq. (19) defines $\vartheta(x)$ but it is not suitable for a numerical evaluation. It is much easier to start from an approximate « ansatz » as follows:

$$\vartheta(x) = \sum_n a_n A_n(x)\,, \tag{41}$$

where the $A_n(x)$ are some simple and well-known functions, for instance powers of x, and the a_n's are constants to be determined by the conditions:

$$\int_0^{2a}\vartheta(x)\varphi_0(k_n,x)\,\mathrm{d}x = 1\,, \tag{42}$$

which can be obtained through Fourier inversion of eq. (19).

Conclusions.

We may sketch the whole procedure in the following steps:

1) From the knowledge of the phase-shifts and of the binding energies of the bound states E_n we reconstruct the function $f(k)$ using the following formula ([6]) ([5]):

$$\log\cdot G(E) = \frac{1}{\pi}\int_0^\infty \mathrm{d}E'\,\frac{\delta(E')}{E'-E} + \sum_n \log\cdot\frac{E}{E+|E_n|} \qquad E, E', \text{real}. \tag{43}$$

([5]) R. Jost and W. Kohn: *Det, Kgl. Danske Vidensk. Selskab. Mat. Fys. Medd.*, **27**, no. 9 (1953).

([6]) H. Umezawa: *Quantum Field Theory*, (Amsterdam 1956) pag. 321.

2) $f(k)$ is then approximated by a polinomial or by any entire function. The zeros of this function are determined. Among them we must find those corresponding to the bound states. We hope that inversely from the knowledge of the zeros one can have a reliable representation of $f(k)$.

3) The kernel (29) is then calculated and eq. (28) solved with one of the methods which we have presented above.

Appendix I

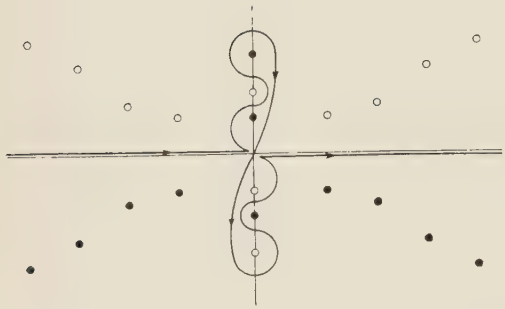

Fig. 1. – ○ zeros of $f(k)$; ● zeros $f(-k)$.

We show here how to derive formula (23) of the text. It is better to work the way back to the customary Stieltjes integral formulation. We can split the integral appearing in (23) into three parts; one stretched along the real axis, the others are closed loops enclosing the singularities arising from the bound-states zeros of $f(k)$ and $f(-k)$ respectively (see Fig. 1).

The contribution of the closed loops can be evaluated with the contour method and it turns out to be the same for both of them.

The result is:

$$(44) \qquad \delta(x-y) = \frac{1}{\pi}\int_{-\infty}^{\infty} \frac{k^2\,\mathrm{d}k}{G(k')}\,\varphi(k,x)\varphi(k,y) + \sum_{\substack{\text{bound}\\ \text{states}}} \frac{2ik_n}{G'(E_n)}\,\varphi(k_n,x)\varphi(k_n,y)\,.$$

This result can be still transformed taking as variable (real) the energy and introducing the density:

$$(45) \qquad \mathrm{d}\varrho(E) = \frac{k\,\mathrm{d}E}{\pi G(E)} \quad E>0; \qquad \mathrm{d}\varrho(E) = \sum_{\substack{\text{bound}\\ \text{states}}} \delta(E+|E_n|)\,\frac{2ik_n}{G'(E_n)}\,\mathrm{d}E\,.$$

We finally get:

$$(46) \qquad \delta(x-y) = \int_{-\infty}^{\infty} \mathrm{d}\varrho(E)\cdot\varphi(k,x)\varphi(k,y)\,,$$

which is the usual way of writing Dirac's function (7) because one has:

$$\int_0^\infty \varphi_n^2(k, x)\,\mathrm{d}x = \frac{G'(E_n)}{2ik_n} \qquad \text{(bound states only)}. \tag{47}$$

* * *

I wish to thank Prof. M. VERDE for many helpful suggestions and for his illuminating criticism.

(7) M. VERDE: *Nuovo Cimento*, **6**, 340 (1957).

RIASSUNTO

Il metodo di Gel'fand e Levitan per la ricostruzione del potenziale dalla funzione spettrale viene reso più semplice e rapido. Si mette pure in evidenza la portata di alcuni teoremi matematici su problemi di carattere pratico.

Pair Effects in the Lee Model.

J. S. Goldstein (*)

Brandeis University - Waltham 54, Mass.

(ricevuto il 26 Maggio 1958)

Summary. — The Lee model of an exactly soluble, renormalizable field theory is extended by allowing the meson to make nucleon pairs, introducing a new nucleon field for the purpose. The theory is still exactly soluble, with the following results; logarithmic divergences remain in the theory after renormalization, and the ghost state is shifted from the V-particle spectrum to the meson spectrum.

1. – Introduction.

The exactly soluble model of a field theory, introduced in 1954 by T. D. Lee [1], has attracted the attention of many writers [2-7]. Since the theory includes self-energy divergences, it is of considerable interest to study the mathematical structure of the renormalization program designed to remove these divergences.

It was observed by Lee that in the limit of point particles, the square of the wave function renormalization constant for the clothed V-particle state becomes negatively infinite. Since it can be shown on quite general grounds [8]

(*) On leave from Baird-Atomic, Inc., Cambridge, Mass.

(1) T. D. Lee: *Phys. Rev.*, **95**, 1329 (1954).
(2) G. Källén and W. Pauli: *K. Dabske Vid. Selskab*, **30**, No. 7 (1955).
(3) K. Ford: *Phys. Rev.*, **105**, 320 (1957).
(4) G. Källén: *CERN*, 57-43 (1957).
(5) Th. Ruijgrok and L. Van Hove: *Physica*, **23**, 880 (1956).
(6) G. Dell'Antonio and F. Duimio: *Nuovo Cimento*, **5**, 1636 (1957); **6**, 751 (1957).
(7) S. Machida: *Prog. Theor. Phys.*, **14**, 407 (1955).
(8) G. Källén: *Nuovo Cimento*, **12**, 217 (1954).

that this quantity should be a probability and hence restricted in value to be between 0 and 1, considerable effort has been put into attempts to understand the consequences of this result. KÄLLÉN and PAULI [2] have shown that this is an essential difficulty of the model, and leads to the existence of another eigenstate of the Hamiltonian having negative norm (ghost state). Attempts to circumvent the difficulty by the introduction of an indefinite metric into the theory are shown by these authors to fail, because the existence of a state of negative norm implies non-unitarity of the S-matrix. It is not clear whether this difficulty arises out of the particular manner in which the Lee model is constructed, or whether it may be true of local field theories in general [3,4].

The Lee model has been extended by RUIJGROK and VAN HOVE [5] in the following way. In the original model, only three different fields are introduced; the V-particle and the N-particle, representing nucleons, and the θ-particle, representing a scalar meson. The only interaction allowed by the Hamiltonian is $V \leftrightarrow N + \theta$. RUIJGROK and VAN HOVE introduce u nuclear fields, V_i, and one meson field θ, the allowed transitions being $V_i \leftrightarrow V_{i+1} + \theta$, where $V_{n+k} \equiv V_k$. Since this model includes overlapping self-energy diagrams, a vertex renormalization is introduced which is related to the charge renormalization. The apparent consequence of the introduction of these extra degrees of freedom into the theory is that even in the limit of point particles the renormalized coupling constant remains finite. However, the difficulty of the ghost state apparently remains [6].

Other examples of exactly soluble field theoretic models have been constructed [8,10-13]. Since the structure of these models is different from that of the Lee model, they will not be discussed here.

The general problem of ghost states in field theories is discussed in considerable detail in references [2-4]. The connection of the ghost states with the problem of self-consistency of field theory is discussed particularly by KÄLLÉN [4].

In the present article, the Lee model has been extended in order to study the effects of allowing the meson to make pairs. There are several ways in which this may be done; the simplest procedure seems to be to introduce a new nucleon field, which we term the χ-particle, and its antiparticle, $\bar{\chi}$, and to allow in addition to $V \leftrightarrow N + \theta$, the transition $\theta \leftrightarrow \chi + \bar{\chi}$. A possibly more

[9] W. THIRRING: *Annals of Physics*, **3**, 91 (1958).
[10] G. WENTZEL; *Helv. Phys. Acta*, **15**, 111 (1942).
[11] MCCORMACK and KLEIN: *Phys. Rev.*, **98**, 1428 (1955).
[12] ARNOUS: *Journ. de Phys.*, **17**, 107 (1956).
[13] E. LOMON: *Nuovo Cimento*, **4**, 106 (1956).
[14] B. LIPPMAN and J. SCHWINGER: *Phys. Rev.*, **79**, 769 (1950).

interesting model is one where the transitions $V \leftrightarrow N + \theta$, $\theta \leftrightarrow N + \bar{N}$ are allowed. The diagrams of Fig. 1 show the possible intermediate states occuring in the clothed V-particle.

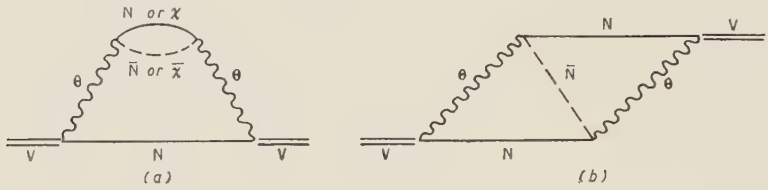

Fig. 1.

It will be seen that the diagram of Fig. 1*b* cannot occur if only the transition $\theta \leftrightarrow \chi + \bar{\chi}$ is allowed. In the appendix it is shown that the model which allows $\theta \leftrightarrow N + \bar{N}$ is soluble in the sense that the one-particle states and the scattering states can be expressed in closed form, but that an integral equation results which has only been solved in a coupling constant expansion. Nevertheless, the basic structure of the two models appears to be the same.

2. – The hamiltonian.

The Hamiltonian for the Lee model, permitting only $V \leftrightarrow N + \theta$, is given in momentum space by

$$H = H_0 + H_1 ,$$

where

$$(1) \qquad H_0 = \sum_p (M_p - \delta M_p)\psi^*(p)\psi(p) + \sum_p T_p \varphi^*(p)\varphi(p) + \sum_p \omega_p a_p^* a_p ,$$

$$(2) \qquad H_1 = g_1 \sum_{pk} (2\Omega\omega_k)^{-\frac{1}{2}} \left[\psi^*(p)\varphi(p-k)a_k + a_k^*\varphi^*(p-k)\psi(p)\right] .$$

In these sums, as well as in all that will follow, it is assumed that a cut-off factor is contained in the summand, although these factors will not be explicitly shown. Alternatively, the sums may be regarded as having an upper limit at some very large but finite momentum, P. The volume of periodicity is taken as Ω, field operators ψ, φ and a are the annihilation operators for the bare V, N and θ particles, respectively, and M_p, T_p and ω_p are the observed energies of the clothed particles. The quantity δM_p is therefore a mass-renormalization counter term for the V-particles. The commutation laws are

$$(3) \qquad [a_k, a_p^*] = \{\psi(k), \psi^*(p)\} = \{\varphi(k), \varphi^*(p)\} = \delta_{kp} ,$$

while all other commutators of field operators with a_k and the other anti-commutators of the nucleon field operators vanish. The quantity g_1 represents the unrenormalized coupling constant for the vertex $\mathrm{V} \leftrightarrow \mathrm{N} + \theta$. As is usual, we put $\hbar = c = 1$.

To this Hamiltonian we now add terms describing the χ-particle and its interaction with the meson field. Thus, if $H = H_0 + H_1 + H_2$,

$$H_0 = \sum_p (M_p - \delta M_p)\psi^*(p)\psi(p) + \sum_p T_p \varphi^*(p)\varphi(p) + \\ + \sum_p (\omega_p - \delta\mu_p) a_p^* a_p + \sum_p E_p \chi^*(p)\chi(p) + \sum_p E_p \bar{\chi}^*(p)\bar{\chi}(p) , \tag{4}$$

$$H_1 = g_1 \sum_{pk} (2\Omega\omega_k)^{-\frac{1}{2}} \left[\psi^*(p)\varphi(p-k)a_k + \text{c.c.}\right] , \tag{5}$$

$$H_2 = g_2 \sum_{pk} (2\Omega\mu)^{-\frac{1}{2}} \left[a_k^* \chi(k-p)\bar{\chi}(p) + \text{c.c.}\right] . \tag{6}$$

The χ-operators have the following anticommutation relations:

$$\left\{\chi(k), \chi^*(p)\right\} = \left\{\bar{\chi}(k), \bar{\chi}^*(p)\right\} = \delta_{kp} . \tag{7}$$

All other anticommutators of χ with itself or other fermion fields vanish, as well as the commutators of the χ-field with a. It is to be noted that in place of the factor $(2\omega_k)^{-\frac{1}{2}}$ which might be expected to appear in H_2, we use instead the factor $(2\mu)^{-\frac{1}{2}}$, where μ is the observed meson mass. If this were not done, the theory would still be soluble, but the renormalization would depend on momentum in a manner adding greatly to the complexity of the renormalization program. It is also to be noted that a mass renormalization counter term for the meson has been added to H_0; this becomes necessary owing to the vacuum polarization diagrams which can now occur (see Fig. 1*a*).

As in the Lee model itself, the present model provides a conservation law for heavy particles. Thus, the following number operators are seen to be conserved with the Hamiltonian $H = H_0 + H_1 + H_2$:

$$Q_1 = \sum_p \psi^*(p)\psi(p) + \sum_p \varphi^*(p)\varphi(p) , \tag{8}$$

$$Q_2 = \sum_p \varphi^*(p)\varphi(p) - \sum_p a_p^* a_p - \tfrac{1}{2} \sum_p \chi^*(p)\chi(p) - \tfrac{1}{2} \sum_p \bar{\chi}^*(p)\bar{\chi}(p) . \tag{9}$$

Thus, the number of N-particles plus the number of V-particles (bare) is conserved in the intermediate states, as in the Lee model; the second relation indicates that the annihilation of an N-particle requires the annihilation of a θ-particle or its equivalent, a χ-$\bar{\chi}$ pair (*).

(*) In this model, the anti-particle does not behave like a hole in an infinite sea, but rather as an ordinary particle. Hence the negative sign in front of the $\bar{\chi}$ number operator.

3. – The one-particle states.

The eigenstates of $H = H_0 + H_1 + H_2$ are most conveniently expressed in terms of the free particle states. It will at once be seen that the vacuum of bare particles is also an eigenstate of H with eigenvalue zero; and that the bare N-, χ- and $\bar{\chi}$-particles are also eigenstates of H with eigenvalues T_p, E_p, E_p, respectively:

$$(10) \qquad \begin{cases} H|0\rangle = 0\,, \\ H\varphi^*(p)|0\rangle = T_p\varphi^*(p)|0\rangle\,, \\ H\chi^*(p)|0\rangle = E_p\chi^*(p)|0\rangle\,, \\ H\bar{\chi}^*(p)|0\rangle = E_p\bar{\chi}^*(p)|0\rangle\,. \end{cases}$$

Because of the possibility of $\theta \leftrightarrow \chi + \bar{\chi}$, the state of one clothed meson is no-longer equal to the state of one bare meson. However, the conservation law (9) allows us to find a simple expression for the clothed one-meson state:

$$(11) \qquad |\theta_k\rangle_c = \alpha_k[a_k^* + \sum_q y(k, q)\chi^*(q)\bar{\chi}^*(k-q)]|0\rangle\,,$$

where α_k is the meson wave function normalization constant, and $y(k, q)$ represents a Fourier coefficient, the value of which is to be determined from the Schrödinger equation. It is readily seen that $H_1|\theta_k\rangle_c = 0$; hence the state (11) is an eigenstate of $H_0 + H_2$. It has been recognized by MACHIDA [7] that this part of the Hamiltonian could be solved exactly for the clothed one-meson state; the solution presented here agrees with that of Machida, although the technique of renormalization used later differs slightly.

The requirement that (11) be an eigenstate of H belonging to the eigenvalue ω_k leads to the following results:

$$(12) \qquad y(k, q) = g_2(2\Omega\mu)^{-\frac{1}{2}}(\omega_k - W_{kq})^{-1}\,,$$

$$(13) \qquad \delta\mu_k = g_2^2(2\Omega\mu)^{-1}\sum_q (\omega_k - W_{kq})^{-1}\,,$$

where the abbreviation W_{kq} is used for $(E_q + E_{k-q})$. It will be observed that the mass renormalization for the meson is more singular, in the limit of no cut-off, than the V-particle mass renormalization found by Lee, to be rederived below.

In similar fashion, the state of one clothed V-particle may be found. The conservation laws indicate a superposition of the following form:

$$(14)\qquad |V_p\rangle_c = \beta_p[\psi^*(p) + \sum_k u(p,k)a_k^*\varphi^*(p-k) + \\ + \sum_{k\,q} v(p;kq)\varphi^*(p-k)\chi^*(q)\bar{\chi}^*(k-q)]|0\rangle\,,$$

where β_p is a normalization constant, and $u(p,k)$, $v(p;kq)$ are again Fourier coefficients to be determined from the Schrödinger equation.

We require now that (14) be an eigenstate of H with eigenvalue M_p; the resulting equations are as follows (*):

$$(15)\qquad v(p;kq) = -g_2(2\Omega\mu)^{-\frac{1}{2}}u(p,k)[T_{p-k} - M_p + W_{kq}]^{-1}\,,$$

$$(16)\qquad u(p,k)[\omega_k - \delta\mu_k + T_{p-k} - M_p] + g_1(2\Omega\omega_k)^{-\frac{1}{2}} + g_2(2\Omega\mu)^{-\frac{1}{2}}\sum_q v(p;kq) = 0\,,$$

$$(17)\qquad \delta M_p = g_1\sum_k (2\Omega\omega_k)^{-\frac{1}{2}}u(p,k)\,.$$

Eq. (16) can be solved for $u(p,k)$ by the elimination of $v(p;kq)$ from eq. (15). The result is

$$(18)\qquad u(p,k) = -g_1(2\Omega\omega_k)^{-\frac{1}{2}}[\omega_k + T_{p-k} - M_p]^{-1}\cdot \\ \cdot\Big[1 + g_2^2(2\Omega\mu)^{-1}\sum_q (W_{kq} - \omega_k)^{-1}(W_{kq} - M_p + T_{p-k})^{-1}\Big]^{-1}\,.$$

In deriving eq. (18), the value of $\delta\mu_k$ has been introduced from eq. (13). The V-mass renormalization then has the form

$$(19)\qquad \delta M_p = (-g_1^2/2\Omega)\sum_k \Big\{\omega_k(\omega_k + T_{p-k} - M_p)\cdot \\ \cdot[1 + (g_2^2/2\Omega\mu)\sum_q (W_{kq} - \omega_k)^{-1}(W_{kq} - M_p + T_{p-k})^{-1}]\Big\}^{-1}\,.$$

4. – χ-$\bar{\chi}$ scattering.

The simplest two-particle scattering state in this theory is the χ-$\bar{\chi}$ scattering. As is to be expected, the part of the Hamiltonian labeled H_1 plays no role, so that the scattering is the same as that calculated by MACHIDA (7)

(*) It is at this point that the advantage of introducing a new χ-field is realized. If the transition $\theta \leftrightarrow N + \bar{N}$ is allowed, eq. (18) becomes an integral equation for $u(p,k)$; in its present form it can be solved algebraically. See Appendix for the derivation of the integral equation.

The scattering eigenstate of H is required to have the following properties: it shall consist of an incoming part which is a plane wave consisting of one χ and one $\bar{\chi}$ with momenta $p-k$ and k, respectively; and a scattered part containing outgoing χ-$\bar{\chi}$ particles. Such a state must have the form

$$(20)\qquad |\chi_{p-k}\bar{\chi}_k\rangle_c^+ = \left[\chi^*(p-k)\bar{\chi}^*(k) + \sum_{k'} \varrho_+(pk;k')\chi^*(p-k')\bar{\chi}^*(k') + ca_p^*\right]|0\rangle$$

where the $(+)$ sign on the distribution $\varrho_+(pk;k')$ indicates that a solution with only outgoing scattered waves is sought. The requirement that (20) be an eigenstate of H with eigenvalue W_{pk} leads to the following equations determining ϱ_+ and c:

$$(21)\qquad \varrho_+(pk;k')[W_{pk}-W_{pk'}] = g_2c(2\Omega\mu)^{-\frac{1}{2}},$$

$$(22)\qquad g_2(2\Omega\mu)^{-\frac{1}{2}}\left[1+\sum_{k'}\varrho_+(pk;k')\right] = c[W_{pk}-\omega_p+\delta\mu_p].$$

The requirement that ϱ_+ represent outgoing waves leads to the following solutions for ϱ_+ and c:

$$(23)\qquad \varrho_+(pk;k') = g_2c(2\Omega\mu)^{-\frac{1}{2}}[W_{pk}-W_{pk'}-i\varepsilon]^{-1},$$

$$(24)\qquad c = g_2(2\Omega\mu)^{-\frac{1}{2}}\Big\{W_{pk}-\omega_k+(g_2^2/2\Omega\mu)\sum_q[(\omega_p-W_{pq})^{-1}-(W_{pk}-W_{pq}-i\varepsilon)^{-1}]\Big\}^{-1},$$

where ε is an infinitesimal positive quantity. Use of the relation

$$\frac{1}{x-i\varepsilon} = P\left(\frac{1}{x}\right)+i\pi\,\delta(x),$$

shows that ϱ_+ does indeed correspond to outgoing waves in configuration space.

With the coefficients ϱ_+ and c determined, it is now possible to calculate the appropriate S-matrix element for χ-$\bar{\chi}$ scattering:

$$(25)\qquad S_p(k_1,k_2) = \delta_{k_1k_2}-2\pi i\,\delta(W_{pk_1}-W_{pk_2})R_p(k_1,k_2),$$

where

$$(26)\qquad R_p(k_1,k_2) = \langle 0|\,\chi(p-k_2)\bar{\chi}(k_2)H_2\,|\chi_{p-k_1}\bar{\chi}_{k_1}\rangle_c^+ .$$

Using eq. (20) together with the definition of H_2, $R_p(k_1k_2)$ is determined as

$$(27)\qquad R_p(k_1k_2) = (g_2^2/2\Omega\mu)\cdot$$
$$\cdot\Big\{W_{pk}-\omega_p+(g_2^2/2\Omega\mu)\sum_q[(\omega_p-W_{pq})^{-1}-(W_{pk}-W_{pq}-i\varepsilon)^{-1}]\Big\}^{-1},$$

where, due to conservation of energy, the momentum k on the right hand side may be taken as either k_1 or k_2. It will be seen (by considering the center of mass system) that only S-wave scattering occurs; hence one obtains for the S-wave scattering phase shift

$$\text{(28)} \qquad \operatorname{tg}\delta = \frac{(\pi g_2^2/2\Omega\mu)\sum_q \delta(W_{pk} - W_{pq})}{(W_{pk} - \omega_p)[1 + (g_2^2/2\Omega\mu)\sum_q (W_{pk} - W_{pq})^{-1}(\omega_p - W_{pq})^{-1}]} .$$

In the center of mass system, this reduces to the simple result

$$\text{(29)} \qquad \operatorname{tg}\delta = \frac{(g_2^2/8\pi\mu)\,|k|\,E_k}{(2E_k - \mu)[1 + (g_2^2/2\Omega\mu)\sum_q (\mu - 2E_q)^{-1}(2E_k - 2E_q)^{-1}]} .$$

In eqs. (28) and (29) the integrals appearing in the denominators are to be taken as principal value integrals. The result (29) agrees with that found by Machida.

5. – N-θ scattering.

The next most simple case of scattering in the theory is N-θ scattering The procedure is essentially the same as in the preceding section. It is convenient to introduce an abbreviation for eq. (11), writing

$$\text{(30)} \qquad |\theta_k\rangle_c \equiv A_k^*\,|0\rangle .$$

An eigenstate of the Hamiltonian is sought consisting of an incident wave containing one N-particle and one *clothed* meson, and containing outgoing waves consisting again of one N-particle and one *clothed* meson. The form of the state must be as follows:

$$\text{(31)} \qquad |N_{p-k}\theta_k\rangle_c^+ = [A_k^*\varphi^*(p-k) + \sum_{k'}\sigma_+(pk;\,k')A_{k'}^*\varphi^*(p-k') + \gamma\psi^*(p) + \sum_{k'q}\tau(pk;\,k'q)\varphi^*(p-k')\chi^*(q)\bar{\chi}^*(k'-q)]\,|0\rangle .$$

Once again it is required that σ_+ be determined so as to yield only outgoing waves in the scattered part.

The state (31) is now required to be an eigenstate of H with eigenvalue

$T_{p-k}+\omega_k$. The resulting equations determining σ_+, γ and τ are

$$\tau(pk;k'q)[T_{p-k}+W_{k'q}-\omega_k-T_{p-k}]= \\ =y(k'q)(2\Omega)^{-\frac{1}{2}}[\gamma g_1\omega_k^{-\frac{1}{2}}+g_2\mu^{-\frac{1}{2}}\sum_q\tau(pk;k'q)], \tag{32}$$

$$\sigma_+(pk;k')[\omega_k+T_{p-k}-\omega_{k'}-T_{p-k'}]= \\ =\alpha_k^{-1}(2\Omega)^{-\frac{1}{2}}[\gamma g_1\omega_k^{-\frac{1}{2}}+g_2\mu^{-\frac{1}{2}}\sum_q\tau(pk;k'q)], \tag{33}$$

$$\gamma[\omega_k+T_{p-k}-M_p+\delta M_p]= \\ =g_1(2\Omega\omega_k)^{-\frac{1}{2}}\alpha_k+g_1\sum_{k'}(2\Omega\omega_{k'})^{-\frac{1}{2}}\sigma_+(pk;k')\alpha_{k'}. \tag{34}$$

The quantities α_k and $y(kq)$ are the same as defined by eq. (11). Introducing the value of $y(kq)$ from eq. (12), these equations may be solved for γ and σ_+, yielding:

$$\sigma_+(pk;k')=\gamma g_1\alpha_{k'}^{-1}(2\Omega\omega_{k'})^{-\frac{1}{2}}[\omega_k+T_{p-k}-\omega_{k'}-T_{p-k'}-i\varepsilon]^{-1}[1+(g_2^2/2\Omega\mu)h_{kk'}]^{-1}, \tag{35}$$

$$\gamma=g_1\alpha_k(2\Omega\omega_k)^{-\frac{1}{2}}\{\omega_k+T_{p-k}-M_p+\delta M_p- \\ -g_1^2\sum_q(2\Omega\omega_q)^{-1}[1+(g_2^2/2\Omega\mu)h_{kq}]^{-1}[\omega_k+T_{p-k}-\omega_{k'_1}-T_{p-k'_1}-i\varepsilon]^{-1}\}^{-1}. \tag{36}$$

The negative imaginary infinitesimal in the denominator of σ_+ ensures that this term corresponds to outgoing waves. The quantity h_{kq} is defined by

$$h_{kq}=\sum_r[T_{p-q}-T_{p-k}+W_{qr}-\omega_k]^{-1}[W_{qr}-\omega_q]^{-1}. \tag{37}$$

All integrals here and in what follows are defined as principal part integrals unless the quantity $-i\varepsilon$ appears explicitly in a denominator.

The R-matrix (see eq. (25)) may now be defined as

$$R_p(k_1k_2)=\langle 0\,|\,A_{k_2}\varphi(p-k_2)H_1\,|\,N_{p-k_1}\theta_{k_1}\rangle_c^+. \tag{38}$$

This definition is valid since $A_k^*\varphi^*(p-k)\,|\,0\rangle$ is an eigenstate of H_0+H_2; H_1 may then be considered as the interaction term leading to scattering. The result is

$$R_p(k_1k_2)=\alpha_{k_1}\alpha_{k_2}g_1^2(4\Omega^2\omega_{k_1}\omega_{k_2})^{-\frac{1}{2}}\{\omega_{k_1}+T_{p-k_1}-M_p+\delta M_p- \\ -g_1^2\sum_{k'}(2\Omega\omega_{k'})^{-1}[1+(g_2^2/2\Omega\mu)h_{k_1k'}]^{-1}[\omega_{k_1}+T_{p-k_1}-\omega_{k'}-T_{p-k'}-i\varepsilon]^{-1}\}^{-1}. \tag{39}$$

At this point it is convenient to introduce the simplification, also made in the Lee model, that the energies of the V and N particles are independent

of momentum, and in fact, that they are equal. Thus

$$T_p = M_p = M \,, \tag{40}$$

with this simplification, $R_p(k_1k_2)$ becomes

$$R_p(k_1k_2) = -\frac{\alpha_{k_1}\alpha_{k_2}g_1^2}{2\Omega\omega_k}\left[\omega_k+\delta M-\frac{g_1^2}{2\Omega}\sum_{k'}\frac{1}{\omega_{k'}}\left(1+\frac{g_2^2}{2\Omega\mu}\,h_{kk'}\right)^{-1}(\omega_k-\omega_k-i\varepsilon)^{-1}\right]^{-1}, \tag{41}$$

$$h_{k'k} = \sum_q (W_{k'q}-\omega_k)^{-1}(W_{k'q}-\omega_{k'})^{-1} \,, \tag{42}$$

$$\delta M = -(g_1^2/2\Omega)\sum_k \omega_k^{-2}[1+(g_2^2/2\Omega\mu)\sum_q W_{kq}^{-1}(W_{kq}-\omega_k)^{-1}]^{-1} \,. \tag{43}$$

Furthermore, since conservation of energy requires $\omega_{k_1} = \omega_{k_2}$ or $|k_1| = |k_2|$, we may write

$$\alpha_{k_1}\alpha_{k_2} = \alpha_k^2 \,. \tag{44}$$

One now finds for the S-wave phase shift

$$\operatorname{tg}\delta = \frac{\dfrac{g\pi_1^2}{2\Omega}\sum_{k'}\dfrac{1}{\omega_{k'}}\left[1+\dfrac{g_2^2}{2\Omega\mu}\,h_{kk'}\right]^{-1}\delta(\omega_k-\omega_{k'})}{\omega_k+\delta M-\dfrac{g_1^2}{2\Omega}\sum_{k'}\dfrac{1}{\omega_{k'}}\left[1+\dfrac{g_2^2}{2\Omega\mu}\,h_{kk'}\right]^{-1}(\omega_k-\omega_{k'})^{-1}} \,. \tag{45}$$

Eq. (45) agrees with Lee's result if g_2 is put equal to zero.

6. – Coupling constant renormalization.

After mass renormalization (eqs. (13) and (43)), there still remain two undefined constants in the theory, g_1 and g_2. It is necessary to renormalize these constants so that the phase shifts given by (28) and (45) no longer contain divergent integrals, if possible. To this end, consider the integral appearing in the denominator of (28); separation of the divergent parts from this integral can be accomplished as follows (it can be done in several different ways):

$$\begin{aligned}\sum_q (W_{pq}-W_{pk})^{-1}(W_{pq}-\omega_p)^{-1} = \\ = \sum_q W_{pq}^{-2} + (\omega_p+W_{pk})\sum_q (W_{pk}-W_{pq})^{-1}(\omega_p-W_{pq})^{-1}W_{pq}^{-1} - \\ - \omega_p W_{pk}\sum_q (W_{pk}-W_{pq})^{-1}(\omega_p-W_{pq})^{-1}W_{pq}^{-2} \,.\end{aligned} \tag{46}$$

It is seen that in the limit of point interaction (no cut-off) the integral in question has a leading divergence which is linear, and in addition, a logarithmic divergence, the coefficient of which depends on the momentum of the scattering particles.

The leading divergence in (46) may be reduced still further:

$$\sum_q W_{pq}^{-2} = \sum_q W_{0q}^{-2} + 4 \sum_q \boldsymbol{p}\cdot\boldsymbol{q} W_{0q}^{-4} + F_p , \tag{47}$$

where F_p represents the remaining terms of the MacLaurin expansion of the integral around $p = 0$; it is easily seen that F_p is proportional to p^2 and is finite in the limit of no cut-off. Furthermore, the second term on the right of (47) vanishes owing to the integration over angles; hence

$$\sum_q W_{pq}^{-2} = \sum_q W_{0q}^{-2} + F_p . \tag{48}$$

The leading (linear) divergence in eq. (28) for the phase shift can be eliminated by a charge renormalization, then, in the following manner. Let

$$Z_2 = 1 + (g_2^2/2\Omega\mu) \sum_q W_{0q}^{-2} , \tag{49}$$

$$f_2^2 = g_2^2 Z_2^{-1} , \tag{50}$$

where f_2 is the renormalized charge. The expression for the phase shift becomes

$$\operatorname{tg}\delta = \frac{(\pi f_2^2/2\Omega\mu) \sum_q \delta(W_{pk} - W_{pq})}{(W_{pk} - \omega_p)\left[1 + \dfrac{f_2^2}{2\Omega\mu} \sum_q \dfrac{W_{pq}(\omega_p + W_{pk}) - \omega_p W_{pk}}{(W_{pk} - W_{pq})(\omega_p - W_{pq}) W_{pq}^2} + \dfrac{f_2^2}{2\Omega\mu} F_p\right]} . \tag{51}$$

It is seen that even after charge renormalization, the scattering vanishes in the limit of point interaction. It is to be considered a defect of the theory that elimination of the linear divergence by renormalization does not eliminate the logarithmic divergence as well. This defect arises from the failure to build a theory with consistent transformation properties, as it is known that such logarithmic terms do not appear after renormalization in a relativistic theory.

It is of interest at this point to calculate the normalization factor of the state $|\theta_k\rangle_c$, which is given by α_k^2:

$$\alpha_k^{-2} = 1 + (g_2^2/2\Omega\mu) \sum_q (W_{kq} - \omega_k)^{-2} = \tag{52}$$

$$= Z_2 \left[1 + \frac{f_2^2 \omega_k}{2\Omega\mu} \sum_q \frac{2W_{kq} - \omega_k}{(W_{kq} - \omega_k)^2 W_{kq}^2} + \frac{f_2^2}{2\Omega\mu} F_k\right] .$$

Since the logarithmic term dominates and is positive, it is seen that Z_2 must be positive in order for the norm α_k^2 to be positive; as discussed earlier, KÄLLÉN [8] has shown on general grounds that this quantity must lie between 0 and 1. However, solving eqs. (49) and (50) for Z_2 in terms of the renormalized charge, one obtains, in analogy to Lee's result

$$Z_2^{-1} = 1 - \frac{f_2^2}{2\Omega\mu} \sum W_{0q}^{-2}, \tag{53}$$

so that if $f_2^2 > ((1/2\Omega\mu) \sum W_{0q}^{-2})^{-1}$, Z_2 is negative. Thus, as shown by KÄLLÉN and PAULI [2], a ghost state for the meson must appear if the cut-off is at sufficiently high momentum.

It is now necessary to carry out the renormalization of g_1. In terms of the renormalized value f_2, the phase shift for N-θ scattering becomes

$$\operatorname{tg}\delta = \frac{(g_1^2\pi/2\Omega Z_2) \sum_q \omega_q^{-1} D_1^{-1}(q, \omega_k)\, \delta(\omega_q - \omega_k)}{\omega_k - (g_1^2/2\Omega Z_2)\left(\sum_q \omega_q^{-2} D_2^{-1}(q) - \omega_q^{-1}(\omega_q - \omega_k)^{-1} D_1^{-1}(q, \omega_k)\right)}, \tag{54}$$

where

$$D_1(q, \omega_k) = 1 + \frac{f_2^2}{2\Omega\mu}\left[\sum_r \frac{W_{qr}(\omega_q + \omega_k) - \omega_q\omega_k}{(W_{qr} - \omega_q)(W_{qr} - \omega_k) W_{qr}^2} + F_q\right], \tag{55}$$

$$D_2(q) = 1 + \frac{f_2^2}{2\Omega\mu}\left[\sum_r \frac{\omega_q}{(W_{qr} - \omega_q) W_{qr}^2} + F_q\right]. \tag{56}$$

The terms in the denominator of eq. (54) may be combined to give the following result:

$$\operatorname{tg}\delta = \frac{(g_1^2\pi/2\Omega Z_2\omega_k) \sum_q \omega_q^{-1} D_1^{-1}(q, \omega_k)\, \delta(\omega_q - \omega_k)}{1 + (g_1^2/2\Omega Z_2) \sum_q \omega_q^{-2}(\omega_q - \omega_k)^{-1} D_1^{-1}(q, \omega_k) D_2^{-1}(q) D_3(q, \omega_k)}, \tag{57}$$

where

$$D_3(q, \omega_k) = 1 + \frac{f_2^2}{2\Omega\mu}\left[\omega_k \sum_r (W_{qr} - \omega_k)^{-1} W_{qr}^{-2} + F_q\right]. \tag{58}$$

We distinguish, at this point, between two types of logarithmic divergences; those which occur from integration over χ-particle momentum, and those which occur from integration over meson momentum. The expression (57) for the phase shift contains both kinds of divergences, while the D-functions contain only divergences of the former kind. We have already seen that it is not possible to go to a point interaction between the θ and χ fields; consequently, it has to be assumed that cut-offs remain in the D-functions, and

that they are therefore finite. The logarithmic divergence which arises from integration over meson momentum may then be eliminated by a charge renormalization of the following kind:

$$f_1^2 = g_1^2 Z_1^{-1}, \tag{59}$$

$$Z_1 = 1 + \frac{g_1^2}{2\Omega Z_2} \sum_q \omega_q^{-3} D_1^{-1}(q, 0) D_2^{-1}(q) D_3(q, 0), \tag{60}$$

$$= 1 + \frac{g_1^2}{2\Omega Z_2} \sum_q \omega_q^{-3} \left(1 + \frac{f_2^2}{2\Omega\mu} F_q\right) D_2^{-2}(q). \tag{61}$$

A straightforward calculation of the wave function normalization factor for the state $|V_0\rangle_c$ yields

$$\beta_0^{-2} = 1 + \sum_k u^2(0, k) + \sum_{kq} v^2(0; kq). \tag{62}$$

A substitution from eqs. (15) and (18), with $T_p = M_p = M$, yields the simple result

$$\beta_0^{-2} = Z_1, \tag{63}$$

a result which also holds in the original Lee model. Since, by the Källén argument, Z_1 must be positive, we must investigate this point. Expressing Z_1 in terms of renormalized quantities only, we obtain

$$Z_1^{-1} = 1 - \frac{f_1^2}{2\Omega Z_2} \sum_q \omega_q^{-3} \left(1 + \frac{f_2^2}{2\Omega\mu} F_q\right) D_2^{-2}(q). \tag{64}$$

It is seen, therefore, that if Z_2 is negative, Z_1 is necessarily positive; consequently, if a ghost state appears for the meson, it no longer appears for the V-particle. But if Z_1^{-1} is in fact a probability, the fact that from (64) its value is greater than unity may lead to difficulties as troublesome as the ghost state.

7. – Conclusions.

The chief result of this paper is probably the additional small insight it gives with respect to the existence of ghost states. It is seen that what is essentially a minor modification of the Lee model is sufficient to eliminate ghosts entirely from the V-particle spectrum, although such abnormal states then appear in the spectrum of the meson. Undoubtedly a further modification of the theory would cause the ghost—perhaps now to be termed the

«galloping ghost» — to appear in the spectrum of the χ-particle, or the N-particle, or anywhere one chooses. It would appear, therefore, that much caution is required in drawing analogies between the Lee model and a real field theory such as quantum electrodynamics, for if all fields require renormalization, there is no reason why the ghost state should appear for the electron, say, and not for the photon.

It is probable that the only kind of field theory which is self-consistent is one in which every field and every vertex requires renormalization, and this clearly excludes both the Lee model and its extension in this paper.

* * *

I would like to thank Prof. S. S. Schweber for many helpful discussions.

Appendix

Three field model with pairs.

We consider here the following Hamiltonian:

$$H_0 = \sum_p (M_p - \delta M_f)\psi^*(p)\psi(p) + \sum_p E(p)[\varphi^*(p)\varphi(p) + \bar{\varphi}^*(p)\bar{\varphi}(p)] + \sum_p (\omega_p - \delta\mu_p)a_p^* a_p \,, \tag{A.1}$$

$$H_1 = g_1 \sum (2\Omega\omega_k)^{-\frac{1}{2}}[\psi^*(p)\varphi(p-k)a_k + \text{c.c.}] \,, \tag{A.2}$$

$$H_2 = g_2 \sum (2\Omega\omega_k)^{-\frac{1}{2}}[a_k^*\varphi(p)\bar{\varphi}(k-p) + \text{c.c.}] \,. \tag{A.3}$$

The clothed one-meson state is then given by

$$|\theta_k\rangle_c = \alpha_k\big[a_k^* + \sum_q y(k,q)\varphi^*(q)\bar{\varphi}^*(k-q)\big]|0\rangle \,, \tag{A.4}$$

with the coefficients α_k and $y(k,q)$ exactly as given in eqs. (12) and (52), and with $\delta\mu_k$ given by eq. (13). The N-N scattering is solved in precisely the same terms as the χ-$\bar{\chi}$ scattering of Sect. 4, and the renormalization of g_2 is unchanged.

The state of one clothed V-particle is now given by

$$|V_p\rangle_c = \beta_p\Big\{\psi^*(p) + \sum_k u(p,k)\varphi^*(p-k)a_k^* + \sum_{kq} v(p;kq)\varphi^*(p-k-q)\bar{\varphi}^*(q)\varphi^*(k)\Big\}|0\rangle \,. \tag{A.5}$$

However, the coefficients u and v are no longer given by eqs. (15) and (16). Instead, application of the Schrödinger equation leads to the following relations:

$$\delta M_p = g_1 \sum_k (2\Omega\omega_k)^{-\frac{1}{2}} u(p, k) , \tag{A.6}$$

$$u(p, k)[E_{p-k} + \omega_k - \delta\mu_k - M_p] + g_1(2\Omega\omega_k)^{-\frac{1}{2}} + \\ + g_2(2\Omega\omega_k)^{-\frac{1}{2}} \sum_q [v(p; p-k, q) - v(p; k-q, q)] = 0 , \tag{A.7}$$

$$v(p; kq)[M_p - E_{p-k-q} - E_q - E_k] = g_2(2\Omega\omega_{p-k})^{-\frac{1}{2}} u(p, p-k) . \tag{A.8}$$

Elimination of v between eqs. (A.7) and (A.8) leads to the following equation for u:

$$u(p, k)D(p, k) = -\frac{g_1}{\sqrt{2\Omega\omega_k}} - \frac{g_2^2}{2\Omega} \sum \frac{u(p, q)}{\sqrt{\omega_k\omega_q}} [M_p - E_{p-k} - E_{p-q} - E_{k-p-q}]^{-1} , \tag{A.9}$$

where

$$D(p, k) = E_{p\ k} + \omega_k - \delta\mu_k - M_p + \frac{g_2^2}{2\Omega\omega_k} \sum_q [M_p - E_{p-k} - E_{k-q} - E_q]^{-1} . \tag{A.10}$$

One no longer can put the energy of the N-particle equal to a constant; as seen from (A.10) such a step leads to meaningless integrals.

The integral equation can, of course, be solved by iteration with respect to g_2^2. The problem solved in the body of this paper then corresponds to the zero-order solution to (A.9) in which the factor $D(p, k)$ is treated exactly. Higher order solutions have not been examined, since it is not felt that the iteration solution will provide any further insight into the problem. The algebraic complexity of the renormalization procedure multiplies rapidly with higher order approximations.

RIASSUNTO (*)

Si estende il modello di Lee di una teoria di campo rinormalizzabile esattamente risolvibile consentendo al mesone di creare coppie di nucleoni introducendo allo scopo un nuovo campo nucleonico. La teoria è ancora esattamente risolvibile, coi seguenti risultati: dopo rinormalizzazione permangono nella teoria divergenze logaritmiche e lo stato fantasma è spostato dallo spettro delle particelle V allo spettro dei mesoni.

(*) *Traduzione a cura della Redazione.*

IL NUOVO CIMENTO Vol. IX, N. 3 1° Agosto 1958

Causality, Complementarity and S-Matrix Formalism in 4 Non-Local Relativistic Theories of Fields.

G. Wataghin

Istituto di Fisica dell'Università - Torino
Istituto Nazionale di Fisica Nucleare - Sezione di Torino

(ricevuto il 1° Luglio 1958)

Summary. — In Sect. **1** a relativistic Lee-model of interacting fields is discussed and the formalism of the proposed non-local theory is illustrated on this example. In Sect. **2** a general formulation of the causality and complementarity in non-local theories of fields is attempted.

1. – The relativistic Lee-Model.

Let us consider 2 scalar fields of, respectively, V, N, ϑ particles and assume that the interaction hamiltonian describes elementary processes $V \rightleftarrows N+\vartheta$. Following Lee, let us examine separately the «sectors» satisfying the conditions: $n_V + n_N = e_1 = \text{const}$; $n_N - n_\vartheta = e_2 = \text{const}$.

Introducing from the beginning the cut-off operators, we can solve the stationary Schrödinger equation in p-space:

$$(1) \qquad \begin{cases} H|z\rangle = E|z\rangle\,, \\ H = H_0 + H'\,, \\ H_0 = \sum_{\boldsymbol{p}} E_V(\boldsymbol{p})\psi_V^*(\boldsymbol{p})\psi_V(\boldsymbol{p}) + \sum_{\boldsymbol{k}} \omega(\boldsymbol{k})a^*(\boldsymbol{k})a(\boldsymbol{k}) + \sum_{\boldsymbol{k}'} E_N(\boldsymbol{k}')\psi_N^*(\boldsymbol{k}')\psi_N(\boldsymbol{k}')\,, \end{cases}$$

H' is the interaction hamiltonian in which relativistic cut-off operators are introduced as functions of invariants I_s, I_t defined in a previous work [1],

[1] G. Wataghin: *Nuovo Cimento*, **5**, 689 (1957); *Varenna Cosmic Ray Conference*. June 1957.

and $|z\rangle$ is an eigen-state of the system which is defined below as a superposition of eigen-states of the free hamiltonian H_0 containing non renormalized parameters M_0, e_0 of mass and charge.

Starting with the self energy problem of the V-particle, we can solve the Schrödinger equation in the center of mass system (CM) in which $\boldsymbol{p}=0$ and $\boldsymbol{k}'=-\boldsymbol{k}$ and write the interaction hamiltonian in the following way:

$$H' = -\frac{g_0}{\sqrt{\Omega}} \sum_{\boldsymbol{k}} \left\{ \frac{1}{\sqrt{2\omega(\boldsymbol{k})}\sqrt{2E_N(-\boldsymbol{k})}} \frac{1}{\sqrt{2}} [\xi] \right\}, \tag{2}$$

where:

$$\xi = f^{(-)}(I_s(|k|)I_t(|k|)\psi_V^*(0)\psi_N(-\boldsymbol{k})a(\boldsymbol{k}) + f^{(+)}(I_s(|k|)I_t(|k|)\psi_V(0)\psi_N^*(-\boldsymbol{k})a^*(\boldsymbol{k})]\},$$

$[a_{\boldsymbol{k}}, a_{\boldsymbol{k}'}] = \delta_{\boldsymbol{k}\boldsymbol{k}'}$ etc.

In the CM system the cut-off operators f^-, f^+ are functions of $|\boldsymbol{k}|$ and can be chosen in such a manner as to give exponentially decaying form-factors in the space and in the time: in (3) g^+, associated with the creation operators, is giving 0 for negative values of time and g^- is giving 0 for positive values of time:

$$\begin{cases} f^- = G(I_s(k))g^-(I_t(k))\; g^+(I_t(M_{0V}, 0)) = \dfrac{1}{(1+\boldsymbol{k}^2l^2)^2} \dfrac{1}{(l(k_0+k_0')+i)} \dfrac{1}{[lM_{0V}-i]}, \\ f^+ = G(I\,(k))g^+(I_t(k))\; g\;\; (I\,(M_{0V}, 0)) = \dfrac{1}{(1+\boldsymbol{k}^2l^2)^2} \dfrac{1}{(l(k_0+k_0')-i)} \dfrac{1}{[lM_{0V}+i]}, \\ k_0+k_0' = \omega(\boldsymbol{k}) + E_N(-\boldsymbol{k}) = \sqrt{M_{0\vartheta}^2+\boldsymbol{k}^2}\sqrt{M_{0N}^2+\boldsymbol{k}^2}. \end{cases} \tag{3}$$

Here l is the universal length. Putting $M_{0N}=1$; $M_{0\vartheta}=1$; $M_{0V}=1$; $l=1$; and solving (1) in the usual way we find:

$$|z\rangle \equiv |V\rangle = N[\psi_V^*(0) + g_0 \sum_{\boldsymbol{k}} \varphi(\boldsymbol{k})\psi_N^*(\boldsymbol{k})a^*(\boldsymbol{k})]|0\rangle, \tag{4}$$

$$\varphi(k) = \frac{g_0}{2\sqrt{\Omega}(1+\boldsymbol{k}^2)^{\frac{5}{2}}[2\sqrt{1+\boldsymbol{k}^2}-i][2\sqrt{1+\boldsymbol{k}^2}-E]}, \tag{5}$$

$$N^{-2} = 1 + \frac{g_0^2}{16\Omega} \frac{1}{(1+\boldsymbol{k}^2)^5[5+4\boldsymbol{k}^2][2\sqrt{1+k^2}-E]^2}, \tag{5'}$$

$$1-E = \frac{g_0^2}{16\Omega} \sum_{\boldsymbol{k}} \frac{1}{(1+\boldsymbol{k}^2)^5(5+4\boldsymbol{k}^2)[2\sqrt{1+k^2}-E]}. \tag{6}$$

From (4) (5) and (5') the mixture of eigen-states which defines the « physical » V-particle is determined.

The particular choice of the cut-off factors in (3) is such that H' remains hermitian, but the virtual states of V, N, ϑ are unstable, decaying with a lifetime of $\tau \lesssim l$. The representation of an unstable virtual state requires some care: the instability of this state is due to the interaction. Therefore such a state is no more an eigen-state of the free hamiltonian H_0, but can be represented as a density matrix of von Neumann as a mixture of infinite eigen-states of H_0 determined by the Fourier-transform of the decaying state. For example, in the proposed formalism the cut-off operators are the Fourier transforms of the form-factors depending on « internal » or relative co-ordinates η, and the factor $l(k_0+k_0'-i)^{-1}$ arises as the Fourier transform of the function $\varphi(\eta_0)$ which is:

$$\varphi = 0\,, \qquad \text{for } \eta_0 < 0,$$

$$\varphi = \exp\,[-i(k_0 + k_0' - il^{-1})\eta_0\,. \qquad \text{for } \eta_0 > 0.$$

We assume that the interaction between fields takes place only if two or more » physical « particles happen to be in the same domain D_l of relative co-ordinates η defined as in ref. ([1]). $|0\rangle$ represents the vacuum of the non-interacting bare particles.

In our example the energy of any virtual state is undetermined at least by the amount of $\tau^{-1} \sim l^{-1} = M_0 = 1$. Thus the representation of the stationary solution (6) is to be considered as a mathematical tool, where $\psi_V^*(\boldsymbol{k})\,|0\rangle$, $a(\boldsymbol{k})\,|0\rangle$ etc. are incomplete representations of the virtual states of bare particles and where $N, g_0, |\Phi(\boldsymbol{k})|^2$ define the statistical composition of the cloud surrounding the « physical » particle. In our example an approximate numerical solution of (6) gives $E \sim 0.91$, and $N^2 \sim 0.94$, if $g^2/4\pi \sim 15$.

The problem of scattering of one ξ-particle on one N or one V-particle can be solved in a similar way with the above method.

The chief difference depends on the choice of the CM system of incoming particles, because it is essential for the method described above that the separation of space and time and, therefore, also the formulation of the stationary Schrödinger equation, must be done in the CM system. The straightforward calculation gives an isotropic distribution in the CM system of the scattered particles and finite total cross-sections σ_{LN} and σ_{LV}. Postulating that these cross-sections should be $\sim l^2$ in the limit $K \to 0$, one finds important relations, which will be discussed in a forthcoming note.

2. – Causality and complementarity in a non local theory.

In accord with Bohr's complementarity principle and Heisenberg's uncertainty relation we can separate the approximate description of the propagation in macroscopic space-time domains of « physical » particles from the

description of short range interactions in which an exchange of momenta, angular momenta or charges takes place, or, more generally, in which particles are created and destructed.

In this initial discussion we shall avoid the consideration of long range fields and shall examine strong short range interactions of the type encountered between nucleons and mesons.

The free field equations of propagation will be considered as giving an approximate description of the propagation in space-time of the probability amplitudes, description adequate to represent interference and diffraction phenomena and some effects of external fields. These equations represent the motion of one « physical » particle non interacting strongly with other physical particles, and thus must contain « renormalized » charge and mass obtained from measurements in the low energy region.

On the other hand we assume the existence of 4-dimensional domains of interaction D_l, where the creation and destruction of particle takes place. It seems obvious that in such domains we cannot apply the propagation equations and control the macroscopic causality. We shall associate the assumption that these domains have in the CM system of incoming interacting particles an extension of $\sim l^4$ ($\Delta x \sim l$; $\Delta t \sim l$), with the assumption that there are no fundamental particles having a mass substantially greater than the nuclear mass M, and thus we shall put $l = M^{-1}$, [$\hbar = 1$; $c = 1$].

The representation of « bare » particles is needed only in the p-space representation used to solve the stationary Schrödinger equation. We assume that the non renormalized masses and coupling constant can be observable in the limit of high energy collision, in cases where the inner structure of the « physical » particle becomes important.

The S-matrix formalism can be formulated in the following way: in a scattering process the interaction problem must be solved in p-space, *e.g.* by means of the stationary Schrödinger equation. The approximate description in space and time of the propagation of scattered particles can be done in the usual way considering asymptotic plane waves corresponding to the outgoing « physical » particles. It must be assumed explicitely that the outgoing particle is created in the interaction domain as a bare particle, but, starting with the moment when this particle goes out of the interaction domain, it is transformed in a « physical » particle through the interaction with the vacuum. The constitution of the cloud surrounding the bare particle is determined solving another problem in the CM system of this particle as in the above described relativistic Lee model ([2]).

([2]) T. D. Lee: *Phys. Rev.*, **95**, 1329 (1954); G. Källén and W. Pauli: *Danske Vid. Selsk.*, (1955).

The claim of macroscopic causality is satisfied in the above formalism in the following way. As illustrated in the case of the interaction hamiltonian H' (2) (3) and in our previous notes (1) the cut-off operator acts in a different way on the created and on the absorbed particles. As a consequence the cut-off operator does not mix outgoing and ingoing waves and one obtains from points of the interaction domain only outgoing waves for future times and only ingoing waves for the past. Therefore no contradiction with the macroscopic causality can arise. But obviously in such an approximate theory we cannot verify the microscopic causality in domains D_l.

RIASSUNTO

Nella Sez. **1** si studia sull'esempio del modello di Lee relativistico il formalismo della teoria non locale proposta dall'autore. Nella Sez. **2** si discute il principio di causalità macroscopica e di complementarità dal punto di vista di questa teoria non locale.

Electronic Equipment for Measuring Ionization in Nuclear Plates.

A. De Marco (*), R. Sanna and G. Tomasini

Istituto di Fisica dell'Università - Genova
Istituto Nazionale di Fisica Nucleare - Sezione di Genova

(ricevuto l'8 Maggio 1958)

Summary. — The drum revolution of a motor-driven mycroscope micrometric eyepiece is read by means of a phototube arrangement originating calibrated electric pulses. The pulses are counted and compared by an equipment incorporating one decade counter tube channel and several condenser storage counters. Final information including track length, mean gap length and gap distribution is directly displayed by electromechanical counters. An analysis of condenser storage counters is given in the Appendix.

1. – Foreword.

Ionization in nuclear plates can be deduced from the measurement of one of the following parameters:

1) $n(r_i)$ = number of gaps wider than one or more given length values r_i, contained within a cell of total length L;

2) l_g = total length of gaps contained within L;

3) w = mean length of gaps.

In order to choose the appropriate parameter and the corresponding measuring method several circumstances must be accounted for, among which:
— variability rate of each parameter as a function of the physical quantity to be evaluated;
— extent of the fluctuations of the given parameter;
— speed of measurement, etc.

(*) At present at CERN, Genève.

Among several authors there is not general agreement on this subject ([1,3]), but it is agreed that the choice of the most suitable parameter should depend upon the actual experimental conditions. It follows hence the expediency of an equipment able to measure, simultaneously and quickly, a number of different parameters. Beside other purposes this equipment will also fulfil that of establishing the most suitable parameter under given conditions, on the basis of a fairly large amount of experimental data obtained under uniform observing conditions.

2. – General description of the equipment.

Equipment on the above mentioned principles have been previously proposed and built in several more or less elaborate models ([2,11]). Our work aims at setting up of one model having the following performances:

a) Reading simultaneously n_0, l_g and $n(r_i)$ for 5 different values of r_i: These values should be adjustable at will within certain limits.

b) Consistency of results. The instrumental errors of the apparatus should be unnoticeable compared with those, merely statistical, bound to the structure of the tracks.

c) The apparatus electronics should be simple to build, operate and mantain.

Our design approach was to keep fixed the objective slit and to mesure directly, *i.e.* without the intermediation of mechanical links, the drum revolution of a thread-and-drum micrometric eyepiece. With reference to Fig. 1. a low speed electric motor M, foot controlled by the operator, drives the central drum D_R of the micrometric eyepiece. The eyepiece drum bears a disc D, whose periphery is milled with 100 teeth. The micrometer body is equipped with a light system, which projects a beam into a phototube through the cuts between the disc teeth.

As disc D revolves, the phototube is hit by a light pulse every time each tooth leaves the light beam. The voltage pulses thus originated across the

(1) P. H. Fowler and D. H. Perkins: *Phil. Mag.*, **46**, 587 (1955).
(2) D. M. Ritson: *Phys. Rev.*, **91**, 1572 (1953).
(3) G. Baroni and C. Castagnoli: *Suppl. Nuovo Cimento*, **12**, 364 (1954).
(4) M. Della Corte: *Nuovo Cimento*, **12**, 28 (1954).
(5) J. E. Hooper, and M. Scharff: *CERN Secr. St. Meas.*, no. 12 (1954).
(6) M. Renardier and Y. Avignon: *Compt. Rend.*, **233**, 393 (1951).
(7) H. M. Mayer: *CERN Secr. St. Meas.*, no. 20 (1955).
(8) M. V. Klein: *Rev. Sci. Instr.*, **28**, 964 (1957).
(9) K. Enslein: Private communication.
(10) G. Cortini, A. Manfredini, A. De Marco, R. Sanna and G. Tomasini: *Report on Padua-Venice Conference*, September 1957.
(11) C. O'Ceallaigh: *CERN Secr. St. Meas.*, no. 11 (1954); see also, R. H. W. Johnston and C. O'Ceallaigh: *Phil. Mag.*, **45**, 424 (1954); *Nuovo Cimento*, **1**, 468 (1955).

phototube output are amplified and shaped by pulse-shaper F into calibrated rectangles of about 225 V amplitude, 10 ms duration. As the micrometer drum has 50 divisions and the disc bears 100 teeth, each pulse corresponds to one half division of the micrometer drum, with our particular set of lenses is equal to a diplacement of 0.04 μm on the plate track.

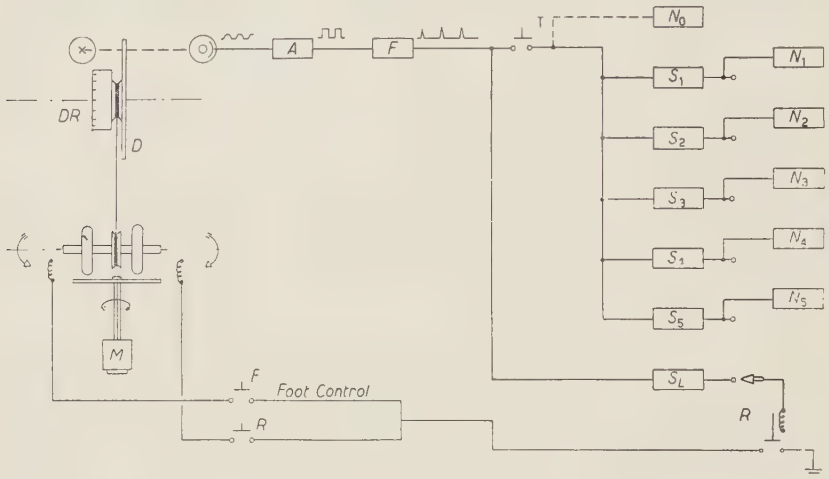

Fig. 1.

All pulses which are outgoing from the pulse shaper when the drum is running are fed to scaler S_L, which hence reads the cell length L. However, the counter N_i is allowed to count the outgoing pulses only while key T is depressed. As a rule, the operator keeps T depressed while the micrometer thread is inside one gap; therefore the figure read by N represents the gap length, $l_g = N_i$ 0.04 μm.

Counter N_0 advances one unit every time the key is depressed, and hence indicates $n(0)$.

The three-digits decade scaler S_L determines the cell length L; in fact its outgoing pulse, which occurs after 1000 standard pulses are fed to the input, energizes stop relay R, which in turn stops the drum drive. Counting circuit S_i (one of the five gap comparing circuits of the apparatus) drives the relating counter N_i in order to advance one digit after every m_i consecutive input pulses, which corresponds to the gap lenght r_i. All the S_i circuits are automatically reset to zero when the operator releases key T. Hence the N_i counters read the quantities $n(r_i)$.

Calibration and quick operational test of each S circuit is accomplished by means of a manual switch allowing the operator to connect the output of the circuit tested into the drive coil of stop relay R. In this way the number of pulses read by N_i at stop is the direct measure of m_i. Motor speed and gearing are designed for driving the micrometer slit at the speed of about 0.3 μm/s; consequently the measuring time is less than 2 min for a cell of 40 μm, and less than one hour is required for measuring one millimeter along a plate track.

3. – Tests performed.

In order that the equipment described may yield reliable results, instrumental errors — *under actual working conditions* — must be small in comparison with the fluctuations due to the statistical nature of the track. To ascertain that this was the case, we performed the following tests:

3·1. *Repeated measurement of a standard length.* – The width of one particular mark of the objective micrometer (simulating a gap of about 2 μm) was measured 1000 times. The results were very well aligned along a Gaussian distribution curve having the variancy of 3.5 pulses (corresponding to 0.14 μm).

We then measured one particular gap 500 times. The gap, lying between two adjacent marks of the objective micrometer, was 10 μm wide. We obtained a variancy of about 2.7 pulses, favourably comparable with the previous result.

3·2. *Repeated measurement of the same track.* – In order to check the apparatus operation under the conditions met while performing the actual measurements, we made repeated measurements of l_g.

Six protonic tracks were measured, for a total length of 400 μm, equal to 10 cells, starting from the end of their ranges. Each measurement was repeated four times. The plates were rather underdeveloped, yielding about 140 gaps every run of 10 cells. Now, if the measurement of a given length yields an instrumental variancy of the order of three pulses, in our instance the expected variancy is of the order of $3\sqrt{140}\sim 35$ pulses.

The measured variancy was of about 40 pulses, which can be favourably compared with the expected result.

3·3. *Combined gap and blob length measurement.* – Measurements of gaps and, subsequently, of blobs, were performed on a group of sixty-four sections, each 400 μm/long, of protonic tracks (that is to say over 640 cells).

The total blob length l_b was obtained by simply inverting the press-release contacts of the key. It was expected that apart of instrumental errors — the sum l_g+l_b would coincide with the total cell length L.

For every cell we computed the difference

$$\Delta = L-(l_g+l_b)\,,$$

which theoretically should fluctuate around zero by effect of instrumental errors. The measurements were grouped per operator, yielding the results of Table I: it appears from the table that the values of $\bar{\Delta}$ are different for each operator, and fairly small compared with the variances. The differences of Δ from zero could hardly be considered as significant, and in any case they may be attributed to causes depending on the operator.

The observed variances are derived from the measurement of an average of 14 gaps per cell; hence each particular value of Δ is derived from a group of 28 length measurements. Dividing the observed variances — *i.e.* the values

of $\sqrt{\Delta^2}$ — by $\sqrt{28}$, we obtain the variances μ, which can be attributed to the measurement of an individual gap, and referred to different operators The results are shown in Table I, last column.

TABLE I.

Operator	$\Delta = \frac{\sum \Delta_i}{n}$	$\sqrt{\Delta^2}$	$\sqrt{\Delta^2 - \overline{\Delta^2}}$	μ
1	+ 9.5	19.6	17,2	3,70
2	+ 4,6	21.2	20.7	4,00
3	— 6.3	25.4	24.8	4.80

The set of measurements described above, shows therefore that instrumental errors *in the actual measurement condition* are of the order of $4 \div 5$ pulses per gap, and have Gaussian fluctuation around zero.

The « intrinsic » fluctuations depending on the variancy of the effective gap length have been computed on the basis of the comparison among measurements performed on different tracks. They are of the order of 60 pulses per cell of stopping protonic track (about 10 gaps), *i.e.* about 19 pulses per gap. The instrumental variancy is therefore far less than the intrinsic variancy.

* * *

We thank Prof. PANCINI, G. CORTINI and A. MANFREDINI very much for the helpful assistence and co-operation in tracing and developing this work, and Dr. G. LUZZATTO for valuable criticism of the analysis.

APPENDIX

Condenser storage counters.

Our measuring unit is similar to those described by other Authors ([5-9]) in that it includes a number of pre-set counters, but differs in that we substituted the conventional scaler chains with the much simpler and more flexible counters of the condenser storage type. These circuits are generally referred to as reliable up to a maximum of 5/10 counts only ([12]); in fact the following analysis, confirmed by experimental results, shows that reliable counts up to at least 100 are quite possible provided that the counted pulses are recurrent at a fairly constant rate.

With reference to the diagram of Fig. 2, the outgoing pulses from cathode follower T_1 have 225 V amplitude, 10^{-2} s duration, ~ 0.1 s recurrency time. The storage condenser, C, is fed via diode T_2 through coupling condenser C_1, whose output is clamped

([12]) MILLMAN-TAUB: *Pulse and Digital Circuits* (New York, 1956), pp. 346-353.

by diode T_2' to the reference level of -150 V. When the operator opens switch S_w the storage condenser is charged by exponential steps until its voltage reaches (after N pulses) the firing potential of thyratron T_3. With the constants shown this potential is approximatively -6 V above cathode, *i.e.* 144 V above the reference level.

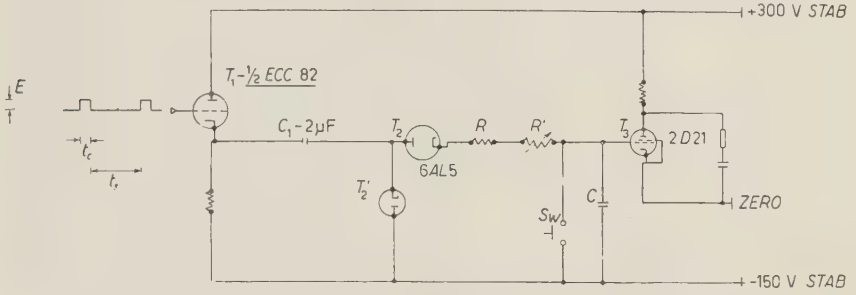

Fig. 2.

The circuit cycle consists of the repetition of alternate charges and discharges which can be evaluated by means of the equivalent circuits of Fig. 3. R_C includes resistors R, R' of Fig. 2 as well as the forward resistence of diode T_2 and the generator internal impedence. R_s includes all the leakages, *i.e.* leakage resistence r_c of condenser C, backward resistence r_d of T_2 and equivalent input (grid) resistence r_T of thyratron T_3.

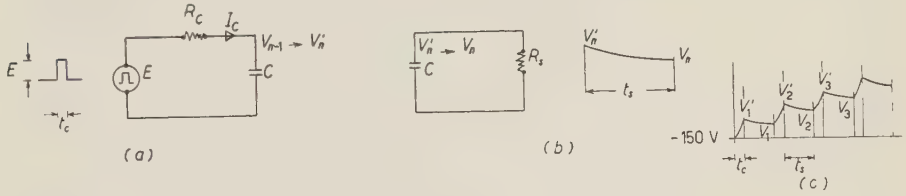

Fig. 3.

The cathode follower internal impedence and the diode forward resistence are only small fractions of the charge limiting resistence, $R+R'$; hence their changes with heater temperature, tube age etc., have little influence on R_c whicy then can be considered a constant of the order of $10^4 \div 10^6$ ohm, depending on the values chosen for C and N.

Of the terms composing R_s, the condenser leakage resistence is of the order $10^{10} \div 10^{11}$ ohms depending on temperature, humidity etc. The thyratron input resistence is also very high as the tube is deionized and works with strongly negative grid bias.

This gives for R_s an order of 10^9 ohm depending essentially on the diode characteristic and variable up to some 30% according to heater temperature etc. These orders of magnitude and variability are taken as basic conditions in the following analysis.

Referring to Fig. 3-*a* (charge) and Fig. 3-*b* (discharge) the network analysis, using the symbols in Fig. 3-*c*, gives:

$$(1) \qquad V_n' = V_{n-1} + (E - V_{n-1})\,(1 - \exp[-t_c/R_c C])\,, \qquad V_n = V_n' \exp[-t_s/R_s C]\,.$$

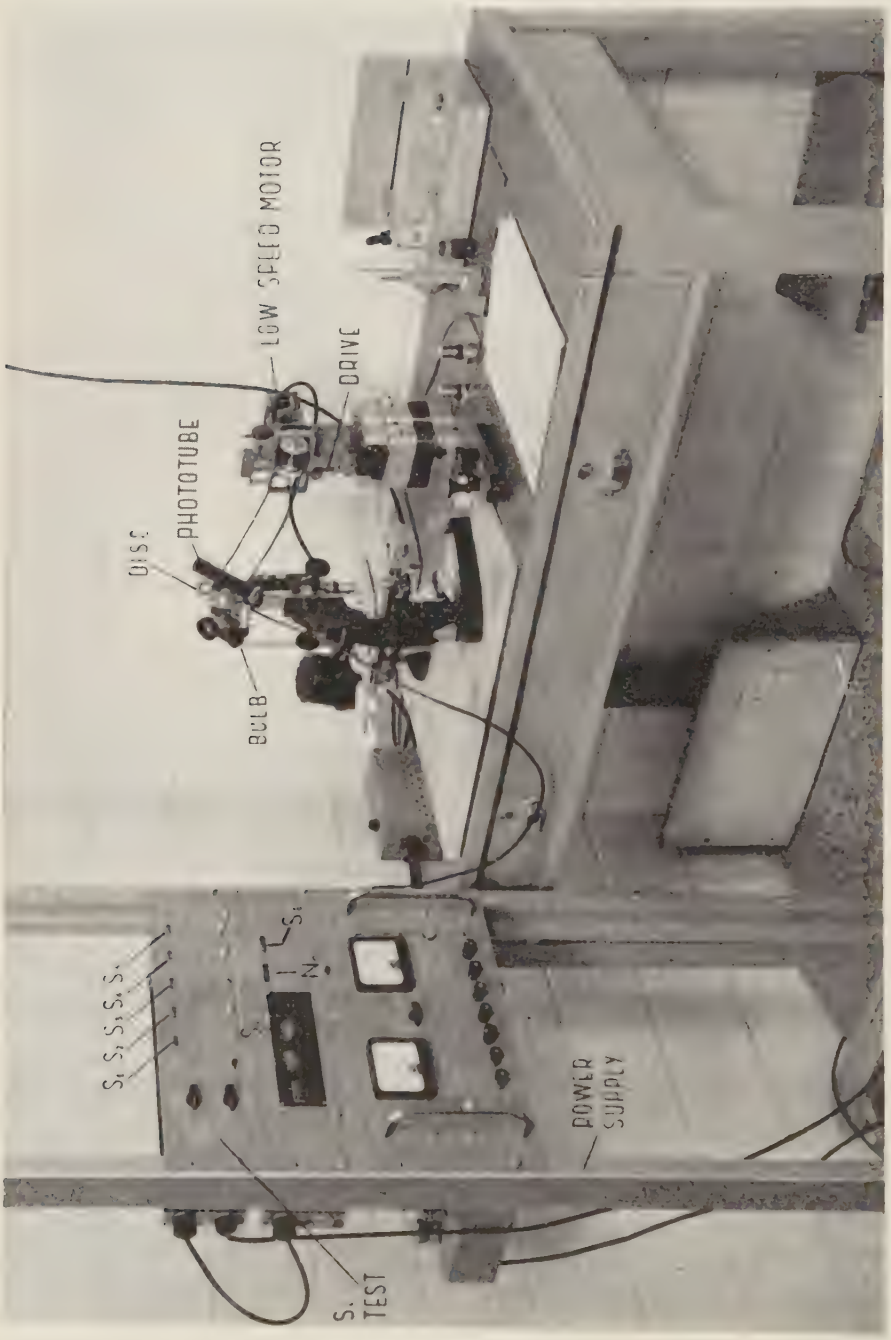
LOW SPEED MOTOR
DRIVE
DISC
PHOTOTUBE
BULB
S, S, S, S, S,
S,
N,
POWER SUPPLY
S. TEST

FIG. 1.

We put

$$u = t_s/R_sC\,; \qquad v = t_c/R_cC$$

and obtain the recurrent equations:

$$V'_n = E(1 - \exp[-v]) + \exp[-(u+v)]V'_{n-1}\,, \tag{2}$$

from which, applying $n-1$ times,

$$V'_n = E(1 - \exp[-v])\,\frac{1 - \exp[-n(u+v)]}{1 - \exp[-(u+v)]}\,. \tag{3}$$

With increasing n, V'_n increases, until for $n = N$, V'_n reaches the predetermined value $V_T = 144$ V by which the thyratron fires. To obtain a good working condition, the final voltage step $\Delta V'_n = V'_n - V'_{n-1}$ must be larger than the spontaneous drift ΔV_T of the firing potential. This limits the maximum possible value N_0 of N.

To calculate N_0 we can neglige u in respect to v in (3) and we get at once

$$\Delta V'_n = E(1 - \exp[-v])\exp[-(n-1)v] \simeq Ev\exp[-(n-1)v]\,.$$

It must be $\Delta V'_n \geqslant \Delta V_t$, so that the limit conditions are met for $\Delta V'_N = \Delta V_T$, that is for

$$N - 1 = \frac{1}{v}\left(\log v + \log\frac{E}{\Delta V_T}\right). \tag{4}$$

Since u is determined by unmodifiable leakages, we look for the optimum value of v (that is the optimum adjustment of C and R_c) required to obtain the largest possible value N_0 of N, keeping u as a constant (small with respect to v so that it may be negliged). Therefore we equate to zero the derivative of N with respect to v.

This condition gives:

$$v_0 = \frac{e\,\Delta V_T}{E} \tag{5}$$

and from (4)

$$N_0 - 1 = \frac{1}{e}\,, \tag{6}$$

while from (3) we obtain, having fixed v and N, and always neglecting u, the optimum firing voltage. This is

$$V_T = E(1 - 1/e)\,. \tag{7}$$

With our values of $\Delta V_T = 0.15$ V and $E = 225$ V, we get from (5), (6) and (7)

$$v_0 \simeq 1.8\cdot 10^{-3}\,, \tag{8}$$

$$N_0 \simeq 550\,, \tag{9}$$

$$V_T = 0.63\,E = 142\text{ V}\,. \tag{10}$$

Our working condition is $u = 5 \cdot 10^{-4}$, so that the value (8) for v_0 would not fulfil the condition $v \gg u$ satisfactorily: as moreover it is advisable to work within safe margins, we have taken $v = 1 \div 20 \cdot 10^{-2}$. Of course, N is correspondingly reduced, because eq. (6) is always satisfied.

The best condition (eq. (10)) for the firing potential is also always satisfied. In our apparatus $V_T = 150 - 6 = 144$ V, as already stated. Now, in order to evaluate the influence on N of the variations of u, we go back to eq. (3) which we develop to the first order in u and v, keeping the exponential only when $(u+v)$ is multiplied by n.

We obtain

$$V'_n = E \frac{v}{u+v} (1 - \exp [n(v+u)])$$

and

$$N = -\frac{1}{v}\left(1 - \frac{u}{v}\right) \log \left[1 - \frac{V'_N}{E}\left(1 + \frac{u}{v}\right)\right].$$

Developing the logarithm to the first order in u/v and using condition (7), one gets in place of eq. (6):

$$N \simeq \frac{1}{v}\left[1 + (e-2)\frac{u}{v}\right]. \tag{11}$$

The maximum value of N that we tested was ~ 100, with $v = 10^{-2}$. As $u = 5 \cdot 10^{-4}$, we had $u/v = 0.05$; $(e-2)u/v \simeq 0.03$. This means that a 30% variation of u gives an error of 1% (that is *one pulse*) in N.

This error is within the overall precision limits of our equipment, hence no particular care was given to improve it. More stringent requirements could be met by stabilization of the storage leak resistence (consisting mainly of the proper choice of diode T_2, stabilization of heater supply, etc.).

RIASSUNTO

La determinazione dei vari parametri di ionizzazione in emulsioni nucleari, viene realizzata per mezzo di un apparecchio semiautomatico associato al micrometro oculare a filo del microscopio. Nella misura si fa ruotare il tamburo del micrometro mediante un motore comandato a pedale dall'operatore. La rotazione del tamburo è letta da un dispositivo foto-elettrico che genera impulsi calibrati. Questi impulsi vengono contati e confrontati da un contatore decadico e da vari contatori ad accumulazione. Le grandezze misurate sono registrate da numeratori telefonici e comprendono: lunghezza totale di traccia misurata, numero dei « gap » e numero dei « gap » di lunghezza maggiore di certi valori prefissati. In appendice è riportata l'analisi dei circuiti integratori ad accumulazione.

Un generatore di treni d'impulsi nel campo dei nanosecondi.

U. Pellegrini

Comitato Nazionale Ricerche Nucleari - Centro Coordinamento Elettronica (*)
Roma

(ricevuto il 24 Maggio 1958)

Riassunto. — Si descrive un generatore di treni d'impulsi adatto per lo studio della strumentazione elettronica ad elevato potere risolutivo (~ 10 ns). Viene discusso lo schema di principio e si riporta quello del circuito realizzato dando le caratteristiche degli impulsi d'uscita dei quali si può variare la durata fino ad un minimo di 15 ns, l'ampiezza da 0 a 5 V; si può inoltre regolare il ritardo fra successivi impulsi e il numero degli impulsi contenuti in un treno.

1. – Premessa.

Nel nostro laboratorio abbiamo realizzato un generatore capace di fornire treni d'impulsi dalle seguenti caratteristiche:

1) durata degli impulsi variabile fino ad un minimo di 15 ns;

2) ritardo variabile fino ad un minimo di 25 ns;

3) ampiezza da 0 fino a 5 V;

4) numero regolabile di unità fino all'ordine di cento.

L'apparecchio è semplice e di facile costruzione, ma richiede un generatore ausiliare perchè deve essere comandato in entrata da un impulso di durata uguale a quella degli impulsi che si desiderano in uscita. Può essere perciò usato insieme ad un generatore con relais a mercurio e cavo formatore, ed è utile abbinare i due apparecchi in un unico complesso che risulta molto più versatile per lo studio della strumentazione elettronica ad elevato potere risolutivo.

(*) Lavoro pubblicato con l'autorizzazione del Comitato Nazionale Ricerche Nucleari.

2. – Schema di principio.

Un generatore di impulsi nel campo delle frequenze VHF è stato già proposto ed analizzato da C. C. CUTLER [1] per applicazione nella tecnica radar e nelle microonde. Il circuito da noi sviluppato è una particolare versione del precedente e consiste essenzialmente di un amplificatore a larga banda non-invertitore polarizzato in entrata all'interdizione e con una reazione positiva ritardata fra entrata ed uscita.

Lo schema di principio è riportato in Fig. 1. Come stadio amplificatore si è usato un pentodo EFP 60 ad emissione secondaria grazie al suo elevato fattore di merito e alla possibilità di prelevare sul dinodo un segnale non sfasato. La reazione positiva fra uscita ed entrata è stabilita dal cavo di ritardo posto fra dinodo e griglia adattato ad entrambi i terminali per eliminare impulsi di riflessione.

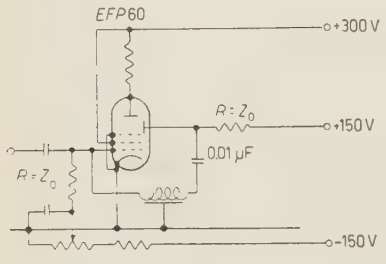

Fig. 1.

Un impulso applicato in entrata e capace di portare la griglia al di sopra dell'interdizione si ritrova con lo stesso segno all'uscita del dinodo. La reazione positiva fa sì che esso ricompaia in entrata dopo un tempo pari al ritardo introdotto dal cavo. L'impulso può circolare più di una volta fra entrata ed uscita ed il numero dei percorsi ciclici è determinato dal valore totale dell'amplificazione e dell'attenuazione lungo l'intera catena di reazione. Ovviamente ad ogni percorso è possibile prelevare un impulso positivo all'uscita del dinodo o negativo all'uscita dell'anodo. La loro durata è determinata sia dalla durata dell'impulso di comando sia dal tempo di salita dello stadio amplificatore; però, quando il comando dura meno del tempo di salita, gli impulsi hanno sempre una durata pari al doppio di tale tempo.

Facendo alcune ipotesi semplificatrici sul funzionamento del circuito, si può valutare l'ampiezza dei successivi impulsi che compaiono in griglia e il loro numero.

Supporremo che quando la griglia della EFP 60 supera l'interdizione, l'amplificazione del dinodo a sia indipendente dal punto di lavoro; inoltre trascureremo tutte le possibili cause di attenuazione del segnale e terremo conto solo della frazione che viene perduta ad ogni ciclo per portare la griglia dalla tensione di polarizzazione alla tensione di interdizione.

Usando le seguenti notazioni:

v = ampiezza del segnale di comando;

kv = frazione del segnale perduta per superare l'interdizione;

a = amplificazione sul dinodo;

τ = ritardo dinodo-griglia;

[1] C. C. CUTLER: *P.I.R.E.*, **43**, 140 (1955).

è facile controllare che, se al tempo $t = 0$ l'ampiezza v_0 dell'impulso applicato sulla griglia è v, il primo impulso di reazione giunto dopo un tempo τ ha un'ampiezza:

$$v_1 = (v - kv)a = v(a - ka); \tag{1}$$

l'ampiezza del secondo impulso giunto dopo un tempo 2τ è:

$$v_2 = v\left[a^2 - k\,(a^2 + a)\right];$$

e il calcolo procede analogamente per i successivi. L'ampiezza dell'impulso ennesimo v_n per $n > 0$ può quindi porsi sotto la forma:

$$v_n = v(a^n - k \sum_1^n{}_m\, a^m)\,. \tag{2}$$

Questa schematizzazione vale in realtà solo se $(a - ka) < 1$. Infatti nel caso opposto si osserva dalla (1) che v_1 è maggiore di v; l'ampiezza dei successivi impulsi aumenta progressivamente finchè si raggiunge la saturazione dove a si annulla. Questo significa che se $(a - ka) > 1$ il circuito può essere posto in uno stato di oscillazione indefinita.

Viceversa nel caso in cui $(a - ka) < 1$, si otterrà un treno d'impulsi con ampiezza decrescente il cui numero è dato dal valore di n per cui v_n si annulla. Tale valore si ricava dalla (2) imponendo che:

$$a^n - k \sum_1^n{}_m\, a^m = 0\,.$$

Questa relazione, con facili trasformazioni, si può porre nella forma:

$$n = \frac{\ln\left(\dfrac{ka^2}{k + (1-k)(1-a)a}\right)}{\ln a}\,, \tag{3}$$

da cui si determina n, numero degli impulsi contenuti in un treno, una volta nota l'amplificazione a l'ampiezza del comando v e la differenza kv fra tensione di interdizione e tensione di polarizzazione di griglia.

3. – Circuito realizzato.

Lo schema elettrico del circuito realizzato è riportato in Fig. 2.

Il cathode follower V_{1a} ha il compito di disaccoppiare l'entrata, in cui è applicato il segnale di comando su cavo da 52 Ω adattato, dal ramo di reazione costituito da una linea di ritardo a 200 Ω. V_2 è lo stadio amplificatore con reazione positiva descritto nella sezione precedente. Sul catodo si è posta una resistenza di 100 Ω che introduce una reazione negativa capace di stabilizzare

l'amplificazione di dinodo a. Ciò è necessario perchè, come si deduce dalla (3), il numero massimo di impulsi può variare fra un treno e il successivo se varia a pur rimanendo costanti k e v.

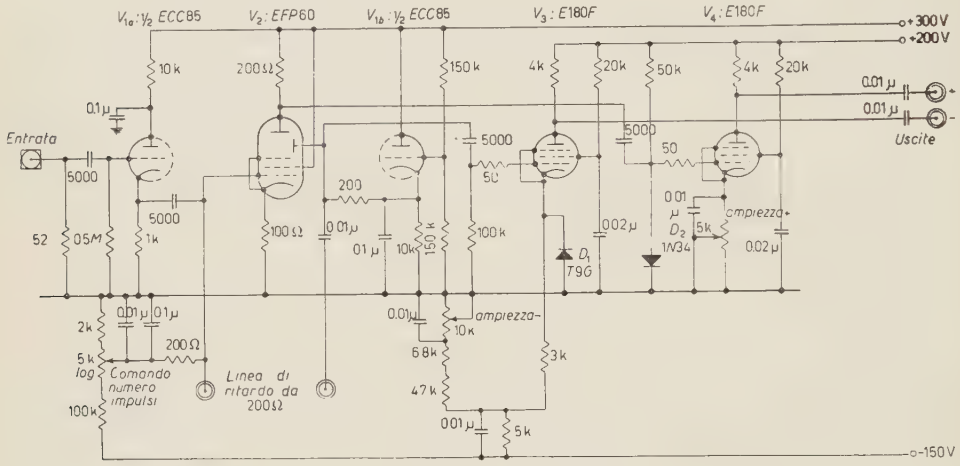

Fig. 2.

Gli impulsi prelevati sulla placca o sul dinodo di V_2 presentano un'ampiezza diversa fra loro come specifica la (2). Abbiamo dunque introdotto gli stadi limitatori V_3 e V_4 con polarizzazione regolabile in maniera da poter variare anche l'ampiezza degli impulsi d'uscita. Il carico di placca di V_3 e V_4 in regime impulsivo è costituito dall'impedenza caratteristica Z_0 dei cavi inseriti nelle boccole d'uscita che vanno adattati sull'altro estremo dove si preleva l'impulso: con cavi da 200 Ω, l'ampiezza massima è di 5 V.

Lo stadio V_3 limita gli impulsi positivi provenienti dal dinodo. Anzichè determinare il taglio mandando la valvola in saturazione, è più efficace adottare lo schema da noi riportato. Normalmente V_3 è polarizzato vicino all'interdizione, sicchè D_1 è in piena conduzione ed il catodo di V_3 è bloccato a massa. All'arrivo d'un impulso positivo la corrente di V_3 aumenta finchè il catodo sale ad una tensione positiva ed interdice D_1. A questo punto, se il carico di placca è di 200 Ω, l'amplificazione si riduce di un fattore circa quindici perchè lo stadio è fortemente controreazionato dalla resistenza di 3 kΩ sul catodo.

Lo stadio V_4 limita gli impulsi negativi prelevati sulla placca della EFP 60. In questo caso è sufficiente affidare il taglio all'interdizione della E 180 F.

Ai terminali dei cavi connessi alle boccole d'uscita si ottengono così treni con impulsi che hanno tutti uguale ampiezza tranne l'ultimo impulso che in genere non è tanto grande da poter essere sufficientemente amplificato e quindi tagliato da V_3 o da V_4. Tuttavia, anche nelle condizioni più sfavorevoli, l'ampiezza dell'ultimo impulso non è mai inferiore alla metà dell'ampiezza del precedente.

L'apparecchio è in funzione nel nostro laboratorio da quattro mesi, viene comandato con gli impulsi di un generatore con relais a mercurio ed è ado-

perato con vantaggio nello studio di apparecchiature di conteggio ad elevato potere risolutivo.

* * *

Desidero ringraziare il Prof. B. Rispoli per gli utili suggerimenti da Lui avuti durante lo svolgimento del lavoro.

SUMMARY

A regenerative pulse generator is described which can be used for generating a group of coded pulses. The operation of the circuit is discussed and the characteristics of the output pulses are given: minimun pulse width and spacing are 15 and 25 nanoseconds respectively; the amplitude and the number of coded pulses are controllable.

L'acceleratore per deutoni da 160 keV dell'I.N.F.N., Sezione di Milano.

L. Colli, S. Micheletti e C. Salvetti

Istituto di Scienze Fisiche dell'Università - Milano
Istituto Nazionale di Fisica Nucleare - Sezione di Milano

(ricevuto il 4 Giugno 1958)

Riassunto. — In questo lavoro viene descritto l'acceleratore elettrostatico per deutoni costruito all'Istituto di Fisica dell'Università di Milano. Questo strumento che è stato particolarmente progettato per fornire una sorgente di neutroni da 14 MeV per mezzo della reazione ${}_1^2\mathrm{D}+{}_1^3\mathrm{T}={}_2^4\alpha+{}_0^1\mathrm{n}+$ $+17.587$ MeV, può fornire un flusso di neutroni di $5\cdot10^9$ neutroni/s in tutto l'angolo solido, alla tensione acceleratrice di 150 kV.

1. – Introduzione.

Nel Marzo del 1958 è entrato in funzione all'Istituto di Fisica di Milano un acceleratore per deutoni che è stato progettato allo scopo di fornire una sorgente di neutroni veloci di notevoli intensità.

È ben noto che per mezzo della reazione ${}_1^2\mathrm{D}+{}_1^3\mathrm{T}={}_2^4\alpha+{}_0^1\mathrm{n}+17.587$ MeV si possono ottenere neutroni dell'energia di circa 14 MeV con una sezione d'urto molto grande, che ha un massimo per l'energia dei deutoni incidenti di 120 keV.

Le caratteristiche di questa reazione, per la quale occorre una relativamente piccola energia dei deutoni, unite al fatto che si possono facilmente preparare ed acquistare le targhette contenenti tritio in forma di dischetti metallici ricoperti di uno strato di zirconio, nel quale è adsorbito tritio in quantità notevole (~1 cc a temperatura e pressione normali) sui quali si può comodamente far avvenire la reazione, permettono di realizzare facilmente sorgenti di neutroni aventi un'intensità che può raggiungere i 10^{10} neutroni/s [1,2] emessi in tutto l'angolo solido e che richiedono la costruzione di un acceleratore che, a causa della relativamente bassa differenza di potenziale richiesta per l'accelerazione dei deutoni, risulta molto semplice e poco dispendioso.

L'acceleratore dell'INFN di Milano che è descritto qui è stato progettato in base ai seguenti criteri:

---

[1] S. G. Forbes, E. R. Graves e R. N. Little: *Rev. Sci. Instr.*, **24**, 424 (1953).
[2] R. A. Peck e H. P. Eubank: *Rev. Sci. Instr.*, **26**, 444 (1955).

1) La sorgente di ioni che fornisce il fascio di deutoni è tenuta a massa e la targhetta nella quale si fa avvenire la reazione D+T è portata a tensione negativa che può arrivare a 160 keV.

Questa disposizione permette una grande semplicità della costruzione, evitando di dover portare a tensione tutti gli strumenti che servono al funzionamento della sorgente di ioni, e permettendo una grande facilità di manovra sulla sorgente stessa anche durante il funzionamento dell'acceleratore. Si ha ancora il vantaggio di poter inserire il sistema di pompaggio per l'alto vuoto direttamente vicino alla sorgente di ioni, cosa che permette di sfruttare tutta la portata della pompa.

2) Per ovviare, almeno in parte, allo svantaggio di non potersi avvicinare molto alla targhetta zirconio-tritio, sorgente dei neutroni, con strumenti di misura, poichè si trova ad alta tensione, il corpo dell'acceleratore è stato costruito in modo che la parete esterna dell'acceleratore intorno al sistema ottico ed alla targhetta, nell'interno del quale è fatto il vuoto, sia un tubo metallico, collegato a massa. Si può così avvicinare i rivelatori fino a 10 cm dalla sorgente di neutroni.

2. – Descrizione dell'acceleratore.

Lo schema generale illustrante la disposizione delle varie parti dell'acceleratore e le caratteristiche esterne dell'impianto sono mostrati in Fig. 1.

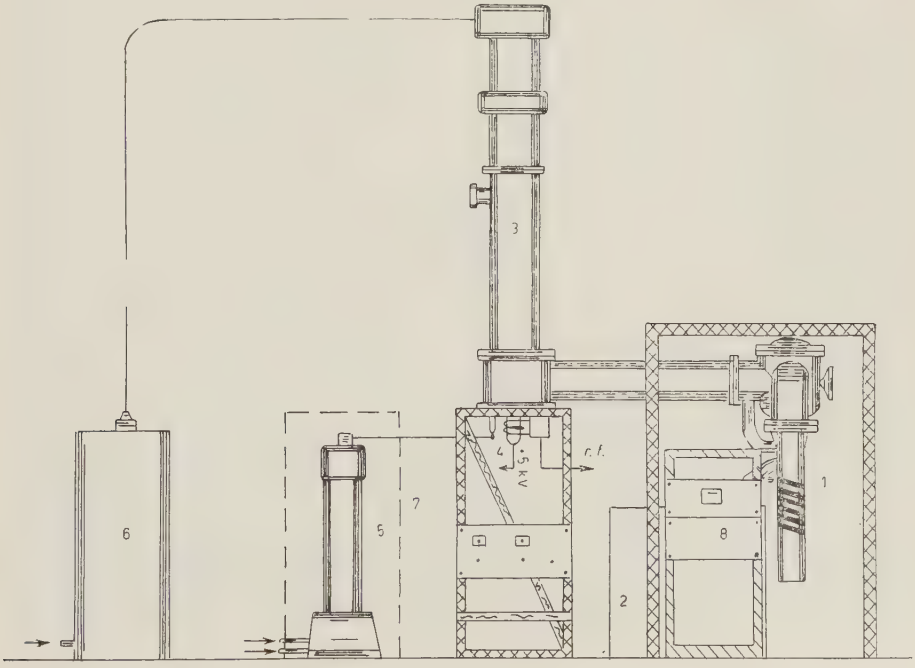

Fig. 1. – Schema generale della disposizione delle varie parti dell'acceleratore. 1) Pompe a diffusione; 2) pompa rotativa; 3) colonna acceleratrice; 4) sorgente di ioni; 5) generatore 50 kV; 6) generatore 160 kV; 7) schermo elettrostatico; 8) generatore di radiofrequenza per la sorgente.

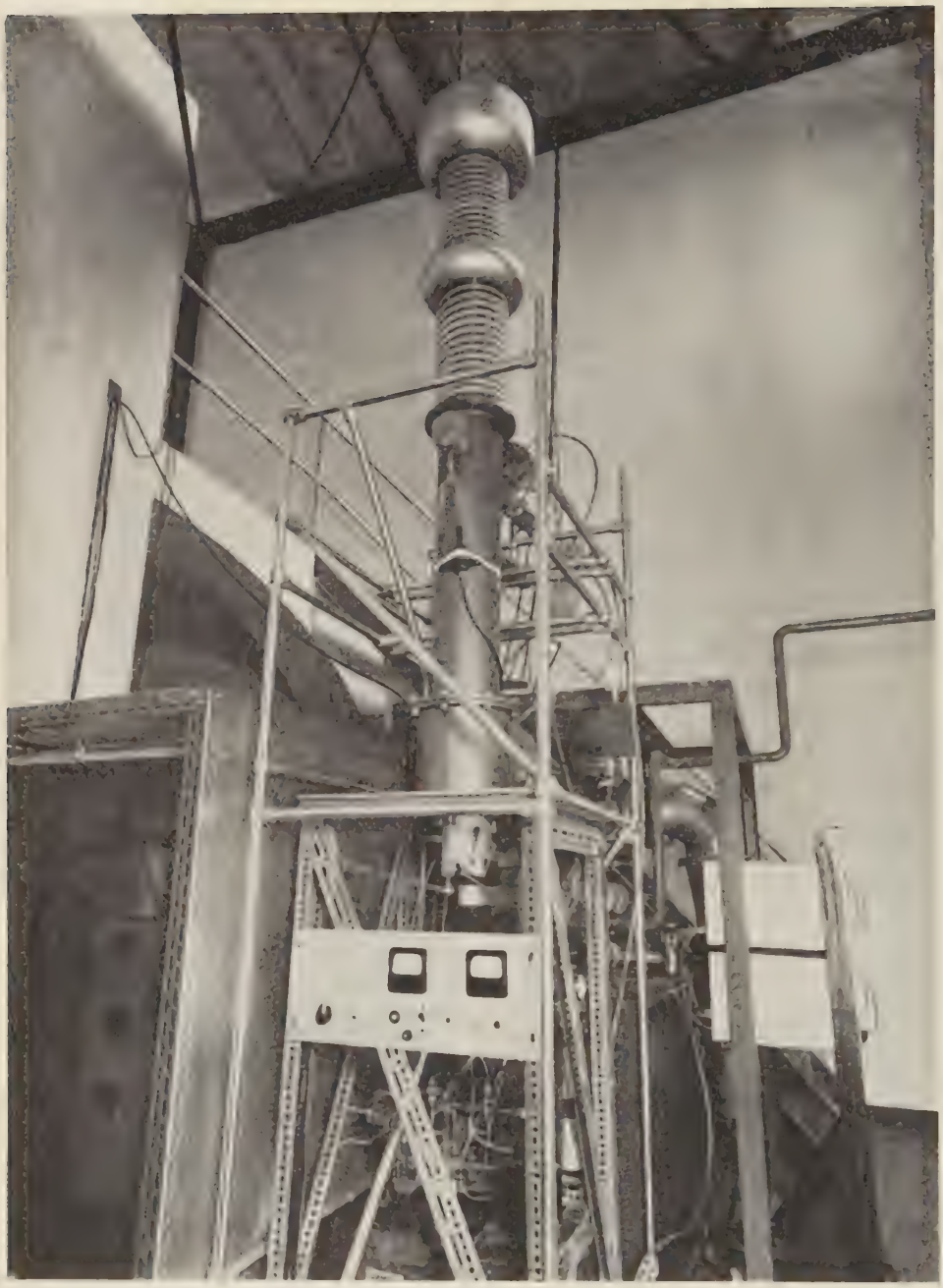

Fig. 2. – L'acceleratore visto dal basso. Nella gabbia di rete che funziona da schermo elettrostatico è visibile la colonna moltiplicatrice del generatore da 50 kV; al centro della figura si vede la sorgente di ioni accesa e la colonna acceleratrice. Attorno agli isolanti di pyrex sono avvolte le resistenze che formano il partitore di tensione. Le flange di ottone cui sono fissate le lenti sono ricoperte da uno schermo elettrostatico di alluminio. A destra è il generatore di radio-frequenza per la sorgente di ioni.

Il sistema di pompaggio è costituito da una pompa rotativa preliminare e da due pompe a diffusione in parallelo, che funzionano ad olio di silicone, per la portata complessiva di 1200 l/s.

Attraverso una valvola di grande luce e un condotto della lunghezza di circa 1 m e del diametro di 20 cm, le pompe sono collegate ad una prima camera dell'acceleratore, che serve da base al tubo proprio di accelerazione e alla quale sono applicate anche la sorgente di ioni ed un passante isolato che introduce nel sistema a vuoto la tensione per la prima lente elettrostatica del sistema di focalizzazione.

Tutto il sistema focalizzante, formato di tre lenti elettrostatiche è mostrato in Fig. 3. Questo sistema, compresa la targhetta, è chiuso entro un tubo di acciaio collegato alla prima camera e quindi posto a massa. Al di sopra di questo sono due flange di ottone isolate tra loro e dal tubo di acciaio da due tubi di pyrex, le quali sostengono le due ultime lenti e la targhetta.

Tutti i cilindri che formano le lenti elettrostatiche sono di acciaio inossidabile con i bordi arrotondati per evitare effetti di scariche fra di essi.

Tutte le tenute di vuoto sono realizzate per mezzo di anelli di neoprene a sezione circolare.

La tensione della prima lente è fornita da un generatore di tensione che può fornire una tensione massima di 50 keV [3] ed una corrente massima di 10 mA. La tensione per le altre due lenti è fornita da un generatore del tipo ad induzione elettrica, ed ha una tensione massima di 160 keV ed una corrente massima di 2.5 mA [4]. La seconda lente viene portata a tensione per mezzo di un potenziometro costituito di resistenze di tipo normale, che viene avvolto intorno ai cilindri di vetro.

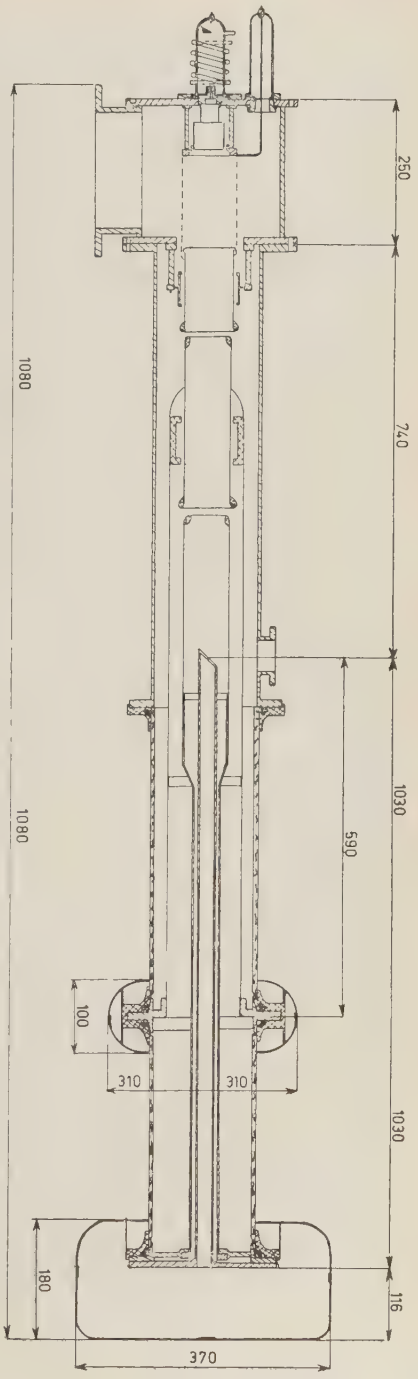

Fig. 3. – Schema della colonna acceleratrice.

[3] Studiato e costruito all'Istituto di Fisica dell'Università di Genova.

[4] Costruito dalla Società S.A.M.E.S.

3. – La sorgente di ioni.

La sorgente di ioni, del tipo a radiofrequenza, è mostrata in dettaglio in Fig. 4. Essa è costituita da un bicchiere di vetro pyrex, fissato alla camera base del tubo per mezzo di guarnizione anulare di gomma al silicone posta sul bordo esterno e tenuta in sede da una flangia metallica.

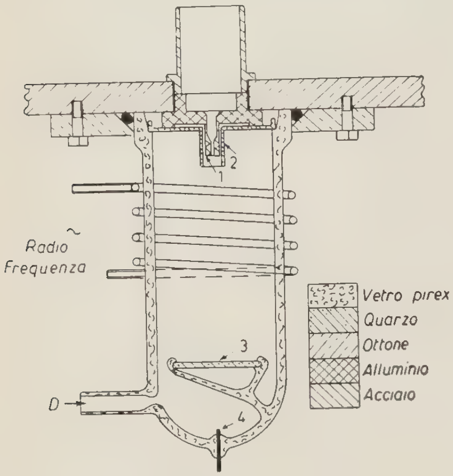

Fig. 4. – La sorgente di ioni a radio-frequenza. 1) elettrodo estrattore in durallumi-nio; 2) rivestimento di quarzo; 3) dischetto di quarzo; 4) elettrodo di tungsteno.

L'elettrodo estrattore, di duralluminio, è avvitato sulla parete della camera ed è protetto da un piattino di quarzo con un tubetto centrale che circonda la punta dell'estrattore.

Nel centro dell'estrattore è un canalino della lunghezza di 6 mm del diametro di 2.4 mm, attraverso il quale esce il fascio di ioni. Sul fondo della sorgente, dalla parte opposta all'estrattore è saldata una bacchetta di tungsteno, passante, che dalla parte interna è riparata da un dischetto di quarzo. Nella sorgente viene immesso deuterio attraverso un usuale purificatore a palladio caldo. La pressione di funzionamento è di circa $1.5 \cdot 10^{-3}$ mm Hg.

La scarica viene eccitata per mezzo di un oscillatore a radiofrequenza a circa 14 MHz che viene accoppiato alla sorgente per mezzo di una spirale di rame. La potenza massima fornita dall'oscillatore è di 200 W. Per estrarre il fascio di ioni si applica una differenza di potenziale di $(3000 \div 4000)$ V tra l'elettrodo superiore estrattore e la bacchetta di tungsteno, portando quest'ultima a potenziale positivo.

In queste condizioni di funzionamento il fascio di ioni estratto, analizzato per mezzo di uno spettrografo di massa costruito a questo scopo, è stato trovato composto per circa l'80% di ioni atomici.

La sorgente è investita da un getto d'aría per il raffreddamento.

4. – Caratteristiche di funzionamento.

L'acceleratore è in funzione da alcuni mesi ed ha dato prova di buona stabilità e riproducibilità delle condizioni di funzionamento; esso viene attualmente usato per lo studio di reazioni nucleari prodotte da neutroni di 14 MeV. Le condizioni di sperimentazione richiedono un flusso di neutroni dell'ordine di 10^9 neutroni/s. Questo flusso è ottenuto con una tensione di estrazione di 2000 V, una tensione alla prima lente di 20000 V e una tensione di accelerazione totale di 150000 V.

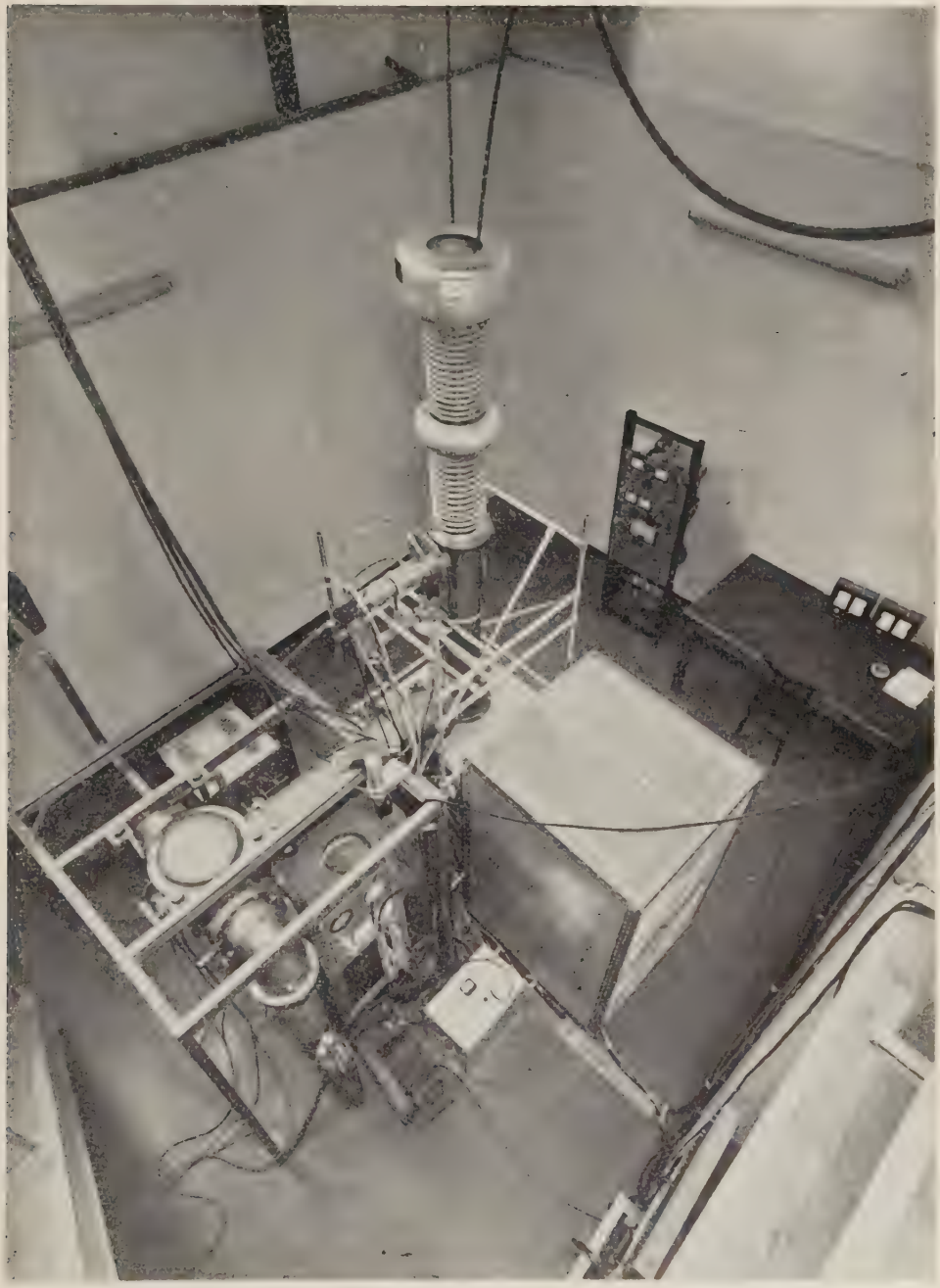

Fig. 5. – L'acceleratore visto dall'alto. A sinistra è visibile il sistema di pompe con il tubo d'attacco alla camera base dell'acceleratore. Accostato al tubo dell'acceleratore all'altezza della targhetta di tritio si vede il rivelatore di protoni usato per l'esperienza ora in corso che è sostenuto da una incastellatura in tubi di alluminio. La tensione acceleratrice è portata alle lenti elettrostatiche dal cavo isolato connesso alla cima dell'acceleratore.

Questo flusso non è il massimo che il tubo può fornire, in quanto possono essere usate tensioni di estrazione più alte senza difficoltà.

Tutta l'apparecchiatura è sistemata in una sola stanza, delle dimensioni di 4×6 m e dell'altezza di 8 m.

I comandi della sorgente di ioni, delle alte tensioni e di tutti gli strumenti elettronici sono posti in un locale attiguo protetto da un muro di mattoni di cemento da dove si possono quindi fare tutte le operazioni di accensione e controllo della macchina.

I neutroni vengono contati per mezzo di un contatore a scintillazione costituito da un cristallo di antracene e da un fotomoltiplicatore, posto alla distanza di circa 1 m dalla targhetta di tritio.

* * *

Gli autori sono lieti di ringraziare il prof. U. Facchini per aver ospitato nel reparto di fisica del CISE le esperienze preliminari sulla sorgente di ioni e il dr. G. Ghilardotti e la dr. Anna Sona per l'aiuto prestato per la messa a punto della stessa sorgente.

SUMMARY

The electrostatic accelerator of the Physics Institute of the University of Milan is here described. This instrument was designed to be used as a 14 MeV neutron source by means of the reaction ${}_1^2\mathrm{D} + {}_1^3\mathrm{T} = {}_2^4\alpha + {}_0^1\mathrm{n} + 17.587$ MeV. A total flux of $5 \cdot 10^9$ neutrons/s can be obtained, with the accelerating potential of 150 kV.

LETTERE ALLA REDAZIONE

(La responsabilità scientifica degli scritti inseriti in questa rubrica è completamente lasciata dalla Direzione del periodico ai singoli autori)

Sound Absorption in Relation to Free Volume of Liquids.

H. Singh

Physics Honours School, Panjab University - Hoshiarpur, India

(ricevuto il 28 Febbraio 1958)

The dependence of sound absorption on free volume in case of rubber-like polymers has been recently investigated by Singh and Nolle [1]. They have shown that in case of high molecular weight polyisobutylene and Hycar OR-15 vulcanizate, for constant viscous loss, the free volume in the medium remains essentially constant. In this case constant viscous loss is defined in two different ways; in the first case the viscous loss is supposed to remain constant when the imaginary part of the bulk wave modulus of the transmission medium remains constant and in the second case the viscous loss is supposed to remain constant when we adjust the temperature and pressure so as to always remain on the peak of the absorption function. In the case of liquids such as alcohols where the entire absorption is attributed to viscous losses, a fixed value of absorption will be a proper criterion for constant viscous loss.

With the passage of sound waves in a liquid the number and size of the holes and hence the free volume in the liquid undergo considerable changes. Certain holes are destroyed whereas new ones are created, at other places. Also the size of the holes changes with changing temperature and pressure. The creation and destruction of holes and the variation in their size involves considerable expenditure of energy which comes from the sound beam. This means that if, by suitably adjusting the temperature and pressure of the medium, the free volume is kept constant, the viscous losses of the medium which are a function of its fluidity will remain constant. In other words, for a constant value of viscous sound absorption the free volume will remain constant. It can thus be argued that in cases where the excess sound absorption is mainly due to bulk viscosity, the measured sound absorption should have the same value as long as the free volume remains constant.

Using the measurements of Carnevale and Litovitz [2] and of Chhapgar [3] the absorption function α/ν^2 at various pressures and temperatures has been calculated for methyl alcohol and

[1] Harkrishan Singh and A. W. Nolle: in press.

[2] E. H. Carnevale and T. A. Litovitz: *J.A.S.A.*, **27**, 547 (1955).

[3] A. F. Chhapgar: *Doctorate Thesis*, Univ. of Bombay, India.

is shown in Fig. 1. For a suitable fixed value of absorption such as the one shown by the line AA' in the figure we find that

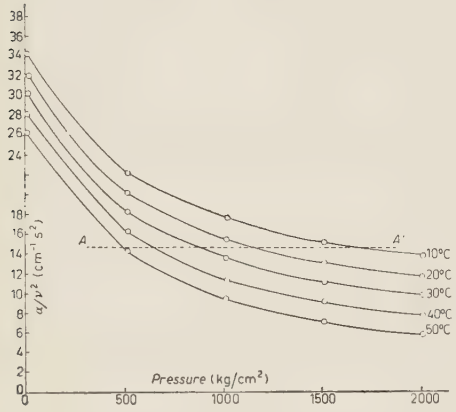

Fig. 1.

to maintain α/ν^2 constant, for a change of pressure from 480 to 1650 kg/cm^2, the temperature needs to be raised from 10 to 50 °C. From BRIDGMAN's ([4]) data on the relative volume of methyl alcohol at various pressures and temperatures, by interpolation we calculate the relative volume at different values of temperature and pressure corresponding to the points lying on the line AA'. The process is repeated for ethyl, n-propyl and n-butyl alcohols and the results are plotted in Fig. 2. The plot clearly indicates that the relative volume remains essentially constant, the maximum change being of the order of 3%, which is fairly small as compared to the inaccuracies in the measurements used for these calculations.

It also follows from the postulate put forth here that in cases where the excess absorption is mainly due to factors other than bulk viscosity, the change in absorption will not be in step with the change in free volume. To check this, same calculations have been repeated for carbon disulphide in which excess absorption is attributed to relaxation processes. Here the absorption values are taken from MIFSUD and NOLLE ([5]) and the relative volume data from BRIDGMAN. As a result, it is found that the relative volume in carbon disulphide changes by about 25% for corresponding change of pressure as compared to 3% in case of alcohols referred to above.

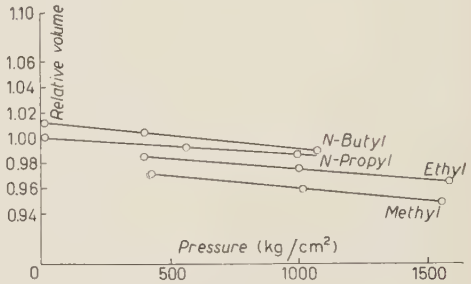

Fig. 2.

Thus it may be concluded that if we adjust so as to always have a constant viscous loss, the free volume which is defined as the total volume of the holes in the liquid essentially remains constant. Also it may be said that the total absorption losses in these alcohols are due to two viscosities *viz.* the shear and bulk viscosities. This also implies that bulk viscosity will be one of the factors contributing towards sound absorption in all alcohols.

([4]) P. W. BRIDGMAN: *The Physics, of High Pressure* (London, 1949).

([5]) J. F. MIFSUD and A. W. NOLLE: *J.A.S.A.*, **28**, 469 (1956).

Question of a Second Neutral Pion (*).

A. M. Baldin (+) and P. K. Kabir (×)

Department of Mathematical Physics - University of Birmingham, England

(ricevuto l'11 Giugno 1958)

A recent analysis (1) has established that the σ_-/σ_+ photoproduction ratio for free nucleons is practically constant near threshold and approximately equal to 1.4 (with about 10% accuracy), in close agreement with the predictions of field theory with a coupling constant (2) of 0.08. This leads to a «theoretical» value of the Panofsky ratio

$$(1) \qquad R = \frac{\sigma(\pi^- + \mathrm{P} \to \pi^0 + \mathrm{N})}{\sigma(\pi^- + \mathrm{P} \to \gamma + \mathrm{N})}$$

of 2.4 ± 0.4 where the error includes the effect of errors in the photoproduction cross-section (1), in the S-phase shifts (5), and in the mass-difference between charged and neutral pions (6). The actual experimental value is reported (7) as 1.52 ± 0.11.

To remove the discrepancy, it was suggested (1) that the neutral pions which are emitted when π^--mesons are absorbed in hydrogen may not be the usual π^0-mesons occurring in symmetric meson theory, but may have isotopic spin $T=0$. We shall see that, to fulfil its purpose, the other properties of the postulated pseudoscalar $T=0$ meson, which we denote by π_0^0, must be assumed to be closely similar to those of the $T=1$ neutral pion, henceforth denoted by π_1^0. When we wish to refer to the two types collectively, we use the old notation π^0. The situation envisaged in (1) could arise, for example, if the mass of the π_1^0 were

$$(2) \qquad m_{\pi_1} > m_{\pi^-} - (m_\mathrm{N} - m_\mathrm{P}) ,$$

(*) This question is also discussed by Y. Yamaguchi (preprint).

(+) Permanent address: Physical Institute of Academy of Sciences of U.S.S.R., Moscow.

(×) Permanent address: Institute of Nuclear Physics, Calcutta.

(1) A. M. Baldin: *Nuovo Cimento* **8**, 569 (1958).

(2) Strictly speaking, the σ_-/σ_+ ratio does not depend on the coupling constant; however, it depends on an unknown parameter $N^{(-)}$ (see ref. (3)). The ratio 1.4 is obtained if this parameter is chosen to yield the observed value (4) of σ_+ with a value of $f^2 = 0.08$. Setting $N^{(-)} = 0$ gives a ratio of 1.3 but requires $f^2 = 0.06$ to obtain σ_+ correctly. On the other hand, if $N^{(-)}$ is adjusted to give $\sigma_-/\sigma_+ = 2.0$, we would require $f^2 = 0.32$ to achieve agreement with σ_+.

(3) G. F. Chew, M. L. Goldberger, F. E. Low and Y. Nambu: *Phys. Rev.*, **106**, 1345 (1957).

(4) M. Beneventano, G. Bernardini, D. Carlson-Lee, G. Stoppini and L. Tau: *Nuovo Cimento*, **4**, 323 (1956).

(5) D. Nagle, F. Hildebrand and R. Plano: *Phys. Rev.*, **105**, 718 (1957).

(6) W. Chinowsky and J. Steinberger: *Phys. Rev.*, **83**, 586 (1953).

(7) J. M. Cassels: *Proc. Seventh Rochester Conference* (1957); J. Fischer, R. March and L. Marshall: (*Phys. Rev.*, **109**, 533 (1958)) report $R = 1.87 \pm 0.10$.

whereas the π_0^0 had the mass usually ascribed to the π^0. Then the emission of π_1^0's would be energetically forbidden in π^--absorption, and only π_0^0's would be emitted. Since these are not related to the charged pions, there would no longer be any direct connection between the experimental Panofsky ratio and the quantity (1) calculated from the cross-sections for change-exchange scattering and threshold pion photoproduction.

For the sake of definiteness, let us assume that the mass 264.3 m_e measured by CHINOWSKY and STEINBERGER [6] is that of the π_0^0 whereas the mass of the π_1^0 is intermediate between this and that of the charged pions.

Before discussing the Panofsky ratio further, let us examine the experimental knowledge of pion phenomena to see whether there really is room for a π_0^0 as postulated. Firstly, the π_0^0 will be, like the π_1^0, unstable against the process

$$\pi^0 \to 2\gamma ,$$

and decay with a lifetime comparable to that of the π_1^0. Techniques of γ-ray measurement are not sufficiently refined to distinguish between the photons in π_0^0- and π_1^0-decay. Note that the decay

$$\pi_1^0 \to \pi_0^0 + \gamma ,$$

is strictly forbidden.

Experiments on charge-independence in nuclear forces clearly do not affect the π_0^0, but those on meson production provide a more stringent test. Charge-independence (and only $T=1$ pions) require the reactions

$$(3) \qquad \begin{cases} \mathrm{P} + \mathrm{P} \to \pi^+ + \mathrm{D} , \\ \mathrm{N} + \mathrm{P} \to \pi^0 + \mathrm{D} , \end{cases}$$

to have identical angular distributions and total cross-sections in the ratio 2:1.

[8] R. SCHLUTER: *Phys. Rev.*, **96**, 734 (1954).

The same restriction is imposed on the pair of reactions

$$(4) \qquad \begin{cases} \mathrm{P} + \mathrm{D} \to \pi^+ + {}^3\mathrm{H} , \\ \mathrm{P} + \mathrm{D} \to \pi^0 + {}^3\mathrm{He} , \end{cases}$$

While the measurements [9] on (4) are not sufficiently accurate to draw any clear conclusion, SCHLUTER [8] finds the condition fairly well fulfilled for (3) for meson momenta from 0.6 μc to 1.3 μc. This does not, however, rule out the π_0^0, since it merely proves that, in the observed energy-range, the amplitudes for the reactions (3) in the state $T=0$ are small compared to those in $T=1$. When we remember that in the latter case the meson can be in a state with $T=\frac{3}{2}$, $j=\frac{3}{2}$ with respect to one of the nucleons of the deuteron, this does not appear unreasonable. In fact, the dominance [10] of the $(\frac{3}{2}, \frac{3}{2})$ resonance for meson-nucleon phenomena below 300 MeV meson energy ensures that the neutral pions observed in most reactions would be π_1^0's (since the π_0^0 could not participate in a meson-nucleon system with $T=\frac{3}{2}$). Thus meson-nucleon phenomena below 300 MeV, the approximate limit of present-day theory, would be largely unaffected by the introduction of the π_0^0. Therefore, the only clear-cut way to settle the question of the existence of a π_0^0 would be to investigate the appearance of neutral pions in a reaction in which all the other participants have isotopic spin $T=0$. The simplest such reaction [11] is

$$(5) \qquad \mathrm{D} + \mathrm{D} \to \pi^0 + {}^4\mathrm{He} ,$$

and the observation of the process (5) would conclusively establish the existence of the π_0^0.

[9] J. BANDTEL, H. FRANK and B. MOYER: *Phys. Rev.*, **106**, 802 (1957).

[10] See *e.g.* F. E. LOW: *Rev. Mod. Phys.*, **29**, 216 (1957).

[11] This reaction is mentioned by YAMAGUCHI although he states that it is forbidden for pseudoscalar π_0^0. We do not agree with this remark.

Returning to the Panofsky ratio, the cross-section for low-energy charge-exchange scattering, assuming the existence of a π_0^0, will be

$$(6) \quad \sigma(\pi^- + \mathrm{P} \to \pi^0 + \mathrm{N}) = \\ = 4\pi \left[\frac{v_0^0}{v_-} |a_0|^2 + \frac{2}{9} \frac{v_1^0}{v_-} |a_1 - a_3|^2 \right],$$

where v_-, v_0^0, and v_1^0 are the velocities of the π^-, π_0^0 and π_1^0 respectively and a_0 is the amplitude for the process

$$\pi^- + \mathrm{P} \to \pi_0^0 + \mathrm{N},$$

for low energies. a_1 and a_3 have their usual meanings [12]. It is then clear that the contribution of the second term in (6) can be reduced, for zero energy of the π^--P system, by decreasing v_1^0; which is the same as taking the π_1^0 mass higher than the value assumed heretofore. Then the values of $|a_0|$ and v_1^0 may be adjusted to yield a value of (6) which leads to a value of R (1) in agreement with the experimental value, *without interfering with the values of* a_1 *and* a_3.

A more interesting situation arises if the π_1^0 mass is assumed to lie above the limit (2). Then the neutral pions emitted in the Panofsky experiment are exclusively π_0^0's and we find

$$(7) \quad |a_0| = 0.10,$$

in units of the meson Compton wavelength, from the experimental value 1.52 for R. At positive energy, both kinds of π^0 will contribute to the charge-exchange scattering, given by (6). But the value of $|a_0|$ (7) is large enough already to account for all the scattering. Therefore, we must set $a_1 \approx a_3$. This would remove a long-standing problem [13] in pion physics which was to explain the opposite signs of a_1 and a_3 in the usual analysis [14].

We consider a_3 to be already determined, since it is obtained from the π^+-P scattering which involves only the $T = \frac{3}{2}$ state and the backward maximum and the Coulomb interference tell us the sign unambiguously. We therefore keep [14] $a_3 = -0.11$ and take a_1 to fit the low-energy elastic π^--P scattering. Because of the experimental bias against small angle scattering events [5], it appears to us to be possible to fit the experimental data almost as well with a negative value of a_1 as with a positive one [15]. This solution amounts to saying that the s-wave π^--P interaction is repulsive, whereas the conventional solution takes it as attractive. This could be decided if the sign of the Coulomb interference were conclusively known either from scattering, or from the level-shift in a mesic H-atom. Unfortunately, experiments on mesic atoms have so far been done only with heavier elements. There, using the simple theory of DESER *et al.* [16], we obtain a level shift of the same sign but about five times larger than the previously calculated value which appeared to agree quite well with experiment [17].

Whether or not the « revolutionary » solution for the s-wave amplitudes is

[12] The scattering in any parity-angular momentum state with $T = \frac{1}{2}$ will now be described in general by a 2×2 matrix determined by *three* real parameters, assuming invariance under time-reversal. This complicates the phase shift analysis, but for pure s-wave scattering, we can define the scattering length a_1 as usual, if $|a_0|$ is small compared to the de Broglie wave length.

[13] M. GELL-MANN and M. L. GOLDBERGER: *Proc. of the Fourth Rochester Conference* (1954).

[14] J. OREAR: *Nuovo Cimento*, **4**, 586 (1956).

[15] There are other experiments, in particular on the angular distribution for elastic π^--P scattering, which would be quite sensitive to this new assignment. However, since they are even more sensitive to the « small » P-phase shifts, no conclusion can be drawn without performing a new phase shift analysis including the new particle.

[16] S. DESER, M. L. GOLDBERGER, W. THIRRING and K. BAUMANN: *Phys. Rev.*, **96**, 774 (1954).

[17] M. STEARNS: *Proc. of the CERN Symposium* (1956).

proved or disproved, it is extremely desirable to perform the experiment (5) to settle the question of a second π^0; if it should indeed be proved to exist, it would be necessary to re-examine, besides the pion-nucleon scattering in $T=\frac{1}{2}$ states, also other problems on which it would have an immediate bearing.

* * *

We are grateful to Professor R. E. PEIERLS for his valuable criticism of this investigation.

The Non-Mesonic Decay in Flight of a He Hyperfragment.

M. Baldo Ceolin, W. F. Fry (*) and H. Huzita (+)

Istituto di Fisica dell'Università - Padova
Istituto Nazionale di Fisica Nucleare - Sezione di Padova

(ricevuto il 19 Giugno 1958)

During a systematic scanning of G-5 emulsions, which had been exposed to a 4.5 GeV pion beam from the Berkeley bevatron, an event was found which is interpreted as a non-mesonic decay in flight of a He hyperfragment. The characteristics of the event are shown in Fig. 1 and Table I. The connecting track, which is black, has many δ-rays along its entire length. Profile

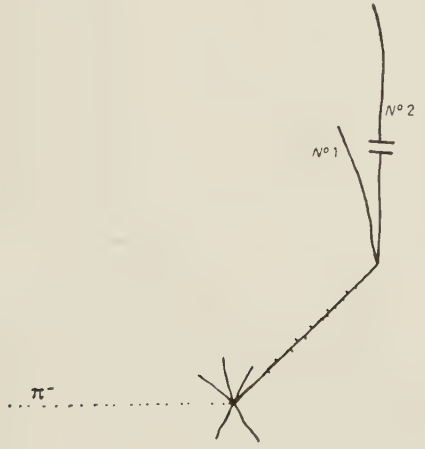

Fig. 1.

Table I.

Type of the parent star	$14 + 0\pi^-$
Connecting track	Length 477 μm Dip angle 39°
Secondary tracks	N. 1 Range 482 μm Energy 9 MeV (if proton)
	N. 2 Range 10.89 mm Energy 56 MeV (proton)

measurements are not consistent with the assumption that the fragment came to rest before producing the secondary star. These measurements also give a charge greater than one for the fragment.

The velocity of the fragment was obtained from the energy distribution of the δ-rays [1] and was found to be

$$\beta = 0.14 \div 0.15 .$$

(*) Present address: Department of Physics, Univ. of Wisc. Madison, Wisc.

(+) On leave of absence from St. Paul's University, Tokyo.

[1] We used the curve of P. Freier, E. J. Lofgren, E. P. Ney and F. Oppenheimer: *Phys. Rev.*, **74**, 1818 (1948).

Using this velocity, the time of flight of the fragment is

$$t = (1.06 \div 1.14) \cdot 10^{-11}\ \mathrm{s}\,.$$

In order to check the reliability of velocity and charge estimates by this method, a similar study has been made on a ^{8}Li hammer track. The hammer track that was chosen was 1 mm long and had a dip of 12°. The properties of the δ-rays along this ^{8}Li track as well as along the connecting track are summarized in Table II. The δ-ray density along the ^{8}Li track increases from zero quite rapidly at a residual range of about 200 μm. This is to be compared with the connecting track which has δ-rays near the secondary star. From this we conclude that the fragment was not at rest when it gave rise to the secondary star.

The number of δ-rays along the connecting track is consistent with a charge of 2 for a velocity which was obtained from the energy distribution of the δ-rays. A charge of 2 is also observed for the secondary particles.

TABLE II.

The connecting track		The hammer track	
Projected distance from the secondary event in μm	Energy of δ-rays in keV	Residual range in μm	Energy of δ-rays in keV
		from 0 at 220 μm	
		no δ-rays with $E \geqslant 10$ keV	
16	15	220	10
—	—	290	12
83	12	295	12
148	14	310	12
150	10	320	10
154	14	335	10
178	11	360	12
193	20	360	12
	—	370	10
270	21	380	13
340	14	400	10
360	14	420	10
		425	12
		435	10
No. of δ-rays $\geqslant 10$ keV = 10		450	12
» $\geqslant 14$ = 7		475	12
» $\geqslant 15$ = 3		480	17
» $\geqslant 20$ = 2		480	12
		495	10
		505	13
		540	13
		565	10
		570	10
		No. of δ-rays $\geqslant 10$ keV = 23	
		» $\geqslant 15$ = 1	

A similiar δ-ray analysis for the ^{8}Li hammer track to obtain its velocity at a chosen point, gives a residual range which is consistent with the observed range, suggesting that the method can be used on tracks which have a residual range of about 600 μm.

For the velocity of the fragment that was obtained from δ-rays, the energy and residual range for the fragment under the following assumptions are:

$$\text{if } {}^4\text{He} \begin{cases} E_{{}^4\text{He}_\Lambda} = (38 \div 44)\ \text{MeV}, \\ R_{{}^4\text{He}_\Lambda} = (550 \div 650)\ \mu\text{m}, \end{cases}$$

$$\text{if } {}^5\text{He} \begin{cases} E_{{}^5\text{He}_\Lambda} = (47 \div 54)\ \text{MeV}, \\ R_{{}^5\text{He}_\Lambda} = (780 \div 980)\ \mu\text{m}. \end{cases}$$

An alternative interpretation of the event as a breakup of a normal He fragment, due to a collision with a heavy nucleus, can be excluded by noting that the kinetic energy of the charged particles, alone, is greater than the total kinetic energy of the fragment. If neutral particles are also considered, the energy discrepancy is even greater.

About 30% of all non-mesonic decays of hyperfragments of He, Li and Be have a proton of energy greater than about 50 MeV [2], therefore the fast proton is not unusual.

* * *

The authors are grateful to Dr. E. J. LOFGREN and others at Berkeley for making the exposures possible.

[2] M. BALDO-CEOLIN, C. DILWORTH, W. F. FRY, W. D. B. GREENING, H. HUZITA, S. LIMENTANI and A. E. SICHIROLLO: *Nuovo Cimento*, **7**, 328 (1958).

Test on the Global Symmetry.

D. Ito, S. Minami (*) and H. Tanaka (+)

Institute of Physics, Tokyo University of Education - Tokyo
(*) *Department of Physics, Osaka City University - Osaka*
(+) *Istituto di Fisica dell'Università - Bologna*
Istituto Nazionale di Fisica Nucleare - Sezione di Bologna

(ricevuto il 24 Giugno 1958)

A note is given on a possible test of the «global symmetry» proposed independently by Gell-Mann [1], Schwinger [2] and Tiomno [3].

According to the idea of the global symmetry the doublet (Σ^+, Y^0) or (Z^0, Σ^-) (*) is coupled to the pion, in absence of K particles, in identically the same way as the proton and neutron. On the other hand, π-Σ scattering is expressed in general by the amplitudes, T_2, T_1 and T_0 corresponding to the iso-spin $I=2$, 1 and 0 respectively, and the π-Λ^0 scattering by the amplitude T of $I=1$ only. Then, if the pion-nucleon scattering is characterized by the amplitudes A and B of iso-spin $I=\frac{3}{2}$ and $\frac{1}{2}$, the above amplitudes T's are easily expressed in terms of A and B as follows:

$$(1)\quad \begin{cases} T_2=A\,, \quad T_1=(A+2B)/3\,, \quad T_0=B\,. \\ T=(2A+B)/3\,. \end{cases}$$

As a simplest result of the above relation the process $\pi^-+\Sigma^+ \rightleftarrows \pi^+ + \Sigma^-$ is expected to be forbidden, but the experimental check will be practically impossible in the present stage. Next, one might take an interest in the simple reaction such as

$$(A)\qquad K^- + p \to \Sigma + \pi\,.$$

However, in such final two body case it would offer a poor test on the global symmetry because of the angular momentum conservation. In other words, if, as expected, the state $J=\frac{1}{2}$ is predominant in K^--p interaction the final state will give a poor information about the state $J=\frac{3}{2}$ which must be a strong interaction by the global symmetry in the final $(\Sigma$-$\pi)$ system. Hence, we shall confine ourselves only to the case of final three body reactions where the conservation of energy and angular momentum appears less restrictive for a pair among the final three particles.

For a convenience of comparison between the (hyperon-π) and (nucleon-π) interactions the three body final states are divided into two classes, that is,

a) the final states consisting of hyperon, pion and nucleon;

(1) M. Gell-Mann: *7-th Rochester Conference* (1957), IX, 6.
(2) J. Schwinger: *7-th Rochester Conference* (1957), IX, 15.
(3) J. Tiomno: *7-th Rochester Conference* (1957), IX, 22.
(*) $\Lambda^0 = \frac{1}{\sqrt{2}}(Z^0 - Y^0)$, $\Sigma^0 \quad \frac{1}{\sqrt{2}}(Z^0 - Y^0)$.

b) the final states consisting of hyperons and pion but without nucleon.

In the case *a*), the following interactions are considered for the incident K^- energy of $(100 \div 500)$ MeV.

$$(B) \qquad K^- + D \to \Sigma + N + \pi$$

$$(C) \qquad K^- + D \to \Lambda^0 + N + \pi .$$

Owing to the iso-spin conservation ($I = \frac{1}{2}$) the iso-spin of the (Σ-π) system in (B) must be $I = 1$ or 0. Then, as is seen from the relation (1), in the reaction

$$(B') \qquad K^- + D \to \Sigma^+ + n + \pi^-$$

the strong interaction in the $(\frac{3}{2}\ \frac{3}{2})$ state should appear mostly between the neutron and π^- (*). So, it would not serve to a direct test of the global symmetry. In this process (B′) most of the energy will be used for exciting the (n-π^-) system to an isobaric state, and the energy distribution of Σ^+ will be inclined to a favour of the low energy.

On the other hand, in the process

$$(C') \qquad K^- + D \to \Lambda^0 + p + \pi^-$$

the system (π^--Λ^0) has only one state $I = 1$, and if the global symmetry (I) really holds the $(\frac{3}{2}\ \frac{3}{2})$ strong interaction should stand in the (π-Λ^0) system rather than in the (π^--p) system. Thus, in place of the (π^--p) center of mass system the Q-value (+) measured in the (π^--Λ^0)center of mass system will show a peak in the $(140 \div 150)$ MeV region. Further, the energy spectrum of the proton will have a same tendency as that of Σ^+ in the reaction (B′) favouring the low energy. On the contrary, if the Q-value and angular correlation in the (π^--p) system are similar to those of the (π^--n) system in (B′) showing a strong $(\frac{3}{2}\ \frac{3}{2})$ resonance and if the momentum spectrum of Λ^0 resembles that of Σ^+ in (B′), the global symmetry will be possibly violated.

In the case *b*), one considers the following interactions:

$$(D) \qquad \pi^+ + p \to \Sigma^+ + \pi^+ + K^0$$

$$(E) \qquad \pi^+ + p \to \Lambda^0 + \pi^+ + K^+ .$$

If the final interaction takes an essential role in the process (D), as a result of the relation (I) the (π^+-Σ^+) system should manifest the strong $(\frac{3}{2}\ \frac{3}{2})$ interaction because the (π^+-Σ^+) system has only a state $I = 2$. Of course, one must take account of the K-particle effect but it will be of minor importance for our qualitative argument so long as the (hyperon-π) interaction be much stronger than the (hyperon-K) interaction. Therefore, in the (π^+-Σ^+) center of mass system the peak of the Q-value lying in the $(140 \div 150)$ MeV region would be a clearer evidence of the global symmetry than given by the process (C′).

In the process (E) only the $I = 1$ state appears for the (π^+-Λ^0) system, but the argument is essentially the same as above.

(*) One may remember that the isobar model of the $(\frac{3}{2}\ \frac{3}{2})$ state was very effective for the system of two nucleons and pion.

(+) The Q-value is defined by $N^+ \to N + \pi + Q$ where N^+ means an isobar nucleon. In other words, for this case, Q is the sum of the kinetic energy of π^- and Λ^0 in the (π^--Λ^0) C.M. system.

On Electromagnetic Corrections from High Energy Virtual Photons.

R. Gatto and M. Ruderman (*)

Istituto di Fisica e Scuola di Perfezionamento in Fisica Nucleare dell'Università - Roma
Istituto Nazionale di Fisica Nucleare - Sezione di Roma

(ricevuto il 26 Giugno 1958)

In this note we wish to comment and expand on the relevance of a recent suggestion on the theory of $\pi \to e + \nu$ decay [1,2].

The magnitude of the electromagnetic corrections to different matrix elements depends on the detailed structure of the interaction considered. Thus, for example, the electron Lamb shift in a vector (Coulomb) or pseudovector field, after charge and mass renormalization, is negligibly dependent on virtual photons more than a few MeV off the energy shell. On the other hand, in a scalar or pseudoscalar field it depends very much on the high energy photons: indeed it is a divergent correction proportional to the logarithm of the maximum momentum of the virtual photons considered. One can make a rough classification into those reactions whose radiative corrections depend strongly upon high momentum virtual photons, those which depend slightly, and those which depend negligibly.
make some remarks on these groupings and on their relation to a point of view which has been suggested for the problem of the smallness of the $\pi \to e + \nu$ rate [1,2].

The radiative corrections to the lepton decay modes of the charged pion ($\pi \to e + \nu$ and $\pi \to \mu + \nu$) depend upon the behaviour of high energy virtual photons for any boson-lepton coupling and especially for that coupling resulting indirectly from a universal $A + V$ baryon-lepton point interaction. In this case the decay matrix element, in the absence of the electromagnetic couplings, is proportional to the electron or muon mass. It has been pointed out that, in so far as the decays $\pi \to e + \nu$ and $\pi \to \mu + \nu$ are representable as occurring at a single point in space-time (the point (x, t) where the pion is annihilated, coincides with the point (x', t') where the lepton pair is created) then the divergent radiative corrections cancel a major part of the effect of mass renormalization [1,2]. The resulting matrix elements turn out to be proportional to the bare (not including electromagnetic corrections) electron or muon mass. Specifically, the matrix element for $\pi \to$ lepton (l) $+ \nu$ was shown to be ex-

(*) John Simon Guggenheim Foundation Fellow on leave from the University of California, Berkeley.

(1) R. Gatto and M. Ruderman: *Nuovo Cimento* **8**, 775, 1958

(2) J. C. Taylor: *Phys. Rev.* (to be published).

pressible to all orders in e^2 as

$$(1) \qquad M_1 = G m_1^{(B)} \varphi_\pi^* (\psi_1 \gamma_5 \psi_\nu) ,$$

with all radiative corrections included. Now, after renormalization of the π and of the electron masses, this is still divergent, the leading term being proportional ro $e^2 G (\ln(\lambda/m)) m_1^{(B)}$, where the virtual photons are limited by $|K|^2 < \lambda^2$ and the matrix element has no radiative corrections left except that one has to replace bare masses by physical masses. Thus, as $\lambda \to \infty$, the ratio of the rates for electron and muon decay is rigorously given by

$$(2) \qquad r = \left(\frac{m_e^{(B)}}{m_\mu^{(B)}}\right)^2 \left(\frac{1-(m_e^2/m_\pi^2)}{1-(m_\mu^2/m_\pi^2)}\right)^2 ,$$

a result which is expected to hold to all orders in e^2 in conventional quantum electrodynamics (Q.E.). The suggested explanation of the anomalously small $(\pi \to e+\nu)/(\pi \to \mu+\nu)$ ratio was based on the proposal that $(m_e^{(B)}/m_\mu^{(B)}) \ll (m_e/m_\mu)$ ([1,2]).

In a more realistic description of the π-lepton decay, (x, t) is different from (x', t'), and we can define $\bar{\lambda}$ such that $|(x-x')^2 - c^2(t-t')^2| \sim 1/\bar{\lambda}^2$. Then the equivalence theorems which lead to Eq. (1) need no longer be valid, even approximately, unless the relevant virtual photons have $K^2 < \bar{\lambda}^2$. If this is not true but if, on the contrary, most of the contributions from virtual photons were to come for $K^2 > \bar{\lambda}^2$, then we would expect the electron mass change to be the dominant electromagnetic correction. The photon, which because of gauge invariance must be emitted from the point $(x, t) = (x', t')$ in the local approximation, as well as from the meson and electron currents, is, in general, emitted with smaller amplitude if $(x, t) \neq (x', t')$. The separation effectively contributes a form factor which « softens » the radiative corrections but not the electron and meson self-energies. Then the new ratio would differ from the previous one (Eq. (2)) only in that the bare masses would be replaced by the observed masses (except for some small terms of order α)

$$(2') \qquad r' = \left(\frac{m_e}{m_\mu}\right)^2 \frac{\left(1-(m_e^2/m_\pi^2)\right)^2}{\left(1-(m_\mu^2/m_\pi^2)\right)^2} .$$

For example we may consider a Fermi-Yang type model for a π^+: a bare proton bound in a ^1S state to a bare antineutron by a static potential. The assumption of a static potential is here only made on grounds of simplicity and it does not affect the main conclusions. Then, after mass renormalizations, all electromagnetic corrections to the pion-lepton decay are finite and of order e^2. In particular there can be nothing to cancel the logarithmically divergent correction expressing the change from $m^{(B)}$ to $m = m^{(B)}(1 + e^2 \log(\lambda/m^{(B)}) + \ldots)$. However if the cut-off photon momentum λ is much less than the momenta of the bound proton then eq. (2) again obtains. Similarly, if the process $\pi^+ \to p + \bar{n} \to l + \nu$ is cut-off for $|p^2| \cong \bar{\lambda}^2$ for the virtual proton or antineutron, then Eq. (2) can be shown to hold if $\lambda^2 < \bar{\lambda}^2$ but Eq. (2') is valid when $\lambda^2 \gg \bar{\lambda}^2$. Now λ is generally assumed to be of the order of the nucleon mass M, since virtual nucleons appear in the intermediate state in the decay, but, of course, the integrals diverge and $\bar{\lambda}$ might, in a correct theory, turn out to be much larger. If, in general, all divergent integrals are cut-off at about the same momentum, then, although the ratio (2) may be expected to hold, it differs negligibly from (2') since $m = m_B(1 + e^2 \ln(M/m_B)) \cong m_B$. If $m \gg m_B$ then $\lambda \gg \bar{\lambda} \sim M$, but then we would expect (2') to hold. We feel that conventional Q.E. can make m differ appreciably from m_B only by making use of photons so very far off the energy shell that the assumptions which lead to (2), $K^2 < \bar{\lambda}^2$, are not valid. Rather, from our experience with simple models, the relation (2') obtains in these cases.

Aside from the question of the ratio r, the attractive notion that all of the electron mass is electromagnetic is incompatible with present Q.E. Even to make most of it electromagnetic requires the unconfortably large cut-off $\lambda \sim me^{137}$. If the photon propagator, K^{-2}, is altered by replacing it by a suitable function $f(K^2)$, the electron mass can be made largely (but not entirely) electromagnetic with photons such that $K^2 \lesssim \bar{\lambda}^2$; moreover with such an alteration in Q.E. Eqs. (1) and (2) remain valid [3]. However an $f(K^2)$ which results in a 100% correction of the electron mass would also be expected to give enormous π^+-π^0 or proton-neutron mass differences. An unspecified change in Q.E., which satisfies our prejudice that electron mass is electromagnetic, may largely restrict virtual photons to the region $K^2 \leqslant \bar{\lambda}^2 \sim M^2$ (the baryon masses are the largest inverse lengths that so far exhibit themselves distinctly in the interactions among particles). Eq. (1) and hence Eq. (2), needs no longer be valid but it would be our hope that it would remain at least approximately valid.

An alteration of Q.E. for $K^2 \gtrsim M^2$ would affect electromagnetic corrections to matrix elements in various degrees:

i) The Lamb shift and the anomalous magnetic moment of the electron are entirely insensitive to any such alteration.

ii) Many matrix elements, although finite after change and mass renormalization, involve virtual photons of sufficiently high momentum ($K \gtrsim M$) that they will be presumably altered. Thus, for example, the radiative corrections to the rate and to the ρ-value of $\mu \to e + \nu + \bar{\nu}$ are finite, after mass renormalization for the $A \pm V$ coupling. However the relevant photon energies extend up to the muon mass. An alteration of Q.E. at 1 GeV may be expected to produce a non-negligible alteration in the electromagnetic corrections. A similar conclusion results for nuclear β-decay where, although the correction is again finite for an $A \pm V$ coupling the relevant virtual photons extend past 1 GeV. As we have already pointed out [1] very accurate measurements of the polarizations of the β particles may provide an important clue.

iii) Among those electromagnetic corrections which are divergent and therefore depend very sensitively upon the high energy virtual photons are the mass differences among members of isotopic mass multiplets ($\pi^{\pm}$-π^0, n-p, $\Sigma^+\Sigma^-$, $\Sigma^{\pm}\Sigma^0$ etc.). Particularly interesting is the large observed Σ^+-Σ^- mass difference which for a charge symmetric pion-baryon interaction would be zero in the absence of K-interactions. Such a large mass difference is the main objection so far to the hypothesis that K-couplings are considerably weaker than π-couplings [4]. An interesting point also arises in connection with the proposed $\Delta T = \frac{1}{2}$ rule for weak interactions. The main objection to this rule comes at present from the ratios of $K^0 \to \pi^+ + \pi^-$ to $K^0 \to \pi^0 + \pi^0$, and of $K^+ \to \pi^+ + \pi^0$ to $K^0 \to 2\pi$. The radiative corrections to the relevant matrix elements are given by divergent expressions very sensitive to high energy photons. The breakdown of $\Delta T = \frac{1}{2}$ in these decay modes, as due to electromagnetic corrections, would certainly be incorrectly estimated from present Q.E. if there is an alteration at 1 GeV. The radiative corrections to $\pi \to e + \nu$ decay of course belong to this group and we have already seen how the magnitude may perhaps be greatly altered. How-

[3] This was shown in reference [1].

[4] M. GELL-MANN: *Proc. of the VII Annual Rochester Conference* (New York, 1957), pp. IX-6; J. SCHWINGER: *Proc. of the VII Annual Rochester Conference* (New York, 1957), pp. IX-15; R. E. MARSHAK: *Proc. of the VII Annual Rochester Conference* (New York, 1957), pp. IX-27.

ever it would be very surprising if the radiative corrections were indeed the explanation of the anomalous $\pi \to e + \nu$ rate while they would not have other significant effects among the processes included in this group.

It must be stressed that if experiment does not indicate slight discrepancies from the predictions from ordinary Q.E. for some of the processes of the group ii) (and the anomalous magnetic moment of the muon agrees accurately with the Karplus-Kroll-Summerfield-Peterman formula) and larger discrepancies for processes of group iii), then we would feel that an explanation of the $(\pi \to e + \nu)/(\pi \to \mu + \nu)$ ratio based upon the hypothesis of an electromagnetic nature of the electron mass would no longer be an attractive one. Present measurements are unfortunately not accurate enough to allow any conclusion.

* * *

We would like to thank Drs. S. Bludman and J. C. Taylor for an interesting correspondence on these subjects, and Drs. M. Cini and B. Touschek for stimulating discussions.

Note added in proof.

A suggestion for the $\pi \to e + \gamma$ to $\pi \to \mu + \gamma$ ratio similar to that proposed in our previous paper (see reference [1]) has been made independently by R. P. Feynman at the last *High Energy Physics Conference* in Geneva (June-July 1958). Differently from us, in his approach Feynman assumes a specific model for the breakdown of quantum electrodynamics.

Il metodo funzionale di Feynman in un semplice modello di teoria dei campi.

R. Cirelli e A. Esteve Pastor (*)

Istituto di Scienze Fisiche dell'Università - Milano
Istituto Nazionale di Fisica Nucleare - Sezione di Milano

(ricevuto il 3 Luglio 1958)

È noto come il metodo funzionale di Feynman (1), per i problemi a un numero finito di gradi di libertà, sia equivalente alla formulazione tradizionale della meccanica quantistica; nel caso di sistemi a infiniti gradi di libertà una dimostrazione completa non è ancora stata data. Scopo della presente nota è di saggiare l'equivalenza del metodo di Feynman con i metodi ordinari della teoria dei campi mediante l'applicazione ad uno dei primi e più semplici modelli risolubili di teoria dei campi: quella di un campo bosonico scalare neutro in interazione con un nucleone infinitamente pesante.

L'hamiltoniana del sistema è

$$H = \sum_k (a_k^+ a_k + \tfrac{1}{2})\omega_k + g \sum_k \frac{1}{(2\omega_k V)^{\frac{1}{2}}} (a_k^+ + a_k) ,$$

dove il significato dei simboli usati è quello corrente; con

$$a_k = \frac{1}{(2\omega_k)^{\frac{1}{2}}} (p_k - i\omega_k q_k) ,$$

$$a_k^+ = \frac{1}{(2\omega_k)^{\frac{1}{2}}} (p_k + i\omega_k q_k) ,$$

tenuto conto che

$$[q_k, p_{k'}] = i\delta_{kk'} ,$$

si ha

$$H = \sum_k \frac{1}{2} [p_k^2 + \omega_k^2 q_k^2] + g \sum_k \frac{1}{V^{\frac{1}{2}} \omega_k} p_k .$$

(*) De l'Instituto de Física del Consejo Superior de Investigaciones Científicas di Madrid.
(1) R. P. Feynman: *Rev. Mod. Phys.*, **20**, 367 (1948); W. Pauli: *Ausgewählte Kapitel aus der Feldquantisierung* (Zürich, 1957), pag. 139.

Il propagatore del sistema è dato, in generale, nell'intervallo $\tau = t - t_0$, da

$$(1)\qquad K(q_1, q_2 \dots q_k \dots, q_1', q_2' \dots q_k' \dots; \tau) = K(q\,|\,q';\tau) = \lim_{\substack{\varepsilon\to 0\\ N\to\infty\\ \tau\ \mathrm{fisso}}} \int \prod_{\alpha=0}^{N-1} K_c(q^{(\alpha+1)}\,|\,q^{(\alpha)};\varepsilon)\,\mathrm{d}q^{(1)} \dots \mathrm{d}q^{(\alpha)} \dots \mathrm{d}q^{(N)} .$$

Nel caso in cui l'interazione non dipenda dal tempo è facile vedere che

$$K(q\,|\,q';\tau) = K_c(q\,|\,q';\tau) ,$$

essendo K_c il propagatore « classico », facilmente calcolabile dall'azione classica

$$S(q\,|\,q';\tau) = \int_{t_0}^{t} L\,\mathrm{d}t' = \int_{t_0}^{t} \Big(\sum_k p_k\dot q_k - H\Big)\,\mathrm{d}t' = \int_{t_0}^{t} \sum_k \frac{1}{2}\Big[\dot q_k^2 - \omega_k^2 q_k^2 - 2\frac{g}{V^{\frac12}\omega_k}\dot q_k + \frac{g^2}{V\omega_k^2}\Big]\mathrm{d}t' =$$

$$= \sum_k \Big\{\frac{\omega_k}{2}\operatorname{cotg}\omega_k(t-t_0)\,[q_k^2(t)+q_k^2(t_0)] - \frac{\omega_k}{\sin\omega_k(t-t_0)}\,q_k(t)\,q_k(t_0) - \\ - \frac{g}{V^{\frac12}\omega_k}\,[q_k(t)-q_k(t_0)] + \frac{1}{2}\frac{g^2}{V\omega_k^2}\,(t-t_0)\Big\} ;$$

quindi

$$K(q\,|\,q';\tau) = D\exp\,[\,i\,S(q\,|\,q';\tau)\,] .$$

con

$$D = \prod_k \left(\frac{\omega_k}{2\pi i\,\sin\omega_k(t-t_0)}\right)^{\frac12} .$$

Se, seguendo una tecnica corrente, si introduce il fattore di spegnimento adiabatico dell'interazione, il propagatore va calcolato rifacendosi alla (1); al risultato si può arrivare con un metodo di ricorrenza che illustriamo per un oscillatore di hamiltoniana

$$\mathcal{H} = \frac{1}{2}\,(p^2+\omega^2q^2) + g\exp\,[-\lambda\,|\,t\,|\,]\frac{1}{V^{\frac12}\omega}\,p .$$

Diviso l'intervallo $\tau \equiv (-t, t)$ in $2N$ parti uguali $\varepsilon = (\tau/2N)$ e preso in ogni intervallo $t_{r+1} - t_r$

$$g_r \equiv g\exp\,[-\lambda\,|\,t_r\,|\,] ,$$

si ha:

$$K(q, q';\, t_1 - t_0) = K_c(q, q';\, t_1 - t_0) ,$$

$$K(q, q';\, t_2 - t_0) = \int K_c(q, q^{(1)};\, t_1 - t_0)\,K_c(q^{(1)}, q';\, t_2 - t_1)\,\mathrm{d}q^{(1)} =$$

$$= \sqrt{\frac{\omega}{2\pi i\,\sin\omega\varepsilon}}\,\sqrt{\frac{\omega}{2\pi i\,\sin\omega\varepsilon}}\exp\left[i\,\frac{\omega}{2}\operatorname{cotg}\omega\varepsilon[q^2+q'^2] + ig_0q - ig_1q'\right]\cdot$$

$$\cdot\int\exp\left[\frac{i\omega}{2}\,\operatorname{cotg}\,\omega\varepsilon\cdot 2q^{(1)2} - i\,\frac{\omega}{\sin\omega\varepsilon}\,(q+q')q^{(1)} + i(g_1-g_0)q^{(1)}\right]\mathrm{d}q^{(1)} =$$

$$= \sqrt{\frac{\omega}{2\pi i\,\sin 2\omega\varepsilon}}\exp\left[i\,\frac{\omega}{2}\operatorname{cotg}\,2\omega\varepsilon(q^2+q'^2) - i\,\frac{\omega}{\sin 2\omega\varepsilon}\,qq'\right]\exp\,[iG_2q - iG_2'q' + iF_2] ,$$

e in generale

$$K(q, q'; t_{r+1} \quad t_0) = \int K(q, q^{(r)}; t_r \quad t_0)\, K_r(q^{(r)}, q'; t_{r+1} \quad t_r)\, \mathrm{d}q^{(r)} =$$

$$= \sqrt{\frac{\omega}{2\pi i \sin(r+1)\omega\varepsilon}} \exp\left[i \frac{\omega}{2} \operatorname{cotg}(r+1)\omega\varepsilon [q^2 + q'^2] - i \frac{\omega}{\sin(r+1)\omega\varepsilon} qq' \right] \cdot$$

$$\cdot \exp\left[i \left(G_r + \frac{(g_{r+1} - G'_r) \sin \omega\varepsilon}{\sin(r+1)\omega\varepsilon} \right) q - i \left(g_{r+1} - \frac{(g_{r+1} - G'_r) \sin r\omega\varepsilon}{\sin(r+1)\omega\varepsilon} \right) q' + i F_{r+1} \right],$$

da cui le formule ricorrenti

$$G'_{r+1} = g_{r+1} - \frac{(g_{r+1} - G'_r) \sin r\omega\varepsilon}{\sin(r+1)\omega\varepsilon} = g_{r+1} - \frac{\sum_{s=1}^{r} (g_{s+1} - g_s) \sin s\omega\varepsilon}{\sin(r+1)\omega\varepsilon} .$$

$$G_{r+1} = G_r + \frac{(g_{r+1} - G'_r) \sin \omega\varepsilon}{\sin(r+1)\omega\varepsilon} = \sum_{n=1}^{n=r} \frac{\sin \omega\varepsilon \sum_{s=1}^{n} (g_{s+1} - g_1) \sin s\omega\varepsilon}{\sin(n+1)\omega\varepsilon \sin \omega\varepsilon} .$$

$$F_{r+1} = \frac{1}{2} \frac{g^2}{V\omega^2} \sum_r \varepsilon \exp[-\lambda |t_r|] - \sum_r \frac{(g_{r+1} - G'_r)^2}{2\omega(\operatorname{cotg} r\omega\varepsilon + \operatorname{cotg} \omega\varepsilon)} .$$

Eseguendo nell'ordine i limiti $\varepsilon \to 0$, $\tau \to \infty$, $\lambda \to 0$ è facile vedere che

$$(\alpha) \qquad G'_N = g , \qquad G_N = 0 , \qquad F_N = \frac{1}{2} \frac{g^2}{V\omega^2} t ,$$

$$(\beta) \qquad G'_{2N} = G_{2N} = 0 , \qquad F_{2N} = \frac{1}{2} \frac{g^2}{V\omega^2} \tau .$$

Con le (α) si ha il propagatore nell'intervallo di tempo che va da $-\infty$ ad un tempo qualsiasi finito; con le (β) si ha il propagatore da $-\infty$ a $+\infty$

$$K(q, q', \tau) = \sqrt{\frac{\omega}{2\pi i \sin \omega\tau}} \exp\left[\frac{i\omega}{2} \operatorname{cotg} \omega\tau (q^2 + q'^2) - \frac{i\omega}{\sin \omega\tau} qq' + \frac{i}{2} \frac{g^2}{V\omega^2} \tau \right] =$$

$$= K_{\text{osc. libero}} \cdot \exp\left[\frac{i}{2} \frac{g^2}{V\omega^2} \tau \right] .$$

Quindi, considerando l'insieme degli oscillatori, si ottiene:

$$K(q_1, q_2 \ldots q_k \ldots, q'_1, q'_2 \ldots q'_k \ldots; \tau) = \prod_k K(q_k, q'_k; \tau)_{\text{osc. lib.}} \exp\left[i \sum_k \frac{1}{2} \frac{g^2}{\omega_k^2 V} \tau \right] .$$

Da questa espressione risulta subito l'aspetto peculiare del modello consistente nell'assenza di diffusione mesone-nucleone; il « fattore di fase »

$$\sum_k \frac{1}{2} \frac{g^2}{V\omega_k^2}$$

dà direttamente l'auto-energia δm del nucleone; inoltre, senza ulteriori complicazioni nei calcoli, facendo interagire il campo bosonico con due nucleoni infinitamente pesanti, si avrebbe, nel fattore di fase, una espressione che, con le usuali manipolazioni, porterebbe al potenziale di Yukawa [2].

* * *

Desideriamo ringraziare vivamente il prof. P. CALDIROLA per il suo costante interessamento; uno di noi (A.E.P.) ringrazia anche la Fundación Juan March per una borsa di studio concessagli.

[2] Cfr. per es., G. WENTZEL: *Quantum Theory of Fields* (New York, 1949), p. 44.

A Discussion of Some Angular Distributions in the Reactions $\pi+N \to \pi+\pi+N$, $N+N \to 2N+\pi$, $\gamma+N \to \pi+\pi+N$.

G. Morpurgo

Istituto di Fisica dell'Università - Parma
Istituto Nazionale di Fisica Nucleare - Laboratori di Frascati

(ricevuto il 14 Luglio 1958)

Some experiments on the reactions $\pi+N \to \pi+\pi+N$; $N+N \to N+N+\pi$ at high energy have been already done [1]; also experiments on the reaction $\gamma+N \to \pi+\pi+N$ are beginning [2]. Of course we are still very far from statistically significant data but one may expect some increase in the future.

The purpose of the present short discussion is to point out that, in presenting the data from the above mentioned reactions, one should plot also certain angular distributions of the final products (in addition to the ones which are commonly given) which may provide valuable information on some significant aspects of the above reactions.

The aspects which we have in mind are two: *a*) to know whether or not two of the three outgoing particles have a preference for some relative angular momentum state, *b*) to find evidence for parity conservation — or non-conservation — in strong interactions from high energy events.

To illustrate point *a*) we shall consider as an example the reaction [3]:

$$\pi+N \to \pi+\pi+N . \tag{1}$$

If, at some energy the relative angular momentum of the two pions shows a preference for some value, this may be an indication for a particularly strong interaction between the two pions when they have that value of the angular momentum. Similarly if the $t=\frac{3}{2}$, $J=\frac{3}{2}$ resonance state of the pion nucleon system has a particularly important

[1] *a*) incident π^-: W. D. Walker, R. Hushfar and W. D. Shephard: *Phys. Rev.*, **104**, 526 (1956); E. Eisberg *et al.*: *Phys. Rev.*, **97**, 797 (1955); W. D. Walker and J. Crussard: *Phys. Rev.*, **98**, 1416 (1955). The Fig. 20 in this paper contains one of the distributions which we shall discuss below. It is the only example we know. *b*) incident p: T. W. Morris *et al.*: *Phys. Rev.*, **103**, 1472 (1956); W. B. Fowler *et al.*: *Phys. Rev.*, **103**, 1479 (1956); W. B. Fowler *et al.*: *Phys. Rev.*, **103**, 1489 (1956); M. M. Block *et al.*: *Phys. Rev.*, **103**, 1484 (1956).

[2] J. Sellen, G. Cocconi, V. T. Cocconi and E. Hart: *Phys. Rev.*, **110**, 779 (1958).

[3] Among the reactions (1) the most convenient is perhaps $\pi^+ + p \to 2\pi + N$.

role (4) in a reaction like (1), in a certain energy interval, one should find the final nucleon and one of the pions (which will be mentioned later) preferentially in a state with total angular momentum $\frac{3}{2}$.

To illustrate point *b*) we notice that, so far, there is no or little evidence for parity conservation in high energy events due to strong interactions. The absence, to a very high degree of accuracy of an electric dipole moment of a nucleon, only depends, as it is well known, on the invariance under T (or CP); and the fact that there is good evidence of parity conservation in strong interactions at low energy (5), does not imply, necessarily, that the same must happen at high energy.

We shall first discuss which angular distributions are important in providing information on point *a*); the same distributions are also of interest for point *b*).

We shall generally call 1, 2, 3, the three outgoing particles from any of the reactions previously mentioned; we are interested in the distribution of angular momentum of the particles 2, 3 in the reference system in which they have opposite momenta; such angular momentum — the relative angular momentum — we call $\boldsymbol{S}$. We may characterize the final state of 1, 2, 3 in the total center of mass system ($\boldsymbol{p}_1+\boldsymbol{p}_2+\boldsymbol{p}_3=0$) giving the momentum $\boldsymbol{p}_1$, the value of S^2 and the component of $\boldsymbol{S}$ along some axis, and the absolute value $|\boldsymbol{p}'|$ of the relative momentum of 2 and 3 in in the reference system in which they have opposite momenta: $\boldsymbol{p}'=\boldsymbol{p}'_2=-\boldsymbol{p}'_3$.

The angular distributions which, we claim, may give information on S are now the following: 1) the distribution in θ, where θ is, for each observed event, the angle between $\boldsymbol{p}_1$ and $\boldsymbol{p}'$; 2) the distribution in φ where φ is the angle between the following two planes: *a*) the plane determined by $\boldsymbol{p}_1$ and the line of flight of the incident particles, *b*) the plane determined by $\boldsymbol{p}_1$ and $\boldsymbol{p}'$. It is apparent that the distributions defined above are the same which have been considered ( ) in the reactions of associated production of hyperons and K particles to get information on the spins of the hyperons: we have simply substituted here the K with the particle 1 and the hyperon with the subsystem of the particles 2 and 3. The differences with respect to the case of the associated production are that:

1) the particles 2 and 3 do not generally have, in their rest system, an even approximately unique Q value;

2) the decay of the subsystem 2+3 is almost simultaneous with its production;

3) the subsystem 2+3 is not generally produced with a unique value of the spin S, but will generally bewn superposition of states with different spins, which will generally interfere.

As far as the points 1) and 2) are concerned they should not influence

(4) For a discussion of the isobaric model compare: S. J. LINDENBAUM and R. M. STERNHEIMER: *Phys. Rev.*, **109**, 1722 (1958) for the case of reaction (1) and *Phys. Rev.*, **105**, 1874 (1957) for the case of the reaction $N+N \rightarrow N+N+\pi$. Our point of view is however somewhat different from that expressed in the above mentioned papers; our question is simply to know whether considering only that subclass of events, which, kinematically could be compatible with the isobaric model, the relative angular momentum of the pion and nucleon from the «decay» of the isobaric state is $\frac{3}{2}$ as it should be; of course it is to be hoped that the subclass of events in question is an appreciable fraction of the total number of the events; it is however difficult to say at present how appreciable it is and the experimental data do not furnish a clear picture.

(5) Compare D. H. WILKINSON: *Phys. Rev.*, **109**, 1603, 1610, 1613 (1958) and the references quoted there.

(6) G. MORPURGO: *Nuovo Cimento*, **4**, 1222 (1956); **5**, 1787 (1957); also the chap. 15 in: C. FRANZINETTI and G. MORPURGO: *Suppl. Nuovo Cimento*, **6**, 469 (1957).

the kind of information on S provided by the angular distributions in θ and φ; as far as the point 3) is concerned the knowledge of the spin distribution of the subsystem $2+3$ is precisely one of the objectives of an investigation like the one proposed here; it must be said however that such an investigation is likely to be fruitful only if one value of S is predominant.

To conclude the distributions in θ and φ defined above will give in principle on S the same kind of information which they are capable of providing on the spin of the hyperon in a reaction of associated production. In particular if we take only those events in which particle 1 goes backward or forward with respect to the direction of the incident beam, we may apply a known argument by ADAIR [7] and get a much more significant information (from the θ distribution).

Consider for instance again the reaction (1); and suppose that we ask to test whether the resonance model is valid, as discussed before, at least for an appreciable subclass of the events [4].

We assume that if an event has taken place through the formation of the resonance state $\pi+\mathrm{N}\to\mathrm{N}^*+\pi_1$ and its subsequent decay $\mathrm{N}^*\to\mathrm{N}+\pi_2$ we may discriminate between π_1 and π_2 (respectively, the pion directly emitted and the pion in the resonance state), on the basis of their energy being in a certain range. We therefore select, among all the events, those in which a pion, which has an energy appropriate to π_1, is produced backward or forward with respect to the incident beam. If the particles 2 and 3 have then a relative total angular momentum $\frac{3}{2}$ one should find a distribution in θ of the form $1+3\cos^2\theta$.

Similarly, if we have some reason to believe, or if we like to test whether the two pions, in the reaction (1) have dominantly some value of the relative angular momentum, we take those events, from reaction (1), in which the final nucleon (particle 1 in this case) goes forward or backward; the distribution in θ is in this case

$$a\cos^{2l}\theta + b\cos^{2l-2}\theta\,.$$

where l is the dominant value of the relative angular momentum for the two pions and a, b arbitrary coefficients.

It has to be pointed out that the above distributions have a determined or almost determined shape because the incident pion is spinless; for photoproduction events or nucleon nucleon collisions the distributions may contain more free parameters.

We now briefly mention the possible effects of parity non conservation [8] on the θ and φ distributions. Again, a discussion similar to that for the associated production may be repeated here [6]; we have that, if parity is not conserved, one may expect in general asymmetries both in the θ and in the φ distribution. We recall that an asymmetry in the φ distribution means that the number of events with $0<\varphi<\pi$ is different from that with $\pi<\varphi<2\pi$; which is the same thing as to say that the numbers of events with a positive or with a negative value of $(\boldsymbol{p}_{\mathrm{inc}}\wedge\boldsymbol{p}_1)\cdot\boldsymbol{p}'$ are different. An asymmetry in the θ distribution means that the number of events with $0<\theta<\pi/2$ is different from that of the events with $\pi/2<\theta<\pi$. It has to be remarked

[7] R. K. ADAIR: *Phys. Rev.*, **100**, 1540 (1955).

[8] We are well aware (G. MORPURGO and B. F. TOUSCHEK: circulated report, June 1957) of the fact that to a γ_5 charge independent strong interaction between pions and nucleons it is not possible to add a parity non conserving term simultaneously maintaining the invariance under time reversal, which of course we want to preserve (electric dipole moments). However a strong parity non conserving process between pions and nucleons might be obtained for instance, without violating time reversal and charge independence, through the intermediary of strong parity non conserving interactions involving hyperons and heavy mesons.

that this last kind of asymmetry is not generally considered in the hyperon case because the assumption is usually made that the strong interactions giving rise to the production of the KY pair conserve the parity; if this is true, it follows that the Y can be polarized only normally to the production plane, which implies no θ asymmetry. It is on the other hand clear that if we look for the possible evidence for non conservation of parity in high energy events we have to look also for θ asymmetries, both in the pion-nucleon reactions considered in this paper, and in the reactions with hyperons and heavy mesons; the fact that, so far, no evidence for θ asymmetries is present in this last kind of reactions [9] (*e.g.* $K^- + p \to \Sigma + \pi$; $\Sigma \to N + \pi$ or $\pi + N \to Y + K$; $Y \to N + \pi$) cannot still be considered a proof that parity is conserved in high energy strong interactions involving hyperons and heavy mesons; it may well be that the longitudinal polarizations of the hyperons emitted begin to be significant only for relativistic velocities of the same, which is not the case for the events studied so far.

To conclude we would like to say that we are perfectly aware, particularly having in mind the sequence of the attempts to determine the spins of the hyperons, of the fact that it will not be easy to collect statistically significant information on the points which we have mentioned; but in any case it will be of some interest to have these distributions slowly inproving; we may repeat in particular, that the method suggested here may prove appropriate to establish the role of the $t = \frac{3}{2}$, $J = \frac{3}{2}$ pion nucleon. resonance in a process like (1).

* * *

I would like to thank prof. G. Salvini for having stimulated my interest in these questions.

[9] For instance in the bubble chamber experiments of the Berkeley group on the reaction $K^- + p \to \Sigma + \pi$ there is, within the errors, no θ asymmetry (by the way, this asymmetry is the same used in testing the parity doublet model and was therefore looked for).

Direttore responsabile: G. POLVANI

Tipografia Compositori - Bologna

Questo fascicolo è stato licenziato dai torchi il 28-VII-1958